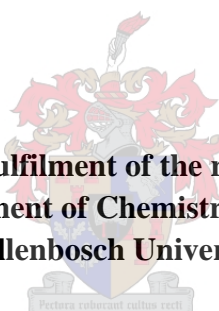


Palladium and Copper Complexes based on Dendrimeric  
and Monofunctional *N, N'* Chelating Ligands as Potential  
Catalysts in the Oxidative Carbonylation of Alcohols

**By**

**Nomvano Mketi**

**A dissertation submitted in fulfilment of the requirements for the degree of  
M. Sc. (Chemistry), Department of Chemistry and Polymer Science at the  
Stellenbosch University**



**Supervisor: S.F. Mapolie**

**March 2010**

## DECLARATION

---

By submitting this thesis electronically, I declare that the entirety of the work contained therein is my own original work, that I am the owner of the copyright thereof (unless to the extent explicitly otherwise stated) and that I have not previously in its entirety or in part submitted it for obtaining any qualification.

Date: .....

## ABSTRACT

---

In this thesis we describe the synthesis of several new *N*-(*n*-propyl)-1-(2-pyridyl and quinolyl)-imine ligands (**ML1-ML4**) as well as peripheral functionalised iminopyridyl and iminoquinolyl poly(propylene-imine) dendrimeric ligands (**DL1-DL8**) with a 1,4-diaminobutane core. The dendrimeric ligands were obtained by modification of the peripheral groups of Generation 1 and Generation 2 poly(propylene-imine) dendrimers, (DAB-(NH<sub>2</sub>)<sub>n</sub>) which are commercially available, with a series of aldehydes. All the ligands were fully characterised by ESI-mass spectrometry, elemental analysis, <sup>1</sup>H & <sup>13</sup>C {<sup>1</sup>H}-NMR, FT-IR and UV/Vis spectroscopies.

These ligands were utilised to synthesise Pd(II) and Cu(I) complexes using appropriate metal precursors. Some of mononuclear complexes, [*N*-(*n*-propyl)-(2-pyridyl and quinolyl) methanimine] dichloro Pd(II) complexes (**C1-C4**) and bis[*N*-(*n*-propyl)-(2-pyridyl and quinolyl) methanimine] copper(I) tetrafluoroborate complexes (**C14**) were structurally characterised. Pd(II) complexes adopted a distorted square-planar geometry around the metal centre while Cu(I) complex exhibit a distorted tetrahedral arrangement around the metal centre. Both Pd(II) and Cu(I) multinuclear complexes (metallodendrimers) were characterised using a range of analytical techniques.

## OPSOMMING

---

In hierdie tesis word die sintese van verskeie nuwe *N*-(*n*-propiel)-1-(2-piridiel) en kinoliel-imien ligande (**ML1-ML4**) sowel as gefunksioneerde imienopiridiel en imienokinoliel poli(propilien-imien) dendrimeriese ligande (**DL1-DL8**) beskryf. Die dendrimeriese ligande was behaal deur die modifikasie van perifere groepe van Generasie 1 en Generasie 2 poli(propilien-imien) dendrimere met 'n reeks aldehiede. Alle ligande was volledig deur ESI-massaspektrometrie, elementele analiese,  $^1\text{H}$  en  $^{13}\text{C}\{^1\text{H}\}$  – KMR, FT-IR en UV/Sigbare spektroskopie gekarakteriseer.

Hierdie ligande was gebruik om Pd(II) en Cu(I) komplekse te berei om van die gepaste metaal voorlopers te gebruik te maak. Sommige van die mono-kern komplekse, [*N*-(*n*-propiel)-(2-piridiel) en kinoliel metanimien] dikloor Pd(II), komplekse (**C1-C4**) en bis[*N*-(*n*-propiel)-(2-piridiel) metanimien] koper(I) tetrafluorboraat, kompleks (**C14**) was struktureël gekarakteriseer. Pd(II) komplekse neem 'n versteurde vierkant valk geometrie om die metaal senter aan, terwyl die Cu(I) kompleks, 'n versteurde tetrahedriese opset rondom die metaal toon.

Beide Pd(II) en Cu(I) multikern komplekse (metaaldendrimere) was deur 'n verskeidenheid van analitiese tegnieke gekarakteriseer.

## ACKNOWLEDGEMENTS

---

First of all I would like to thank the Almighty God for making this possible for me; his glory was with me all the way. He is the controller of everything.

Secondly I would like to express my sincere thanks to Professor Selwyn F Mapolie for his unconditional support, guidance, worthwhile advice and patience, because of him this research project was successful.

Thirdly I like to thank Dr Hendrik van der Westhuizen from SASOL under whose mentoring this project was completed.

I would also like to thank the staff in the Department of Chemistry and Polymer Science, Stellenbosch University especially CAF group for assisting with various analytical techniques.

I'm indebted to Dr C.E Strasser, Mr A. Swartz and Dr J. Gertenbach for performing X-ray analysis during this study and for their meaningful suggestions.

I would also like to thank my colleagues from the Organometallic Group, Rehana Malgas-Enus, Jane Mugo, Mteteleli Sibaca, Yolanda Tancu, Hennie Kotze, Andrew Swartz, Wallace Manning and Dannie van Niekerk for their friendship, extensive support, small talk and their co-operation in the laboratory.

Financial contribution from SASOL and THRIP is also gratefully acknowledged.

Lastly but not least I would like to thank my family and friends, Mr & Mrs Mketi, Samkelwe N Mketi, Monica Mketi, Mkhanyiseli L Mketi, Thandokazi Mketi, Sibusiso Mketi and Mr M.B Mbotshane for their encouragement and inestimable support throughout the completion of this and other previous degrees.

## CONFERENCE CONTRIBUTIONS

---

Nomvano Mketto and S.F Mapolie

***The development of new dendrimeric N, N' donor ligands for the synthesis of palladium complexes.***

Cape Organometallic Symposium, Cape Town, South Africa, 2008.

Nomvano Mketto and S.F Mapolie

***Pd (II) and Cu (I) Monomeric and Dendrimeric Complexes of Di-imine Ligands as Catalyst Precursors for Alcohol oxidation.***

Catalysis Society of South Africa, Cape Town (Goudini Spa), South Africa, 2009.

## TABLE OF CONTENTS

---

<b>Declaration</b>	<b>I</b>
<b>Abstract</b>	<b>II</b>
<b>Opsomming</b>	<b>III</b>
<b>Acknowledgements</b>	<b>IV</b>
<b>Conference Contributions</b>	<b>V</b>
<b>Table of Contents</b>	<b>VI</b>
<b>List of Figures</b>	<b>VII</b>
<b>List of Schemes</b>	<b>X</b>
<b>List of Tables</b>	<b>XII</b>
<b>Abbreviations</b>	<b>XIV</b>
<b>Chapter one:</b> <i>A brief review of the transformation of alcohols via oxidative carbonylation to their corresponding carbonates:</i>	
<i>Catalytic systems and reaction parameters</i>	<i>1</i>
<b>Chapter two:</b> <i>Synthesis and characterization of monofunctional and Multifunctional (dendrimeric) iminopyridyl and iminoquinolyl di-imine ligands</i>	<i>37</i>
<b>Chapter three:</b> <i>Palladium(II) complexes based on mono and multifunctional di-imine ligands: Synthesis and characterization</i>	<i>70</i>
<b>Chapter four:</b> <i>Cationic mono and polynuclear Cu(I) complexes based on pyridyl and quinolyl-imine ligands: Synthesis and characterization</i>	<i>99</i>
<b>Chapter five:</b> <i>Summary and Future work</i>	<i>124</i>
<b>Appendix</b>	<i>127</i>

## LIST OF FIGURES

---

### **Chapter One: A brief review of the transformation of alcohols via oxidative carbonylation to their corresponding carbonates: Catalytic systems and reaction parameters.**

<b>Figure 1.1:</b> Catalytic cycle for DMC production via the EniChem process (LIQUID PHASE)	6
<b>Figure 1.2:</b> Catalytic cycle for DMC via the UBE process (GAS PHASE)	8
<b>Figure 1.3:</b> [ <i>N</i> -Alkyl-(2-pyridyl) methanimine] copper (I) cationic complex and [Cu <sub>1</sub> (biQ-COOR)] <sup>+</sup> BF <sub>4</sub> <sup>-</sup> complex	10
<b>Figure 1.4:</b> Homogeneous Pd-6, 6'-disubstituted-2, 2'-bipyridyl complexes and Pd dinuclear complex bridged with pyridylphosphine ligand	16
<b>Figure 1.5:</b> General structures of the three types of di-imine ligands	18
<b>Figure 1.6:</b> Heterogeneous <i>N,N'</i> donor palladium (II) complexes	19
<b>Figure 1.7:</b> General structure of a generation 3 dendrimer	22
<b>Figure 1.8:</b> An example of continuous membrane reactor	23
<b>Figure 1.9:</b> Divergent route and convergent route for synthesis of dendrimers	24
<b>Figure 1.10:</b> General structures of metallodendrimers	27
<b>Figure 1.11:</b> Schematic drawing of G <sub>0</sub> -NH <sub>2</sub> PAMAM and PPI dendrimers	28
<b>Figure 1.12:</b> Examples of PPI dendrimers	29
<b>Figure 1.13:</b> Dendritic wedges of Pd and Ni complexes	30
<b>Figure 1.14:</b> Pd (II)-phosphine complex modified poly (etherimine) dendrimer	31

### **Chapter Two: Synthesis and characterization of monofunctional and Multifunctional (dendrimeric) iminopyridyl and iminoquinolyl di-imine ligands.**

<b>Figure 2.1:</b> General structures of three types of di-imine ligands	38
<b>Figure 2.2:</b> Massa's bidentate iminopyridine ligands	40
<b>Figure 2.3:</b> Monofunctional iminopyridylimine di-imine ligands	40
<b>Figure 2.4:</b> Multifunctional iminopyridylimine di-imine ligands	41



<b>Figure 2.5:</b> Bis-thio -bis-quinoline ligands	42
<b>Figure 2.6:</b> Possible fragmentation pathway of monofunctional di-imine ligands (ML1-ML4)	47
<b>Figure 2.7:</b> <sup>1</sup> H-NMR (CDCl <sub>3</sub> , 400MHz) spectra of monofunctional di-imine ligands (ML1&ML4) and the numbering schemes for <sup>1</sup> H & <sup>13</sup> C-NMR assignments for ML1-ML4	48
<b>Figure 2.8:</b> <sup>13</sup> C-NMR (CDCl <sub>3</sub> , 400MHz) spectrum of monofunctionalised Methyl-pyridine ligand (ML1)	50
<b>Figure 2.9:</b> G2 dendrimeric <i>N, N'</i> donor ligands [DL5-DL8]	53
<b>Figure 2.10:</b> ESI mass spectrum of DL5	58
<b>Figure 2.11:</b> EIS mass spectrum of DL7	60
<b>Figure 2.11:</b> <sup>1</sup> H-NMR (CDCl <sub>3</sub> , 400MHz) spectrum of generation-1 multifunctional di-imine ligands (DL1&DL3) and the numbering system for <sup>1</sup> H & <sup>13</sup> C-NMR assignments	62

**Chapter three: Palladium(II) complexes based on mono and multifunctional di-imine ligands: Synthesis and characterization.**

<b>Figure 3.1:</b> Pyridyl-imine palladium(II) dichloride complexes	71
<b>Figure 3.2:</b> ESI-mass spectrum of C2	79
<b>Figure 3.3:</b> (A) ESI-MS simulated isotopic distribution of [M-2Cl], (B) [M-C <sub>2</sub> H <sub>5</sub> ], (C) [M <sup>+</sup> ] and (D) experimentally ESI mass spectrum of C2	81
<b>Figure 3.4:</b> The molecular structure of C1 showing crystallographic numbering	82
<b>Figure 3.5:</b> The molecular structure of C2 showing crystallographic numbering	83
<b>Figure 3.6:</b> The molecular structure of C3 showing crystallographic numbering	85
<b>Figure 3.7:</b> The molecular structure of C4 showing crystallographic numbering	86
<b>Figure 3.7:</b> (A) First generation propylene-imine quinolyl (B) second generation poly (propylene-imine) pyridylimine/quinolylimine palladium(II) metallodendrimers	89
<b>Figure 3.8:</b> <sup>1</sup> H-NMR spectrum of C6	91

**Chapter Four: Cationic mono and polynuclear Cu(I) complexes based on pyridyl and quinolyl-imine ligands: Synthesis and characterization.**

<b>Figure 4.1:</b> (A) mononuclear (B) trinuclear copper(I) tetrafluoroborate complexes	100
<b>Figure 4.2:</b> UV/Vis absorption spectrum of C13-C15 in DCM solution (10 <sup>-5</sup> M) at	

room temperature	106
<b>Figure 4.3:</b> UV/Vis absorption spectrum of <b>C16</b> in DCM solution ( $10^{-5}$ M) at room temperature	107
<b>Figure 4.4:</b> The molecular structure of <b>C14</b> showing crystallographic numbering	108
<b>Figure 4.5:</b> (A) First generation propylene-imine quinolyimine (B) second generation poly (propylene-imine) pyridylimine and quinolyimine copper(I) tetrafluoroborate metallodendrimers	111
<b>Figure 4.6:</b> ESI-M spectrum of first generation poly (propylene imine) pyridylimine Copper(I) tetrafluoroborate <b>C18</b>	114
<b>Figure 4.7:</b> ESI-MS spectrum of second generation poly (propylene-imine) pyridylimine copper(I) tetrafluoroborate <b>C22</b>	116
<b>Figure 4.8:</b> Absorption spectra of iminopyridyl-copper(I) metallodendrimers in acetonitrile solution ( $10^{-5}$ M)	119
<b>Figure 4.9:</b> Absorption spectra of iminoquinolyl-copper(I) metallodendrimers in acetonitrile solution ( $10^{-5}$ M)	119

## LIST OF SCHEMES

---

### **Chapter One: A brief review of the transformation of alcohols via oxidative carbonylation to their corresponding carbonates: Catalytic systems and reaction parameters.**

<b>Scheme 1.1:</b> Illustration of the phosgenation process	5
<b>Scheme 1.2:</b> Two steps of EniChem process showing oxidative carbonylation of methanol	5
<b>Scheme 1.3:</b> Six alternative synthetic routes for production of DMC	6
<b>Scheme 1.4:</b> Two steps of UBE process showing oxidative carbonylation of methanol	7
<b>Scheme 1.5:</b> Zeolite-encapsulated Co-Schiff base complex as active catalysts in synthesis of DMC	9
<b>Scheme 1.6:</b> Synthesis of DPC from transesterification of DMC with phenol	12
<b>Scheme 1.7:</b> Proposed mechanism of DPC via direct oxidative carbonylation of phenol	13
<b>Scheme 1.8:</b> Polycarbonates synthesis from transesterification of bis-phenol (BPA) and DPC	15
<b>Scheme 1.9:</b> Effect of 6, 6'- substituents in homogeneous Pd-2'2'-bipyridyl complexes	17
<b>Scheme 1.10:</b> Proposed reaction for production of DMC/DPC	22

### **Chapter Two: Synthesis and characterization of monofunctional and Multifunctional (dendrimeric) iminopyridyl and iminoquinolyl di-imine ligands.**

<b>Scheme 2.1:</b> Synthesis of sulfonate $\beta$ -di-imine ligands	38
<b>Scheme 2.2:</b> Synthesis of <i>N</i> -aryl-2-thienyl substituted 1, 4-diazabutadiene (di-imine) ligands	39
<b>Scheme 2.3:</b> Synthesis of the dinuclear Zn (II) dichloride complexes of symmetric Schiff-base with extended quinoline side arms	42

<b>Scheme 2.4:</b> Synthesis of monofunctional di-imine ligands ( <b>ML1-ML4</b> )	43
<b>Scheme 2.5:</b> Synthesis of monofunctional di-imine ligands ( <b>DL1-DL4</b> )	54
<b>Scheme 2.6:</b> Fragmentation pathway of <b>DL5</b>	59
<b>Scheme 2.7:</b> Fragmentation pathway of <b>DL9</b>	61

**Chapter Three: *Palladium(II) complexes based on mono and multifunctional di-imine ligands: Synthesis and characterization.***

<b>Scheme 3.1:</b> (A) Neutral mononuclear and binuclear Pd(II) dichloride complexes, (B) Cationic mononuclear and binuclear Pd(II) dichloride complexes	72
<b>Scheme 3.2:</b> Unconjugated di-imine Pd(II) complexes	73
<b>Scheme 3.3:</b> Synthesis of mononuclear palladium(II) dichloride complexes based on pyridyl and quinolyl-imine ligands	74
<b>Scheme 3.4:</b> Possible fragmentation pathway of palladium(II) dichloride complexes ( <b>C2</b> )	80
<b>Scheme 3.5:</b> Synthesis of first generation poly (propylene-imine) pyridylimine palladium(II) metallodendrimers	88

**Chapter Four: *Cationic mono and poly-nuclear Cu(I) complexes based on pyridyl and quinolyl-imine ligands: Synthesis and characterization.***

<b>Scheme 4.1:</b> Synthesis of cationic mononuclear copper(I) tetrafluoroborate complexes based on pyridyl and quinolyl-imine ligands	101
<b>Scheme 4.2:</b> Synthesis of first generation poly (propylene-imine) pyridylimine copper(I) tetrafluoroborate metallodendrimer ( <b>C17-C19</b> )	110
<b>Scheme 4.3:</b> Fragmentation pathway of first generation poly (propylene-imine) pyridylimine copper(I) tetrafluoroborate complex <b>C18</b>	115
<b>Scheme 4.4:</b> Fragmentation pattern of second generation poly (propylene-imine) pyridylimine copper(I) tetrafluoroborate complex <b>C22</b>	117

## LIST OF TABLES

---

**Chapter One: *A brief review of the transformation of alcohols via oxidative carbonylation to their corresponding carbonates: Catalytic systems and reaction parameters.***

**Table 1.1:** Homogeneous vs. heterogeneous catalysis 21

**Chapter Two: *Synthesis and characterization of monofunctional and Multifunctional (dendrimeric) iminopyridyl and iminoquinolyl di-imine ligands.***

**Table 2.1:** Characterisation data of monofunctional di-imine ligands (ML1-ML4) 45

**Table 2.2:**  $^1\text{H}$ - Chemical shifts of non-functional di-imine ligands (ML1-ML4) 49

**Table 2.3:**  $^{13}\text{C}$   $\{^1\text{H}\}$  - Chemical shifts of non-functional di-imine ligands (ML1-ML4) 51

**Table 2.4:** Characterisation data of multifunctional dendrimeric di-imine ligands (DL1-DL8) 55

**Table 2.5:**  $^1\text{H}$ - Chemical shifts of multi-functionalised dendrimeric ligands (DL1-DL4) 63

**Table 2.6:**  $^1\text{H}$ - Chemical shifts of multi-functionalised dendrimeric ligands 64

**Table 2.7:**  $^{13}\text{C}$   $\{^1\text{H}\}$  - Chemical shifts of multi-functional dendrimeric ligands (DL1-DL8) 65

**Chapter Three: *Palladium(II) complexes based on mono and multifunctional di-imine ligands: Synthesis and characterization.***

**Table 3.1:** Characterisation data of mononuclear Pd(II) complexes (C1-C4) 76

**Table 3.2:**  $^1\text{H}$ - Chemical shifts of mononuclear Pd(II) complexes (C1-C4) 77

**Table 3.3:** Selected bond lengths (Å) and angles ( $^\circ$ ) for the core of C1 83

**Table 3.4:** Selected bond lengths (Å) and angles ( $^\circ$ ) for the core of C2 84

**Table 3.5:** Selected bond lengths (Å) and angles ( $^\circ$ ) for the core of C3 85

<b>Table 3.6:</b> Selected bond lengths (Å) and angles (°) for the core of <b>C4</b>	87
<b>Table 3.7:</b> Characterisation data of metallodendrimeric Pd(II) complexes ( <b>C7-C12</b> )	92

**Chapter Four: *Cationic mono and poly-nuclear Cu(I) complexes based on pyridyl and quinolyl-imine ligands: Synthesis and characterization.***

<b>Table 4.1:</b> Characterisation data of mononuclear Cu(I) complexes ( <b>C13-16</b> )	103
<b>Table 4.2:</b> <sup>1</sup> H- Chemical shifts of mononuclear Cu(I) complexes ( <b>C13-16</b> )	104
<b>Table 4.3:</b> FT-IR and UV/Vis spectroscopic data for mononuclear cationic copper(I) complexes	106
<b>Table 4.4:</b> Selected bond lengths (Å) and angles (°) for the core of <b>C14</b>	108
<b>Table 4.5:</b> Characterisation data of cationic copper(I) metallodendrimeric complexes ( <b>C17-C24</b> )	112
<b>Table 4.6:</b> <sup>1</sup> H-NMR data cationic copper(I) metallodendrimers ( <b>C17-C24</b> )	113
<b>Table 4.7:</b> Infra-red and UV/Vis spectroscopic data for cationic copper(I) metallodendrimers	118

## ABBREVIATIONS

---

Å	Angstrom
MeCN	Acetonitrile
BQ	benzoquinone
p-BQ	para-benzoquinone
Br	Broad
calcd	Calculated
δ	chemical shift
D	Doublet
DMSO	Dimethylsulfoxide
DCM	Dichloromethane
DMSO-d <sub>6</sub>	deuterated dimethylsulfoxide
ESI-MS	electron spray ionisation mass spectrometry
FT-IR	Fourier transform infrared spectroscopy
EWG	Electron-withdrawing group
Et	Ethyl
g	gram(s)
GC	gas chromatography
GC-MS	Gas chromatography mass spectrometry
h	hours
HQ	hydroquinone

Hz	hertz
i-Pr	isopropyl
IR	Infrared
<i>J</i>	coupling constant
m	Multiplet
Me	Methyl
Me-pyr	Methyl-pyridine
mp	melting point
m/z	mass to charge ratio
MHz	Megahertz
min	Minutes
ml	Millilitres
mmol	Millimoles
NMR	nuclear magnetic resonance
nd	not determined
PhOH	Phenol
ppm	parts per million
s	Singlet (NMR)
t	Triplet
t-Bu	Tertiar butyl
THF	Tetrahydrofuran
UV/Vis	ultraviolet-visible spectroscopy



## CHAPTER ONE

### A BRIEF REVIEW OF THE TRANSFORMATION OF ALCOHOLS VIA OXIDATIVE CARBONYLATION TO THEIR CORRESPONDING CARBONATES: CATALYTIC SYSTEMS AND REACTION PARAMETERS.

---

---

#### CONTENT

1.1	INTRODUCTION TO CARBONYLATION OF ALCOHOLS	2
1.2	OXIDATIVE CARBONYLATION OF ORGANIC ALCOHOLS	2
1.3	ORGANIC CARBONATES	3
1.3.1	Dimethyl Carbonates (DMC)	3
	<i>1.3.1.1 Homogeneous Cu(I) complexes</i>	10
1.3.2	Diphenyl Carbonates (DPC)	11
	<i>1.3.2.1 Direct oxidative carbonylation of phenol</i>	13
	<i>1.3.2.2 Use of DPC in industry</i>	15
1.4	EXAMPLES OF METAL COMPLEXES THAT HAVE BEEN USED TO CATALYSE FORMATION OF DPC	16
	1.4.1 Homogeneous catalysts	16
	1.4.2 Heterogeneous catalysts	18
1.5	CATALYSIS	20
1.6	DENDRIMERS	22
	1.6.1 Two synthetic approaches for dendrimers	24
	<i>1.6.1.1 Divergent approach</i>	24
	<i>1.6.1.2 Convergent approach</i>	25
	1.6.2 Properties of dendrimers	25
1.7	METALLODENDRIMERS	26
	1.7.1 Metallodendrimers in catalysis	28
1.8	CONCLUDING REMARKS	32
1.9	SCOPE AND OUTLINE OF THE ENTIRE THESIS	32
1.10	REFERENCES	34

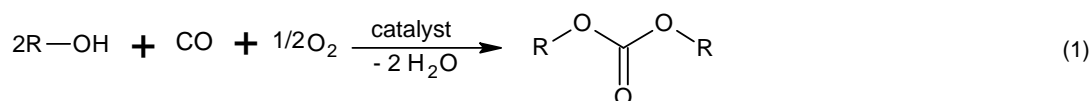
## 1.1 INTRODUCTION TO CARBONYLATION OF ALCOHOLS

Carbonylation of alcohols is a general method for the production of carboxylic acid derivatives and is usually based on transition metal catalysed reactions involving CO (carbon monoxide) and often carried out in a homogeneous fashion. Today more than 70% of synthetic acetic acid production is based on rhodium or iridium catalysed methanol carbonylation. The capacity of world-scale plants using this technology are around  $5 \times 10^5$  tons per year. Carbonylation can also be applied to alkynes, alkenes, esters and organic halides as substrates. More recently, cationic palladium complexes with chelating bis-phosphines have been developed that show great promise in industrial processes. Walter Reppe at BASF introduced the term carbonylation to describe a number of reactions he discovered. Since then, any reaction in which carbon monoxide, alone or together with other components (e.g.  $H_2/O_2$ ), is introduced into an organic molecule in the presence of a catalyst is called a carbonylation reaction [1]. The latter reaction is of major importance both from an academic and an industrial chemical point of view. Due to its availability, price and reactivity patterns, carbon monoxide is becoming more and more an important building block for fine and bulk chemicals. The major reaction types of carbon monoxide have comprehensively been discussed by several leading experts both from academia and industry. Carbonylation reactions such as hydroformylation, alkoxy-carbonylations, CO/olefin-copolymerization, Pauson-Khand reactions and others have been known since 1938 [2]. In this study the main focus is on oxidative carbonylation of alcohols.

## 1.2 OXIDATIVE CARBONYLATION OF ORGANIC ALCOHOLS

Oxidative carbonylation is a type of carbonylation reaction. It differs from others since molecular oxygen together with carbon monoxide are used. Oxidative carbonylation of alcohols/phenols to their corresponding carbonates is a well known organic reaction and is normally a redox reaction. In all types of carbonylation reactions there are three steps that are involved. The first step is the oxidative addition of the substrate to the metal centre which increases the oxidation state of the metal by two. The second step is the

formation of an intermediate by migratory "insertion" of CO (carbonyl). The final step is always the reductive elimination to yield the desired product [3]. This reaction is normally catalyzed by a number of metal complexes including Pd, Cu, Pt, Co, Ni, Rh, Hg, Se and Ir [4]. Oxidative carbonylation involves the insertion of carbon monoxide into a R-O bond of the substrate e.g. alcohol in the presence of molecular oxygen and the active catalyst to form a desired product (carbonate) and with water as a by-product (Equation 1).



[R]: Alkyl / Aryl

### 1.3 ORGANIC CARBONATES

Organic carbonates are very important in industry because of their wide range of applications. For example, dimethyl carbonate (DMC) is a colourless liquid with a pleasant odour. It is non toxic to the environment and not hazardous to human health. It is used as a methylating agent because of its versatility, which reduces the toxicity and the corrosive effect. Secondly, it can also act as a solvent in paints and adhesives. Thirdly, it is used as an oxygenate in gasoline to reduce vehicle emissions which are associated with environmental and health risks [3-6]. On the other hand diphenyl carbonate (DPC) is an important precursor for the production of polycarbonates via melt-polymerisation [5]. These polycarbonates are excellent engineering thermoplastics and can be substitutes for metals and glass because of their good impact strength, heat resistance and transparency [7].

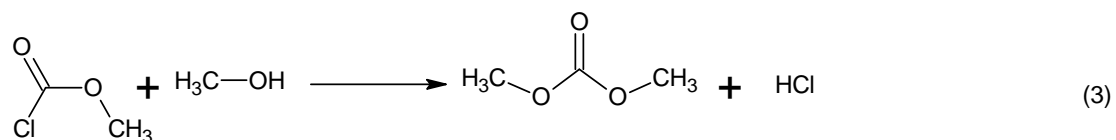
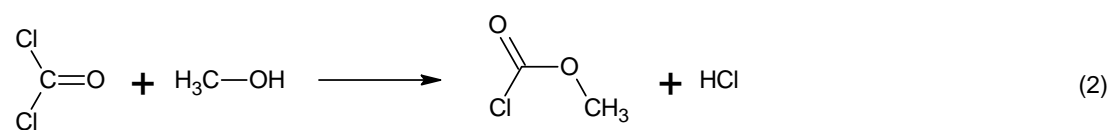
#### 1.3.1 Dimethyl Carbonate (DMC)

There are many methods that have been employed for the production of DMC. These methods include phosgenation of methanol, methanol oxy-carbonylation, methanol reaction with urea, methylnitrite carbonylation, transesterification of urea and methanol reaction with CO<sub>2</sub>, etc [8].

The phosgenation process was the first method used for the production of DMC. This process involves the reaction between phosgene ( $\text{COCl}_2$ ) and methanol ( $\text{MeOH}$ ) to form methylchloroformate as an intermediate species. The latter reacts in the second step with a second molecule of methanol to form the expected product (DMC). Both steps generate  $\text{HCl}$  as a by-product (Scheme 1.1) and it is well known that  $\text{HCl}$  is a toxic substance which is very harmful to the environment. The phosgene gas which is also known as carbonyl chloride is an extremely poisonous gas on its own. This chemical was extensively used during World War I as a choking (pulmonary) agent. Among the chemicals that were used in the war, phosgene was responsible for the large majority of deaths [9]. Phosgene has poor solubility in water and when inhaled deeply into lungs it slowly hydrolyses to form hydrochloric acid and carbon dioxide. Hydrochloric acid causes pulmonary edema [10]. Since the 1980's the phosgenation process has not been used because of the production of  $\text{HCl}$  and toxicity of  $\text{COCl}_2$  gas. Since then many researchers have attempted to develop alternative environmentally friendly methods. Some of these methods are illustrated in Scheme 1.3 below.

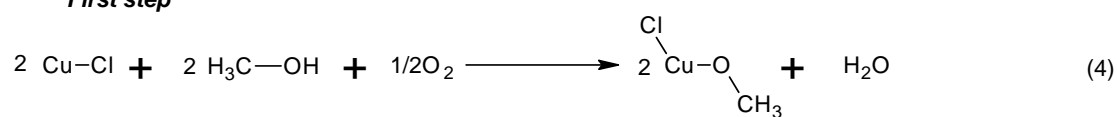
However, there are two large scale commercial methods that are known for the production of DMC. The first one is the **ENIchem (Italy)** process which was developed in 1983. This process uses a homogeneous copper(I) chloride catalyst in the oxidative carbonylation of methanol and uses molecular oxygen and carbon monoxide only. This reaction consists of two steps (see Scheme 1.2). The first step involves the oxidative conversion of cuprous chloride ( $\text{Cu}^{+1}$ ) into cupric alkoxy chloride ( $\text{Cu}^{+2}$ ) in the presence of molecular oxygen. Then in the second step, the cupric alkoxy chloride is reduced to an organic carbonate and cuprous chloride is regenerated [11].

The catalytic scheme for this process is illustrated in Figure 1.1. In the first step molecular oxygen is introduced in order to oxidize cuprous chloride in the presence of methanol to form cupric methoxychloride. Then cupric methoxychloride undergoes reduction under  $\text{CO}$  gas which is promoted by small amounts of cupric species such as  $\text{CuX}_2$  (steps 2-4). In step 5 the methoxy species undergoes nucleophilic attack by a second molecule of methanol which leads to the formation of DMC [3].

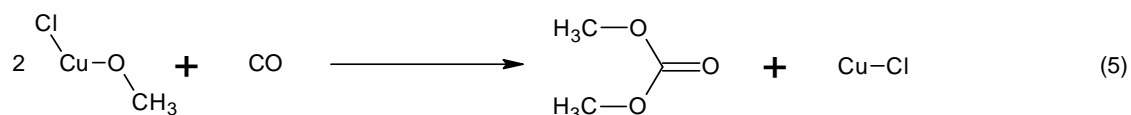


**Scheme 1.1:** Illustration of the phosgenation process

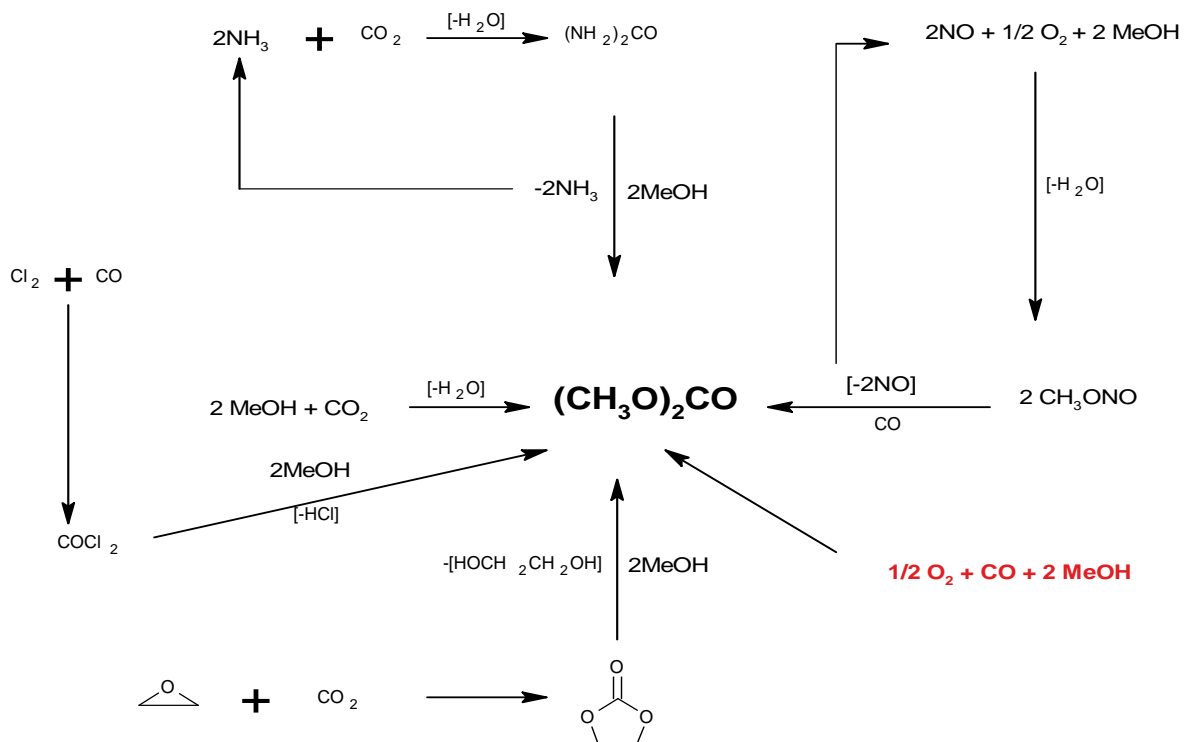
**First step**



**Second step**



**Scheme 1.2:** Two steps of EniChem process showing oxidative carbonylation of methanol



**Scheme 1.3:** Six alternative synthetic routes for production of DMC [3].

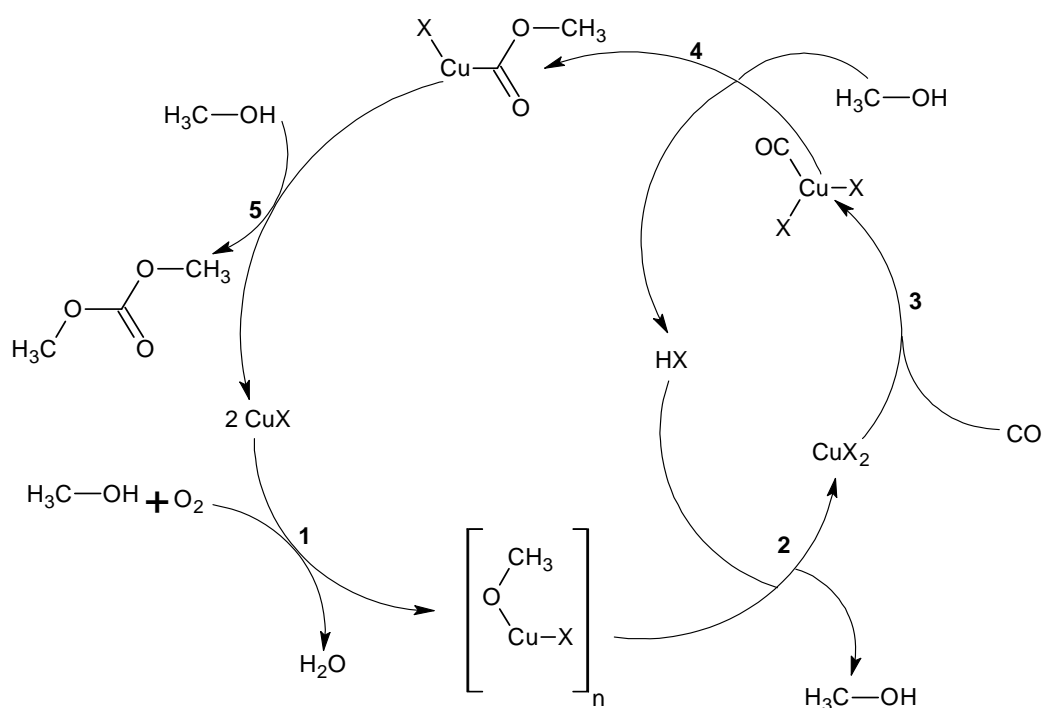


**Figure 1.1:** Catalytic cycle for DMC production via the EniChem process (LIQUID PHASE) [3].



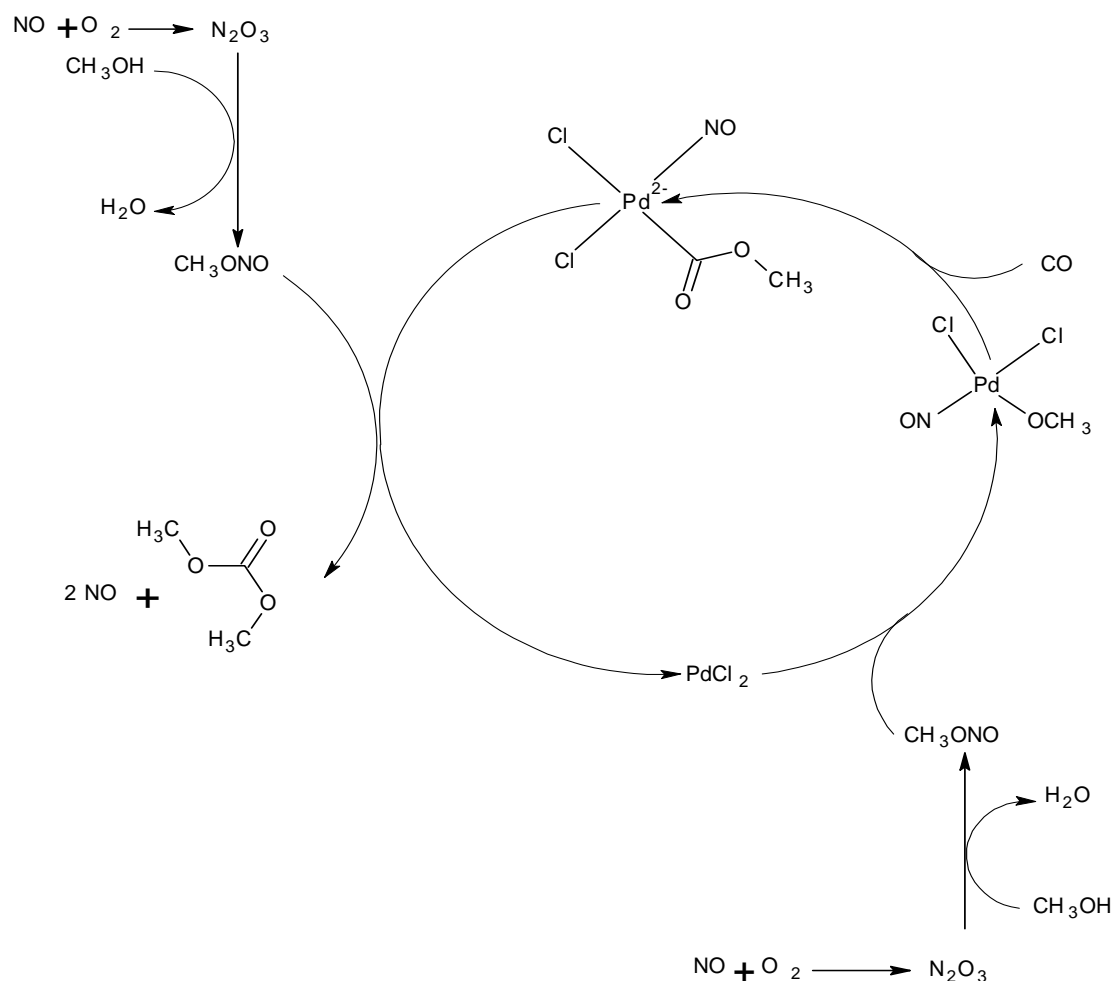
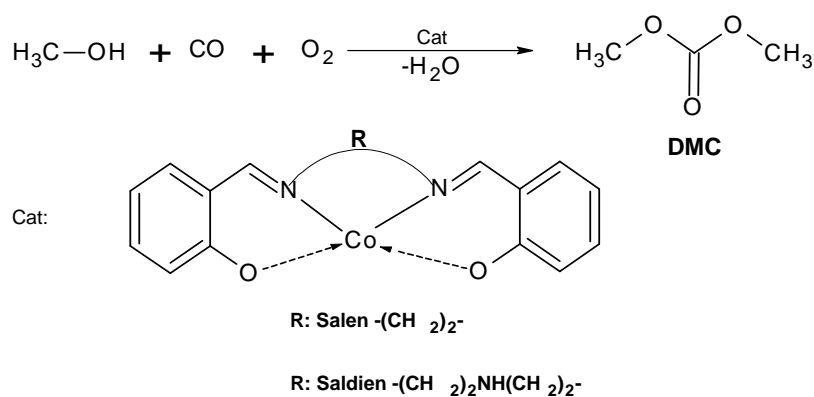


**Figure 1.2:** Catalytic cycle for DMC via the UBE process (GAS PHASE) [3].

However there are two disadvantages that are associated with the EniChem method. The first is the fact that cuprous chloride is sparingly soluble in methanol and as a result the substrate cannot react with the catalyst effectively to form an active intermediate. Secondly, cuprous chloride is highly corrosive to metallic vessels due to the existence of the  $\text{Cl}^-$  ions and the redox reaction of  $\text{Cu(I)}$  [12]. In order to overcome these two problems researchers have been studying alternative methods that can be employed in order to modify this type of catalyst. The use of basic additives as promoters (such as amines and pyridines), room temperature ionic liquids as promoters [(BDMI $\text{m}$ ) $\text{BF}_4$ , (BPy) $\text{Cl}$ , (BPy) $\text{BF}_4$  and (OMIm) $\text{BF}_4$ ], immobilized copper/palladium catalysts, Schiff base copper / palladium complexes, as well as the effect of various types of chelating



ligands such as O-O, N-O, N-S, N-N and N-P [2-12] have been investigated as alternatives. Cu-Y zeolite catalysts were also used in an attempt to minimise the problem of leaching of the Cl<sup>-</sup> ions. Much of the work that uses Cu/Zeolites as catalyst was done by King *et al* [14]. They claim that their catalytic system is highly active and that it has minimal deactivation as compared to the carbon-supported CuCl<sub>2</sub> catalytic system [14]. These workers discovered that chloride is replaced by the zeolites. King *et al.* also claimed that their copper (I) zeolites showed higher selectivity as compared to the copper (I) chloride salt. In this reaction the first step involves the oxidation of methanol on the copper site to form cupric methoxide. The insertion of CO into the metal-oxide bond forms a carbomethoxide (rate determining step). Then MeOH and molecular oxygen react with the carbomethoxide to form DMC [13].



**Scheme 1.5:** Zeolite-encapsulated Co-Schiff base complex as active catalysts in synthesis of DMC [15].

Zhu *et al.* also studied zeolite-encapsulated cobalt Schiff base complexes with a four carbon spacer between the di-imine functionalities as shown in Scheme 1.5 [15]. They reported that the activity, selectivity and corrosion rate of their system was better than compared to neat cobalt complexes. The most active, stable and recyclable encapsulated cobalt catalysts for this catalytic reaction was discovered to be that of Co (sal-ophen)-Y and it showed good activity and selectivity even after the 5<sup>th</sup> run [16]. Recently Zhong *et al.* reported that the main by-product in the oxidative carbonylation of methanol catalysed by copper exchanged zeolite Y are dimethoxymethane (DMM) and methyl-formate (MF)

and the conversion of methanol to DMC was very low due to low loading of the metal onto the zeolite [17]. There have been many attempts to develop catalyst systems [16-19] based on zeolite encapsulated metal complexes, however the problem was low metal loading, leading to ineffective catalysts.

### 1.3.1.1 *Homogeneous copper(I) complexes*

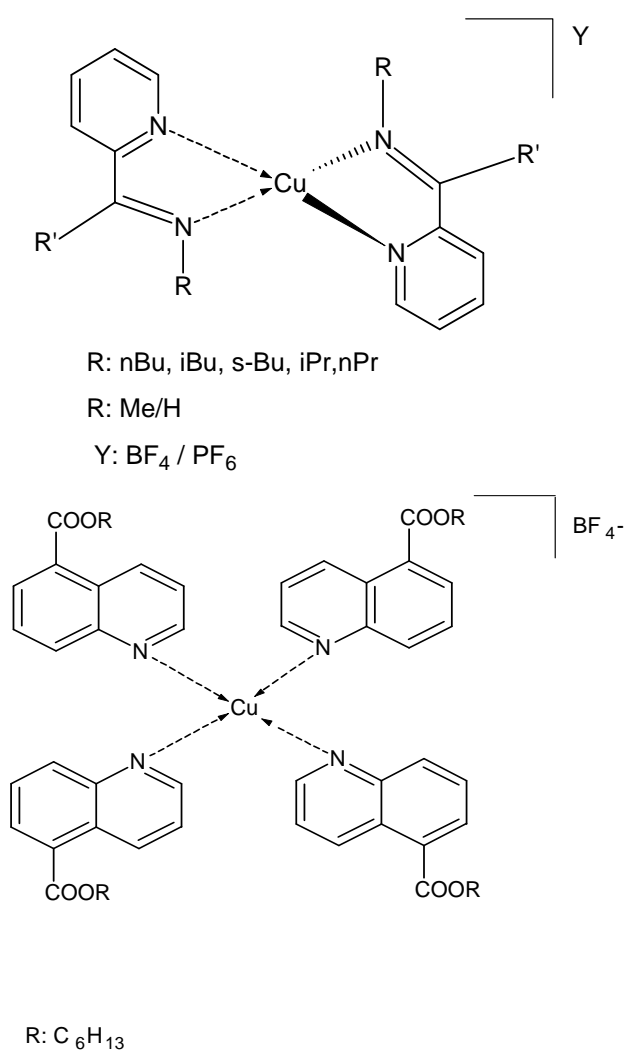
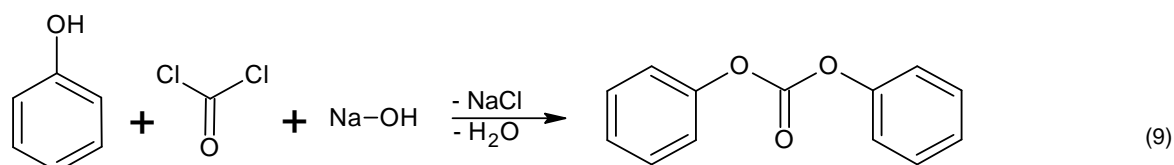


**Figure 1.3:** *[N-Alkyl-(2-pyridyl) methanimine] copper(I) cationic complex [20] and [Cu<sub>1</sub>(biQ-COOR)]<sup>+</sup>BF<sub>4</sub><sup>-</sup> complex [21]*

In order to avoid any corrosion effect of the copper(I) chloride and its leaching, in this study we aim to develop new copper(I) complexes with *N, N'* donor ligands without the

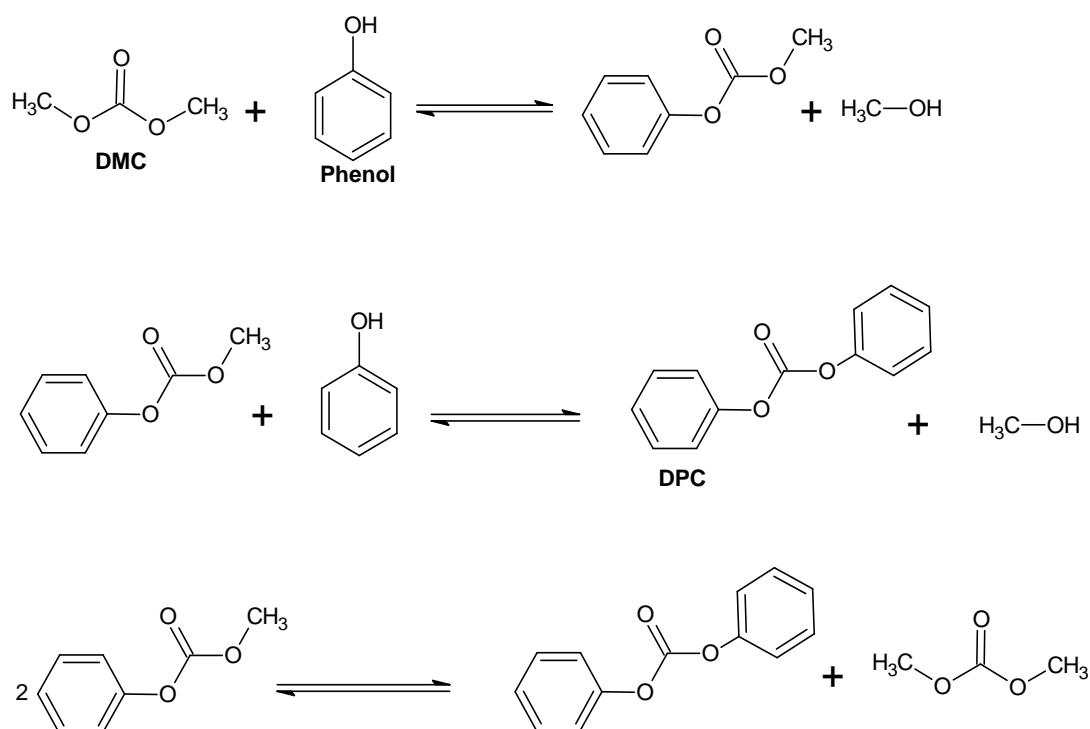
interference of chloride ions. Many research groups have managed to develop such systems for numerous catalytic reactions such as atom-transfer polymerization [20] and as electro-catalysts for O<sub>2</sub> activation in the oxidation of alcohols [21]. Fu *et al.* also reported such types of copper complexes and they discovered that these are easily synthesized. These complexes are strongly distorted around the metal centre [22]. Raab *et al.* reported similar complexes in the oxidative carbonylation of methanol. The outcome of their study showed that the activity, conversion and selectivity in methanol carbonylation strongly increases if three or four strong *N, N'* donor ligands coordinate to copper [23]. Our copper complexes will be based on these types of systems. The bulkiness of the complex in Figure 1.3 increases the selectivity in most reactions and they are regarded as very stable complexes. They can be easily recrystallised via slow diffusion of diethyl-ether into dichloromethane solution at low temperatures [20, 21].

### 1.3.2 Diphenyl Carbonate (DPC)



Diphenylcarbonate (DPC) is considered to be a replacement for phosgene (COCl<sub>2</sub>) in the synthesis of polycarbonates. Conventional production of DPC involves reactions of phosgene and phenol in the presence of a base such as NaOH or KOH (Equation 9). However, the phosgenation process has drawbacks such as use of COCl<sub>2</sub> gas as raw material, use of methylene chloride (dangerous) as a solvent and the production of chloride salts. For these reasons, environmentally friendly processes for synthesis of DPC have been proposed and developed in the past few decades in order to minimize social and environmental effects of pollution [2, 24, and 25]. So far, the most attractive alternative methods that can be used to substitute phosgene appeared to be transesterification of DMC and phenol, see Scheme 1.6 [19,26-28, 66-67], direct oxidative carbonylation of phenol with CO and O<sub>2</sub> [29, 30] and transesterification of

dialkyl oxalates and phenol [31]. The most favoured process of the above mentioned ones is the direct oxidative carbonylation because it is a one step process and theoretically it produces water as the sole by-product. There is a lot of work that has been done in studying this catalytic process [32-35].

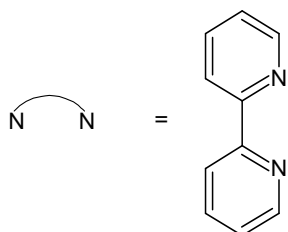
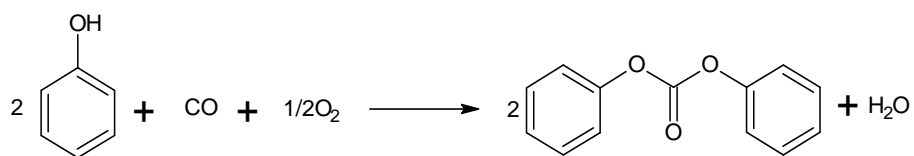
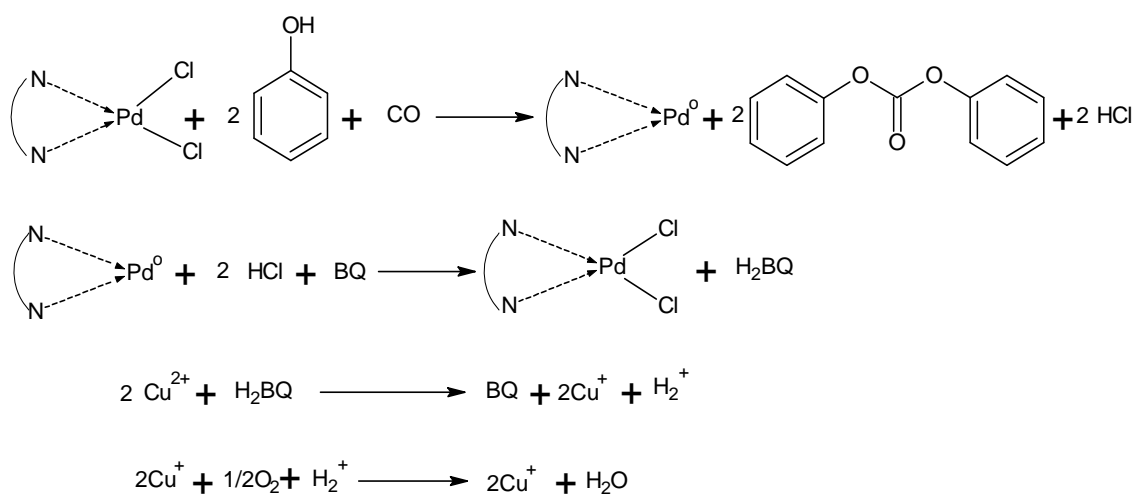


**Scheme 1.6:** Synthesis of DPC from transesterification of DMC with phenol [19].

Interesting work in direct oxidative carbonylation of phenols with carbon monoxide and molecular oxygen has been reported by Hallgren *et al.* [36, 37] where the reaction of phenol with CO and O<sub>2</sub> at atmospheric pressure and room temperature was studied using a palladium(II) dichloride complex and a tertiary amine to produce DPC and arylsalicylates. They pointed out that the conversion of phenol to DPC requires re-oxidation of reduced Pd and regeneration of an active species of Pd(II). That is why direct oxidative carbonylation of phenol is regarded as a slow catalytic reaction, therefore Pd(II) salts need a co-catalyst such as Cu, V, Co and Mn salts to achieve a rapid re-oxidation of metallic palladium [38]. Ishii and co-workers tried to employ a dinuclear

bridged palladium complex and they discovered that the activity of the catalyst increases because of the extra active site (second palladium) [8].

### 1.3.2.1 *Direct oxidative carbonylation of phenol*



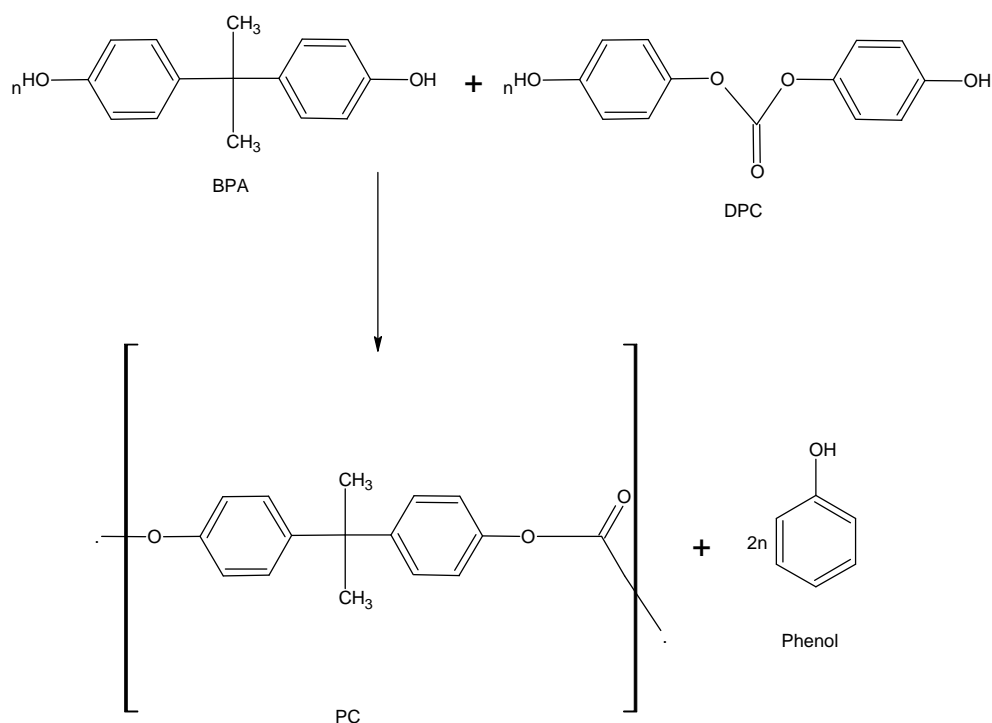
BQ: benzoquinone (organic co-catalyst)

$\text{Cu}^{+2}$ : CuO (metal co-catalyst)

**Scheme 1.7:** Proposed mechanism of DPC via direct oxidative carbonylation of phenol [39]

In the first step of DPC synthesis in Scheme 1.7, DPC is formed from phenol and carbon monoxide with concomitant reduction of Pd(II) to Pd (0) and formation of 2 HCl. This reaction is catalytic by means of a system in which Pd re-oxidation is mediated by the addition of an organic co-catalyst [*p*-benzoquinone (BQ)] and of a metal co-catalyst [CuO]. It is proposed that BQ which is reduced to hydroquinone by HCl reoxidises Pd(0) to Pd(II) while the metal co-catalyst is reduced from Cu(II) to Cu(I) by H<sub>2</sub>QB which is reoxidised to BQ. Oxygen and protons (from 2HCl) close the cycle with re-oxidation of the reduced metal co-catalyst and the formation of water (by-product) [40]. There are many by-products that could be associated with this catalytic reaction; but these differ depending on the type of catalytic system employed. Goyal *et al.* [41] reported that *o*-phenylene carbonate was the main by-product while Ishii *et al.* [42] claimed that phenyl salicylate was the main by-product, Xue *et al.* [43] pointed out that *p*-benzoquinone, phenyl acetate and tributylamine were the main by-products in their reaction. Fan *et al.*[4,39] speculated that in their OIH-DACH-PdCl<sub>2</sub>-Cu<sub>2</sub>O-THF (OIH-DACH: functionalized silica modified by 1,2-diaminocyclohexane) catalytic system phenyl salicylate, tributylamine, *p*-bromophenols and phenyl acetate were detected as main by-products, whereas their OIH-DACH-PdCl<sub>2</sub>-Co(OAc)<sub>2</sub>-CH<sub>2</sub>Cl<sub>2</sub> catalytic system only showed phenyl acetate as the only detected main by-product.

### 1.3.2.2 Use of DPC in industry



**Scheme 1.8:** Polycarbonates synthesis from transesterification of bis-phenol (BPA) and DPC [44].

Diphenyl carbonate is a precursor in the production of polycarbonates which are widely employed as engineering plastic in various applications. The melt transesterification method has advantages over interfacial phosgene methods like lower cost and environmental benign. Melt transesterification is a reversible reaction and the reaction by-product is phenol (see Scheme 1.8) which can be easily distilled off to reach high molecular weight.

## 1.4 EXAMPLES OF METAL COMPLEXES THAT HAVE BEEN USED TO CATALYSE FORMATION OF DPC

### 1.4.1 Homogeneous catalysts

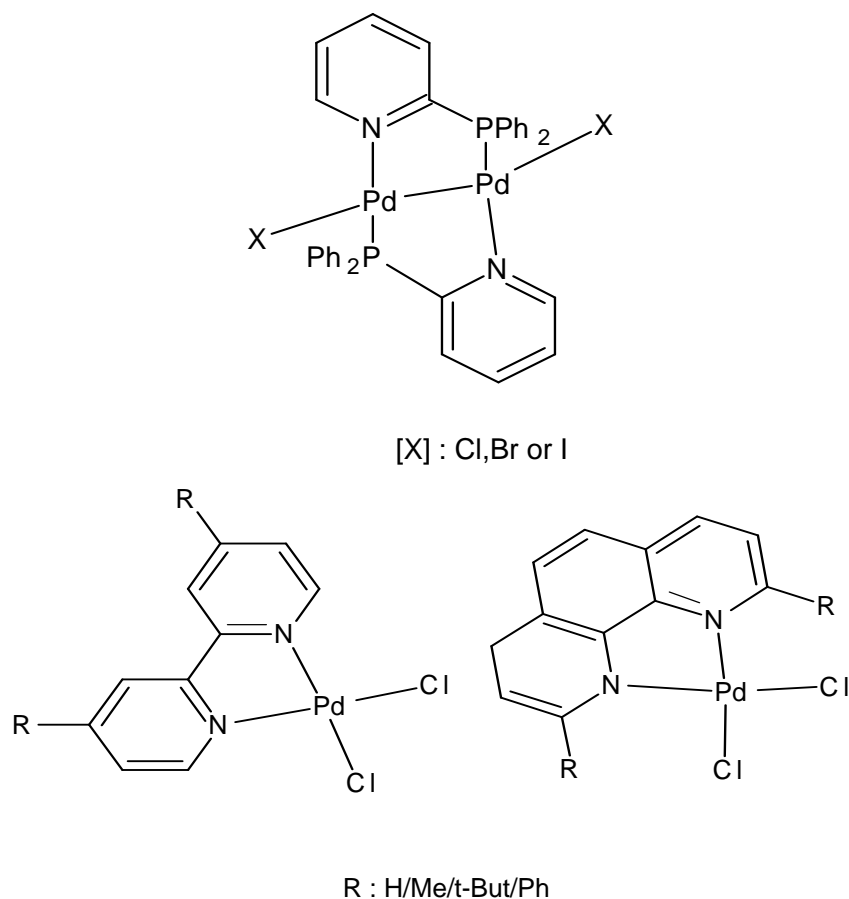
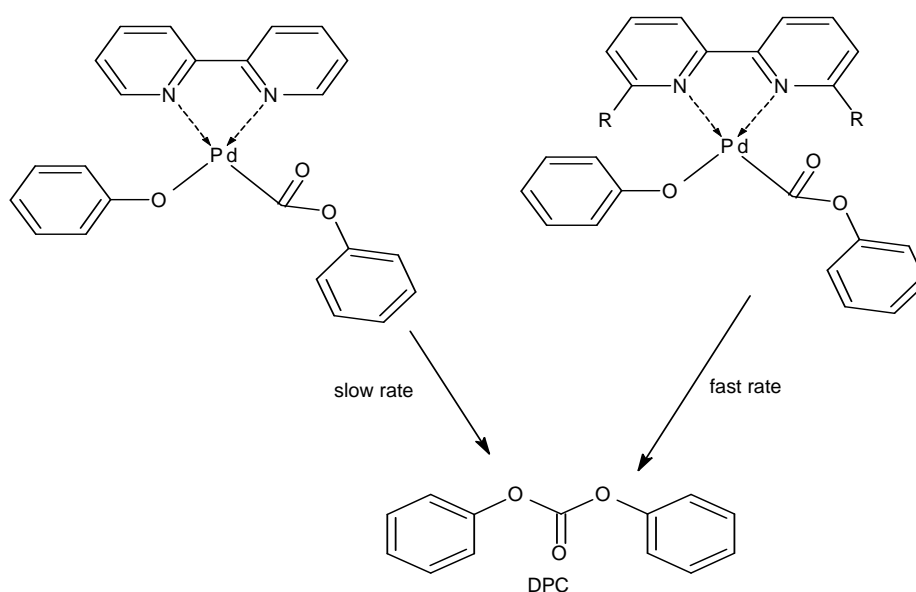


**Figure 1.4:** Homogeneous Pd-6, 6'-disubstituted-2, 2'-bipyridyl complexes [44] and Pd dinuclear complex bridged with pyridylphosphine ligand [42].

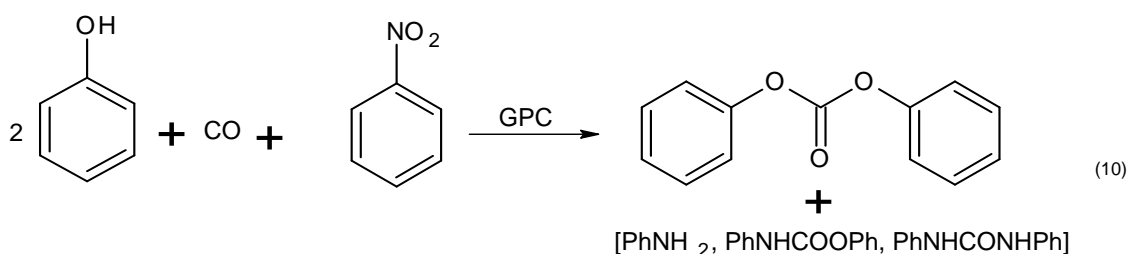
Yasuda *et al.* [44] investigated the effect of bulky ligands on the synthesis of DPC. They discovered that the more bulky the ligand, the more selective the palladium complex. Moiseev *et al.* [45] reported that giant palladium-561 clusters (GPC) were effective in the synthesis of DPC with concomitant reduction of nitrobenzene which was acting as an



oxidizing agent (Equation 10). It was discovered that the use of the above complexes (Figure 1.4) gave higher T.O.F values reaching up to 68.8 (mol-DPC/mol Pd h) under high CO pressure and the presence of 3Å molecular sieves which serve as a drying agent to absorb water molecules (by-product). Water molecules will react with starting material (CO) of this reaction and that will lead to formation of carbon dioxide. The formation of CO<sub>2</sub> will have a negative effect on the selectivity of the catalysts. The presence of the alkyl substituents at the 6, 6'-position of the bipy rings accelerate activity because there is steric repulsion of the R groups and the phenoxycarbonyl units at the Pd centre in the phenoxycarbonyl intermediate, illustration in Scheme 1.10 [42,65].



**Scheme 1.9:** Effect of 6, 6'-substituents in homogeneous Pd-2'2'-bipyridyl complexes [42].



In most cases di-imine ligands were used to complex palladium and copper salts to form  $N, N'$  chelating catalysts. The facet of interest in such ligands is their ability to undergo redox chemistry. Pyridine is known as a good  $\pi$ -acceptor, so the electrons of the metal centre from d-orbital are delocalized around the  $\pi$ -conjugated pyridine ring which makes the  $\pi$ -back bonding to be more effective. This delocalization stabilizes the whole complex [46]. There are three types of di-imine ligands; that is  $\alpha$  di-imine,  $\beta$  di-imine and  $\gamma$  di-imine. They experience differences in forming metal complexes. Unlike the analogous  $\alpha$  and  $\beta$  di-imine ligands, reaction of the  $\gamma$  di-imine ligands with  $\text{Pd}(\text{CH}_3\text{CN})\text{Cl}_2$  form dinuclear palladium complexes. The latter ligands do not coordinate with the Pd(II) centre in a chelating fashion but instead adopt a monodentate coordination mode. Their reactions with palladium acetate result in C-H activation, which forms trinuclear palladacycles [47].

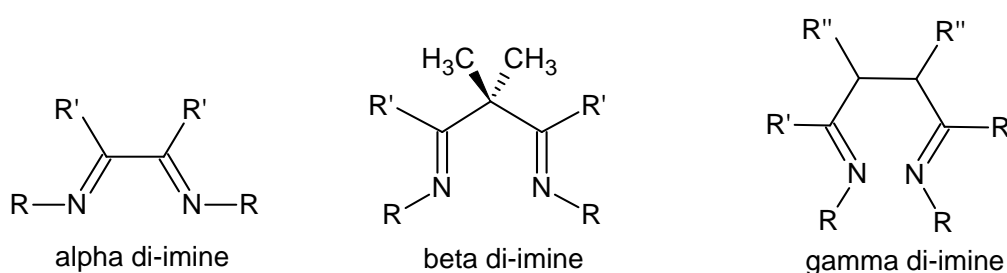


**Figure 1.5:** General structures of the three types of di-imine ligands [47].

#### 1.4.2 Heterogeneous catalysts

It has been reported that when using heterogeneous catalysts in Figure 1.6, reaction parameters such as temperature, time, pressure and quantity of inorganic co catalyst affect the leaching of Pd significantly. One needs to carefully monitor these parameters so that he/she chooses the best. Some researchers report that very low yields of DPC were produced (around 13.7%), because of Pd loss from 2.7wt%-4.0wt% [4, 39, 69]. There are many literature reports wherein  $N, N'$  donor ligands are used as stabilising agents in copper and palladium complexes employed in the production of DMC and DPC. This type of ligand system is recommended because it also minimizes the

corrosion of the reactor material by the chloride anions [48]. Palladium has been also used because it favours square planar coordination, thus forcing the reagents (alcohol and CO) to interact in the catalytically more favoured cis position [4, 39-44, 48]. Copper on the other hand has been used since it can be oxidised and reduced very easily.

The large-scale industrial application of catalysts makes high demands upon these catalysts in order to meet technical, economical, and environmental requirements. Thus, the catalyst should be cost-efficient in terms of catalyst costs per kilogram product. Catalyst separation from the product should be facile in order to avoid contamination of the latter with catalyst residues. In the down-stream processing, the catalyst should not interfere negatively with the waste-water treatment or affect the waste-water quality in a negative way that conflicts with environmental legislation [49-50].

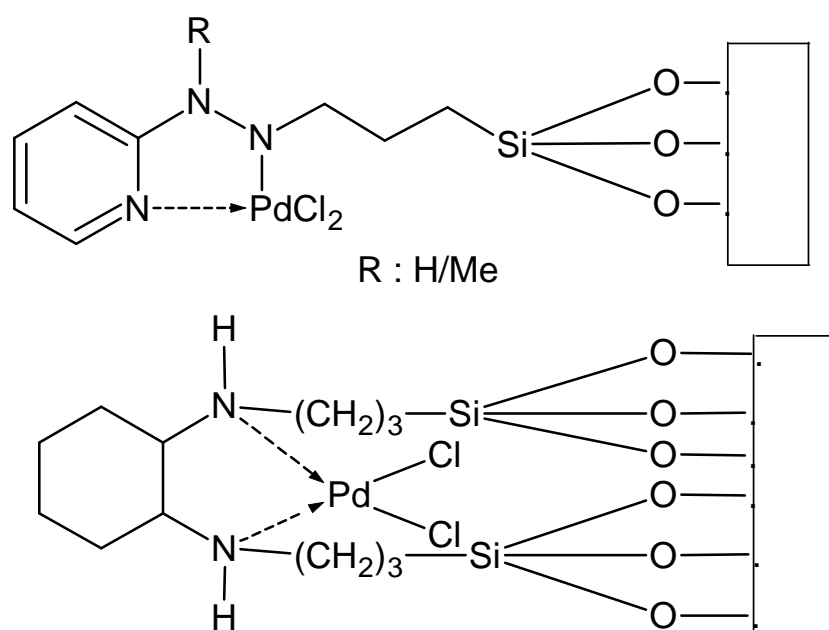


**Figure 1.6:** Heterogeneous *N, N'* donor palladium(II) complexes [4, 39]

## 1.5 CATALYSIS

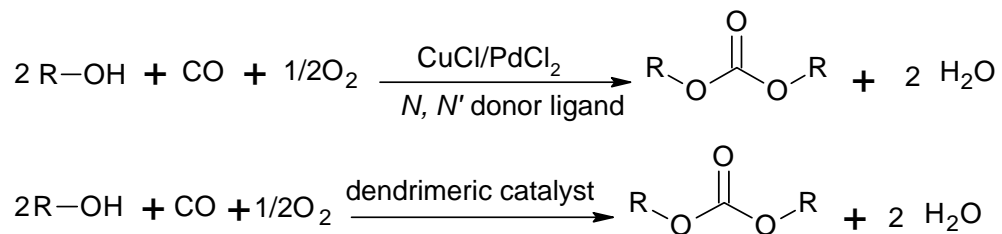
Catalytic reactions such as oxidative carbonylation can be achieved by using either homogeneous or heterogeneous catalysts. However each of these two approaches has their own advantages and disadvantages that need to be balanced, see Table 1.1. To solve this problem researchers have tested several concepts to combine the advantages of homogeneous and heterogeneous catalysis. The heterogenization of homogeneous catalysts exhibits the cross fertilization of both systems by combining most of their advantages [5]. It was discovered that the most effective heterogenization process is the immobilization of the homogeneous catalyst onto a support. Amongst all of the supported catalysts, polymer supported metal complexes are one of the most used since the structures of the active sites in the polymer-supported catalyst are well defined and uniform [6]. Once immobilized, the active sites of the "heterogeneous" catalyst can retain the features of the original homogeneous catalyst, provided that the heterogenization process was well designed [7].

**Table 1.1: Homogeneous vs. heterogeneous catalysis**

<b>Homogeneous Catalysis</b>	<b>Heterogeneous Catalysis</b>
Monophasic system	Multiphasic system
Easily synthesized	Require multi-synthetic steps
High selectivity	Low selectivity
High activity (rate)	Low activity (rate)
Difficulties in separation of desired product	Easy separation of desired product from reaction mixture.
Non-recyclable catalysts	Recyclable catalysts
Generate large amount of waste material	Waste material is limited

In this study we will attempt to bridge the gap between homogeneous and heterogeneous catalysis by developing new *N, N'* donor chelating ligands based on dendrimer scaffolds of poly(propylene-imine) diaminobutane (DAB) dendrimers as our organic support. These dendrimeric ligands will then be complexed to copper and palladium to form metallodendrimers. The metallodendritic catalysts will be evaluated in the catalytic carbonylation reaction of alcohols to form organic carbonates (Scheme 1.10). These multinuclear dendrimeric catalysts will be compared against model mononuclear complexes to evaluate their effect on activity and selectivity. It was discovered that

dendrimeric supports can also minimize the corrosion rate and also improve the stability of the catalyst [51].



**Scheme 1.10:** Proposed reaction for production of DMC/DPC.

## 1.6 DENDRIMERS

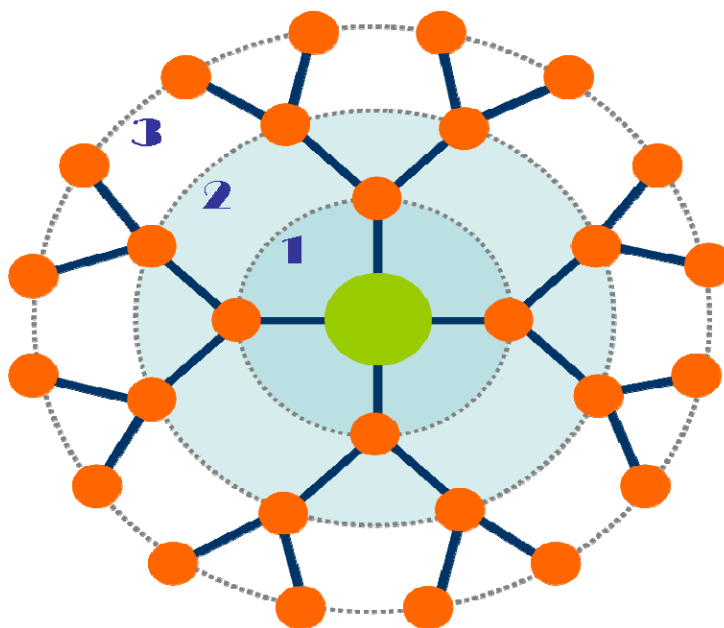


**Figure 1.7:** General structure of a generation 3 dendrimer

Dendrimers are built from a series of branches around an inner core, providing products of different generations and offer intriguing possibilities in this regard. They can be synthesised from almost any core molecule and the branches similarly constructed from any bi-functional molecule, while the terminal groups can be modified chemically to achieve charged, hydrophilic, or hydrophobic surfaces. Their dimensions are extremely small, having diameters (depending on generation) in the range of 2 to 10 nm; that is they are authentic nanoparticles. Normal synthetic processes do not allow for the growth of infinitely large dendrimers, usually because of steric problems. They can be synthesised starting from the central core and working toward the periphery (divergent synthesis), or in a “top-down” approach starting from the outermost residues (convergent synthesis), or built up from component dendrons, either by their covalent attachment or by their self-assembly [49]. Both the core and periphery strategies lead to catalysts that are sufficiently larger than most substrates and products, thus separation by modern membrane separation techniques can be applied. These novel homogeneous catalysts can be used in continuous membrane reactors, which will have major advantages particularly for reactions that benefit from low substrate concentrations or suffer from side reactions of the product [1].

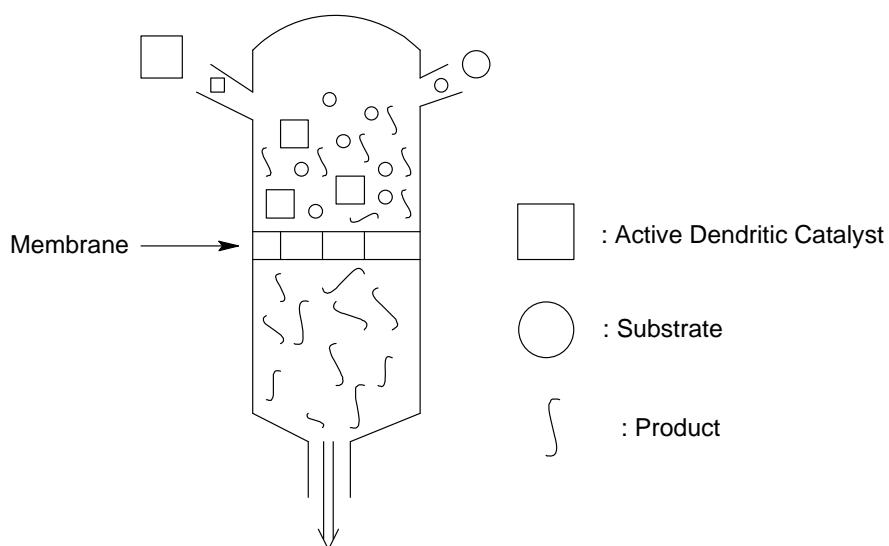


**Figure 1.8:** *An example of continuous membrane reactor*

### 1.6.1 Two synthetic approaches for dendrimers

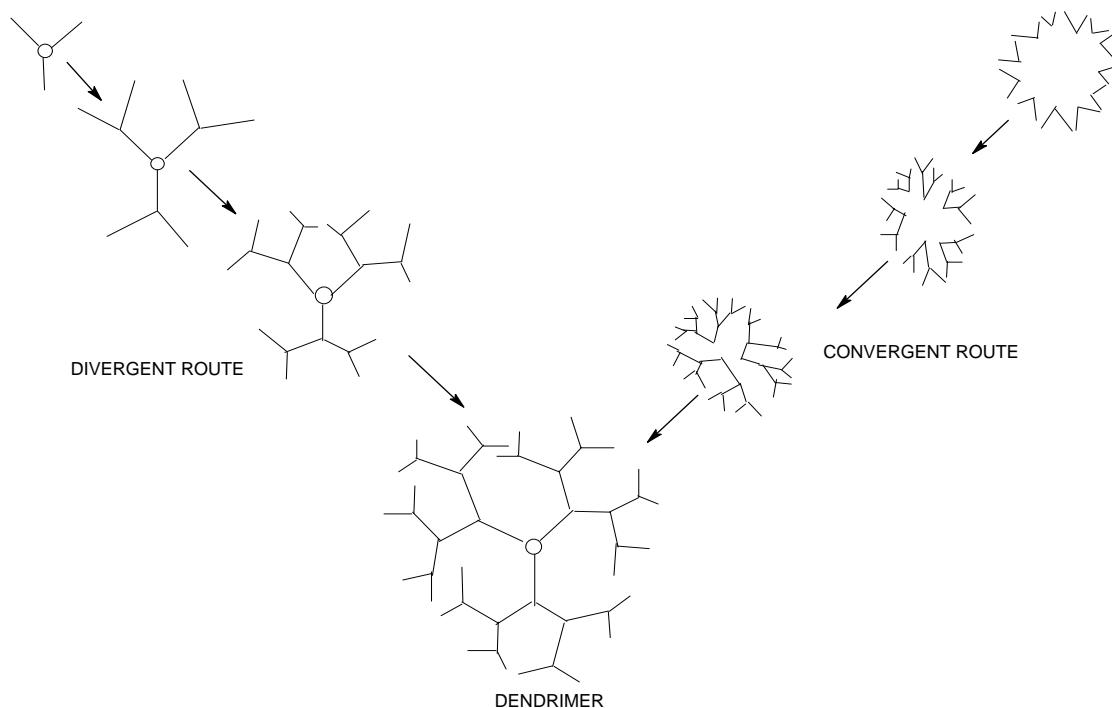


**Figure 1.9:** Divergent route and convergent route for synthesis of dendrimers

#### 1.6.1.1 Divergent approach

This name comes from the way in which the dendrimer grows outwards from the core, diverging into space as shown in Figure 1.9. Starting from a reactive core, a generation is grown, and then the new periphery of the molecule is activated for reaction with more monomer. The two steps can then be repeated. The divergent approach is successful for the production of large quantities of dendrimers since, in each generation-adding step, the molar mass of the dendrimer is doubled. Very large dendrimers have been prepared in this way, but incomplete growth steps and side reactions lead to the isolation and characterization of slightly imperfect samples [11]



### 1.6.1.2 Convergent approach

The 'convergent' approach was developed as a response to the weakness of the divergent synthesis. Convergent growth begins at what will end up being the surface of the dendrimer and works inwards by gradually linking surface units together with more monomers (Figure 3). When the growing wedges are large enough, several are attached to a suitable core to give a complete dendrimer. The advantages of convergent growth over divergent growth stems from the fact that only two simultaneous reactions are required for any generation-adding step. Most importantly, this protocol makes the purification of perfect dendrimers simple [11].

### 1.6.2 *Properties of dendrimers*

- Efficient membrane transport — Dendrimers have demonstrated rapid transport capabilities across biological membranes.
- High loading capacity — Dendrimer structures can be used to carry and store a wide range of metals, organic or inorganic molecules by encapsulation and absorption.
- High uniformity and purity — The synthetic process used produces dendrimers with uniform sizes, precisely defined surface functionality, and very low impurity levels.
- Low toxicity — most dendrimer systems display very low cytotoxicity levels.
- Low immunogenicity — Dendrimers commonly manifest a very low or negligible immunogenic response when injected or used topically.

## 1.7 METALLODENDRIMERS

The loading of any metal to a dendrimeric structure forms a new compound called a metallodendrimer. All possible general structures of metallodendrimers are illustrated in Figure 1.10 below. These types of metallodendrimeric compounds have been used in many catalytic reactions such as Heck-coupling, metathesis, polymerisation etc [52-55]. They are very stable compounds and they can be easily synthesised. They are normally characterised by proton NMR, FT-IR, elemental analysis, mass spectrometry etc. Organometallic catalysis using dendrimers was first reported by van Koten and since then a variety of ligands and catalytically active transition metals have been incorporated at various locations within the dendrimer [52, 56].

All known general different types of metallodendrimers are shown in Figure 1.10, and they are used in different applications depending on the way of anchoring the metal. The metallodendrimer illustrated in Figure 1.10(i) is normally used in homogeneous catalysis and the metals are anchored on the periphery groups. The advantage of this type is that they can be easily synthesized, and in this project we have concentrated on type (i) metallodendrimers.

Metallodendrimers constitute a very promising class of well-defined hyperbranched polymers, whose interest is mainly driven by their potential use as selective and recoverable homogeneous catalysts. In many cases, the metallic centres are grafted to the periphery of the dendrimer, due to the simplicity of this synthetic method from a practical point of view. However, a lot of examples are also known in which the metallic centres are located inside the dendritic structure, either at the core or within the branches [50].

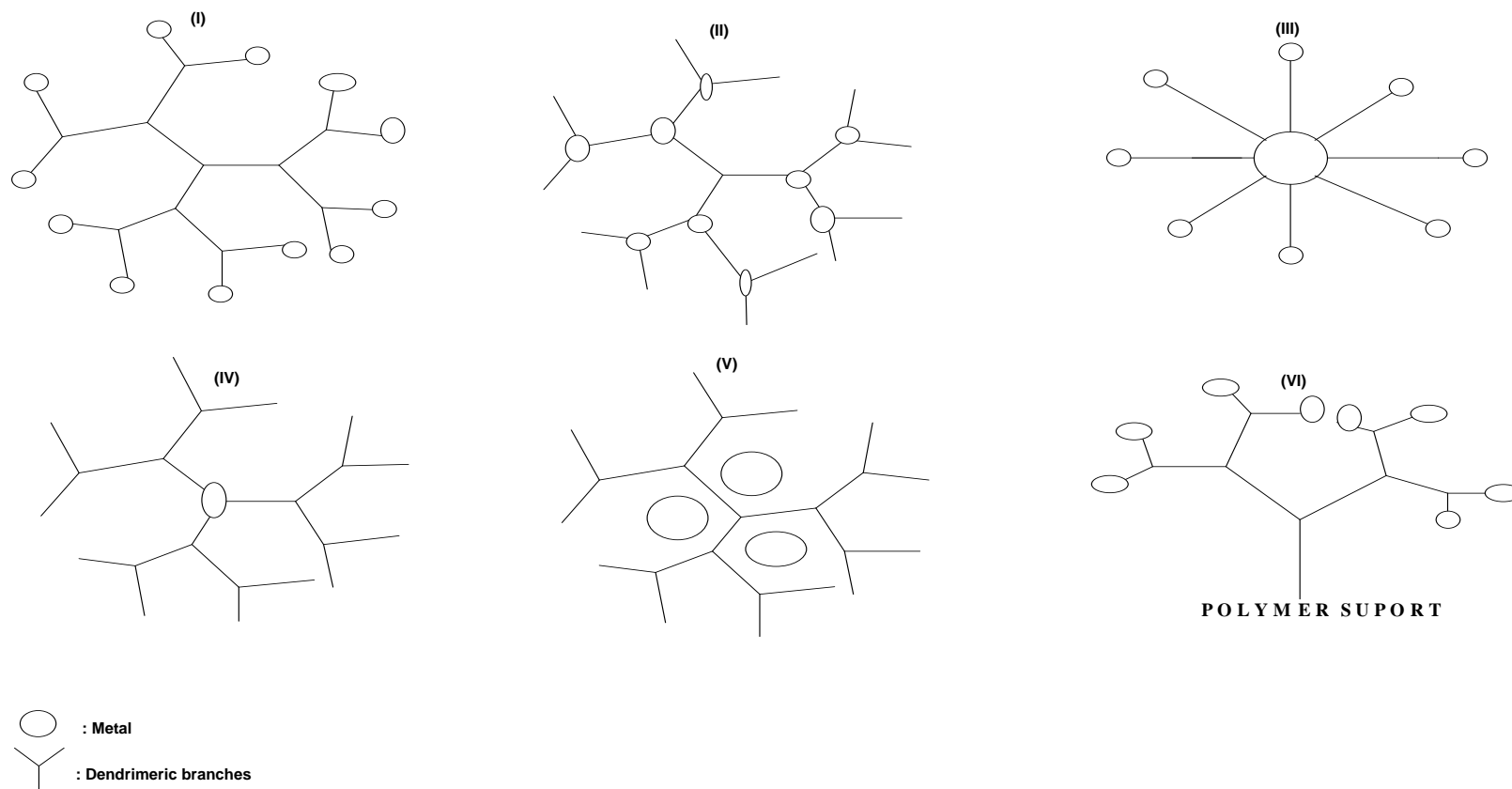


**Figure 1.10:** General structures of metallodendrimers i) Metal located at the termini of the dendritic branches, ii) Metal located at or near focal point of branches, iii) Metal located at the termini of the star branches, iv) Metal located at the centre (core), v) Metal encapsulated inside the dendron, vi) Metal dendron attached to a polymer supported with the metal located at the termini of the branches.

### 1.7.1 Metallodendrimers in catalysis

Metallodendrimers have been used as active catalysts in several catalytic reactions [52-59]. Heck coupling of iodobenzene was catalysed by Pd(II) dichloride complex which was incorporated onto the core of the functionalized dendrimer [56]. Cyclocarbonylation reactions have been reported which were catalysed by recyclable palladium complexes which were located on the periphery of a functionalized dendrimer [52].

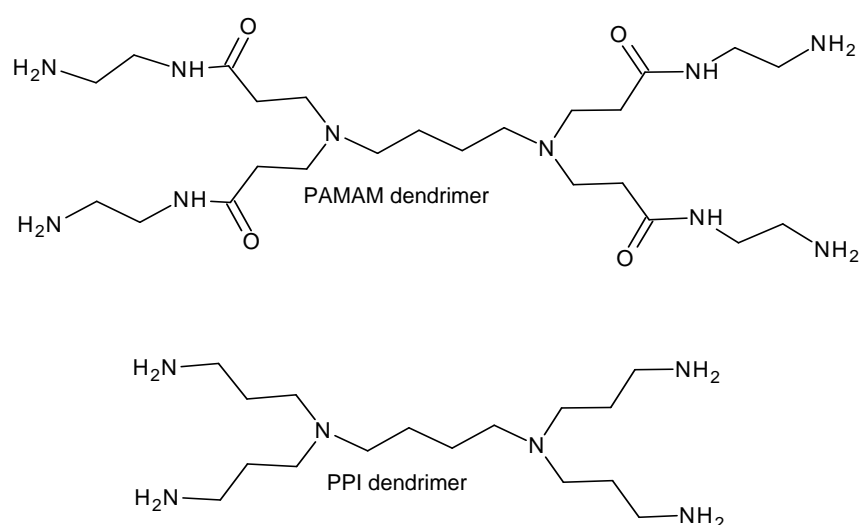


**Figure 1.11:** Schematic drawing of G<sub>0</sub>-NH<sub>2</sub> PAMAM and PPI dendrimers [60]

PAMAM (polyamidoamine) and PPI poly(propylene-imine) dendrimers have been used extensively in different catalytic reactions because of their easy accessibility. These dendrimers are first modified by anchoring metal complexes onto the peripheral branches to form dendritic catalysts (metal nanoparticle-dendrimer composites) before they can be used as active catalysts [60]. In our group we are more interested in the modification of poly(propylene-imine) diaminobutane (DAB) core dendrimers. DAB cored dendrimers were firstly synthesized by Meijer *et al.* [61], and are now commercially available from DSM<sup>®</sup>. In recent papers, we reported the synthesis and full characterization of iminopyridyl

terminally modified poly(propylene-imine) dendrimers and their subsequent Ni and Pd complexes. The catalytic activity of these catalysts was tested in ethylene polymerization [55], ethylene oligomerisation [57], norbornene polymerization [58], and in Heck reactions [59]. Karakhanov *et al* tested the catalytic activity of Pd and Cu complexes which were immobilized onto different poly(propylene-imine) (PPI) diaminobutane and diaminohexane dendrimers in Wacker-oxidation of 1-alkenes in a mixture of alcohol and water at 60-80°C and 0.5 MPa of oxygen. It was noted that selectivity of these catalysts increases with the dendrimer generation. It was also reported that the rate of the reaction was slightly lower for DAH-based catalysts as compared with those of DAB [62].

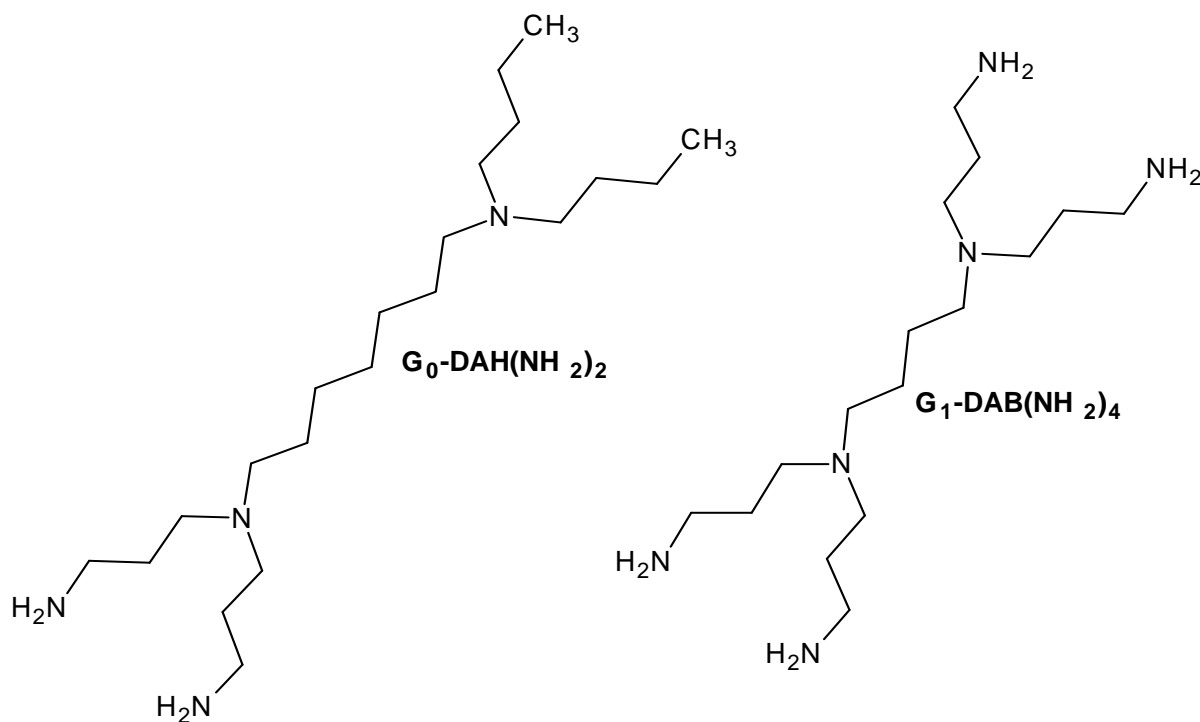


**Figure 1.12:** Examples of PPI dendrimer [62]

In 2005 Blom *et al.* developed new  $\alpha$  di-imine Ni and Pd complexes which contained dendritic wedges of the poly (benzylphenylether) type. These catalysts were then evaluated in ethene oligomerisation [54]. In this study the active metal is located at the core of the dendrimer wedge in order to possibly control the micro-environment around the catalytic centre and thus allow modification of the catalytic selectivity [63]. The direct steric control around the catalytic centre may also be controlled by appropriate *ortho* substitution thereby

favouring oligomerisation. The heteroatomic functionality for attachment of the dendritic wedges is introduced at the *para*-position and thus remote from the active catalytic centre in order to minimize unfavourable interactions. These types of catalysts were also reported by Overret and co-workers. They employed Fe bis(imino) pyridyl dendritic wedges in alkene oligomerisation [64].

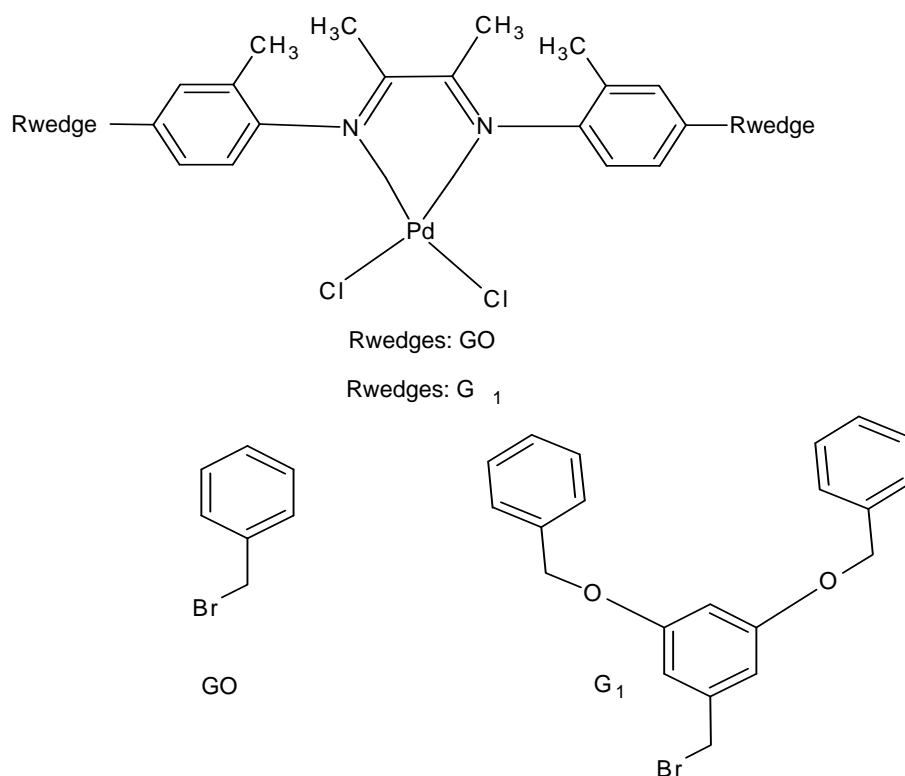


**Figure 1.13:** Dendritic wedges of Pd and Ni complexes [54]

Krishna and co-workers reported Heck coupling of various alkene substrates which were catalysed by Pd(II) phosphine complexes modified by poly (ether-imine) dendrimers. They managed to synthesise mono-nuclear, G-1, G-2 and G-3 analogues of this system. They claimed that their complexes were air-stable in the solid state, but in solution phase these complexes were air sensitive over an extended period. Decomposition of the mono-nuclear analogue was slow as compared to the dendrimeric catalyst. They also reported that the activity of the catalysts increased with an increase in the generation number [53].

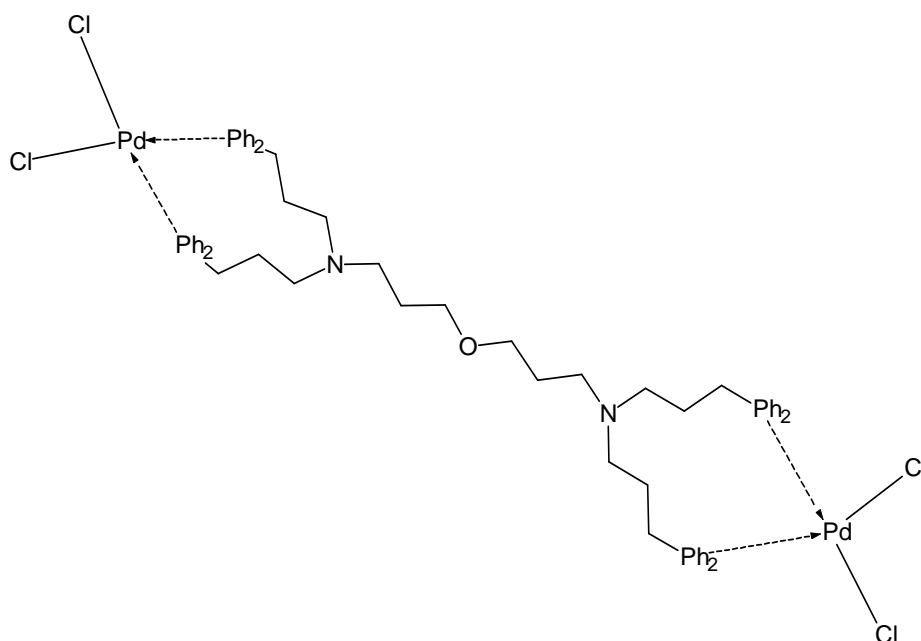


**Figure 1.14:** *Pd(II)-phosphine complex modified poly (ether-imine) dendrimer [53]*

Malgas and co-workers reported the successful synthesis of active dendritic nickel catalysts for ethylene oligomerisation. They also noticed that the higher the dendrimer generation, the higher the catalytic activity as a result of the increased number of active sites. The types of oligomers that were formed differed with dendrimer generation. Generation 1 catalyst formed short chain oligomers whereas generation 2 catalyst formed waxy high molecular weight products. It can be concluded that the dendrimer also impacts on the selectivity of the catalysts [57].

## 1.8 CONCLUDING REMARKS

From the afore going discussion in this chapter, it is clear that oxidative carbonylation of alcohols to the analogous carbonates is a significant process and has gained importance in both academia and in the chemical industry. From reported literature results it is apparent that the synthesis of DMC is more readily facilitated by using copper(I) chloride based catalysts while palladium(II) dichloride based catalysts are more effective for the production of DPC. A main disadvantage of the copper(I) chloride systems is the leaching of  $\text{Cl}^-$  ions due to catalyst instability. This is discussed in some detail in this chapter. Attempts to remedy this situation are also discussed.

The chapter also discussed the merits of immobilizing the oxidation catalysts using both inorganic and organic supports. In the case of the former encapsulation of active catalysts into zeolites and immobilization on mesoporous silica is also outlined. The chapter concludes with a motivation for using dendrimers as immobilizing agents. A brief overview of dendrimers especially its application in catalysis is also given in the latter part of the chapter.

## 1.9 SCOPE AND OUTLINE OF THE ENTIRE THESIS

The main objective of this thesis is to develop new *N,N'* donor ligands and the subsequent coordination of these to palladium and copper salts to form mononuclear and multinuclear Pd(II) and Cu(I) complexes. The full characterization of these complexes is also discussed.

**Chapter one** of this thesis deals with a literature review of the main developments in oxidative carbonylation. In this chapter an attempt is made to clearly show the importance of the continuous production of organic carbonates. Challenges and problems that are associated with this catalytic reaction are discussed. In addition the previous attempts to overcome these problems are summarised. Finally the chapter concludes with a proposal of how we may attempt to provide possible solutions.

The second chapter deals with the actual synthesis of two types of *N, N'* donor ligands. Types 1 are the monofunctional di-imine ligands and type 2 are the multifunctional (dendrimeric) di-imine ligands. Type 1 di-imine ligands are synthesised from the reaction of n-propylamine with various types of aldehydes via a Schiff base condensation reaction. The type 2 di-imine ligands are synthesised in a similar way by reaction of [DAB-(NH<sub>2</sub>)<sub>n</sub>] poly(propylene-imine) (PPI) dendrimers with similar aldehydes. The chapter gives full characterisation data for all the new ligands. This includes various spectroscopic data amongst which are <sup>1</sup>H and <sup>13</sup>C –NMR, FT-IR, ESI-mass spec data. Elemental analysis results are also given for the various ligands.

**Chapter three** is focused on the synthesis and characterisation of Pd(II) complexes of the various di-imine ligands reported in **chapter 2**. The chapter once again gives full characterisation data for all the complexes formed. This includes a range of spectroscopic



data. In some cases the mononuclear metal complexes were also characterized by means of Single crystal x-ray diffraction analysis and the structures of four complexes are reported.

Synthesis of cationic copper(I) complexes is discussed in **Chapter 4**. Both dendrimeric and mono-nuclear copper complexes were fully characterized by  $^1\text{H}$  and  $^{13}\text{C}$  –NMR, FT-IR spectroscopy, ESI-mass spec data. Four mononuclear copper complexes were also characterized by Single X-ray diffraction analysis. Due to time constraints none of the complexes prepared were actually tested for their catalytic activity in oxidative carbonylation of alcohols. The application of these complexes as catalysts in the above processes is suggested for a future study.

**1.10 REFERENCES**

- [1] E.Yoshisato, S.Tsutsumi, *J.Org.Chem.*33 (1968) 869.
- [2] A.G.Shaikh, S.Sivaram, *Chem.Rev.*96 (1996) 951.
- [3] D.Delledome, F.Rivelti, U.Romao, *Appl.Catal. A: General* 221 (2001) 241.
- [4] A.J.B. Robertson, “*Catalysis of Gas Reactions by Metals*. Logos Press”, London, 1970.
- [5] Y.Ono, *Pure Appl.Chem.* 68 (1996) 367.
- [6] K. Tomishige, T. Sakaihorii, *Appl. Catal. A: General* 181 (1999) 95.
- [7] W. Dong, X. Zhou, *Appl. Catal. A: General* 334 (2008) 100.
- [8] H. Ishii, H. Goyal, *J. Mol.Catal. A: General* 148 (1999) 289.
- [9] W.G Eckert, Mass death by gas or chemical poisoning, historical perspective. *Am J Forensic Med Pathol.* 12 (1991) 119.
- [10] T.P. Kennedy, J.R. Hoidal, *J. Appl Physiol.*, 67 (1989) 2542.
- [11] A. Morean, *Electrochim, Acta*, 26 (1998) 1609.
- [12] W. Mo, H. Xiong, *J. Mol. Catal. A: General* 247 (2006) 227.
- [13] F.Rivetti, *Chemistry* 3 (2000) 497.
- [14] S.T. King, *J. Catal.* 161 (1996) 530.
- [15] J.C.Lim, C.S .Cheng, *J. Chinese Inst. Chem .Eng.* 38 (2007) 29.
- [16] D .Zhu, F.M .Mei, L. Chen, *Energy & Fuel*, 23 (2009) 2359.
- [17] Y. Zhong, A.T. Bell, *J. Catal.*, 255 (2008) 153.
- [18] L.J.Chen, J. Boo, F.M. Mei, G.X. Li, *Catal. Commun.* 9 (2008) 658.
- [19] G.X. Li, L.J. Boo, F.M. Mei, *Appl. Catal. A* (2008).
- [20] D.M. Haddleton, D.J. Duncalf, *Eur. J.Inorg. Chem.* (1998) 1799.
- [21] T.V. Magdesieva, *Electrochem. A:* 53 (2008) 3960.
- [22] W.Fu, X. Gen, *Inorg. Chim. Acta.* 360 (2007) 2758.
- [23] V. Raab, M. Merz, J. Sundermeyer, *J. Mol. Catal.* 175 (2001) 51.
- [24] J. Beranek, J. Hlavackova, *Nucl. Acid Chem.* 2 (1978) 999.
- [25] Y. Ono, *Appl. Cat. A: Gen.* 155 (1997) 133.
- [26] K.S. Oh, B.G. Lee, M.S. Han, Y.G. Shul, *React. Kinet.Cat. Lett.* 77 (2002) 51.
- [27] W.B. Kim, Y.G. Kim, J.S. Lee, *Appl. Catal. A: Gen.* 194/195 (2000) 403.
- [28] F.M. Mei, G.X. Li, J. Nie, H.B. Xu, *J. Mol. Catal. A: Chem.* 184 (2002) 456.

- [29] X.B. Ma, J.L. Gong, S.P. Wang, N. Gao, D.L. Wang, X. Yang, F. He, *Catal. Commun.* 5 (2004) 101.
- [30] J.L. Gong, X.B. Ma, X. Yang, S.P. Wang, S.D. Wen, *Catal. Commun.* 5 (2004) 179.
- [31] X.B. Ma, H.L. Nguo, S.P. Wang, Y.L. Sun, *Fuel Process. Technol.* 83 (2003) 275.
- [32] Y.M. Chang, C.M. Shu, *J. Therm. Anal. Catal.*, 193 (2008) 135.
- [33] B.G. Woo, K.Y. Chal, *J. Appl. Polym. Sci.* 80 (2001) 1253.
- [34] B.K. Won, Y.G. Kim, J.S. Lee, *Appl. Catal, A: General*, 403 (2000) 194.
- [35] B.K. Won, Y.G. Kim, J.S. Lee, *Catal. Lett.*, 59 (1999) 83.
- [36] J. E. Hallengren, R.O. Mathews, *J. Organomet. Chem.* 175 (1979) 135.
- [37] J. E. Hallengren, R.O. Mathews, *US Patent* 4,349,485 (1982).
- [38] J. E. Hallengren, R.O. Mathews, *J. Organomet. Chem.* 204 (1981) 135.
- [39] G.Fan, T.Li, G.Li, *Appl. Organomet. Chem* 20 (2006) 656.
- [40] A. Vavasori, L. Toniolo, *J. Mol. Catal. A*.151 (2000) 37.
- [41] M. Goyal, R. Nagahata, *J. Mol. Catal. A: Chem.* 137 (1999) 147.
- [42] H. Ishii, M. Goyal, *Appl. Catal. A: General* 201 (2000) 101.
- [43] W. Xue, J. Zhang, *J. Mol. Catal. A: Chem.* 232 (2005) 77.
- [44] H. Yasuda, *J. Mol. Catal. A: Chemical* 236 (2005) 149.
- [45] I. Moiseev, M. Vargaftik, *J. Mol. Catal: A. Chem.* 108 (1996) 77.
- [46] Y. Soto, Y. Saume, *J. Mol. Catal. A: Chem* 130 (1998) 139.
- [47] M.J. Chitanda, D.E. Prokopchuk, *Organometallics.* 27 (2008) 2337.
- [48] Y. Seto, M. Kagotani, *J. Mol. Catal. A: 151* (2000) 79.
- [49] C. Satmarel, A. Gurtounko, *Macromolecules*, 36 (2003) 486
- [50] A. Caminade, J. Majoral, *Coord. Chem. Rev.* 249 (2005) 1917.
- [51] W.P. Jencks, "Catalysis in Chemistry and Enzymology" McGraw-Hill, New York, 1969
- [52] S. Lu, H. Alper, *Chem. Eur. J.*, 13 (2007) 5908.
- [53] T.R. Krishna, N. Jayaraman, *Tetrahedron*, 60 (2004) 10325.
- [54] B. Blom, M.J. Overet, R. Meijboom, J.R. Moss, *Inorg Chim. Acta.* 358 (2005) 3491.
- [55] G. S. Smith, R. Chen, S. Mapolie, *J. Organomet. Chem.*, 673 (2003) 111.
- [56] T. Mu, D. Feng, S. Fen, *J. Phys. Chem Part C*, 112 (2008) 5952.
- [57] R. Malgas, S.F. Mapolie, S.O. Ojwach, G.S. Smith, J. Darkwa, *Catal. Commun.* 9 (2008) 1612.
- [58] R. Malgas-Enus, S.F. Mapolie, G.S. Smith, *J. Organomet. Chem.* 693 (2008) 2279.

- 
- [59] G.S. Smith, S.F. Mapolie, *J. Mol. Catal. A: Chem* 213 (2004) 187.
- [60] H.S. Li, T.A. Konovalova, *J. Phys. Chem.* 113 (2009) 5358.
- [61] E.M.N. de-van Brabander Berg, E.W. Meijer, *Angew. Chem. Int. Ed. Engl.* 32 (1993) 1308.
- [62] E.A. Karakhanov, A.L. Maximov, *J. Mol. Catal. A: Chem.* 297 (2009) 73.
- [63] G.E. Oosterom, J.M. Frechet, *Angew. Chem, Int. Ed. Engl.* 40 (2001) 1828.
- [64] M.J. Overett, R. Meijboom, J.R. Moss, *Dalton Trans.* (2005) 551.
- [65] A.G. Shaikh, S. Sivaram, *Chem. Rev.* 96 (1996) 951.
- [66] S.P. Wang, X.B. Ma, H.L. Ngou, J.L. Gong, X. Yang, G.H. Xu, *J. Mol. Catal. A: Chem.* 214 (2004) 273.
- [67] S.P. Wang, X.B. Ma, H.L. Ngou, J.L. Gong, X. Yang, G.H. Xu, *Chinese J. Anal. Chem.* 30 (2002) 829.
- [68] T. Liu, C. Chang, *J. Chinese Inst of Chem. Engin.* 38 (2008) 29.
- [69] G. Fan, J. Huang, *J. Mol. Cat A: Chemical* 267 (2007) 34.

## CHAPTER TWO

# SYNTEHSIS AND CHARACTERISATION OF MONOFUNCTIONAL AND MULTIFUNCTIONAL (dendrimeric) IMINOPYRIDYL AND IMINOQUINOLYL DI-IMINE LIGANDS.

---

### CONTENT

2.1 INTRODUCTION TO DI-IMINE LIGANDS	38
2.1.1 Iminopyridyl-imine ligands	39
2.1.2 Iminoquinolyl-imine ligands	41
2.2 RESULTS AND DISCUSSION	43
2.2.1 Synthesis and characterisation of <i>N</i> -( <i>n</i> -propyl)-1-(2-pyridyl and quinolyl)-imine ligands	43
2.2.1.1 <i>FT-IR spectroscopy of ML<sub>n</sub> ligands</i>	44
2.2.1.2 <i>ESI mass spectrometry and elemental analysis of ML<sub>n</sub> ligands</i>	46
2.2.1.3 <i><sup>1</sup>H &amp; <sup>13</sup>C {<sup>1</sup>H}-NMR studies of ML<sub>n</sub> ligands</i>	46
2.2.2 Synthesis and characterisation of [G1&2 DAB-dendr-(NH <sub>2</sub> )-1-(2-pyridyl and quinolyl)-imine] ligands	52
2.2.2.1 <i>FT-IR spectroscopy of DL<sub>n</sub> ligands</i>	54
2.2.2.2 <i><sup>1</sup>H &amp; <sup>13</sup>C {<sup>1</sup>H}-NMR studies of DL<sub>n</sub> ligands</i>	56
2.2.2.3 <i>ESI mass spectrometry of DL<sub>n</sub> ligands</i>	57
2.3 CONCLUDING REMARKS	66
2.4 EXPERIMENTAL SECTION	66
2.4.1 General remarks	66
2.4.2 Materials	67
2.5 SYNTHESIS OF <i>N,N'</i> DONOR LIGANDS	67
2.5.1 Monofunctional di-imine ligands (Type 1) <b>ML1-ML4</b>	67
2.5.2 Multifunctional G1&2 poly (propylene-imine) dendrimeric ligands (Type 2) <b>DL1-DL8</b>	68
2.6 REFERENCES	69

## 2.1 INTRODUCTION TO DI-IMINE LIGANDS

Di-imine ligands are a family of Schiff-base compounds where two or more nitrogen atoms are used as donor sites. Currently there are three well known types of di-imine ligands, which include  $\alpha$  di-imine,  $\beta$  di-imines and  $\gamma$  di-imines (Figure 2.1). Preparation routes to these are similar viz. via Schiff-base condensation of ketones or aldehydes with any primary-amine [1]. Di-imines are well known ligands and have been used as catalyst stabilisers in many catalytic processes such as olefin polymerisation, Heck coupling, Suzuki coupling, olefin oligomerisation and in atom transfer polymerisation [2-8]. They can be complexed to various transition metals to form stable metal complexes which act as active catalysts. Guo *et. al* reported an efficient synthesis, characterisation and application of  $\beta$  di-imines as supporting ligands in the palladium catalysed Suzuki coupling reaction of phenyl bromide and phenyl boronic acid [9]. Powell and co-workers carried out interesting work on the synthesis of thiophene-substituted 1, 4-diazobutadiene ( $\alpha$  di-imine) ligands and their conversion to phosphonium tri-iodide salts [10].

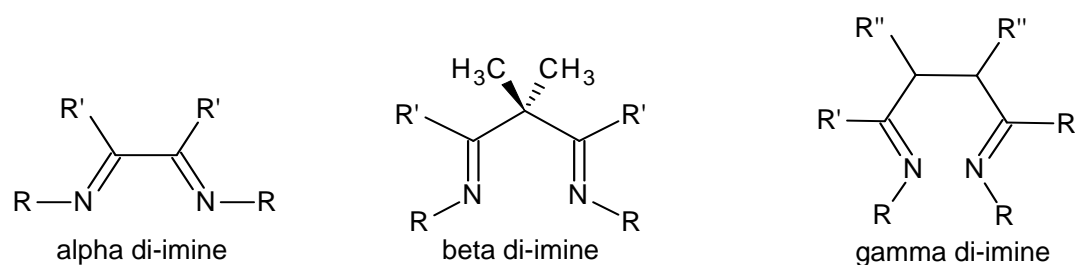
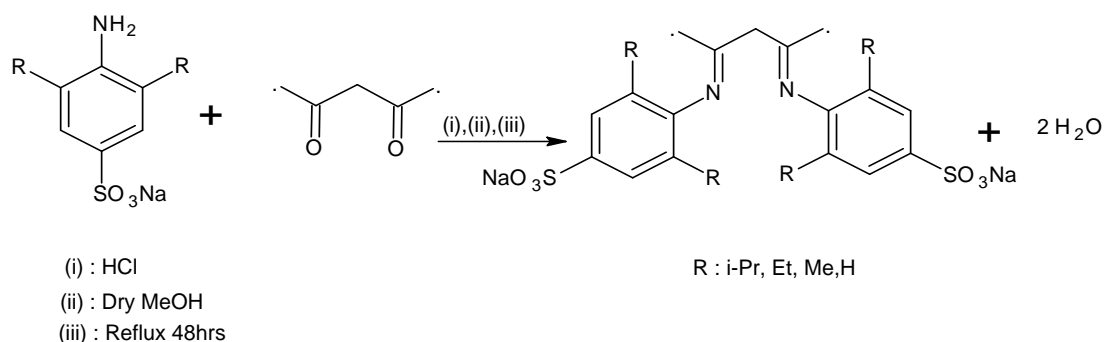
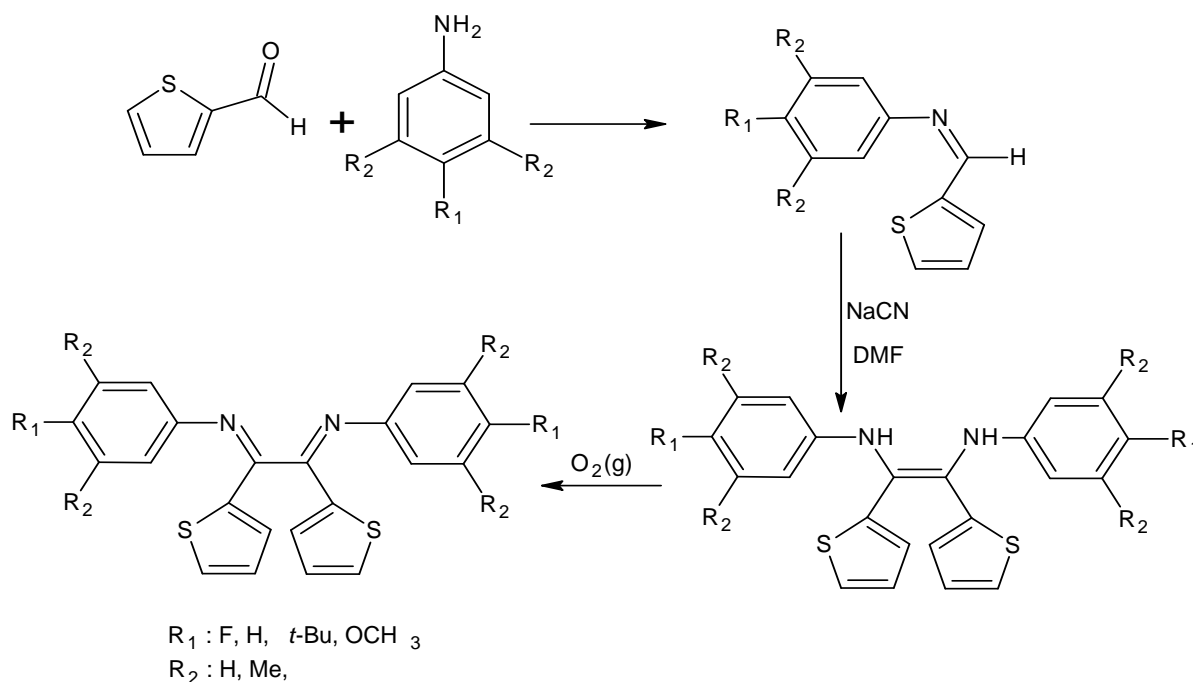


**Figure 2.1:** General structures of three types of di-imine ligands [1].



**Scheme 2.1:** Synthesis of sulfonate  $\beta$  di-imine ligands [9].



**Scheme 2.2:** Synthesis of *N*-aryl-2-thienyl substituted 1, 4-diazabutadiene ( $\alpha$  diimine) ligands [10].

### 2.1.1 Iminopyridyl-imine ligands

A series of *N*-alkyl-(2-pyridyl) methanimines were previously synthesised and characterised by Haddleton and co-workers [2]. This involved Schiff base condensation of ketones or aldehydes with alkyl-amines forming various di-imine ligands with water as a by-product. Several other pyridyl-imine ligands have since been prepared. Copper(I) metal salts have been coordinated to these ligands to form various bis [*N*-alkyl-(2pyridyl) methanimine] copper(I) complexes. Massa *et al* [3], investigated redox properties of  $[\text{Cu}(\text{L}_2)]^+$  and  $[\text{Cu}(\text{L})(\text{PPh}_3)_2]^+$  complexes with systematic variation of aliphatic rings in the iminopyridine ligand (L). A series of di-imine ligands were synthesised which differ in the aliphatic ring substituents (size of ring varies from three to seven).

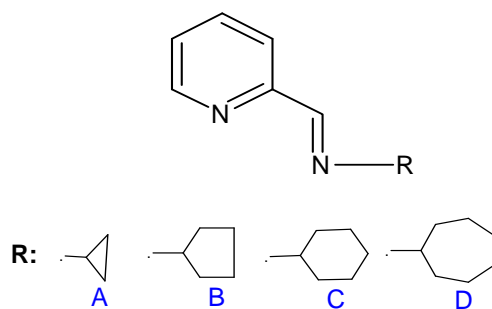
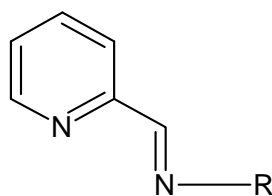


**Figure 2.2:** *Massa's bidentate iminopyridine ligands* [3]

In our group Chen *et al* and Cloete *et al* reported a series of {*N*-alkyl-*N*-[pyridin-2-ylmethylene] di-imine ligands. They claimed that when these ligands were complexed to [bis(acetonitrile)palladium(II) chloride] they form stable complexes with different activity and selectivity due to different ligand environments [4, 5]. Similar work has also been done by Smith *et al* [6] using poly(propylene-imine) dendrimeric ligands. It was noted that their catalysts have higher reaction rates as compared to the analogous mononuclear complexes. An advantage of using dendrimeric ligands is the ability to form multinuclear complexes which promise high activity. An example of this type of dendrimeric ligand is illustrated in Figure 2.4.



- R:**
- A** -CH<sub>2</sub>CH=CH<sub>2</sub>
  - B** -C<sub>6</sub>H<sub>4</sub>CH=CH<sub>2</sub>
  - C** -C<sub>6</sub>H<sub>4</sub>OH
  - D** -C<sub>3</sub>H<sub>7</sub>

**Figure 2.3:** *Monofunctional iminopyridylimine di-imine ligands* [5]



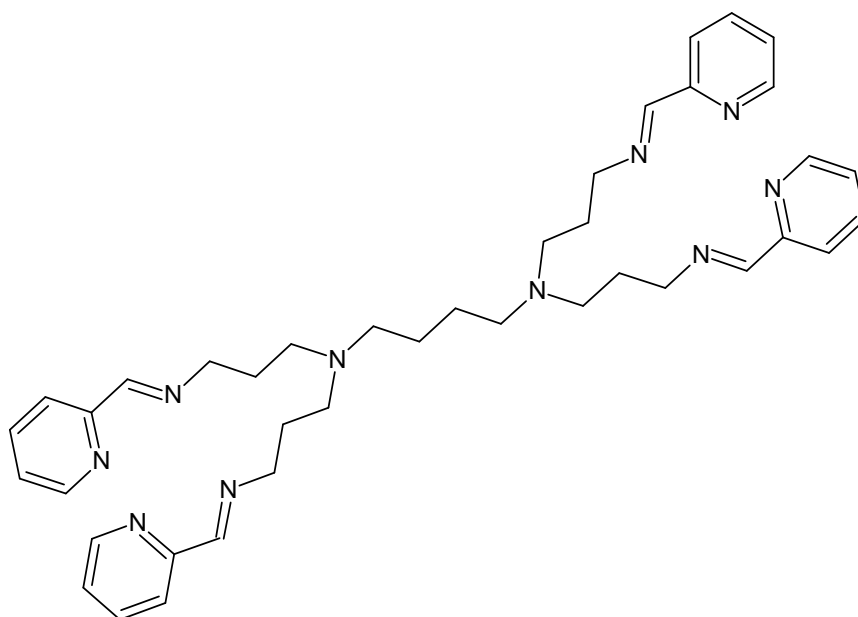


**Figure 2.4:** Multifunctional iminopyridylimine di-imine ligand [6]

### 2.1.2 Iminoquinolyl-imine ligands

These ligands are similar to pyridyl-imine ligands. The only difference is that quinoline is used instead of pyridine. The synthesis of four enantiomerically pure bis-(imine-quinoline) ligands was reported by Prema et al [7]. It was discovered that these ligands tend to favour bis (bidentate) coordination when reacted with  $ZnCl_2$  and their zinc complexes have a single stranded helical motif with M helicity. Amendola also reported similar ligands which they called bis-thio-bis-quinoline ligands [8]. These ligands were complexed with either Cu(I) or Cu(II). The copper complexes were very stable in both solid and solution states. X-ray diffraction and a number of spectroscopic measurements of these complexes revealed that they formed mononuclear species with tetrahedral geometry for Cu(I) and square-planar for Cu(II) around the metal centre [8].

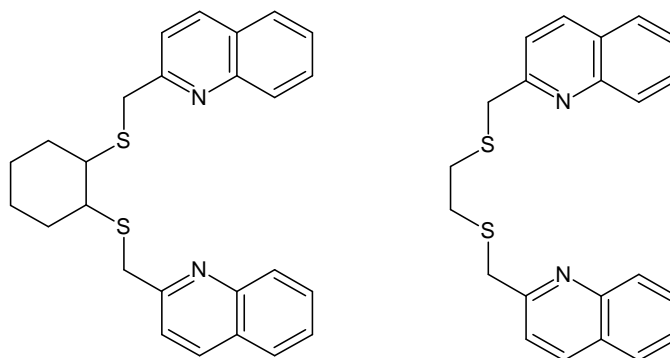
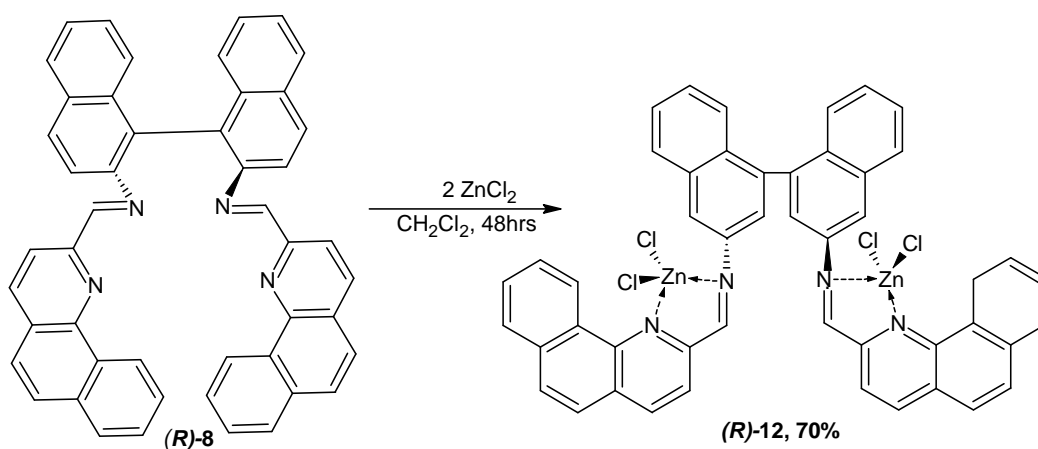


**Figure 2.5:** Bis-thio-bis-quinoline ligands [8]



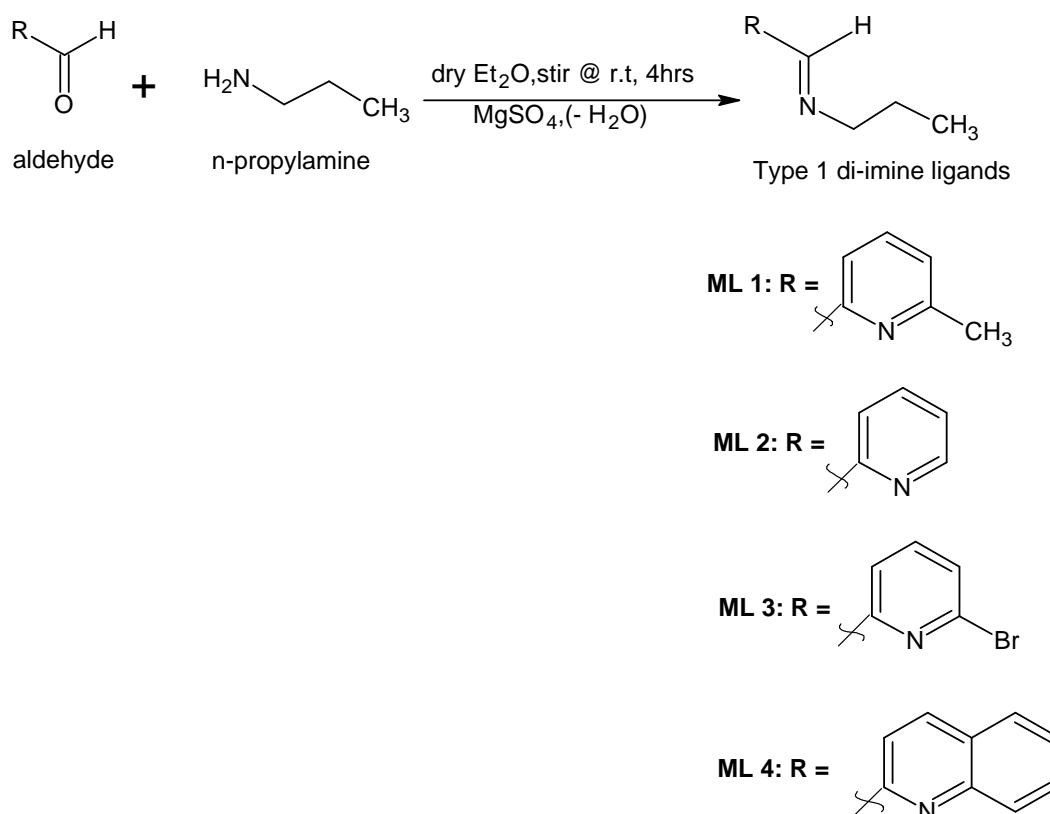
**Scheme 2.3:** Synthesis of the dinuclear Zn(II) dichloride complexes of symmetric Schiff-base with extended quinoline side arms [7].

In this chapter we report the synthesis and characterisation of a series of dendritic iminopyridyl and iminoquinolyl ligands based on polypropylene imine dendrimers with a 1, 4-diaminobutane core (Type 2). Type 1 ligands are the monofunctional analogues based on *N*-propyl-(2-pyridyl) methanimines.

## 2.2 RESULTS AND DISCUSSION

### 2.2.1 Synthesis and characterisation of *N*-(*n*-propyl)-1-(2-pyridyl and quinolyl) imine ligands

The procedure that was used to prepare these ligands is similar to that of Haddleton *et al.* [2], Chen *et al.* [4] and Cloete *et al.* [5]. The synthesis of both pyridyl and quinolyl mono-functionalised ligands was carried out by Schiff base condensation of *n*-propylamine with the corresponding aldehyde in 1:1 ratio with removal of water by using anhydrous magnesium sulphate as shown in Scheme 2.4. After isolation by filtration and reduction of the solvent under vacuum, the pyridylimines (**ML1-ML3**) and quinolylimine (**ML4**) compounds were easily purified by dissolving in diethyl-ether and cooling overnight at  $-5^{\circ}\text{C}$  in order to precipitate out any unreacted aldehyde.



**Scheme 2.4:** Synthesis of monofunctional di-imine ligands (**ML1-ML4**)

All monofunctional ligands were obtained as low viscosity oils in good yields (70-88%), which showed some decomposition when left for prolonged periods at room temperature. However, there was no decomposition at all when the oils were stored at -4°C for extended periods. All the ligands are soluble in common organic solvents such as CH<sub>2</sub>Cl<sub>2</sub>, CHCl<sub>3</sub>, toluene, DMSO, hexane, pentane, CH<sub>3</sub>CN etc. These ligands were fully characterised by <sup>1</sup>H & <sup>13</sup>C-NMR spectroscopy, FT-IR (ATR) spectroscopy, ESI-mass spectrometry and by elemental analysis. Results are shown in Tables 2.1 & 2.3. According to our knowledge, all these ligands are new except for **ML2** which has been already reported by Cloete and co-workers in our group [5].

#### 2.2.1.1 FT-IR spectroscopy

The infra-red spectroscopic investigation of pyridylimine ligands shows three strong bands which appeared at approximately 1647-1650, 1567-1590 and 1550-1573 cm<sup>-1</sup> and were assigned to  $\nu(\text{C}=\text{N})$  vibration and the pyridine-ring  $\nu(\text{C}=\text{N})$  &  $\nu(\text{C}=\text{C})$  vibrations respectively. However, for the quinolyimine ligand (**ML4**) a different infra-red spectrum was obtained which showed strong bands at 1642, 1595 and 1557 cm<sup>-1</sup>, ascribed to  $\nu(\text{C}=\text{N})$  vibration and quinoline-ring  $\nu(\text{C}=\text{N})$  &  $\nu(\text{C}=\text{C})$  vibrations respectively. Table 2.1 indicates  $\nu(\text{C}=\text{N})$  vibrations of the free imine group. These results confirm that the aldehydes have condensed with the amino group of the propylamine chain to form the corresponding imines.

**Table 2.1:** Characterisation data of monofunctional di-imine ligands (**ML1-ML4**)

Mono-functional ligands	Physical Appearance	% Yield	FT-IR (ATR) $\nu$ (C=N) $\text{cm}^{-1}$	Molecular Formula	ESI-MS $[\text{M}+\text{H}]^+$ (m/z) Calculated (Found)	Micro-analysis Calculated (Found)		
						%C	%H	%N
<b>ML1</b>	Colourless oil	70	1651	$\text{C}_{10}\text{H}_{14}\text{N}_2 \cdot 0.26$ $\text{CH}_2\text{Cl}_2$	162.2 (163)	64.01 (64.65)	7.47 (7.16)	11.94 (11.81)
<b>ML2</b>	Pale-yellow oil	86	1651	$\text{C}_9\text{H}_{12}\text{N}_2 \cdot 0.18$ $\text{CH}_2\text{Cl}_2$	148.2 (149)	66.14 (66.63)	7.35 (7.60)	17.15 (17.36)
<b>ML3</b>	Colourless oil	88	1649	$\text{C}_9\text{H}_{11}\text{BrN}_2$	227.1 (229)	47.60 (47.78)	4.85 (4.81)	12.33 (12.02)
<b>ML4</b>	Orange oil	80	1646	$\text{C}_{13}\text{H}_{14}\text{N}_2 \cdot 0.15$ $\text{CH}_2\text{Cl}_2$	198.3 (199)	74.03 (74.75)	6.64 (6.74)	13.29 (13.22)

### 2.2.1.2 *ESI mass spectrometry and elemental analysis*

Electron spray ionisation mass spectrometry is a suitable method for the characterisation for all these monofunctional di-imine ligands. All the mass spectra of these ligands show molecular ion peaks which correlate well with the calculated mono-isotopic molecular mass with an addition of 1 proton as shown in Table 2.1. All mono-functional ligands showed a common peak at  $m/z$  60 which corresponds to the cation of a propylamine chain and the most abundant peak (base peak) correlates well with the parent ion with one hydrogen ion [ $M^+ + H$ ]. The ESI-mass spectrum of **ML2** also showed a peak at  $m/z$  107 which is the result of the dissociation of the propyl chain ( $M^+ - pr$ ). Electron spray ionisation spectra of **ML2**, **ML3** and **ML4** show the presence of a potassium adduct ( $M^+ + K$ ) at  $m/z$  189, 269 and 239 respectively. However, the spectrum of **ML1** shows the presence of a sodium adduct ( $M^+ + Na$ ) at  $m/z$  185. The spectrum of **ML3** shows an isotopic cluster due to the presence of the two isotopes of the bromine ( $^{79}Br$  and  $^{81}Br$ ). The general fragmentation pattern of the mono-functional di-imine ligands (**ML1-ML4**) is presented in Scheme 2.5.

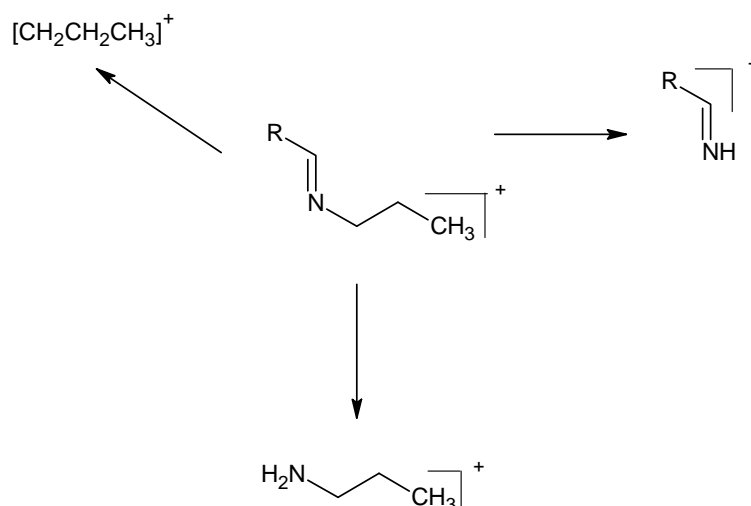
Elemental analysis results are presented in Table 2.1 and they are largely in agreement with the proposed formulations expected although several of them show some evidence of solvent inclusion (DCM) which is also seen in the  $^1H$ -NMR spectra of these compounds. It was difficult to remove residual solvent even under vacuum. These results also reveal that the condensation reaction of propylamine with various aldehydes was successful.

### 2.2.1.3 *$^1H$ & $^{13}C\{^1H\}$ NMR studies of (N-(n-propyl)-1-(2-pyridyl or quinolyl) imine ligands*

All proton NMR spectra of monofunctional di-imine ligands (**ML1-ML4**) show the expected signals for the aliphatic protons in the region  $\delta$  0.93 ppm to  $\delta$  3.65 ppm and the aromatic region protons from  $\delta$  7.16 ppm to  $\delta$  8.65 ppm. The spectra in the aliphatic region show similar trends except for **ML1**. This ligand has a signal at  $\delta$  2.58 ppm corresponding to the three protons (H-10) of methyl substituent at position six of the pyridine ring. The proton NMR results of the monofunctional di-imine ligands are

presented in Table 2.2 and the numbering scheme is illustrated in Figure 2.6 below. H-6 for **ML1** and **ML3** is a doublet as expected for both ligands but that of **ML3** is deshielded because of the influence of the bromide substituent at position six of the aromatic ring. H-9 of the unsubstituted pyridine ligand (**ML2**) is the most deshielded proton ( $\delta$ 8.65 ppm) as compared to the other protons because of the strong influence of the nitrogen of the pyridine ring. Evidence of a condensation reaction is clearly seen in these  $^1\text{H-NMR}$  spectra by a downfield shift of the  $\text{CH}_2$  signals adjacent to the N of the starting propylamine from 3.55 ppm to 3.67 ppm as a result of it now being adjacent to an imine unit. The most significant signal is around  $\delta$ 8.3 ppm (H-4) for pyridine ligands and around  $\delta$ 8.55 ppm for **ML4**. This signal is due to the proton of  $\text{HC=N}$  group which is a result of the condensation reaction.  $^1\text{H-NMR}$  spectra of **ML1&ML4** are illustrated in Figure 2.6.

Further characterisation of the ligands using  $^{13}\text{C-NMR}$  spectroscopy revealed signals for the carbons of the imine functionality between  $\delta$ 159.96-162.64 ppm. Aliphatic carbons are observed up-field as expected ( $\delta$ 11.23-63.71 ppm) and the aromatic carbons are downfield between  $\delta$ 118.70-158.04 ppm as shown in Table 2.3.



**Scheme 2.5:** Possible fragmentation pathway of monofunctional di-imine ligands (**ML1-ML4**).

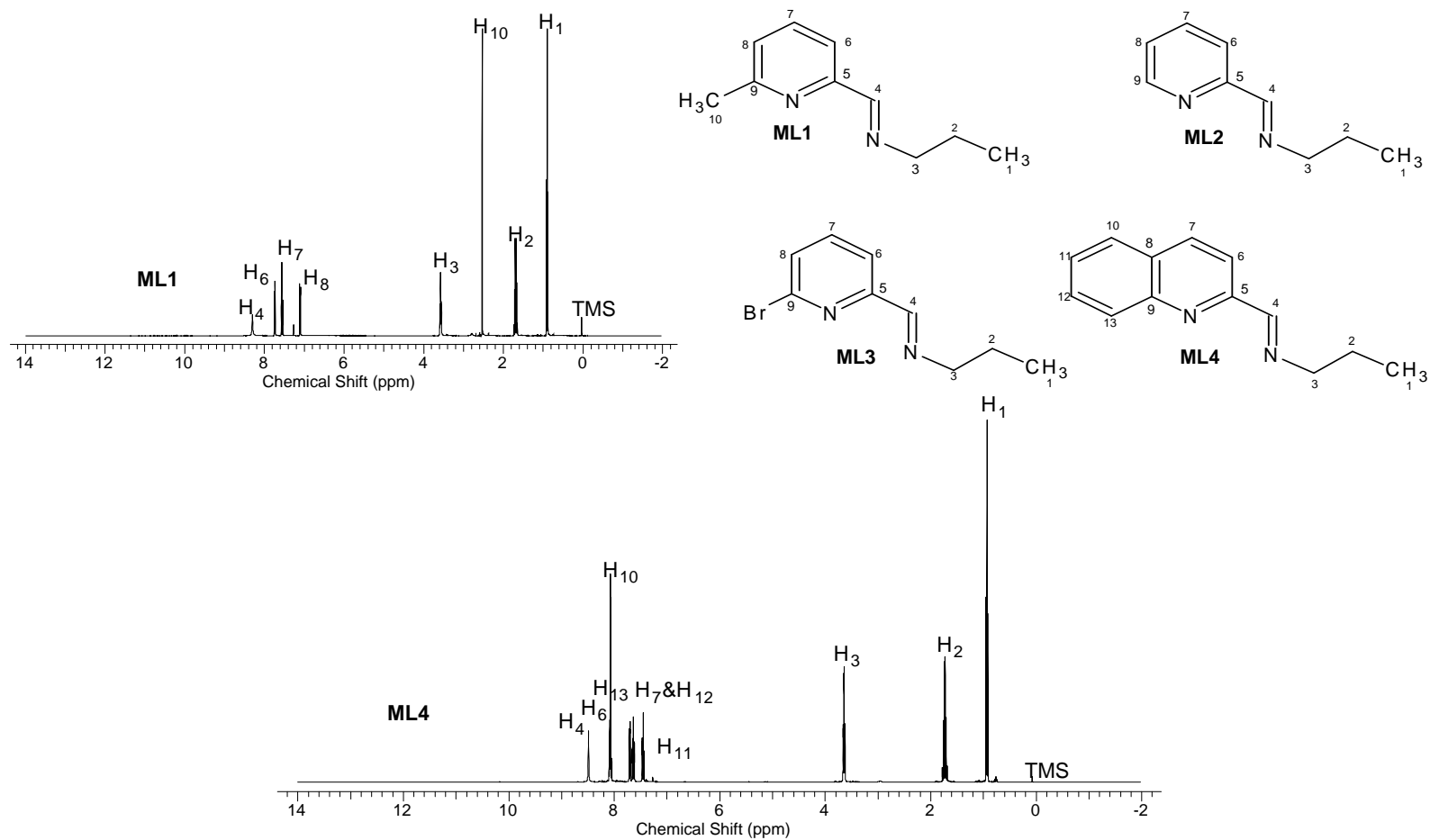


**Figure 2.6:**  $^1\text{H}$ -NMR ( $\text{CDCl}_3$ , 400MHz) spectra of monofunctional di-imine ligands (**ML1**&**ML4**) and the numbering schemes for  $^1\text{H}$  &  $^{13}\text{C}$ -NMR assignments for **ML1-ML4**.



**Table 2.2:**  $^1H$  - Chemical shifts of monofunctional di-imine ligands (**ML1-ML4**)

Compounds	Aliphatic protons $\delta$ (ppm)				Aromatic protons $\delta$ (ppm)								
	H-1	H-2	H-3	H-4	H-6	H-7	H-8	H-9	H-10	H-11	H-12	H-13	CH <sub>3</sub>
<b>ML1</b>	1.06 (t,3H)	1.78 (m,2H)	3.65 (t,2H)	8.38 (s,1H)	7.78 (d,1H)	7.60 (t,1H)	7.16 (d,1H)						2.58 <sup>a</sup> (s,3H)
<b>ML2</b>	0.97 (t,3H)	1.77 (m,2H)	3.65 (t,2H)	8.36 (s,1H)	7.97 (d,1H)	7.74 (t,1H)	7.27 (t,1H)	8.65 (d,1H)					
<b>ML3</b>	0.93 (t,3H)	1.73 (m,2H)	3.61 (t,2H)	8.29 (s,1H)	7.47 (d,1H)	7.58 (t,1H)	7.94 (d,1H)						
<b>ML4</b>	1.00 (t,3H)	1.76 (m,2H)	3.76 (t,2H)	8.55 (s,1H)	8.21 (d,1H)	7.86 (d,1H)			8.12 (d,1H)	7.57 (t,1H)	7.74 (t,1H)	8.16 (d,1H)	

<sup>a</sup> Me-pyr (CH<sub>3</sub>)

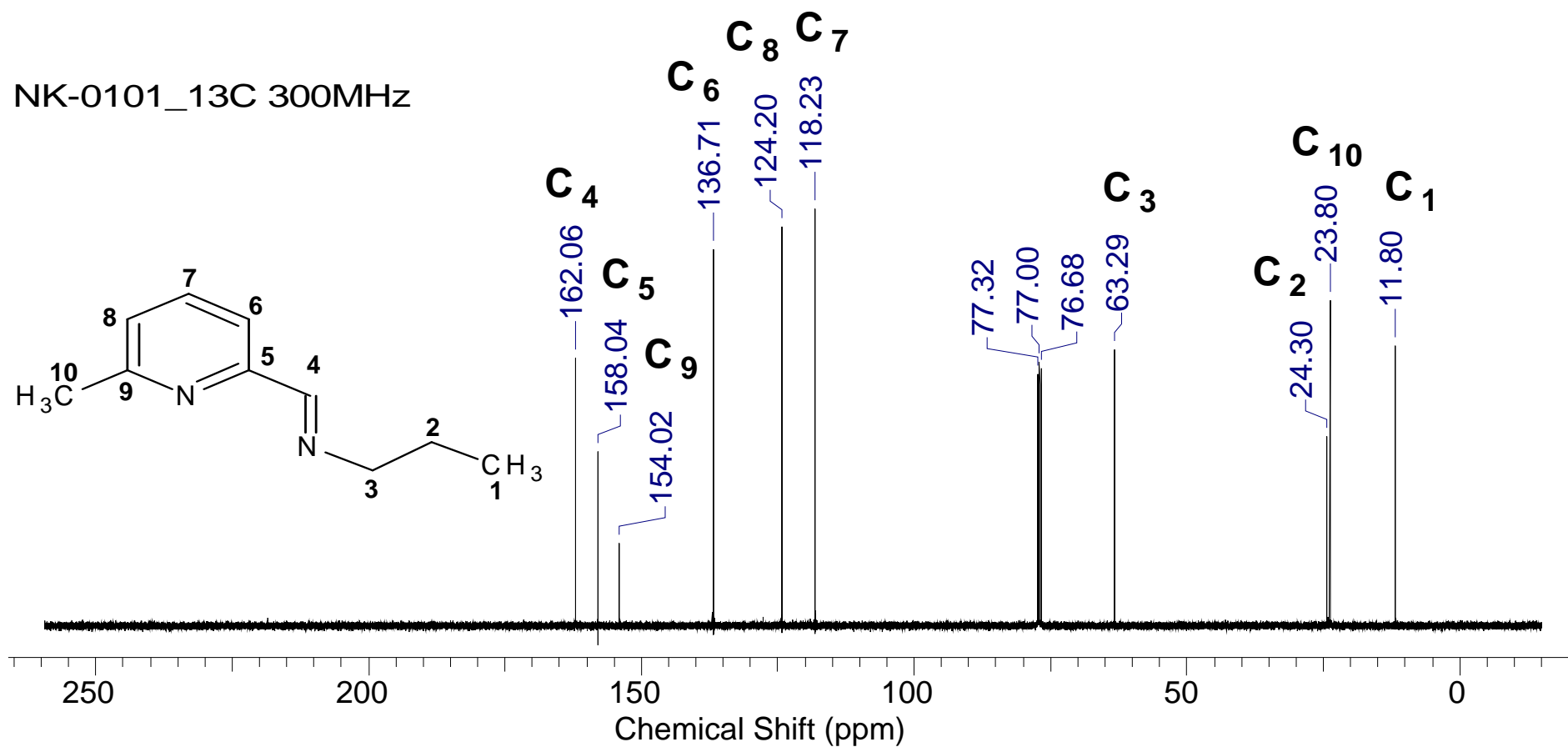


**Figure 2.7:**  $^{13}\text{C}$ -NMR ( $\text{CDCl}_3$ , 400MHz) spectrum of monofunctional Methyl-pyridine ligand (MLI).

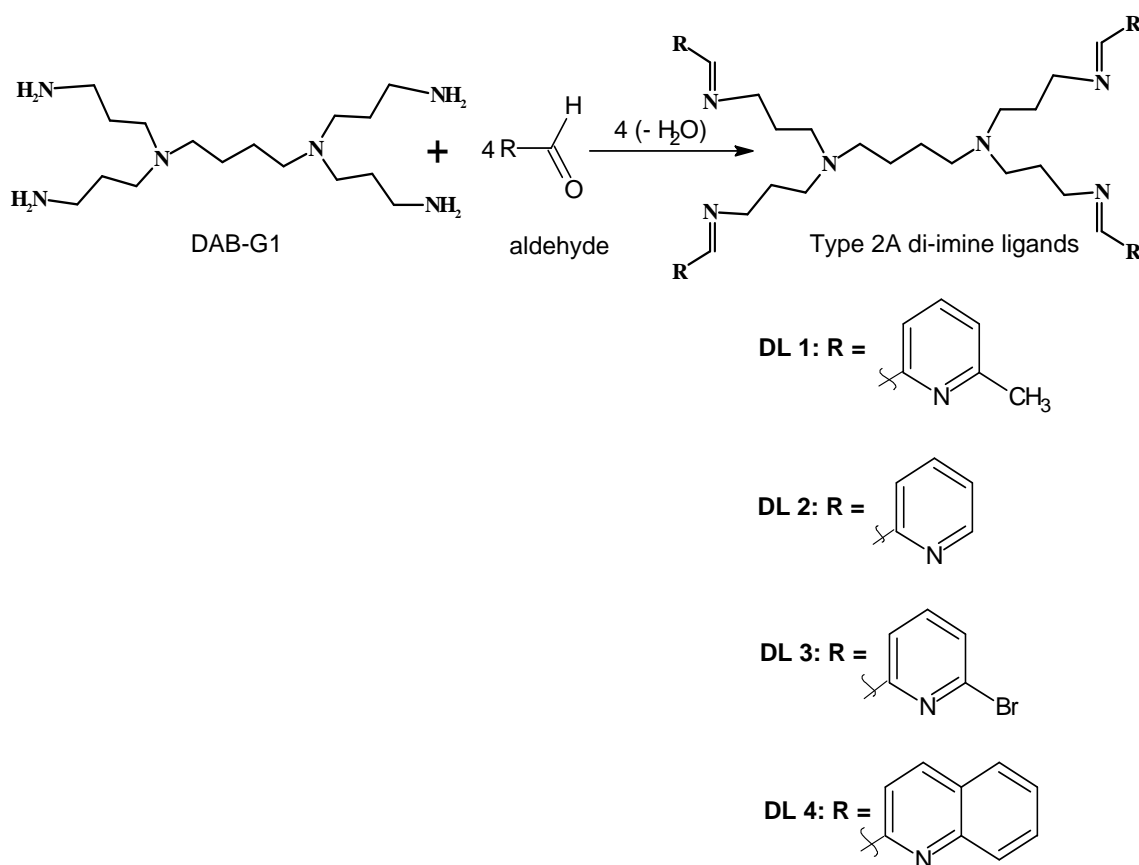
**Table 2.3:**  $^{13}\text{C}$   $\{^1\text{H}\}$  - Chemical shifts of monofunctional di-imine ligands (**ML1-ML4**)

Compounds	Aliphatic carbons $\delta$ (ppm)							Aromatic carbons $\delta$ (ppm)					
	<b>C-1</b>	<b>C-2</b>	<b>C-3</b>	<b>C-4</b>	<b>C-5</b>	<b>C-6</b>	<b>C-7</b>	<b>C-8</b>	<b>C-9</b>	<b>C-10</b>	<b>C-11</b>	<b>C-12</b>	<b>C-13</b>
<b>ML1</b>	11.80	23.80	63.29	162.06	158.04	136.71	118.23	124.20	154.02	24.30 <sup>a</sup>			
<b>ML2</b>	11.65	23.66	63.08	161.53	154.45	136.30	120.98	124.39	149.18				
<b>ML3</b>	11.23	23.28	62.71	159.96	155.32	138.36	119.19	128.52	141.02				
<b>ML4</b>	12.21	24.23	63.71	162.64	155.19	136.38	118.70	127.64	148.08	128.88	129.78	129.99	127.89

<sup>a</sup> Me-pyr (CH<sub>3</sub>)

### 2.2.2 Synthesis and characterisation of [G-1&2 DAB-dendr-(NH<sub>2</sub>)-1-(2-pyridyl and quinolyl)-imine ligands.

The preparation of generation 1 (**DL1-DL4**) and generation 2 (**DL5-DL8**) dendrimeric *N, N'* donor ligands was performed using the method by Smith *et al.* [6, 9] and Malgas *et al.* [12, 13]. The ligands were synthesised via Schiff base condensation of the 1, 4-diaminobutane poly (propylene-imine) dendrimer [DAB-(NH<sub>2</sub>)<sub>n</sub>] (*n* = 4 or 8) with an appropriate aldehyde. The ratio of [DAB-(NH<sub>2</sub>)<sub>n</sub>] to aldehyde was 1:4 for **DL1-DL4** and 1:8 for **DL5-DL8**. The preparation of generation-1 dendrimeric ligands is illustrated in Scheme 2.6 and the general structures of generation 2 dendrimeric ligands are shown in Figure 2.8.



**Scheme 2.6:** Synthesis of multifunctional di-imine ligands (**DL1-DL4**)

Preparation of the dendrimeric ligands (**DL1-DL8**) was carried out over an extended period of time to ensure complete modification of peripheral amino groups of the PPI dendrimer with the corresponding aldehyde. All these ligands were isolated as crude oily products which were all washed extensively with a large excess of de-ionised water to remove any unreacted DAB G1 or G2. In the case of **DL3**, a pure white solid product was obtained by recrystallization from  $\text{CH}_2\text{Cl}_2$ : hexane mixture at  $-5^\circ\text{C}$ . **DL4** was purified by refluxing in hot pentane at  $36^\circ\text{C}$  resulting in the isolation of a yellow solid from the original oily residue. The work-up used for **DL4** was also employed in attempting to purify other ligands but in these cases the products were obtained as pure oils.

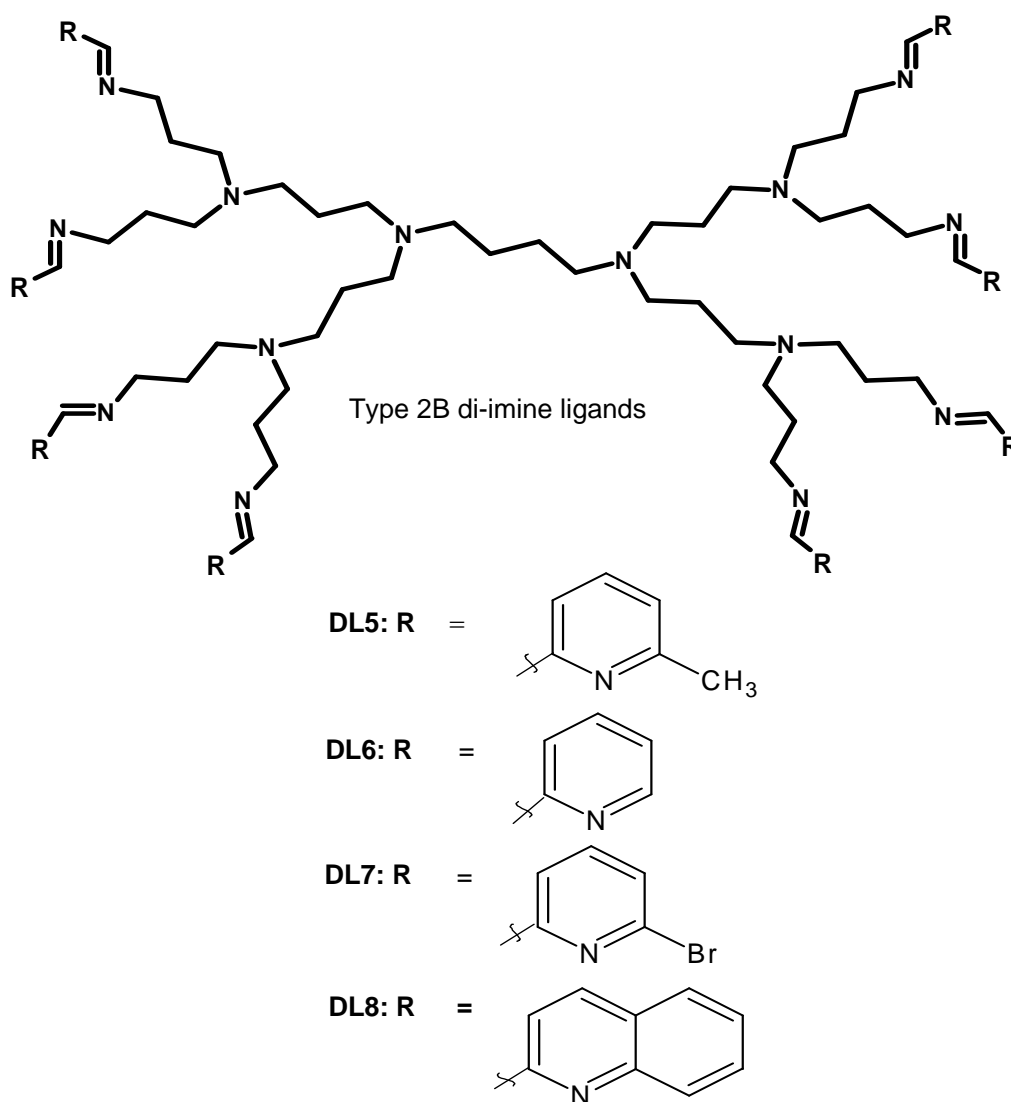


**Figure 2.8:** G2 dendrimeric *N,N'* donor ligands [**DL5-DL8**]

As far as we are aware all 6 dendrimeric ligands (**DL1**, **DL3-DL5**, **DL7 & DL8**) are new and are now reported here for the first time. Ligands (**DL2 & DL6**) were previously published by Smith and co-workers [6, 9]. The two solid ligands are very stable compounds at room temperature and the oils were stored at  $-5^{\circ}\text{C}$  to reduce any decomposition. These ligands were soluble in most common polar solvents such as  $\text{CH}_2\text{Cl}_2$ ,  $\text{CHCl}_3$ , THF,  $\text{Et}_2\text{O}$ ,  $\text{CH}_3\text{CN}$  and the non-polar solvent toluene but the quinolyl and Br-pyridyl ligands were not soluble in  $\text{CH}_3\text{CN}$ . All these functionalised dendrimeric ligands were fully characterised by  $^1\text{H}$  &  $^{13}\text{C}$ -NMR spectroscopy, FT-IR spectroscopy, ESI-mass spectrometry and elemental analysis as shown in Tables 2.4-2.7.

#### 2.2.2.1 *FT-IR spectroscopy*

Infra-red spectra of dendritic ligands were obtained using an ATR accessory. The  $\nu(\text{C}=\text{N})$  stretching modes for the pyridyl-imines are observed around  $1650\text{ cm}^{-1}$  and for quinolylimines around  $1642\text{ cm}^{-1}$  (Table 2.4). In the case of the pyridine based ligands this is consistent with the data obtained for monofunctional ligands. For quinoline based ligands this is significantly lower than what was observed for monofunctional ligands because of a huge amount of electron delocalisation around the quinoline ring.

The infra-red investigation of pyridylimine ligands shows three strong bands which appeared in the regions  $1647\text{-}1650$ ,  $1567\text{-}1590$  and  $1550\text{-}1573\text{ cm}^{-1}$ , assigned to imine  $\nu(\text{C}=\text{N})$  vibrations and pyridine-ring  $\nu(\text{C}=\text{N})$  &  $\nu(\text{C}=\text{C})$  vibrations respectively. However, for the quinolylimine ligands (**DL4 & DL8**) different infra-red spectra were obtained which show strong bands in the range  $1642\text{-}1644$ ,  $1595\text{-}1596$  and  $1557\text{-}1561\text{ cm}^{-1}$ , ascribed to  $\nu(\text{C}=\text{N})$  vibration of the imine functionality and quinoline-ring  $\nu(\text{C}=\text{N})$  &  $\nu(\text{C}=\text{C})$  vibrations respectively. Table 2.4 shows the  $\nu(\text{C}=\text{N})$  vibration of the isolated imine i.e. the non-ring  $\text{C}=\text{N}$  bonds. These results confirm that the aldehydes have condensed with the amino groups on the periphery of the dendrimer forming the corresponding imines. Elemental analysis results are presented in Table 2.4, which also indicate that the condensation reaction of the dendrimer (DAB-G1 or G-2) with various aldehydes was successful because some of the results correspond well with the expected molecular formula of the ligands with solvent inclusion.

**Table 2.4:** Characterisation data of multifunctional dendrimeric di-imine ligands (**DL1-DL8**)

Dendrimeric ligands	Physical Appearance	% Yield	FT-IR (ATR) $\nu_{\text{C=N}}$ $\text{cm}^{-1}$	ESI-MS $[\text{M+H}]^+$ (m/z) Calculated (Found)	Molecular Formula	Micro-analysis Calculated (Found)		
						%C	%H	%N
<b>DL1</b>	Colourless oil	76	1648	729 (730)	$\text{C}_{44}\text{H}_{60}\text{N}_{10} \cdot 0.25 \text{CH}_2\text{Cl}_2$	70.87 (70.19)	8.07 (8.24)	18.69 (19.10)
<b>DL2</b>	Yellow oil	71	1648	672 (673)	$\text{C}_{40}\text{H}_{52}\text{N}_{10} \cdot 0.3 \text{CH}_2\text{Cl}_2$	68.82 (68.88)	7.46 (7.65)	20.07 (19.79)
<b>DL3</b>	White solid	91	1651	988 (989)	$\text{C}_{40}\text{H}_{48}\text{Br}_4 \text{N}_{10}$	48.60 (49.00)	4.89 (5.47)	14.17 (14.59)
<b>DL4</b>	Yellow solid	90	1643	873 (874)	$\text{C}_{56}\text{H}_{60}\text{N}_{10} \cdot 0.2 \text{CH}_2\text{Cl}_2$	75.86 (75.70)	6.79 (7.06)	15.75 (16.37)
<b>DL5</b>	Colourless oil	95	1648	1598 (1599)	$\text{C}_{96}\text{H}_{136}\text{N}_{22} \cdot 0.5 \text{CH}_2\text{Cl}_2$	70.72 (70.25)	8.37 (8.65)	18.81 (19.48)
<b>DL6</b>	Deep-yellow oil	89	1648	1486 (1487)	$\text{C}_{88}\text{H}_{120}\text{N}_{22} \cdot 0.5 \text{CH}_2\text{Cl}_2$	69.62 (69.61)	7.93 (8.13)	20.13 (20.58)
<b>DL7</b>	Deep-orange oil	88	1649	2117(1086 <sup>a</sup> )	$\text{C}_{88}\text{H}_{112}\text{Br}_8 \text{N}_{22}$	49.92 (49.98)	5.33 (5.71)	14.55 (15.64)
<b>DL8</b>	Colourless oil	93	1644	1886 (944 <sup>a</sup> )	$\text{C}_{120}\text{H}_{136}\text{N}_{22} \cdot 2 \text{CH}_2\text{Cl}_2$	71.28 (71.79)	6.82 (7.15)	14.99 (16.03)

<sup>a</sup> Doubly charged parent ion.

### 2.2.2.1 $^1\text{H}$ & $^{13}\text{C}\{^1\text{H}\}$ -NMR studies of dendrimeric ligands (**DL1-DL8**)

Both proton and carbon-13 nuclear magnetic resonance spectra of the dendritic ligands were obtained in deuterated chloroform. The spectra of these ligands revealed the symmetric nature of the dendritic structures and the data obtained are shown in Tables 2.6 & 2.7. Both dendrimeric DAB generation 1 and 2 di-imine ligands (**DL1-DL8**) show similar trends especially for the aliphatic protons of the core as well as the arms of the dendrimer. For these ligands, evidence of successful Schiff base condensation is noted by the presence of the  $\text{H-C=N}$  (H-6, G1/H-9, G2) signal around  $\delta$ 8.3 ppm for those ligands that are based on pyridine and around  $\delta$ 8.55 ppm for those ligands based on quinoline. There is also another significant shift that relates to condensation products. Around 3.7 ppm there is a signal due to  $\text{CH}_2$  (H-5, G1/H-8, G2) groups adjacent to the imine moieties ( $=\text{N-CH}_2$ ). The proton signals for internal branches of the dendrimer are seen between  $\delta$ 1.41-3.8 ppm and these results correlate well with previous results in our group by Smith *et al.*[6,9], van Wyk *et al* [14] and Malgas *et al.*[12,13]. The protons assigned to the aryl pyridine and quinoline units are observable downfield between  $\delta$ 7.25-8.12 ppm as expected. In the case of G2 ligands (**DL5-DL8**) we observe an overlapping of the signals for H-3 with H-6 and of H-4 with H-7 because of their similar chemical environment.

Similar to the proton NMR data, Carbon 13 data also confirms the symmetrical nature of the dendritic ligands. Carbon 13 nuclear magnetic resonance spectra correlate well with the expected results for all the multifunctional dendrimeric ligands (**DL1-DL8**). All the chemical shifts for G1 & G2 can be assigned to their appropriate carbons, the six carbons of the dendritic core framework region are observable around  $\delta$ 21-59 ppm and those of the aromatic region are clearly seen at around  $\delta$ 117-157 ppm. Carbon 12/15 i.e. the methyl substituent at position six of the pyridine ring (**DL1 & DL5**) overlaps with carbon 2 ( $\text{CH}_2$ ) of the dendritic side arm ( $\text{CH}_2$ :  $\delta$ 24.27ppm and  $\text{CH}_3$ :  $\delta$ 24.53 ppm). The carbon signal for the  $\text{HC=N}$  group appeared approximately at  $\delta$ 162 ppm for all of the compounds. These results are tabulated in Table 2.7



### 2.2.2.2 ESI mass spectrometry

Further characterisation of dendrimeric ligands was done by using electron spray ionization mass spectrometry which confirmed the molecular mass of the expected compounds (**DL1-DL8**). The spectra of these ligands show intense peaks which are due to multiply charged parent ions, especially for generation 2 dendrimeric ligands (**DL5-DL8**). **DL5** also shows this phenomenon with the parent ion peak  $[M+H]^+$  at  $m/z$  1599 but the base peak at  $m/z$  800 correlates well with a doubly charged parent ion. The spectrum also shows a triply charged parent ion at  $m/z$  533 which is also observable in the ESI mass spectra of other G2 dendrimeric di-imine ligands. The fragmentation pathway of this compound (**DL5**) is shown in Scheme 2.7 and its corresponding mass spectrum is shown in Figure 2.9. The spectrum of **DL7** shows a peak at 1058  $m/z$  which is also due to a doubly charged parent ion, the spectrum of this compound is very complex because of the isotopic cluster due to two bromine isotopes as discussed previously for the mass spectrum of **ML3**. The fragmentation pathway of this compound is shown in Scheme 2.6 which is similar to that of **DL7**. The latter also shows a peak at  $m/z$  706 which is attributed to triply charged parent ion.

All the electron spray ionisation mass spectra of the di-imine ligands show the expected parent ion and the results can be accounted for (Table 2.1) and are consistent with those reported for other dendrimeric ligands by van Wyk *et al* [14].

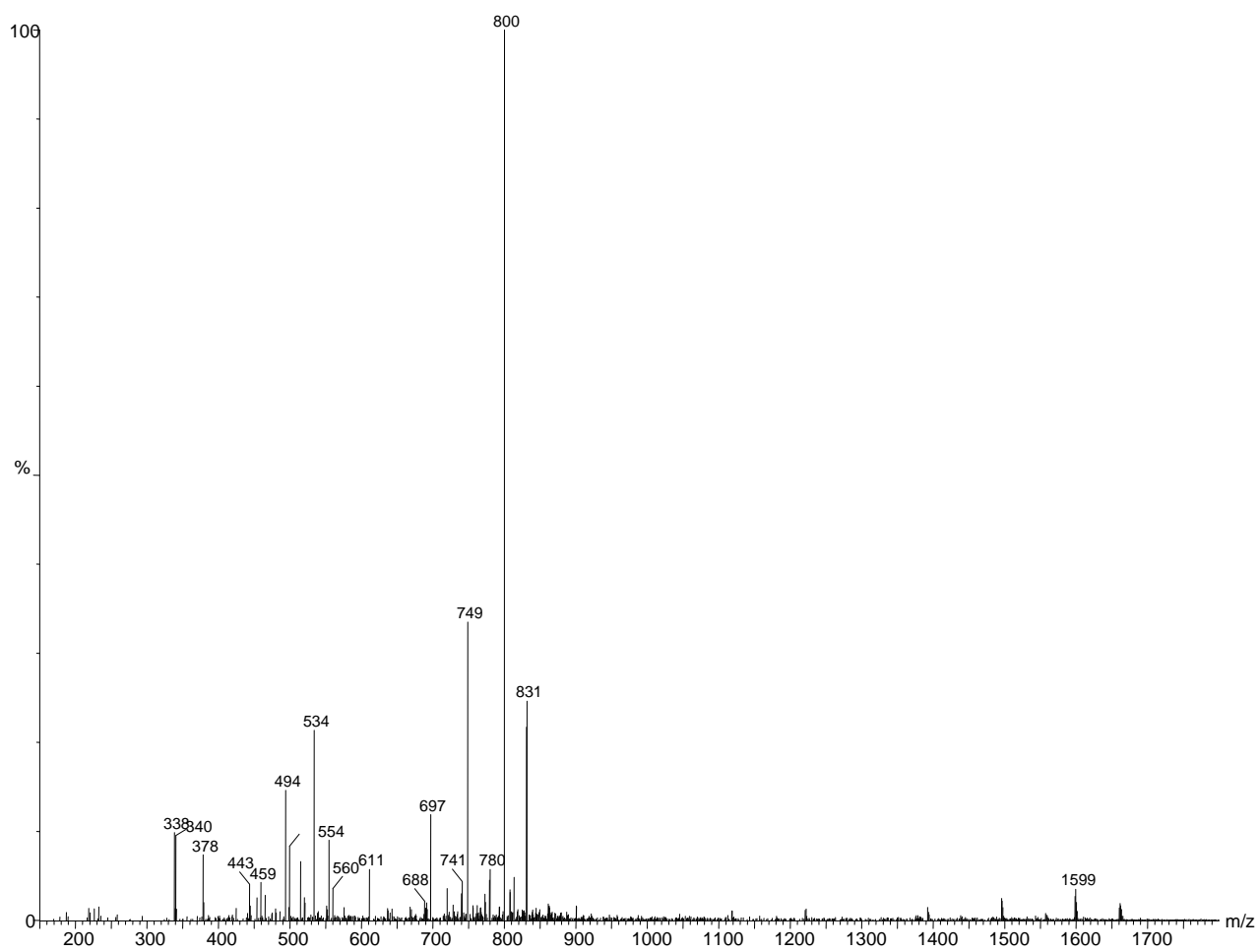
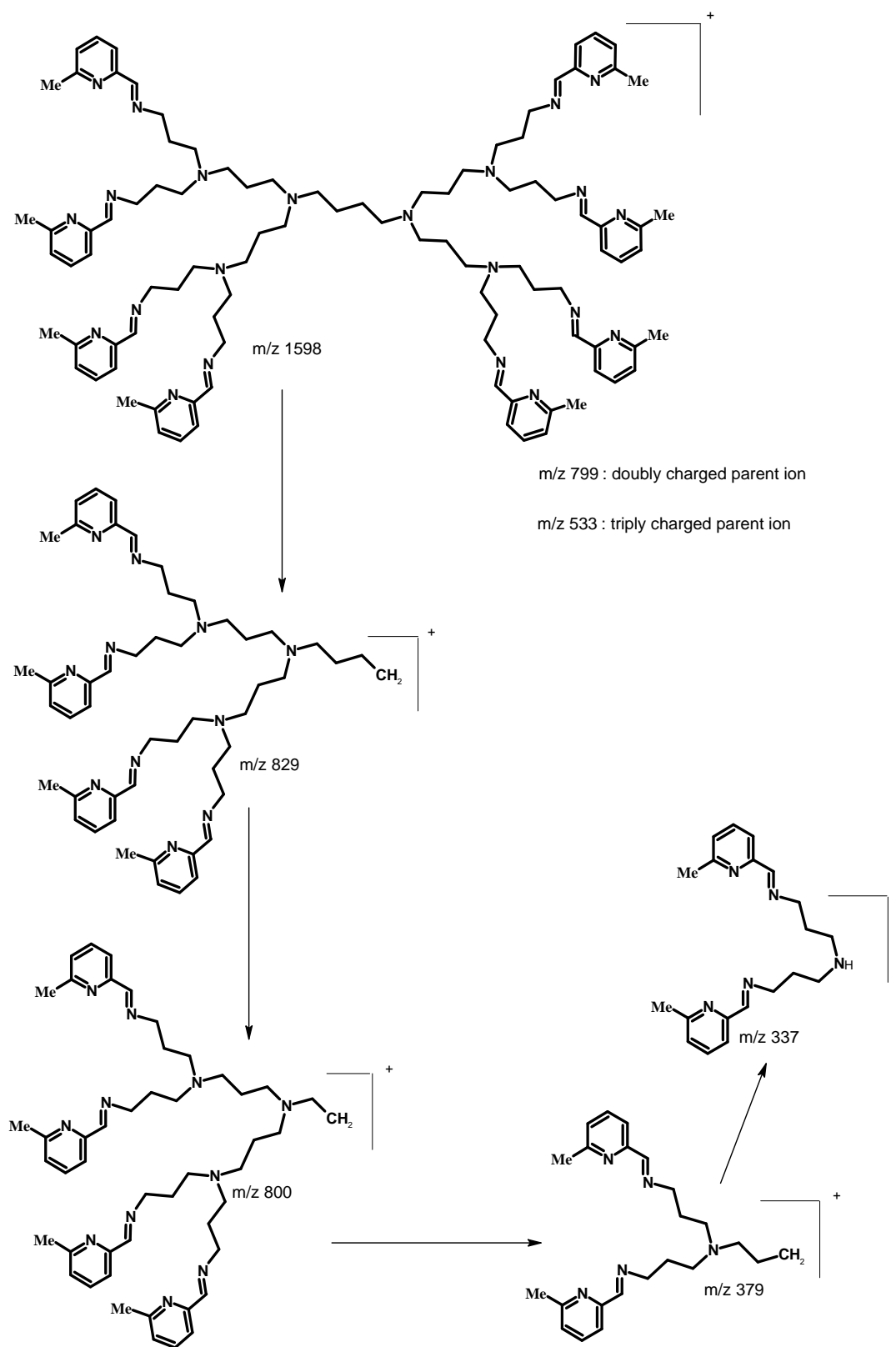


**Figure 2.9:** ESI mass spectrum of DL5



**Scheme 2.7:** Fragmentation pathway of DL5

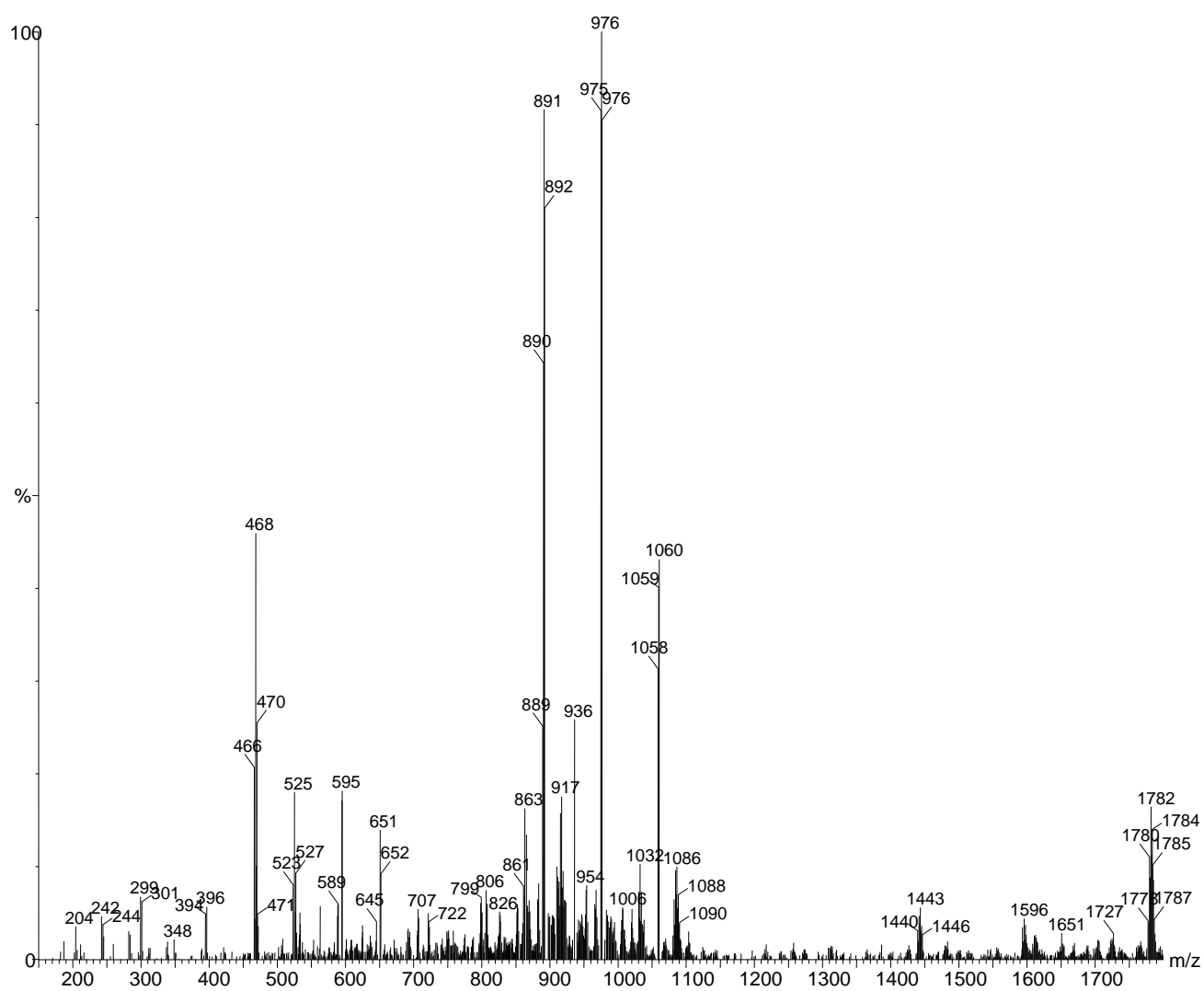
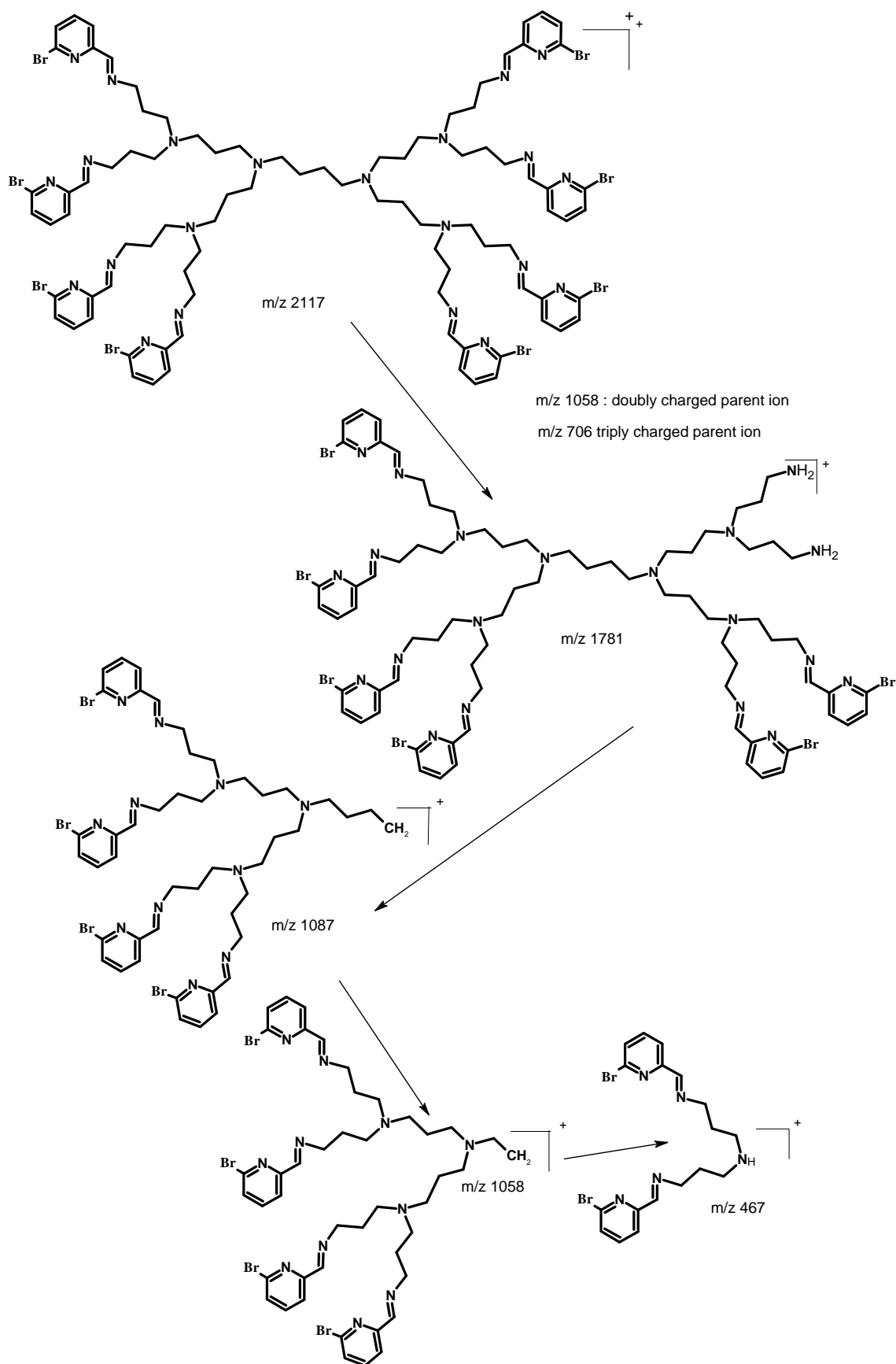
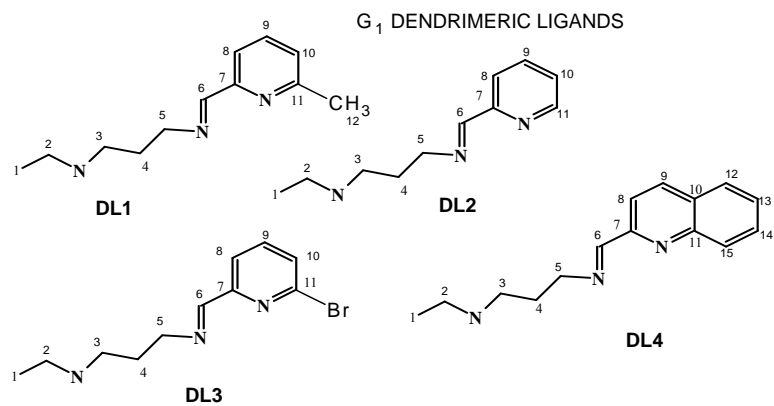


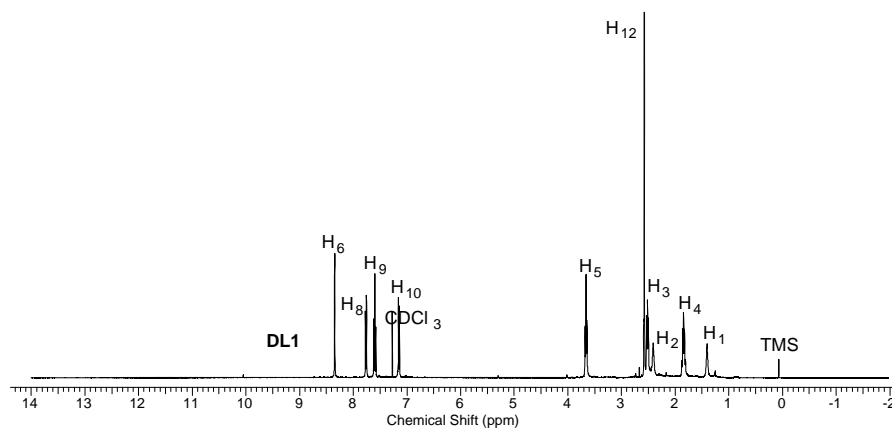
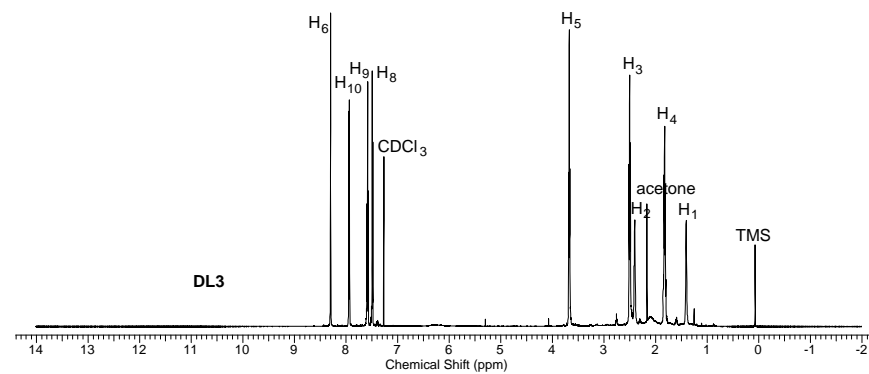
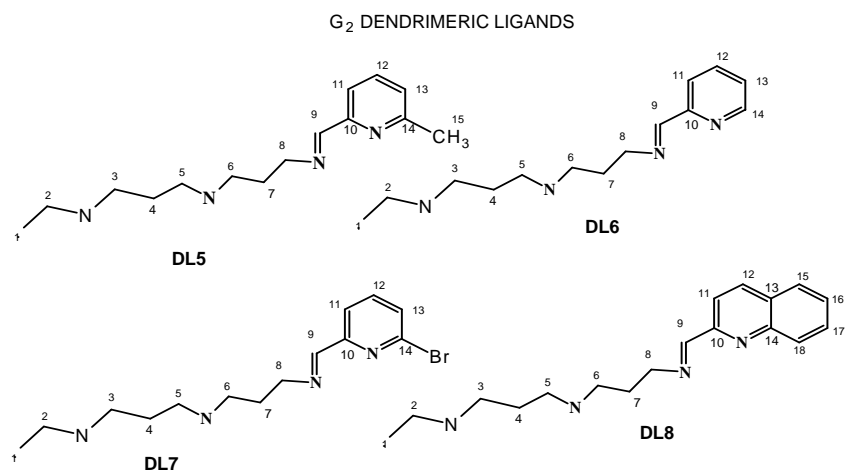
**Figure 2.10:** ESI mass spectrum of DL7



Scheme 2.8: Fragmentation pathway of DL7



**NB: Only shows arms and the first two carbons of the dendrimeric core .**



**Figure**

**2.11:**  $^1\text{H-NMR}$  ( $\text{CDCl}_3$ , 400MHz) spectrum of generation-1 multifunctional di-imine ligands (**DL1&DL3**) and the numbering system for  $^1\text{H}$  &  $^{13}\text{C-NMR}$  assignments.

**Table 2.5:** <sup>1</sup>H- Chemical shifts of multifunctional dendrimeric ligands (DL1-DL4)

Protons	DL1	DL2 <sup>a</sup> (ppm)	DL3	DL4
H-1	1.54 (m,4H)	1.4 (m,4H)	1.41 (m,4H)	1.45 (m,4H)
H-2	2.65 (t,4H)	2.42 (t,4H)	2.40 (t,4H)	2.44 (t,4H)
H-3	2.71 (t,8H)	2.53 (t,8H)	2.50 (t,8H)	2.56 (t,8H)
H-4	1.97 (qn,8H)	1.85 (qn,8H)	1.83 (qn,8H)	1.89 (qn,8H)
H-5	3.79 (t,8H)	3.68 (t,8H)	3.68 (t,8H)	3.76 (t,8H)
H-6	8.46 (s,4H)	8.36 (s,4H)	8.30 (s,4H)	8.55 (s,4H)
H-8	7.89 (d,4H)	7.95 (d,4H)	7.50 (d,4H)	8.11 (d,4H)
H-9	7.71 (t,4H)	7.71 (t,4H)	7.59 (t,4H)	8.09 (d,4H)
H-10	7.25 (d,4H)	7.29 (t,4H)	7.93 (d,4H)	
H-11		8.63 (d,3H)		
H-12	2.54 (s,3H) <sup>a</sup>			7.73 (d, 4H)
H-13				7.70 (t,4H)
H-14				7.53 (t,4H)
H-15				8.12 (d, 4H)

<sup>a</sup> Me-pyr (CH<sub>3</sub>)

**Table 2.6:**  $^1\text{H}$ - Chemical shifts of multifunctional dendrimeric ligands

Protons	DL5	DL6 (ppm)	DL7	DL8
H-1	1.49(m,4H)	1.36(m,4H)	1.38(m,4H)	1.38(m,4H)
H-2	2.51(t,4H)	2.41(t,4H)	2.39(t,4H)	2.41(t,4H)
H-3&6	2.64(t,24H)	2.52(t,24H)	2.51(t,24H)	2.56(t,24H)
H-4&7	1.69 (qn,24H)	1.84(qn,24H)	1.82(qn,24H)	1.88(qn,24H)
H-5	1.96(qn,24H)	1.57(qn,24H)	1.58(qn,24H)	1.59(qn,24H)
H-8	3.77 (t,16H)	3.58(t,16H)	3.49(t,16H)	3.73(t,16H)
H-9	8.46(s,8H)	8.36(s,8H)	8.29(s,8H)	8.52(s,8H)
H-11	7.89(d,8H)	7.96(d,8H)	7.49(d,8H)	8.12 (d,8H)
H-12	7.71(t,8H)	7.70(t,8H)	7.58(t,8H)	8.09(d,8H)
H-13	7.25(d,8H)	7.28(t,8H)	7.95(d,8H)	
H-14		8.61(d,8H)		
H-15	2.69 <sup>a</sup> (s,8H)			7.73(d,8H)
H-16				7.71(t,8H)
H-17				7.53(t,8H)
H-18				8.13(d,8H)

<sup>a</sup> Me-pyr ( $\text{CH}_3$ )



**Table 2.7:**  $^{13}\text{C}$   $\{^1\text{H}\}$  - Chemical shifts of multifunctional dendrimeric ligands (**DL1-DL8**)

Compounds	Aliphatic carbons (ppm)								Aromatic carbons (ppm)							
	C-1	C-2	C-3	C-4	C-5	C-6	C-7	C-8	C-9	C-10	C-11	C-12	C-13	C-14	C-15	C-16
<b>DL1</b>	24.27	24.59	28.20	51.67	52.24	59.54	162.04	118.21	124.07	136.57	153.96	157.86	54.13			
<b>DL2</b>	22.68	25.53	28.62	52.05	54.42	59.94	162.23	121.55	124.92	136.84	149.73	154.97				
<b>DL3</b>	22.56	24.75	27.75	51.18	53.62	58.99	160.09	119.18	128.53	138.37	141.04	155.31				
<b>DL4</b>	21.98	25.21	28.20	51.67	54.08	59.59	162.44	118.33	127.26	136.48	147.68	129.36	129.54	127.63	128.78	154.76
<b>DL5</b>	24.27	24.59	28.20	51.67	52.24	59.54	162.04	118.21	124.07	136.57	153.96	157.86				
<b>DL6</b>	23.43	24.28	28.17	51.66	53.13	59.54	161.80	121.17	124.51	136.45	149.30	154.53				
<b>DL7</b>	23.44	25.20	28.16	51.64	53.03	59.44	160.48	119.63	128.97	138.80	141.46	155.71				
<b>DL8</b>	22.01	24.92	27.82	51.27	52.76	59.20	161.95	117.93	127.20	135.99	147.26	128.95	129.13	127.46	128.80	154.36

## 2.3 CONCLUDING REMARKS

In this chapter we have fully discussed the synthesis of two types of *N, N'* donor ligands, whereby Type 1 are the monofunctional di-imine ligands (Scheme 2.4) and Type 2 are the multifunctional (dendrimeric) di-imine ligands (Scheme 2.6 and Figure 2.8). Type 1 di-imine ligands have been easily synthesised from the reaction of *n*-propylamine with various types of aldehydes via a Schiff base condensation. The Type 2 di-imine ligands are synthesised in a similar way by reaction of [DAB-(NH<sub>2</sub>)<sub>*n*</sub>] polypropylene-imine (PPI) dendrimers with similar aldehydes. Most of these ligands were isolated as oils in very good yields (70%-95%). These compounds showed some decomposition when left at room temperature for prolonged periods. Type 1 ligands (**ML1-ML4**) were purified by addition of Et<sub>2</sub>O to precipitate out all the unreacted aldehyde, whereas Type 2 ligands (**DL1-DL8**) were just refluxed in hot pentane. Dendrimeric ligands were further purified by washing with de-ionised water. The ligands (**DL1-DL8**) were characterised using a number of spectroscopic methods. All of the results correlate well with the expected structure of the condensation products. From the results and the discussion of this chapter we can conclude that we have successfully synthesised and characterised 12 di-imine ligands, nine of which are new.

## 2.4 EXPERIMENTAL SECTION

### 2.4.1 *General Remarks*

All manipulations involving air-sensitive and/or moisture-sensitive compounds were performed in a nitrogen-filled glove box or under an atmosphere of purified dry nitrogen using standard Schlenk techniques. IR spectra were recorded as oils or solids by using ATR on a Nicolet Aneta 330 FT-IR spectrometer. NMR spectra were recorded on a Varian Unity Inova instrument (<sup>1</sup>H at 300/400/600 MHz, <sup>13</sup>C at 75 MHz). Chemical Shifts are reported in ppm and referenced to residual proton and carbon signals (7.25 and 77ppm) for CDCl<sub>3</sub> respectively. (+ESI) mass spectrometric characterisation was done using a Waters API Quattro Micro instrument with direct injection of DCM solutions, MS settings were as follows: capillary voltage 3.5Kv, cone voltage 15 RF1 40, cone gas 50L/h, desolvation temperature 400°C and

desolvation gas 500L/h. Elemental analyses were done at the Micro-analytical laboratory of the Chemistry Department at University of Cape Town.

## 2.4.2 Materials

All solvents were purchased from Aldrich or Kimix Chemicals (South Africa), and they were refluxed over appropriate drying agents and distilled prior to use: diethyl ether and toluene over sodium wire and benzophenone, dichloromethane and acetonitrile over phosphorous pentoxide, hexane and pentane over sodium wire. All the various aldehydes: 2-pyridinecarboxyaldehyde, 2-quinolinecarboxyaldehyde, 6-bromo-2-pyridinecarboxyaldehyde and 6-methyl-2-pyridinecarboxyaldehyde were purchased from Sigma-Aldrich together with n-propylamine. G1 and G2 poly(propylene-imine) DAB-cored dendrimers were purchased from SymoChem in the Netherlands. All the aldehydes and amines were used without any further purification.

## 2.5 Synthesis of N, N' donor ligands

### 2.5.1 *Monofunctional di-imine ligands (type 1) ML1-ML4*

All monofunctional ligands were prepared using a similar procedure that was described by Haddleton et al [2], Chen et al [4] and Cloete et al [5]. The appropriate amount of aldehyde was transferred into a 100 ml Schlenk tube. **ML1**:6-methyl-2-pyridinecarboxyaldehyde (0.20 g, 1.65 mmol) and 10 ml of dry diethyl ether was allowed to dissolve by means of stirring at room temperature for 5 minutes. After that, 2-3 g of anhydrous MgSO<sub>4</sub> was added and the colourless solution was cooled in an ice bath during the addition of n-propyl-amine. The mixture was allowed to stir for 4 hours at room temperature, after which the solution was filtered by means of gravity. The solvent was removed under vacuum and the residual oil was then further purified by addition of diethyl-ether at -4°C to precipitate out any unreacted aldehyde. After decanting the solvent, ligand was dried under vacuum for 3-4 hours. Ligands **ML1-ML4** were isolated as oils and they were successfully characterized by <sup>1</sup>H & <sup>13</sup>C NMR spectroscopy, FT-IR spectroscopy, ESI-MS and elemental analysis, results are tabulated in Tables 2.1-2.3.

### 2.5.2 Multifunctional G1 & G2 poly (propylene-imine) dendrimeric ligands (type2) DL1-DL8.

These ligands were prepared by using the same procedure used by Smith *et al* [6, 9] and Malgas *et al* [12, 13]. The process for **DL1** is described as an example. A 100 ml Schlenk tube was charged with nitrogen gas followed by 15 ml of dry toluene and 3 g of anhydrous MgSO<sub>4</sub>. Then an appropriate amount of 6-Methyl-2-pyridinecarboxyaldehyde (0.270 g, 2.17 mmol) was dissolved into the toluene by stirring at room temperature for 5 minutes. A sample of DAB-dendr-(NH<sub>2</sub>)<sub>4</sub> generation one ( 0.180 g, 0.56 mmol) was dissolved in dry toluene (10 ml). This colourless solution was added to the stirring solution of aldehyde and MgSO<sub>4</sub> by means of a syringe. The colourless mixture was allowed to stir at room temperature for 2 days. The mixture was filtered by gravity and the solvent was removed by rotary evaporator leaving colourless oil. The product was then dissolved in dry DCM (10 ml) and extracted with de-ionized water (7x30 ml) to remove any unreacted DAB. The organic layer was then collected, dried over anhydrous MgSO<sub>4</sub> and filtered by gravity. After removal of the solvent by rotary evaporator, the product was refluxed overnight in hot pentane (36 °C) to remove any unreacted aldehyde. In a similar way **DL3** and **DL4** were obtained as a white and a yellow solid respectively. Other ligands were obtained as pure oils. Ligands **DL1-DL8** were successfully characterised by <sup>1</sup>H & <sup>13</sup>C-NMR spectroscopy, FT-IR, ESI-MS and elemental analysis. Characterisation data are given in Tables 2.5-2.7.

**2.6 REFERENCES**

- [1] M.J.Chitanda, D.E.Prokopchuk, *Organomet.* 27 (2008) 2337.
- [2] D.M.Haddleton, D.J.Duncalf, *Eur. J.Inorg.Chem.* (1998) 1799.
- [3] W.Massa, S.Dehghampour, *Inorg.Chem.* 362 (2009) 2872.
- [4] R. Chen, J.Bacsa, S.F.Mapolie, *Polyhedron.* 22 (2003) 2855.
- [5] J.Cloete, S.F.Mapolie, *J. Mol. Catal. A:* 243(2006) 221.
- [6] G.Smith, R.Chen, S.F.Mapolie, *J. Organomet.Chem*, 673 (2003) 111.
- [7] D.Prema, A.V.Wiznycia, *Dalton Trans.* (2007) 4788.
- [8] V.Amandola, C.Mangano, *Inorg.Chem.* 42 (2003) 6056.
- [9] G.S.Smith, S.F.Mapolie, *J. Mol.Catal.A: Chem* 213 (2004) 187
- [10] X.Guo, J.Zhou, X.Li, H.Sun, *J.Organomet.Chem*, 693 (2008) 3692.
- [11] A.B.Powell, J.R.Brown, K.V.Vasudevan, A.H.Cowley,*Dalton.Trans.* (2009) 2521.
- [12] R.Malgas, S.F.Mapolie, S.O.Ojwach, G.S. Smith, J.Darkwa, *Catal.Commun.* 9 (2008) 1612.
- [13] R. Malgas-Enus, S.F.Mapolie, G.S. Smith, *J. Organomet. Chem.* 693 (2008) 2279.
- [14] J.L. van Wyk, *Mono-nuclear and multinuclear salicylaldimine metal complexes as catalysts precursors in the oxidation of phenol and cyclohexane*, PhD Thesis, University of the Western Cape (2008).

## CHAPTER THREE

### Pd(II) COMPLEXES BASED ON MONO AND MULTI-FUNCTIONAL DIIMINE LIGANDS: SYNTHESIS AND CHARACTERISATION.

---

#### CONTENT

3.1 INTRODUCTION	72
3.2 RESULTS AND DISCUSSION	75
3.2.1 Synthesis of mono-nuclear [N-(n-propyl)-(2-pyridyl and quinolyl-methanimine] dichloro Pd (II) complexes , <b>C1-C4</b>	75
3.2.1.1 <i>Infrared and <sup>1</sup>H-NMR spectroscopic studies of mono-nuclear Complexes</i>	76
3.2.1.2 <i>ESI mass spectrometry and elemental analysis of C1-C4</i>	79
3.2.1.3 <i>Single X-ray crystallographic studies of Pd (II) mono-nuclear Complexes</i>	83
3.3 Synthesis of multinuclear dendrimeric Pd (II) complexes, <b>C5-C12</b>	88
3.3.1 <i><sup>1</sup>H &amp; <sup>13</sup>C{<sup>1</sup>H}-NMR spectroscopic studies of dendrimeric complexes</i>	91
3.3.2 <i>FT-IR spectroscopic studies of C5-C12</i>	91
3.4 CONCLUDING REMARKS	95
3.5 EXPERIMENTAL SECTION	96
3.5.1 General remarks and instrumentation	96
3.5.2 Materials	96
3.6 SYNTHESIS OF MONONUCLEAR AND MULTINUCLEAR Pd(II) COMPLEXES	97
3.6.1 Mononuclear [N-(n-propyl)-(2-pyridyl and quinolyl)-methanimine dichloro Pd(II) complexes, <b>C1-C4</b>	97
3.6.2 Multinuclear [G1&2_DAB-dendr-(NH <sub>2</sub> ) <sub>n</sub> -1-(2-pyridyl and quinolyl)-imine] dichloro Pd (II) complexes, <b>C5-C12</b>	97
3.7 X-RAY CRYSTALLOGRAPHIC STUDIES FOR <b>C1-C4</b>	98
3.7.1 Description of crystals for <b>C1 &amp; C2</b> and refinement parameters for data collections, see Appendix	98

## CHAPTER THREE

### **Pd(II) COMPLEXES BASED ON MONO AND MULTI-FUNCTIONAL DIIMINE LIGANDS: SYNTHESIS AND CHARACTERISATION.**

---

3.7.2	Description of crystals for <b>C3</b> & <b>C4</b> and refinement parameters for data collections, see Appendix	98
3.8	STRUCTURAL DETERMINATION	99
3.9	REFERENCES	100

### 3.1 INTRODUCTION

As stated in Chapter one of this thesis, late transition metal complexes with nitrogen based ligands have been employed in a wide range of applications in both homogeneous and heterogeneous catalysis [1-11]. Considerable attention has lately been focussed on the synthesis of multinuclear organometallic compounds based on the expectation that their reactivity in catalysis will have a significantly positive effect as compared to that of analogous mononuclear species [6-8]. Pyridyl-imine metal complexes, both multinuclear and mononuclear with long chain spacers have been reported recently [1, 3, 4, 6, 7&10]. Kettunen and co-workers reported the synthesis of Pd(II) diimino-bispyridine complexes (see Scheme 3.1) with an axial biphenyl back-bone [8]. These complexes showed activity in norbornene polymerisation. In their study, they discovered that the cationic complexes were square-planar with Pd centres coordinated to all four nitrogen donors that lead to inactivity of these complexes towards norbornene polymerisation [8]. Similar complexes were also reported by Cloete and Chen [3 & 4]. Pelagatti *et al.* reported some interesting work on the synthesis of pyridyl-imine palladium(II) and (0) complexes and they also tested the catalytic activity of these in the Heck-coupling of iodobenzene with methyl acrylate. It was noted that Pd<sup>+2</sup> complexes have high reactivity as compared to their analogous neutral complexes. Reactivity among the Pd<sup>+2</sup> catalysts was as follows B>C>>A, which can be accounted for using steric effects [10].

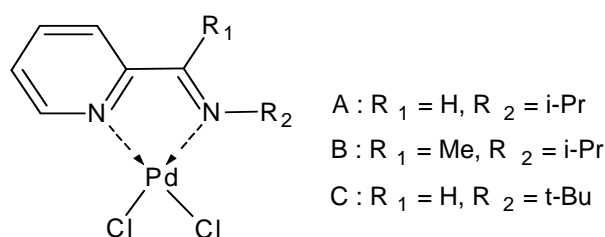
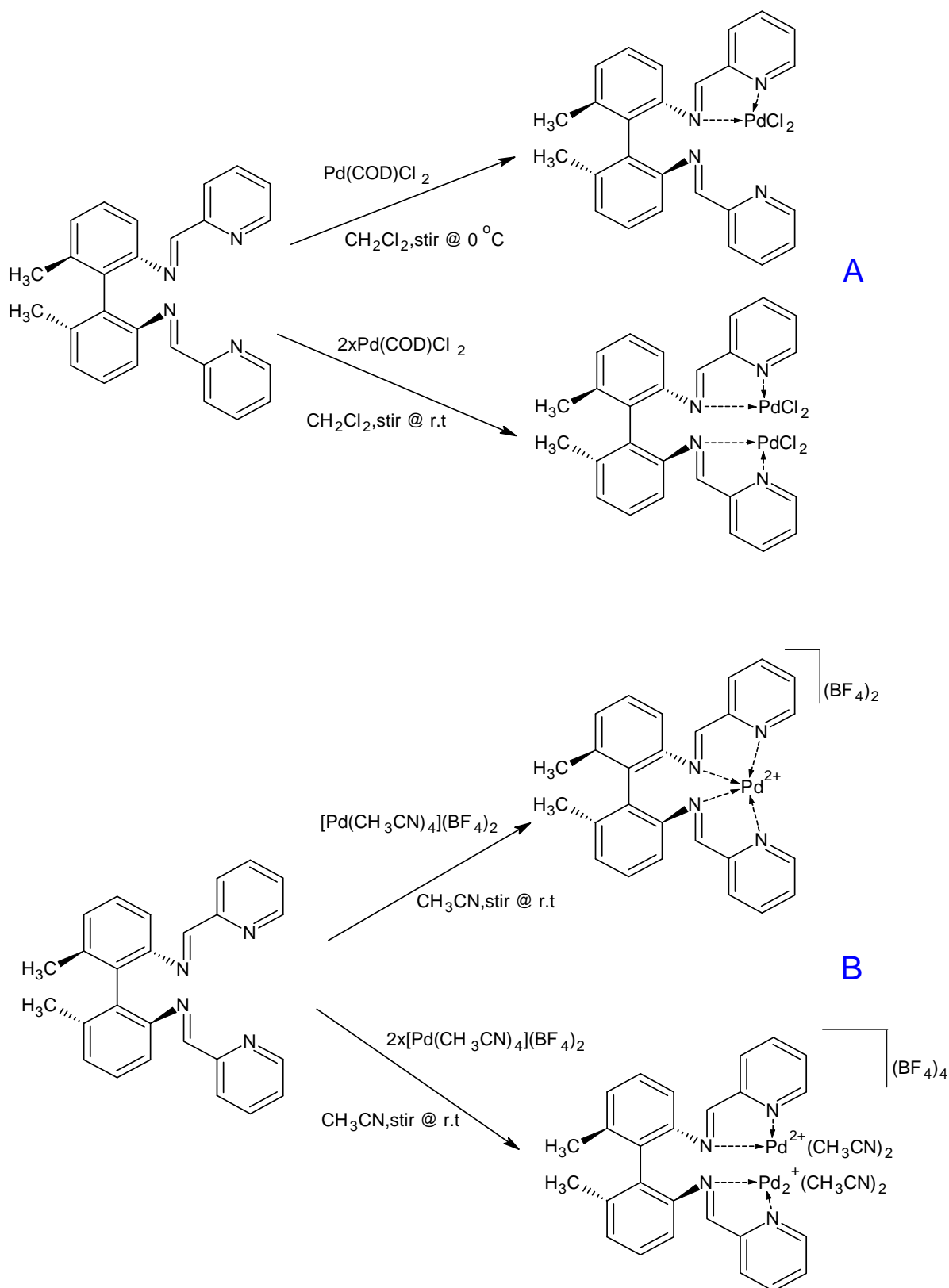


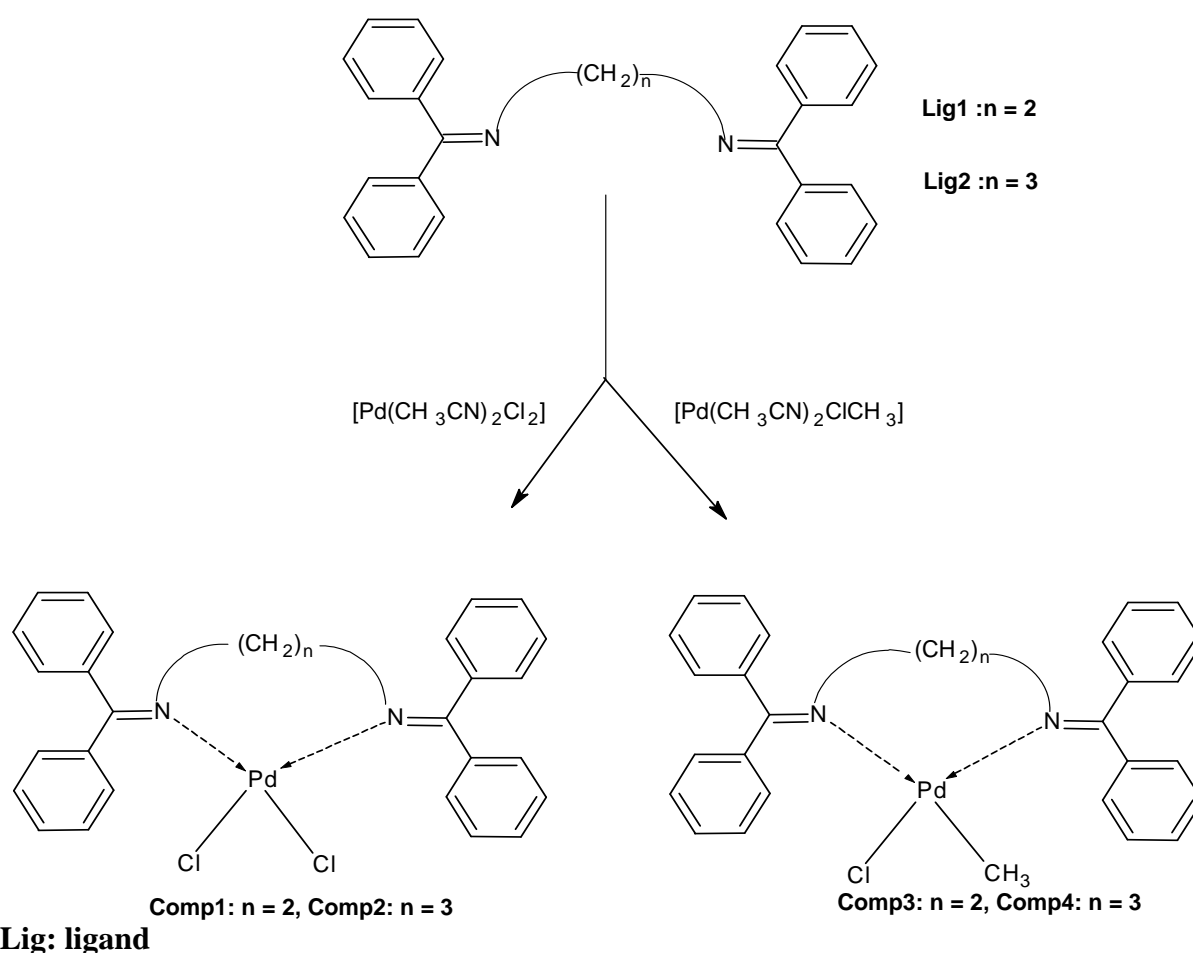
**Figure 3.1:** *Pyridyl-imine palladium(II) dichloride complexes [10]*





**Scheme 3.1:** (A) Neutral mononuclear and binuclear Pd(II) dichloride complexes, (B) Cationic mononuclear and binuclear Pd(II) dichloride complexes [8].

Nelana and co-workers recently synthesised unconjugated di-imine palladium complexes (see Scheme 3.2) and they tested the catalytic activity of these complexes in Heck coupling of iodobenzene and methyl acrylate or butyl acrylate [9]. They concluded that these complexes have higher catalytic activity as compared to palladium(II) dichloride salt. It was thus suggested that di-imine ligands effectively stabilise the Pd(0) colloids that act as the catalytically active sites in the Heck-coupling reactions [9]. A quinoline-2-carboimine palladium(II) complex immobilised on MCM 41 was developed by Kommura and co-workers [11]. This catalyst showed reactivity towards Sonogoshira coupling reactions of terminal alkynes with aryl halides [11].



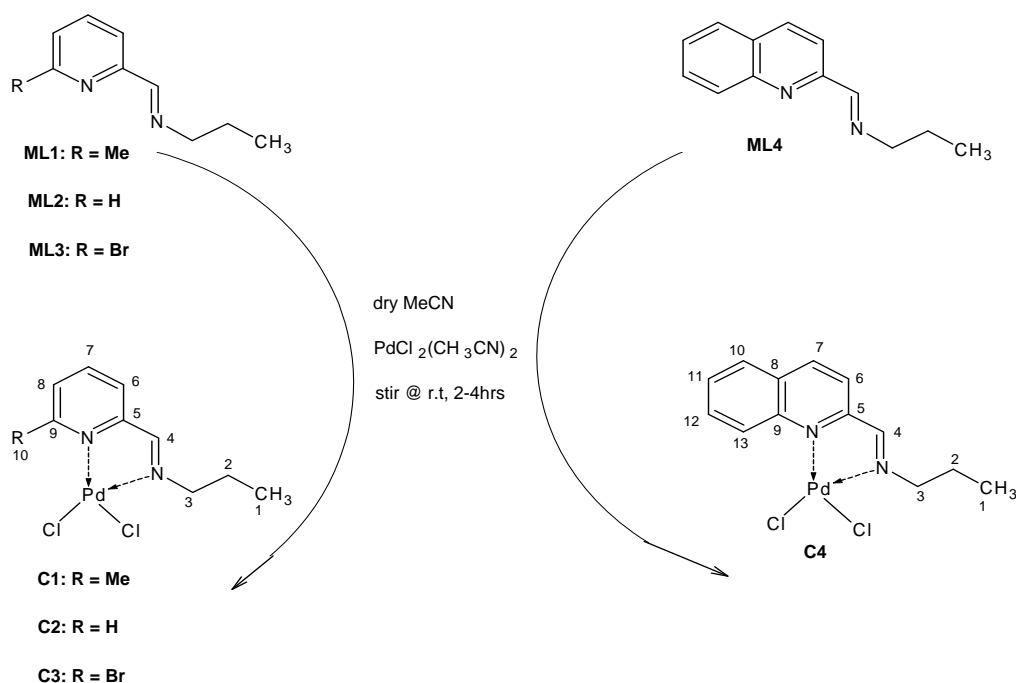
**Scheme 3.2:** Unconjugated di-imine Pd(II) complexes [9]

In this chapter we report the synthesis of several mononuclear and multinuclear Pd(II) complexes based on both pyridyl-imine and quinolyl-imine ligands.

## 3.2 RESULTS AND DISCUSSION

### 3.2.1 Synthesis of mononuclear *[N-(n-propyl)-(2-pyridyl and quinolyl-methanimine)] dichloro Pd(II) complexes, C1-C4*

Palladium complexes were synthesized by modifying a procedure that was used by Chen *et al* [3] and Cloete *et al* [4]. Subsequent reactions of equimolar amounts of the monofunctional ligands (**ML1-ML4**) with  $\text{PdCl}_2(\text{CH}_3\text{CN})_2$  resulted in the formation of *[N-(n-propyl)-1-(2-pyridyl/quinolyl) methanimine]* dichloro palladium complexes (**C1-C4**). All of the complexes were isolated as yellow solids and they were very stable in the solid state but in  $\text{CH}_2\text{Cl}_2$  or  $\text{CHCl}_3$  solutions they tend to undergo demetallation which results in the formation of palladium black ( $\text{Pd}^0$ ). **C2** and **C4** were only soluble in DMSO. **C1** & **C3** were recrystallised by dissolving in DCM and cooling the solution at  $-5^\circ\text{C}$  for 48 hours. **C2** & **C4** crystals on the other hand were grown from diffusion of EtOH into DMSO solutions at room temperature. These prisms and needle shaped crystals with yellow-red appearance were suitable for single crystal X-ray diffraction analysis.



**Scheme 3.3:** Synthesis of mononuclear palladium(II) dichloride complexes based on pyridyl and quinolyl-imine ligands.

### 3.2.1.1 *Infrared and <sup>1</sup>H-NMR spectroscopic studies of mononuclear complexes*

The proton NMR spectra of all mono-nuclear palladium(II) complexes (**C1-C4**) show similar trends especially in the aliphatic region. For all of these compounds there is a down-field shift of the proton signals in the aromatic region upon complexation. This reveals the existence of strong coordination of both pyridine nitrogen and the imine nitrogen to the palladium centre. In the case of the unsubstituted pyridyl-imine palladium complex (**C2**) there is a significant downfield shift of both the imine proton ( $H-C=N$ ) from 8.3 ppm in the free ligand spectrum to 8.6 ppm in the complex and the protons of the  $CH_2$  group adjacent to the imine moiety ( $=N-CH_2$ ) from 3.57 ppm to 3.68 ppm. These protons are assigned as H-4 and H-3 respectively (see Table 3.2). **C1&3** show an up-field shift of the imine proton to 8.17 ppm and 8.22 ppm respectively. However the situation is different in the case of the quinoline based complex (**C4**). Here the imine proton shifted from 8.55 ppm in the free ligand to 8.94 ppm of the complex while the  $CH_2$  protons adjacent to the imine group shifted from 3.61 ppm to 3.76 ppm.

Infra-red spectra of all pyridyl-imine palladium complexes (**C1-C3**) showed a distinct shift of the  $\nu(C=N)$  band which normally occurs around  $1650\text{ cm}^{-1}$  in the free ligand and which upon coordination occurs around  $1600\text{ cm}^{-1}$ . For **C4** the  $\nu(C=N)$  stretch occurs at  $1597\text{ cm}^{-1}$ . The shifting of the  $C=N$  band in these complexes is caused by the coordination of the metals into the di-imine ligands. This coordination reduces the electron density in the  $C=N$  bond due to electron density flowing from the ligand to the metal centre. These results are within the range of those published for similar complexes [3 & 4].

**Table 3.1:** Characterisation data of mononuclear Pd(II) complexes (C1-C4)

Mono-nuclear complexes	Physical Appearance	% Yield	Melting Point (°C)	FT-IR (ATR) $\nu$ (C=N) $\text{cm}^{-1}$	Molecular Formula	ESI-MS [M+H] <sup>+</sup> (m/z) Calculated (Found)	Micro-analysis Calculated (Found)		
							%C	%H	%N
<b>C1</b>	Yellow needles	73	182-185	1602	C <sub>10</sub> H <sub>14</sub> Cl <sub>2</sub> N <sub>2</sub> Pd	339.53 (340)	35.37 (35.29)	4.16 (4.11)	8.25 (8.00)
<b>C2</b>	Yellow prisms	83	152-155	1598	C <sub>9</sub> H <sub>12</sub> Cl <sub>2</sub> N <sub>2</sub> Pd	325.53 (326)	33.21 (33.21)	3.72 (3.68)	8.61 (8.32)
<b>C3</b>	Red prisms	76	140-142	1589	C <sub>9</sub> H <sub>11</sub> BrCl <sub>2</sub> N <sub>2</sub> Pd	404.43 (405)	26.73 (26.80)	2.74 (2.42)	6.93 (6.69)
<b>C4</b>	Orange prisms	79	185-190	1597	C <sub>13</sub> H <sub>14</sub> Cl <sub>2</sub> N <sub>2</sub> Pd	375.59 (376)	41.57 (41.26)	3.76 (3.63)	7.46 (7.35)

**Table 3.2:** <sup>1</sup>H- Chemical shifts of mononuclear Pd(II) complexes (C1-C4)

Pd <sup>2+</sup> complexes	Aliphatic protons ä(ppm)				Aromatic protons ä(ppm)							
	H-1	H-2	H-3	H-4	H-6	H-7	H-8	H-9	H-10	H-11	H-12	H-13
<b>C1</b>	0.93 (t,3H)	1.87 (m,2H)	3.81 (t,2H)	8.17 (s,1H)	7.70 (d,1H)	7.93 (t,1H)	7.44 (d,1H)		3.10 <sup>a</sup> (s,3H)			
<b>C2</b>	0.89 (t,3H)	1.82 (m,2H)	3.68 (t,2H)	8.60 (s,1H)	8.10 (d,1H)	8.33 (t,1H)	7.86 (t,1H)	8.98 (d,1H)				
<b>C3</b>	0.94 (t,3H)	1.88 (m,2H)	3.81 (t,2H)	8.22 (s,1H)	7.82 (d,1H)	7.86 (t,1H)	7.88 (d,1H)					
<b>C4</b>	0.91 (t,3H)	1.87 (m,2H)	3.76 (t,2H)	8.94 (s,1H)	8.81 (d,1H)	8.18 (d,1H)			8.12 (d,1H)	7.83 (t,1H)	7.93 (t,1H)	7.79 (d,1H)

<sup>a</sup> Me-pry CH<sub>3</sub>.

### 3.2.1.2 *ESI mass spectrometry and elemental analysis studies of C1-C4*

Micro-analysis data obtained for palladium complexes confirmed a 1:1 ratio of metal to ligand as depicted in Scheme 3.3.

The successful coordination of ligands **ML1-ML4** to palladium was also established by positive ion electron spray ionisation mass spectrometry. The ESI-mass spectra of the palladium complexes showed isotopic clusters because of the six natural occurring stable isotopes of palladium and the two chloride isotopes which have significant natural abundances [13-17]. The mass spectra of these mononuclear palladium complexes (**C2-C4**) differ depending on the different conditions that were employed to record the spectra. It was observed that at a high desolvation temperature (400°C) and low cone voltage (15V), the spectra of these complexes show peaks which correspond to bimetallic species with an inclusion of acetonitrile solvent (Scheme 3.4). Similar observations were previously reported for other palladium complexes. Tomazela et al reported dimerisation of palladacycles in acetonitrile solution and they also observed chloride/acetonitrile exchange [16]. Tjosaas and co-workers also observed acetate/acetonitrile exchange in their six-membered ring acetate-bridged palladacycles  $[\text{Pd}_2\text{Lig}_2(\text{OAc})_2+\text{H}]^+$  [17]. They also reported that the ESI-mass spectra had base peaks which correspond to the monomer [17]. In our case, the bimetallic species undergoes a complex fragmentation process. The first step involves the loss of a propyl chain  $(-\text{C}_3\text{H}_9)^+$  resulting in the formation of  $[\text{Pd}_2(\text{i-Cl})_2\text{L}_2-\text{C}_3\text{H}_9]^+$  species with the most abundant peak at  $m/z$  619. Bach and co-workers reported formation of monomeric, dimeric and trimeric species of the  $[\text{Pd}(\text{en})\text{Br}_2]$  complex. They also observed sodium adducts of these species without acetonitrile inclusion [13]. From these reports it can be concluded that dimerisation during mass spectral analysis is common for some mono-nuclear palladium (II) complexes. An example of the fragmentation pattern of these complexes is shown in Scheme 3.4 and a mass spectrum is illustrated in Figure 3.2.

However when the mass spectral analysis is conducted at lower desolvation temperature (350°C) and higher cone voltage (35V), the spectra of **C1-C4** showed peaks that correspond to their mononuclear ions. **C2** showed four sets of peaks in the mass spectrum. The first one is due to the sodium adduct of the parent ion  $[\text{M}+\text{Na}]^+$  at  $m/z$  348.9 and the second one at  $m/z$  332 is due to the loss of  $\text{CH}_3$  of the aliphatic chain  $[\text{M}+\text{Na}]-\text{CH}_3$ . The most abundant peak is due to loss of  $-\text{C}_2\text{H}_5$  from parent ion

[M-C<sub>2</sub>H<sub>5</sub>] resulting in a peak at m/z 296. Tjosaas *et al* [17] reported that the cone voltage may be altered to vary the energy of the ions formed in the ESI-MS. They also observed important differences in complexes of the type PdL (OAc)<sub>2</sub> by studying ESI-mass spectra using cone voltages 10, 30, 40 and 50V. Neo *et al* [14] observed different ESI-mass spectra of PdCl<sub>2</sub>(Ph<sub>2</sub>P(CH<sub>2</sub>)<sub>5</sub>PPh<sub>2</sub>) with an increase in cone voltage. They noted that at low cone voltage (20V), the solvated species (ion) was the base peak, but the unsolvated species was dominant at 50V. From these reports it can be concluded that solvent ligands, like acetonitrile do not survive under increased cone voltage conditions.

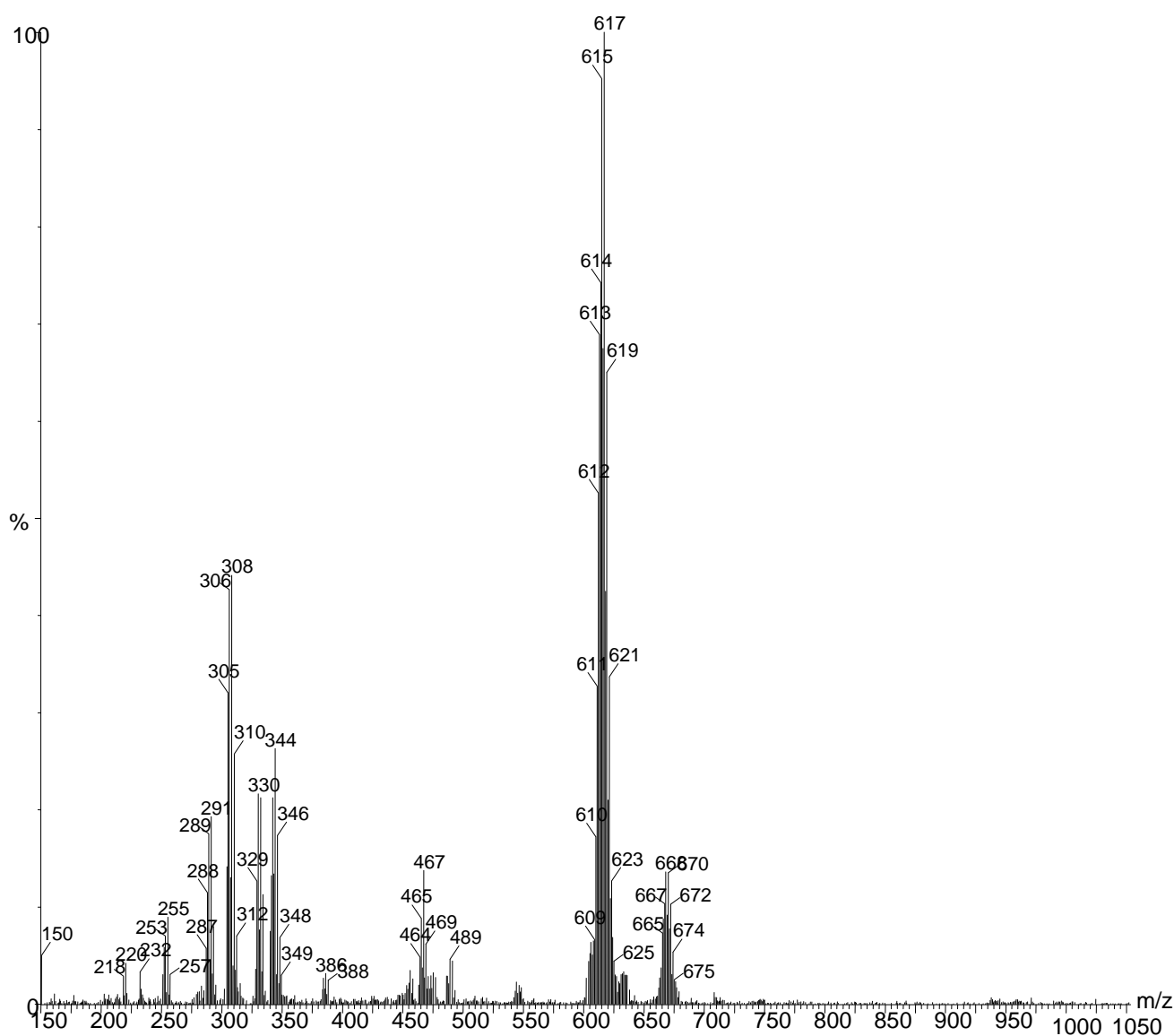
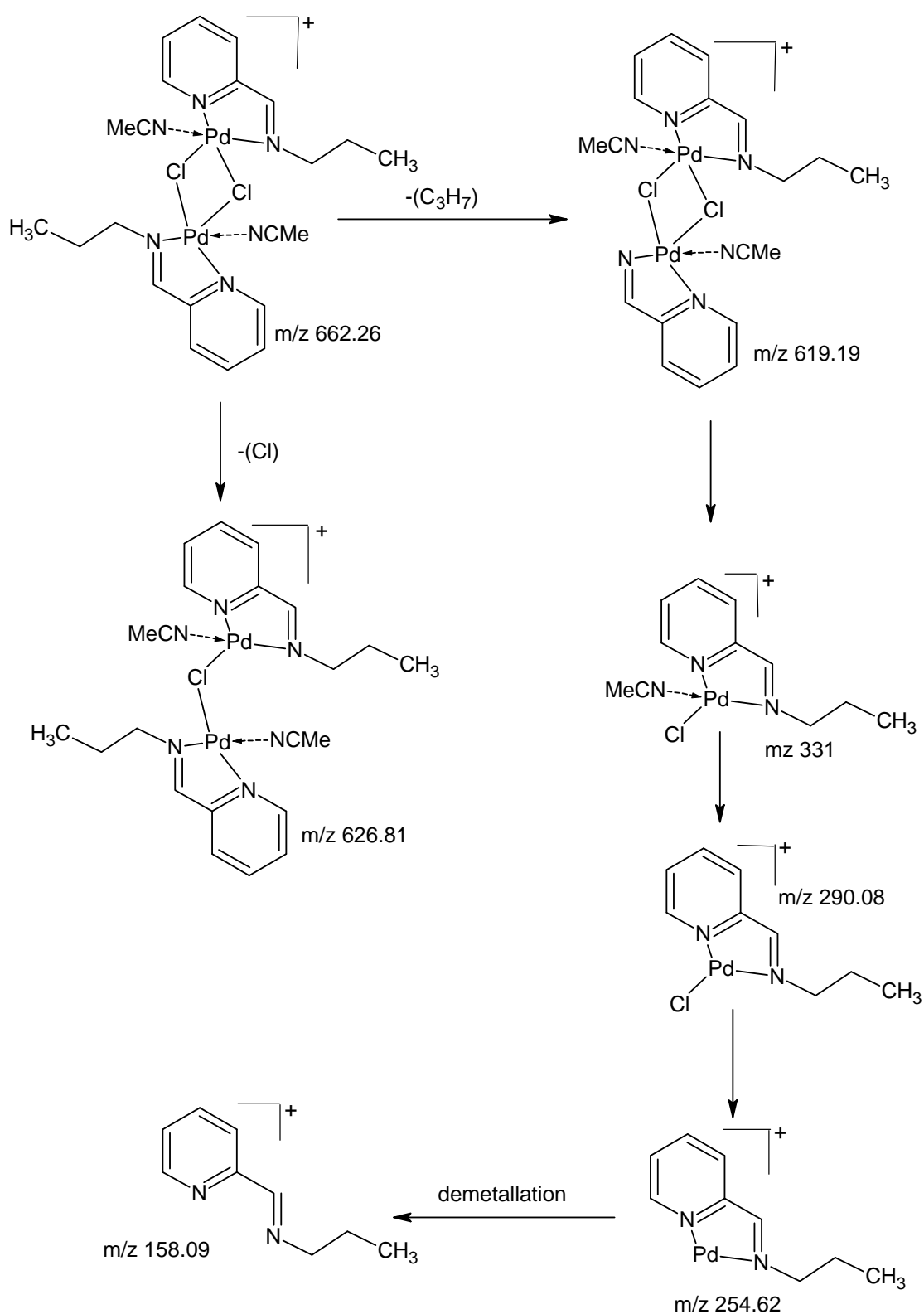


**Figure 3.2:** ESI-mass spectrum of C2





**Scheme 3.4:** Possible fragmentation pathway of palladium(II) dichloride complex (C2)

The simulated mass spectrum of **C2** is shown in Figure 3.3. As it can be seen, there is an excellent agreement between the experimentally observed and simulated isotopic distribution pattern. This type of agreement is found for all complexes **C1-C4**.

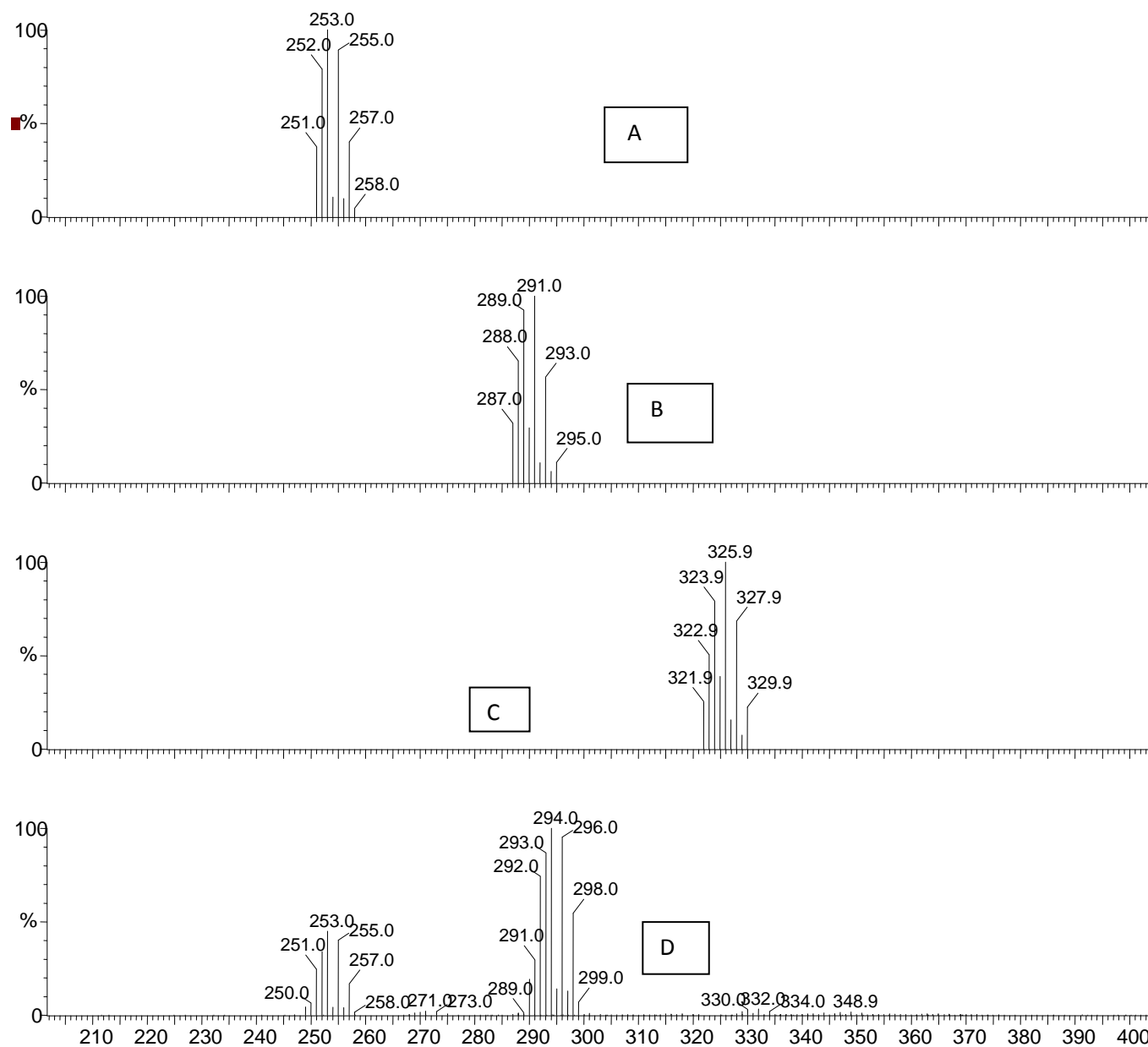
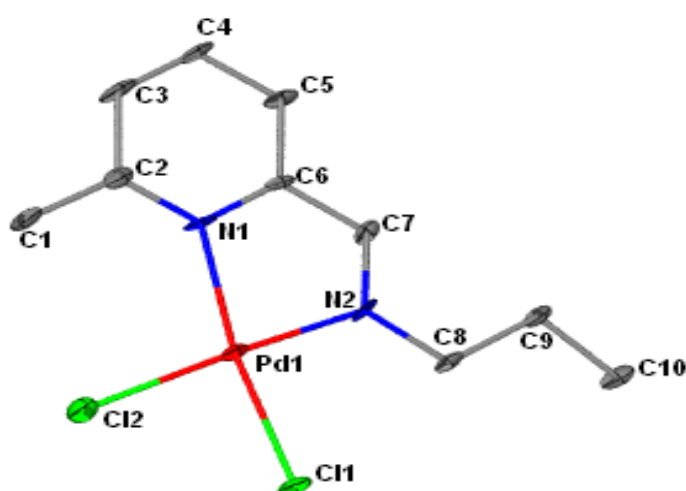


**Figure 3.3 :** (A) ESI-MS simulated isotopic distribution of  $[M-2Cl]$ , (B)  $[M-C_2H_5]$ , (C)  $[M^+]$  and (D) experimentally ESI mass spectrum of **C2**

### 3.2.1.3 Single-Crystal X-ray crystallographic studies of Pd(II) mononuclear complexes

Crystals of **C1-C4** suitable for X-ray diffraction analysis were obtained as previously described above. The crystal structural data and crystal refinement parameters for some of the complexes are presented in Tables 3.8 & 3.9. The coordination geometry for the palladium complexes can best be described as distorted square-planar. This is a usual for some of palladium(II) complexes [3].

#### *Structural description of C1*

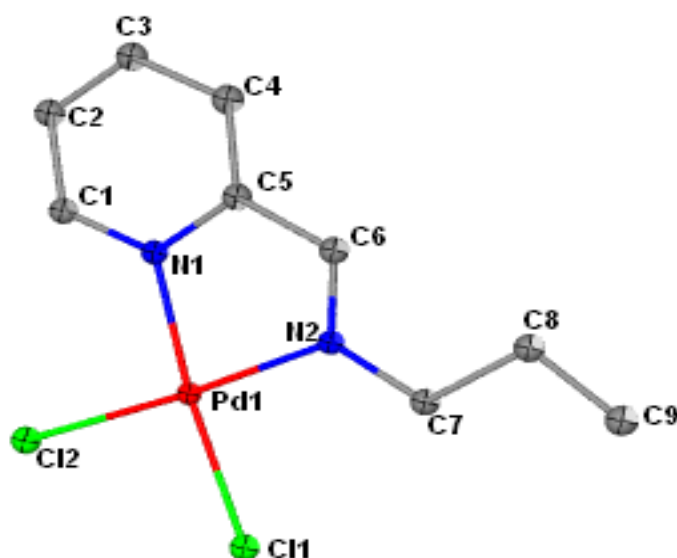


**Figure 3.4:** The molecular structure of **C1** showing crystallographic numbering.

The molecular structure of **C1** is depicted in Figure 3.4 with selected bond lengths and angles around the metal centre provided in Table 3.3. The molecular structure clearly shows that one ligand is coordinated to one palladium atom in a bidentate fashion as reported for similar complexes [3]. The geometric environment around the palladium centre is a distorted square-planar with bond angles N(1)-Pd-N(2), N(1)-Pd-Cl(1), N(2)-Pd-Cl(1), N(2)-Pd-Cl(2), Cl(1)-Pd-Cl(2), and N(1)-Pd-Cl(2) observed to be 80.61(3), 171.5(2), 91.7(2), 175.1(5), 85.61(10) and 102.3(2) respectively. There are similarities in these bond angles with those reported by Chen *et al* [3] for the [*N*-octyl-*N*-(pyridin-2-ylmethylene)amine] dichloro palladium(II) complex. It has been discovered that the bond angles and lengths for these complexes (**C1-C4**) were in coincide with the similar published structures [3 & 8].

**Table 3.3:** Selected bond lengths ( $\text{\AA}$ ) and angles ( $^\circ$ ) for the core of **C1**

Bond length ( $\text{\AA}$ )		Bond angles ( $^\circ$ )	
Pd-N(1)	2.129 (8)	N(1)-Pd-N(2)	80.61 (3)
Pd-N(2)	2.015 (7)	N(1)-Pd-Cl(1)	171.5 (2)
Pd-Cl(1)	2.281 (2)	N(2)-Pd-Cl(1)	91.7 (2)
Pd-Cl(2)	2.304 (2)	N(2)-Pd-Cl(2)	175.1 (5)
N(2)-C7	1.285 (2)	Cl(1)-Pd-Cl(2)	85.61 (10)
N(1)-C6	1.342 (1)	N(1)-Pd-Cl(2)	102.3 (2)
C6-C7	1.460 (3)		

*Structural description of C2***Figure 3.5:** The molecular structure of **C2** showing crystallographic numbering.

X-ray analysis of complex (**C2**) in Figure 3.5 once again revealed the coordination of one ligand per palladium centre with two chloride groups attached to the palladium. As for **C1** the geometry around metal centre is also observed to be distorted square planar (see Table 3.4). It has been noted that the bond angles N (1)-Pd-Cl (1) [ $174.67^\circ$  (9)] and N(2)-Pd-Cl (2) [ $175.89^\circ$  (9)] are larger than analogous angles for **C1**. This indicates that the distortion around palladium is not as great as observed for

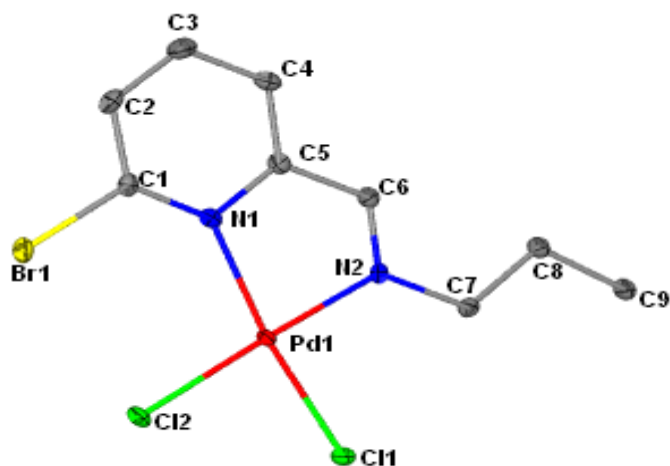
**C1** even though the ligands are coordinated in the same fashion. The greater distortion in **C1** could be due to the presence of the methyl group at position six of the pyridine ring, which is not the case in **C2**. The bond angles [N(1)-Pd-Cl(1) 174°] and [N(2)-Pd-Cl(2) 175°] are exactly the same as those reported by Chen *et al* [3] in their pyridyl-imine complex of palladium(II).

**Table 3.4:** Selected bond lengths ( $\text{\AA}$ ) and angles ( $^\circ$ ) for the core of **C2**

Bond length ( $\text{\AA}$ )		Bond angles ( $^\circ$ )	
Pd-N(1)	2.025 (3)	N(1)-Pd-N(2)	80.81 (12)
Pd-N(2)	2.022 (3)	N(1)-Pd-Cl(1)	174.67(9)
Pd-Cl(1)	2.2784 (9)	N(2)-Pd-Cl(1)	93.96 (9)
Pd-Cl(2)	2.3052 (9)	N(2)-Pd-Cl(2)	175.89(9)
N(1)-C5	1.3563 (5)	Cl(1)-Pd-Cl(2)	90.14 (3)
N(2)-C6	1.285 (5)	N(1)-Pd-Cl(2)	95.309 (9)
C5-C6	1.454 (5)		

### *Structural description of C3*

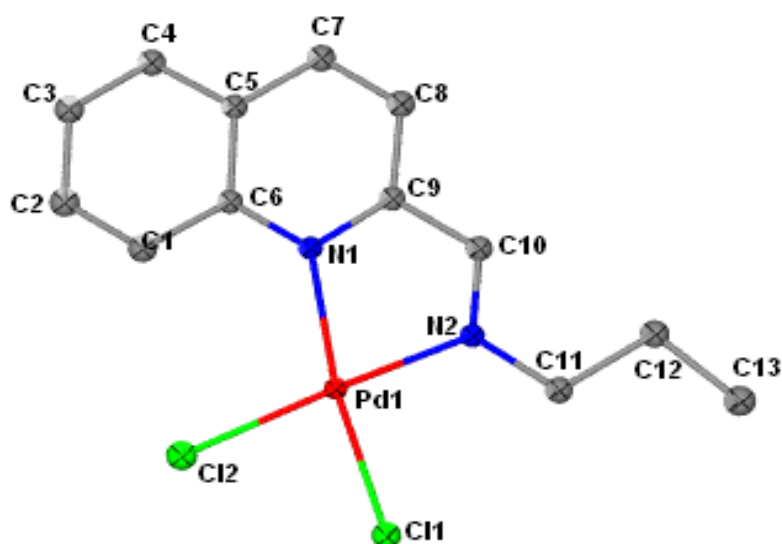
The ORTEP diagram of the molecular structure of **C3** (Figure 3.6) depicts a bidentate coordination system with one 6-bromopropyl-pyridin-2-ylmethylene-amine ligand coordinated to the palladium centre. Bond distances and angles around palladium are presented in Table 3.5. As for **C1** and **C2** the coordination around the metal centre is observed to be distorted square planar. However the distortion around the metal centre is observed to be much greater in **C3** as compared to **C1** & **C2**. The evidence is from the bond angle N(2)-Pd-Cl(2) which is found to be 176.99° (4). This greater distortion is attributed to the bromide substituent at the six position of the pyridine ring which creates a highly steric environment.



**Figure 3.6:** The molecular structure of **C3** showing crystallographic numbering.

**Table 3.5:** Selected bond lengths ( $\text{\AA}$ ) and angles ( $^\circ$ ) for the core of **C3**

Bond length ( $\text{\AA}$ )		Bond angles ( $^\circ$ )	
Pd-N(1)	2.142 (2)	N(1)-Pd-N(2)	80.63(8)
Pd-N(2)	2.017 (2)	N(1)-Pd-Cl(1)	172.43(6)
Pd-Cl(1)	2.2776 (6)	N(2)-Pd-Cl(1)	91.81(6)
Pd-Cl(2)	2.2948 (7)	N(2)-Pd-Cl(2)	176.99(6)
N(1)-C5	1.372 (3)	Cl(1)-Pd-Cl(2)	85.84(2)
N(2)-C6	1.270 (3)	N(1)-Pd-Cl(2)	101.72(6)
C5-C6	1.463 (3)		
C1-Br	1.878 (3)		

*Structural description of C4*

**Figure 3.7:** *The molecular structure of C4 showing crystallographic numbering.*

The molecular structure for the quinoline palladium(II) complex (**C4**) is shown in Figure 3.7, with selected bond lengths and angles around the metal centre listed in Table 3.6. As in the case of the other palladium(II) dichloride complexes (**C1-C3**), the molecular structure of **C4** revealed coordination of one ligand to one palladium atom in a bidentate fashion through the pyridine nitrogen (N1) and imine nitrogen (N2). The bond length of the two carbons linking the pyridine and imine together is similar to that of palladium structures reported herein (equal to 1.460 Å), with the exception of **C4** where it is longer (see Tables 3.3-3.6). This is because of the influence of the bulkiness of the quinoline ring. The geometry around the palladium centre is also distorted square-planar as shown by selected bond angles in Table 3.6.

**Table 3.6:** Selected bond lengths ( $\text{\AA}$ ) and angles ( $^\circ$ ) for the core of **C4**

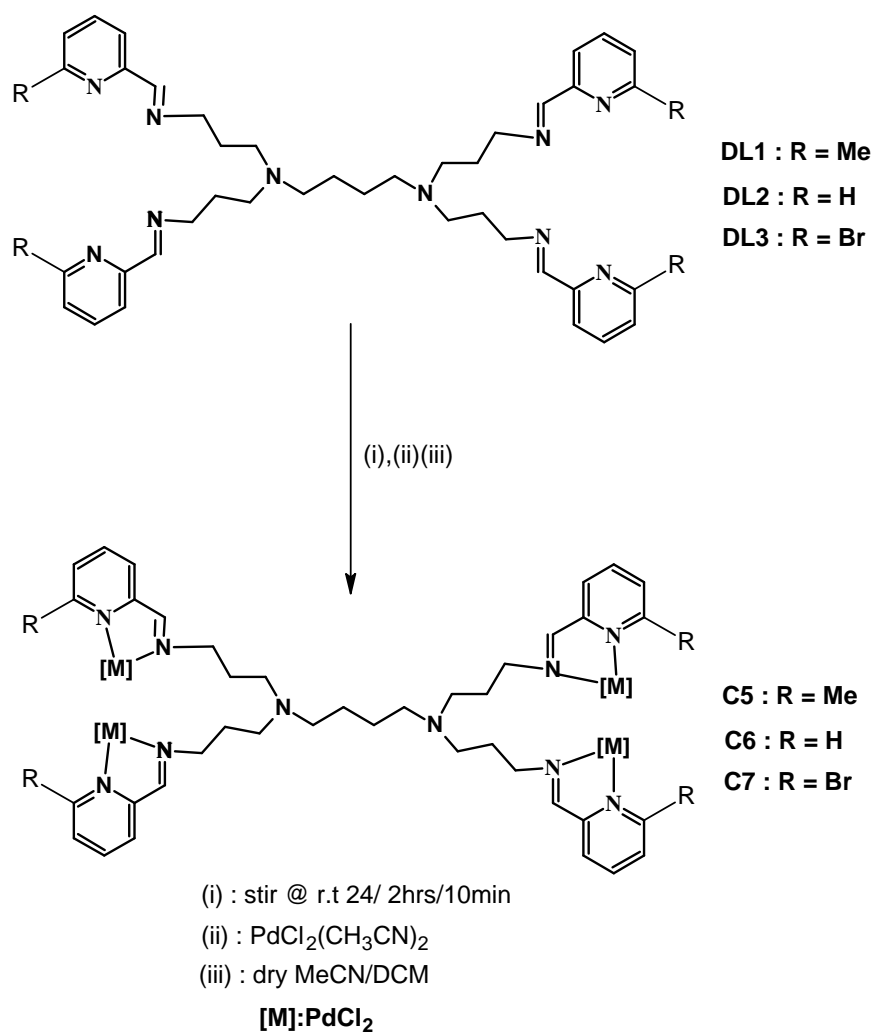
Bond lengths ( $\text{\AA}$ )		Bond angles ( $^\circ$ )	
Pd-N(2)	2.018 (5)	N(1)-Pd-N(2)	80.37 (6)
Pd-N(1)	2.131 (5)	N(1)-Pd-Cl(1)	171.98 (4)
Pd-Cl(1)	2.277 (6)	N(2)-Pd-Cl(1)	91.71 (4)
Pd-Cl(2)	2.313 (7)	N(2)-Pd-Cl(2)	174.85 (4)
N(1)-C(9)	1.339 (2)	Cl(1)-Pd-Cl(2)	84.79 (9)
N(2)-C(10)	1.274 (2)	N(1)-Pd-Cl(2)	103.19 (4)
C(9)-C(10)	1.461 (2)		

### 3.3 Synthesis of multinuclear dendrimeric Pd(II) complexes, C5-C12.

Multinuclear palladium complexes were synthesized by modifying a procedure that was used by Smith *et al* [7], van Wyk *et al* [20] and Malgas *et al* [18 & 19]. Palladium complexes **C5-C12** were obtained by peripheral functionalisation of the dendrimeric ligands (**DL1-DL8**) with  $\text{PdCl}_2(\text{CH}_3\text{CN})_2$  in dry DCM/MeCN under inert atmosphere. All complexes were isolated as very stable yellow-orange solids in moderate to good yields. These peripherally bound Pd dendrimers were only soluble in DMSO, and they were purified by extensively washing the complexes with DCM in order to remove any unreacted ligand or palladium precursor. The reaction time was crucial in the formation of these complexes because it was noted that with time the imine ligand hydrolyses to form the corresponding aldehyde. This hydrolysis process seemed to be mediated by the metal as no such hydrolysis occurred in the absence of the metal. Complexes **C5** and **C9** were stirred for two hours to prevent formation of palladium black ( $\text{Pd}^0$ ). However complexation of **DL4** & **DL8** with palladium precursor was carried out for 10 minutes because with prolonged reaction period the formation of hydrolysis products were observed. The same problem was observed in the synthesis of **C7** and **C11**. For these two complexes a decrease in the reaction time did not prevent hydrolysis which appeared to be an extremely fast reaction as compared to the complexation reaction. The structures of the metallodendrimers with  $\text{PdCl}_2$  moieties bonded to pyridylimino and quinolylimino



units were confirmed by  $^1\text{H}$  &  $^{13}\text{C}$ -NMR spectroscopies in DMSO- $d_6$  and solid state FT-IR spectroscopy.



**Scheme 3.5:** Synthesis of first generation poly (propylene-imine) pyridylimine palladium(II) metallodendrimers.

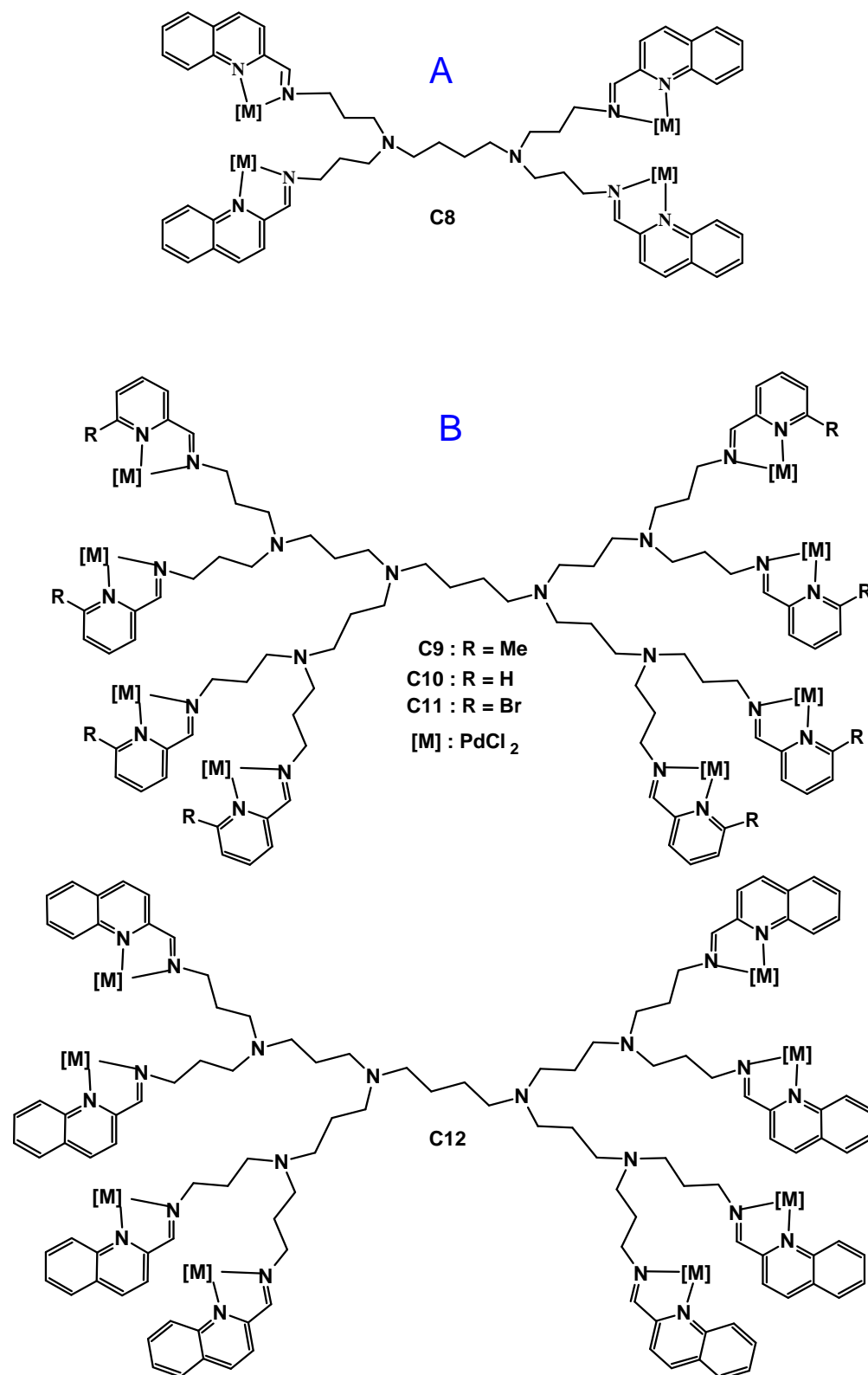


**Figure 3.8:** (A) First generation propylene-imine quinolyl (B) second generation poly (propylene imine) pyridylimine/quinolylimine palladium(II) metallodendrimers.

### 3.3.1 $^1\text{H}$ & $^{13}\text{C}\{^1\text{H}\}$ -NMR spectroscopic studies of dendrimeric complexes

The structures of metallodendrimeric complexes with  $\text{PdCl}_2$  moieties bonded to pyridylimino/quinolylimino units were established by nuclear magnetic resonance studies in  $\text{DMSO-d}_6$ . The proton NMR spectra of these complexes showed broadened peaks as compared to their analogous mononuclear complexes as shown in Figure 3.9. NMR signals due to aliphatic protons of the dendrimer core, side-arms and those of the pyridine/quinoline ring occur at chemical shifts similar to those of the parent ligands which were discussed in **Chapter 2**. The only difference is the fact that in the complexes there is a slight downfield shift. This down-field shift occurs drastically for the proton of the imine moiety ( $\text{HC}=\text{N}$ ) and the protons of the  $\text{CH}_2$  group adjacent to the imine moiety ( $\text{H}_2\text{C}-\text{N}=\text{CH}$ ). This is because coordination of the ligand to the metal is via pyridine/quinoline nitrogen and imine nitrogen. In the case of pyridine based palladium complex **C6**, the imine proton shifted from 8.36 ppm (ligand) to 8.66 ppm (complex) which was similar to that observed for mono-nuclear complexes. Smith *et al* also observed similar shifts [6&7]. Carbon-13 nuclear magnetic resonance spectroscopy was also used to investigate evidence of complexation. All complexes gave relatively poor quality spectra because of the poor solubility of these compounds. Even so all peaks could be assigned to the corresponding carbons.

### 3.3.2 *FT-IR spectroscopic studies of C5-C12*

Infra-red spectroscopy was also used as an investigation tool to determine complexation of dendrimeric ligands and the results are shown in Table 3.7 which shows  $\nu(\text{C}=\text{N})$  stretches for the complexes. As discussed in the case of mono analogues, the  $\nu(\text{C}=\text{N})$  vibrations shifted to lower wave numbers as compared to the dendrimeric ligands. Metallodendrimers also showed a band around  $3385\text{ cm}^{-1}$  which is a characteristic of water coordination to the metal centre; this is the evidence of a hydrolysis reaction as reported in literature [9]. Unlike mononuclear analogues, metallodendrimers do not melt they decompose at high temperatures as compared to the mononuclear complexes, see Table 3.7. From these results it can be concluded that metallodendrimers have high thermal stability. Due to poor solubility of these

compounds (**C5-C12**) mass spectrometry was not obtained, but some of these complexes showed good micro-analysis results, see table 3.7.

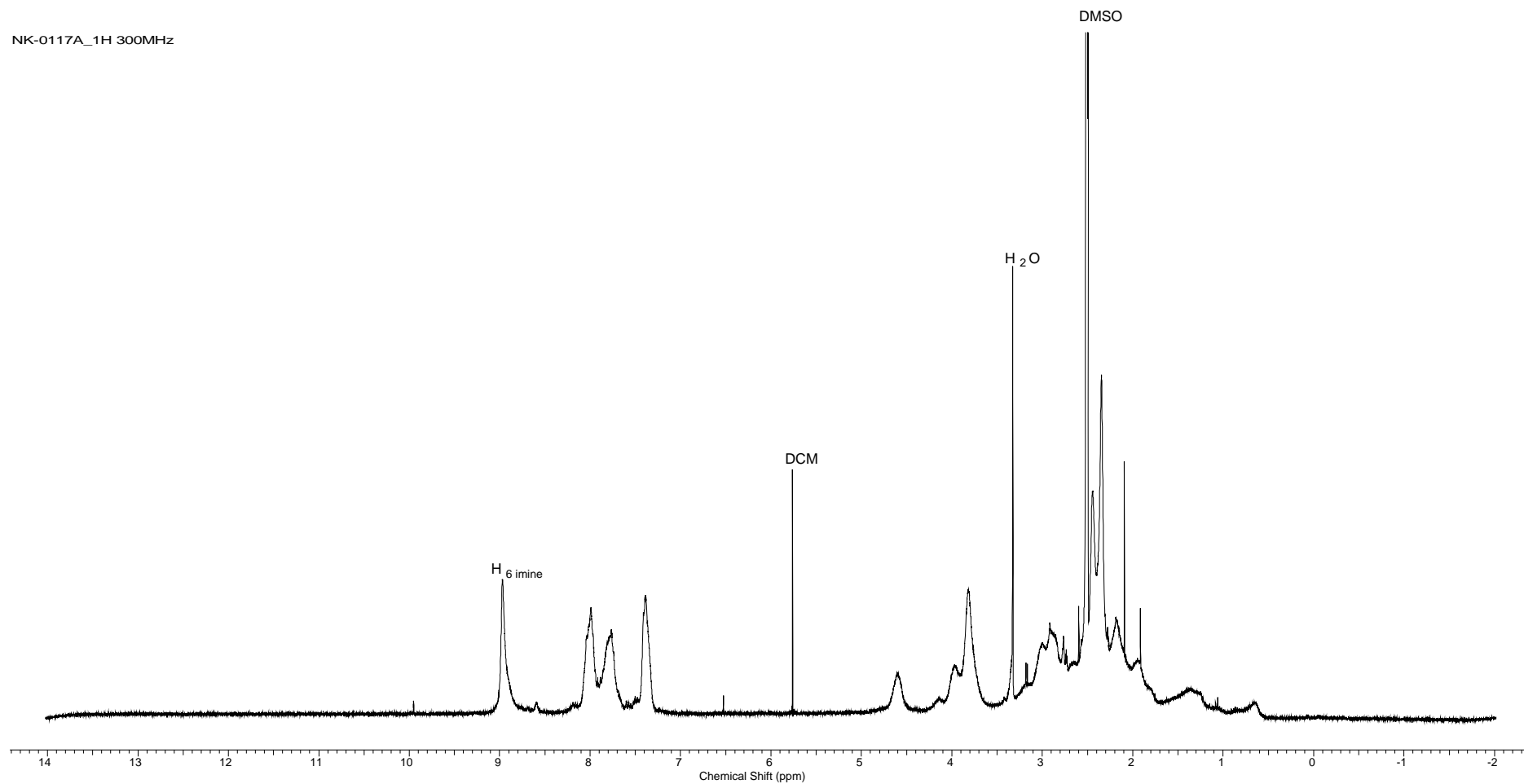


**Figure 3.9:**  $^1\text{H-NMR}$  spectrum of C6

**Table 3.7:** characterisation data of metallodendrimeric Pd(II) complexes (C7-C12)

Multinuclear complexes	Physical Appearance	% Yield	Decomposition Point (°C) <sup>a</sup>	FT-IR (ATR) $\nu$ (C=N) $\text{cm}^{-1}$	Molecular Formula	Micro-analysis Calculated (Found)		
						%C	%H	%N
C5	Orange	82	190	1601	C <sub>45</sub> H <sub>63</sub> Cl <sub>8</sub> N <sub>10</sub> Pd <sub>4</sub>	36.74(37.00)	4.20(4.02)	9.74(9.40)
C6	Light-orange	96	200	1599	C <sub>41</sub> H <sub>55</sub> Cl <sub>8</sub> N <sub>10</sub> Pd <sub>4</sub>	34.76(34.33)	3.79(4.12)	10.13(10.05)
C7	Bright-yellow	81	200	1590	C <sub>41</sub> H <sub>51</sub> Br <sub>4</sub> Cl <sub>8</sub> N <sub>10</sub> Pd <sub>4</sub>	<b>n.d<sup>b</sup></b>		
C8	Deep-orange	86	200	1598	C <sub>57</sub> H <sub>63</sub> Cl <sub>8</sub> N <sub>10</sub> Pd <sub>4</sub>	42.50(41.99)	3.82(3.78)	8.85(8.55)

C9	Orange	85	200	1602	$C_{104}H_{160}Cl_{16}N_{22}Pd_8$	39.82(39.52)	5.14(5.03)	9.82(9.77)
C10	Yellow	93	205	1599	$C_{96}H_{144}Cl_{16}N_{22}Pd_8$	38.12(38.04)	4.80(4.77)	10.19(10.07)
C11	Yellow	70	210	1589	$C_{96}H_{136}Br_8Cl_{16}N_{22}Pd_8$		<b>n.d<sup>b</sup></b>	
C12	Orange	71	222	1597	$C_{128}H_{160}Cl_{16}N_{22}Pd_8$		<b>n.d<sup>b</sup></b>	

<sup>a</sup>:These complexes do not melt, they change colour to brown at higher temperatures.

<sup>b</sup>:Not determined

### 3.4 CONCLUDING REMARKS

A number of mononuclear [*N*-(*n*-propyl)-(2-pyridyl/quinolyl) methanimine dichloro Pd(II) complexes have been successfully synthesized and characterised with a number of spectroscopic techniques. These complexes were synthesized by reacting monofunctional ligands (**ML1-ML4**) with palladium bis(acetonitrile)dichloride precursor in a 1:1 ratio. All the characterisation data were consistent with the expected results. Single X-ray diffraction analysis showed that around the palladium centre we have distorted square planarity. The distortion was even greater for **C1** and **C3** because of the substituents at position six of the pyridine ring.

The synthesis and characterisation of generation 1 & 2 metallodendrimers were also discussed in this chapter. These complexes were synthesized by using a similar procedure that was used for mononuclear analogues. The reaction time for these complexes was very crucial, because with time they tend to favor a hydrolysis reaction to form the corresponding aldehyde and amine. To minimise the occurrence of hydrolysis products, these reactions were monitored by <sup>1</sup>H-NMR spectroscopy. The bromo-substituted metallodendrimers (**C7** & **C11**) tend to undergo this hydrolysis in a very short period of time. It is suspected that the bromide substituent enhances the hydrolysis reaction. From all the results in this chapter it can be concluded that 3 new mono-nuclear palladium(II) dichloride complexes and 6 new palladium(II) metallodendrimers have been successfully synthesised and characterised by a number of spectroscopic methods. Micro-analysis results are confirming the purity compounds. Metallodendrimers showed high thermal stability as compared to their mononuclear analogues.



## 3.5 EXPERIMENTAL SECTION

### 3.5.1 *General remarks and instrumentation*

All manipulations involving air-sensitive and/or moisture-sensitive materials were performed in a nitrogen-filled glove box or under an atmosphere of purified dry nitrogen using standard Schlenk techniques. IR spectra were recorded as solids by using an ATR accessory on a Nicolet Aneta 330 FT-IR spectrometer. NMR spectra were recorded on a Varian Unity Inova instrument ( $^1\text{H}$  at 300 or 400 MHz,  $^{13}\text{C}$  at 75 or 100 MHz). Chemical Shifts are reported in ppm and are referenced to residual proton and carbon signals (7.25 and 77ppm) for  $\text{CDCl}_3$  respectively and 2.50 and 39.0 ppm for  $\text{DMSO}-d_6$ . MS-(+ESI) spectrometric characterisations were done by using a Waters API Quattro Micro instrument with direct injection of DCM solution, MS settings were as follows: capillary voltage 3.5Kv, cone voltage 15 RF1 40, cone gas 50L/h, desolvation temperature  $400^\circ\text{C}$ , desolvation gas 500L/h and cone gas 50L/h. Elemental analysis was performed by the University of Cape Town Micro-analytical Laboratory.

### 3.5.2 *Materials*

All solvents were purchased from Sigma-Aldrich or Kimix Chemicals (South Africa), and they were refluxed over appropriate drying agents and distilled prior to use: diethyl ether and toluene over sodium wire and benzophenone, dichloromethane and acetonitrile over phosphorous pentoxide, hexane and pentane over sodium wire. Dimethyl sulfoxide (DMSO) was used as received without any further purification. The palladium precursor  $[\text{Pd}(\text{CH}_3\text{CN})_2\text{Cl}_2]$  was prepared according to literature procedures [21 & 22].

### 3.6 SYNTHESIS OF MONONUCLEAR AND DENDRIMERIC Pd(II) COMPLEXES

#### 3.6.1 Mononuclear [*N*-(*n*-propyl)-(2-pyridyl and quinolyl) methanimine] dichloro Pd(II) complexes, C1-C4.

These complexes were prepared by using a similar procedure that was used by Chen *et al* [3] and Cloete *et al* [4]. Synthesis of **C1** is described as an example. Palladium bis-(acetonitrile) dichloride precursor (0.1985 g, 0.755 mmol) was introduced into a 100ml Schlenk tube which had previously been purged with nitrogen gas. The precursor was then dissolved in 10 ml of dry acetonitrile, and a deep-red solution was observed. Then a colourless solution of monofunctional methyl-pyridine ligand **ML-1** (0.200 g, 1.35 mmol) in 10 ml of dry acetonitrile was introduced into the above solution via a syringe. A dark-orange solution was observed immediately. This reaction was stirred at room temperature for 1 hour, after which the solvent was removed under vacuum and a deep-orange sticky residue was obtained. The residue was dissolved into DCM and layered with pentane and stored at -5°C yielding orange shiny needle-like crystals which were suitable for single X-ray analysis. Crystals were washed with an ice cold mixture of DCM/pentane (1:1) and dried under vacuum. All complexes were then characterised by <sup>1</sup>H and <sup>13</sup>C-NMR, FT-IR, MS (ESI) and elemental analysis.

#### 3.6.2 Multinuclear [*G*-1&2\_DAB-dendr-(NH<sub>2</sub>)<sub>*n*</sub>-1-(2-pyridyl and quinolyl)-imine] dichloro Pd(II) complexes, C5-C12.

Dendrimeric palladium dichloride complexes of pyridylimine and quinolyimine ligands were synthesised by the same method employed by Smith *et al* [6 & 7], van Wyk *et al* [20] and Malgas *et al* [18 & 19]. **Complex 5** is used as an example to describe the synthesis of these complexes (**C5-C12**). Palladium bis (acetonitrile) dichloride precursor (0.143 g, 0.549 mmol) was transferred to a 100 ml Schlenk tube followed by 10 ml of dry acetonitrile, upon stirring at room temperature under nitrogen gas a deep-red solution was observed. Separately G-1 Me-pyridine

dendrimeric ligand (**DL1**) (0.100 g, 0.137mmol) was dissolved in 5 ml of dry acetonitrile. This colourless solution was added drop-wise into the stirring solution of the palladium precursor. Immediately a yellow precipitate formed. This reaction was allowed to proceed for two hours. After the removal of solvent, an orange solid residue was obtained which was washed with dry DCM (10 ml x 7) in order to remove any unreacted substrate. All eight complexes (**C5-C12**) were characterised by FT-IR,  $^1\text{H}$  &  $^{13}\text{C}$ -NMR spectroscopies. Results are listed in Table 3.7.

### 3.7 X-RAY CRYSTALLOGRAPHIC STUDIES OF C1-C4.

#### 3.7.1 *Description of crystals for C1 & C2 and refinement parameters for data collections, see Appendix.*

**C1:** Needle shaped yellow crystals with approximate dimensions 0.59x0.08x0.04mm<sup>3</sup>. Refinement of 138 parameters based on all 2522 reflections yielded  $R_1= 0.0669$  and  $wR_2= 0.1571$  for  $I > 2\sigma(I)$  (1942 reflections).

**C2:** Prism shaped yellow crystals with approximate dimensions 0.18x0.11x0.09mm. Refinement of 58 parameters based on all 3768 reflections yielded  $R_1= 0.0439$  and  $wR_2= 0.1074$  for  $I > 2\sigma(I)$  (3171 reflections).

#### 3.7.2 *Description of crystals for complexes C 3& C4 and refinement parameters for data collections see Appendix.*

**C3:** Prism shaped red crystals with approximate dimensions 0.146x0.139x0.110mm. Refinement of 137 parameters based on all 2634 reflections yielded  $R_1= 0.0231$  and  $wR_2= 0.0544$  for  $I > 2\sigma(I)$  (2444 reflections).

**C4:** Prism shaped orange crystals fragment with approximate dimensions 230x140x100mm<sup>3</sup>. Refinement of 163 parameters based on all 2725 yielded  $R_1 = 0.0174$  and  $wR_2= 0.0450$  for  $I > 2\sigma(I)$  (2811 reflections).

### 3.8 STRUCTURAL DETERMINATION (C1-C4)

Single crystals of C1-C4 were mounted on a fine focus sealed tube. The crystal data were collected at 100(2) K on a Bruker APEX-CCD area detector diffractometer with a MoK $\alpha$  radiation ( $\lambda = 0.71073 \text{ \AA}$ ) by using a  $\omega$ -2 $\theta$  scan mode. Data collection and reduction were performed using *SMART* and *SAINTE* software. All the structures were solved by direct methods and non-hydrogen atoms were subjected to an isotropic refinement by full-matrix least squares on  $F^2$  using *SHELXTL* package [ref]. Structural refinement and solutions were obtained by *SHELXL* and *SHELXS* respectively.

**3.9 REFERENCES**

- [1] D.M. Haddleton, D.J. Duncalf, *Eur. J. Inorg.Chem.* (1998) 1799.
- [2] W. Massa, S. Dehghampour, *Inorg .Chem.* 362 (2009) 2872.
- [3] R. Chen, J. Bacsá, S.F. Mapolie, *Polyhedron.* 22 (2003) 2855.
- [4] J.Cloete, S.F. Mapolie, *J. Mol. Catal. A:* 243(2006) 221.
- [5] T. Kylmala, N. Kuuloja, Y.Xu, K. Rissanen, R. Franzen, *Eur J. Chem* (2008) 4019.
- [6] G. Smith, R. Chen, S. Mapolie, *J.Organomet.Chem,* 673 (2003) 111.
- [7] G. Smith, S.F. Mapolie, *J. Mol .Catal .A:* Chem 213 (2004) 187.
- [8] M .Kettunen, C .Vedder, H-H .Britzinger, I .Mutikainen, M .Leskela, T .Repo, *Eur .J .Inorg .Chem* (2005) 1081.
- [9] S .Nelana, J .Cloete, G .Lisenskey, E .Nordlander, I .Guzei, S .Mapolie, J Darkwa, *J. Mol. Catal. A:* 285 (2008) 72.
- [10] P .Pelagatti, M .Corcell, M .Costa, S .Ianeli, C .Pelizzi, D .Pogoline, *J. Mol. Catal. A:* 226 (2005) 107.
- [11] K .Komura, H .Nakamura, Y .Sugi, *J. Mol .Catal. A:* 293(2008) 72.
- [12] S .Bach, T .Sepeda, G .Merrill, J .Walmsley, *J. Am. Soc .Mass Spectrom.* 16 (2005) 1461.
- [13] W .Zawartka, A .Gniewek, A .Trzeciak, J .Ziolkowski, J .Pernak, *J. Mol. Catal .A:* 304 (2009) 8.
- [14] K .Neo, Y .Neo, S .Chien, G .Tan, A .Wilkins, W .Henderson, T .Hor, *Dalton Trans.*, (2004) 2281.
- [15] D .Tomazela, F .Gozzo, G .Ebeling, P .Livotto, M .Eberlin, J .Dupont, *Inorg Chim .Act.* 357 (2004) 2349.
- [16] F .Tjosaas, A .Fiksdahl, *J.Organomet .Chem.* 692 (2007) 5429.
- [17] P .Chardrasokaran, J .Mague, M. Balakrishna, *Inorg .Chem,* 45 (2006) 6678 .
- [18] R .Malgas, S.F .Mapolie, S.O .Ojwach, G .S Smith, J .Darkwa, *Catal . Commun.* 9 (2008) 1612.
- [19] R . Malgas-Enus, S.F .Mapolie, G.S . Smith, *J. Organomet. Chem.* 693 (2008) 2279.
- [20] J.L van Wyk, *Mono-nuclear and multinuclear salicylaldimine metal complexes as catalysts precursors in the oxidation of phenol and cyclohexane,* PhD Thesis, University of the Western Cape (2008).

- [21] D .Drew, J.R .Doyle, *Inorg .Synth*, 13 (1972) 47.  
[22] G.K .Anderson, M .Lin, *Inorg .Synth*, 28 (1990) 60.

## CHAPTER FOUR

### CATIONIC MONO AND POLY-NUCLEAR Cu(I) COMPLEXES BASED ON PYRIDYL AND QUINOLYL-IMINE LIGANDS: SYNTHESIS AND SPECTROSCOPIC CHARACTERISATION.

---

---

#### CONTENT

4.1 INTRODUCTION	104
4.2 RESULTS AND DISCUSSION	105
4.2.1 Bis[N-(n-propyl)-1-(2-pyridyl and quinolyl) methanimine] Cu(I) Tetrafluoroborate complexes, <b>C13-C16</b>	105
4.2.1.1 <i>Infrared and <sup>1</sup>H-NMR spectroscopic studies of mononuclear         Complexes</i>	106
4.2.1.2 <i>ESI mass spectrometric studies of mononuclear complexes</i>	109
4.2.1.3 <i>UV/Vis spectroscopic studies of mononuclear Cu(I)         complexes</i>	109
4.2.1.4 <i>Single-Crystal X-ray crystallographic studies of cationic         mononuclear Cu(I) complexes</i>	111
4.2.2 Synthesis of cationic multinuclear dendrimeric Cu(I) complexes	113
4.2.2.1 <i>Mass spectrometric studies of polynuclear copper (I)         complexes</i>	114
4.2.2.2 <i>UV/Vis and Infrared spectroscopic studies of polynuclear         copper(I) complexes</i>	116
4.2.2.3 <i>Micro-analysis and <sup>1</sup>H-NMR spectroscopic studies of         polynuclear copper(I) complexes</i>	118
4.3 CONCLUDING REMARKS	120
4.4 EXPERIMENTAL SECTION	121
4.4.1 General remarks and instrumentation	121
4.4.2 Materials	121
4.5 SYNTHESIS OF MONO AND POLYNUCLEAR COPPER(I) COMPLEXES	122

## CHAPTER FOUR

### CATIONIC MONO AND POLY-NUCLEAR Cu(I) COMPLEXES BASED ON PYRIDYL AND QUINOLYL-IMINE LIGANDS: SYNTHESIS AND SPECTROSCOPIC CHARACTERISATION.

---

---

4.5.1	Mononuclear Bis[N-(n-propyl)-1-(2-pyridyl and quinolyl)-methanimine] Cu(I) Tetrafluoroborate complexes, <b>C13-C16</b>	122
4.5.2	Multinuclear [G1&2_DAB-dendr-(NH <sub>2</sub> ) <sub>n</sub> -1-(2-pyridyl and quinolyl)-imine] Cu(I) Tetrafluoroborate complexes, <b>C17-C24</b>	122
4.6	X-RAY CRYSTALLOGRAPHY	123
4.6.1	Description of crystals for <b>C14</b> and refinement parameters for data collections, see Appendix	123
4.7	REFERENCES	124



## 4.1 INTRODUCTION

Copper(I) complexes based on di-imine ligands are of growing interest as most of these complexes combine remarkable features such as ease of preparation, reversible electrochemical behaviour, light absorption in the visible spectral region, long-lived electronically excited states and intense luminescence [1-11]. However, the emission signal from the charge transfer (CT) excited state of copper(I) complexes is typically weak and short-lived because of the lowest-energy CT state of a  $d^{10}$  system involving excitation from metal-ligand d-orbitals [3 & 6]. Scott and co-workers reported the synthesis of copper(I) Tetrafluoroborate complexes with binaphthylidene and biquinoline ligands. These complexes showed irreversible reduction processes [7]. As it was reported in Chapter 3, multinuclear complexes are of great interest because of their higher activity as compared to their mononuclear analogues. Lind *et al* [8] reported the synthesis of trinuclear copper(I) complexes containing 3,4,9,10,15,16-hexamethyl-1,6,7,12,13,18-hexaazatrinaphthylene which showed two bands in the visible region attributed to ligand-centred and MLCT transitions respectively.

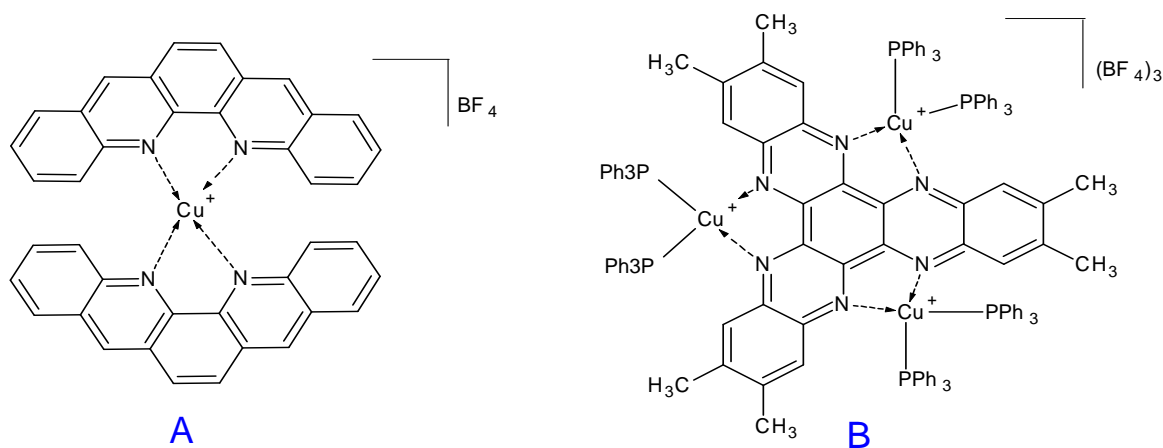


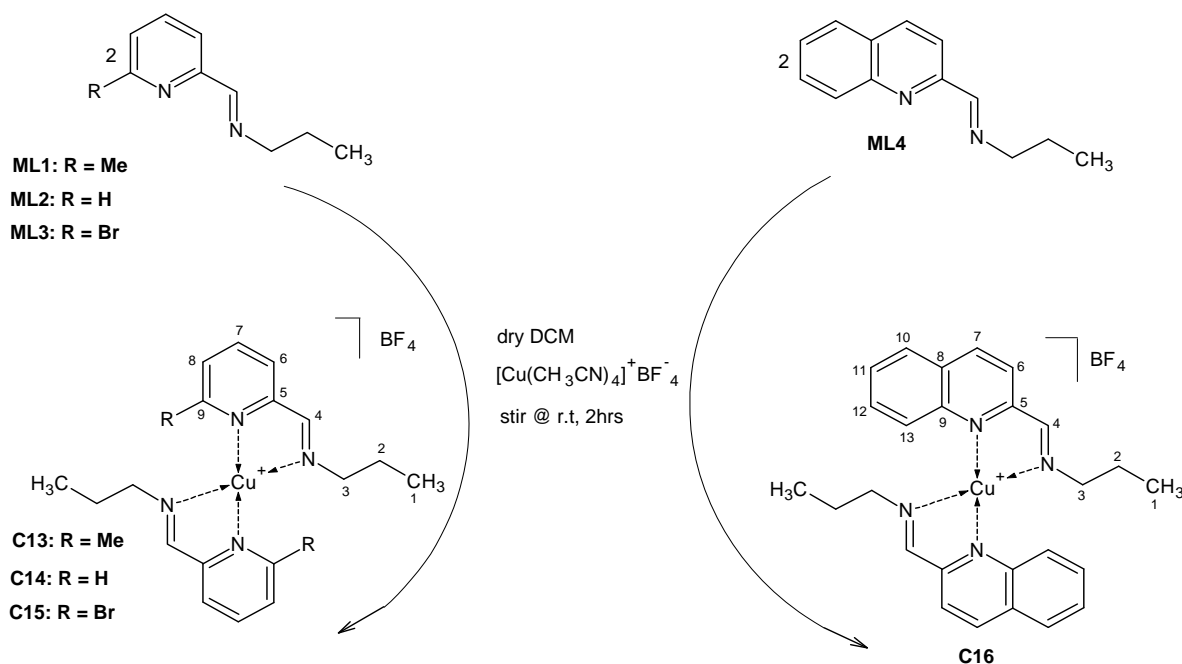
**Figure 4.1:** (A) mononuclear (B) trinuclear copper(I) tetrafluoroborate complexes [7&8]

In this Chapter we report the synthesis and spectroscopic characterisation of some copper(I) mononuclear and multinuclear dendrimeric tetrafluoroborate complexes.

## 4.2 RESULTS AND DISCUSSION

### 4.2.1 Bis[*N*-(*n*-propyl)-1-(2-pyridyl and quinolyl) methanimine] Cu(I)Tetrafluoroborate complexes, C13-C16.

Copper complexes were prepared by the same procedure that was reported by Haddleton *et al* [9] and by Fu *et al* [11]. All copper(I) complexes (**C13-16**) were prepared by reacting monofunctional di-imine ligands (**ML1-ML4**) with tetrakis(acetonitrile)copper(I) tetrafluoroborate as the metal precursor by using a 1:2 ratio of metal precursor to ligand. The synthesis is illustrated in Scheme 4.1. **C13 & C14** were isolated as dichroic blocks and plates respectively. Dichroic means the crystals display a green or yellow colour under polarized light depending on the angle of the light source. **C15** was obtained as deep-red needle-like crystals whereas **C16** formed deep-purple prisms. These crystals were obtained after slow diffusion of Et<sub>2</sub>O into very concentrated DCM solutions of **C13-C16**. These complexes, **C13-C16** were very stable at room temperature in the solid state but they show some decomposition when left in solution for prolong periods. The complexes were soluble in common organic solvents such as CHCl<sub>3</sub>, CH<sub>2</sub>Cl<sub>2</sub>, CH<sub>3</sub>CN and THF. They were obtained in very good yields and they were characterised by various analytical techniques as shown in Tables 4.1-4.4.



**Scheme 4.1:** Synthesis of cationic mononuclear copper(I) tetrafluoroborate complexes based on pyridyl and quinolyl-imine ligands.

#### 4.2.1.1 Infrared and <sup>1</sup>H-NMR spectroscopic studies

IR spectra of the copper complexes (**C13-16**) showed that complexation of ligands **ML1-4** in 2:1 ratio of ligand to the copper precursor was successfully achieved, because there is a significant change in position of the  $\nu$  (C=N) band in the IR spectrum. For **C13**, **C14** & **C16**, this band occurs around 1590 cm<sup>-1</sup>. The presence of an electron-withdrawing group at position six of the pyridine ring influenced the position of the  $\nu$ (C=N) stretch for **C15** at a lower wave-number (1582 cm<sup>-1</sup>). It is suspected that an EWG reduces the delocalisation of electron density in the pyridine ring which affects the  $\nu$ (C=N) stretch. These results are within the range of those published for similar complexes [1, 2 & 12]. These previously reported complexes also show a very broad and intense band at 1030-1032 cm<sup>-1</sup> which was not observed in the case of free mono-functional ligands. This band is due to vibrations of the B-F bond of the BF<sub>4</sub><sup>-</sup> counter ion.

<sup>1</sup>H-NMR spectral data obtained for these cationic copper complexes together with the relevant assignments are provided in Table 4.2. The data obtained supports the structures depicted in Scheme 4.1, and are in good agreement with proton NMR data observed for other copper complexes [9-11]. The resonance for the HC=N proton is observed as a sharp singlet downfield as compared to their analogous ligands in the region  $\delta$  8.53-9.19 ppm in the spectra of all complexes. This confirms coordination of the ligands to the copper metal. The chemical shifts due to the protons of the aromatic rings are similar to those of the ligands, but there is a slightly downfield shift due to coordination of the metal. The methyl substituent in the six position of the pyridine ring in **C13** is observed as a sharp upfield singlet at  $\delta$  2.1 ppm. The aliphatic protons of **C13** & **C14** are exactly the same, in that H-1, H-2 and H-3 occur at 0.81, 1.56 and 3.76 ppm respectively for both complexes. For **C15** there is a slight downfield shift (H1:0.87, H2:1.63 & H3:3.83 ppm). The presence of the bromide substituent at position six of the pyridine ring plays a big role in this. The proton NMR data obtained for these complexes confirm that copper(I) complexes are diamagnetic (d<sup>10</sup>), because all the peaks can be clearly defined and resolved, which is not the case for d<sup>9</sup> systems.

**Table 4.1:** Characterisation data of mononuclear Cu(I) complexes (C13-16)

Mono-nuclear complexes	Physical Appearance	% Yield	Melting Point (°C)	Molecular Formula	ESI-MS [M+H] <sup>+</sup> (m/z) Calculated (Found)	Micro-analysis Calculated (Found)		
						%C	%H	%N
C13	Deep-red needles	85	85-87	C <sub>20</sub> H <sub>28</sub> BCuF <sub>4</sub> N <sub>4</sub>	474.81 (475)	n.d	n.d	n.d
C14	Dichroic plates	78	105-108	C <sub>9</sub> H <sub>12</sub> BCuF <sub>4</sub> N <sub>4</sub>	359.95 (361)	48.39 (47.92)	5.41 (5.59)	12.54 (12.71)
C15	Dark-brown needles	80	145-147	C <sub>18</sub> H <sub>22</sub> BBr <sub>2</sub> CuF <sub>4</sub> N <sub>4</sub>	604.55 (605)	n.d	n.d	n.d
C16	Dark-purple prisms	83	155-159	C <sub>13</sub> H <sub>14</sub> BCuF <sub>4</sub> N <sub>4</sub>	460.07 (461)	57.10(57.44)	5.16(5.18)	10.24(9.91)

**Table 4.2:**  $^1\text{H}$ - Chemical shifts of mononuclear Cu(I) complexes (**C13-16**)<sup>a</sup>

<b>Cu<sup>I</sup> complexes</b>	<b>Aliphatic protons</b>				<b>Aromatic protons</b>							
	<b><math>\delta</math> (ppm)</b>											
<b>c</b>	H-1	H-2	H-3	H-4	H-6	H-7	H-8	H-9	H-10	H-11	H-12	H-13
<b>C13</b>	0.81 (t,3H)	1.55 (m,2H)	3.76 (t,2H)	8.86 (s,1H)	7.88 (d,1H)	8.10 (t,1H)	7.67 (d,1H)		2.18 <sup>b</sup> (s,3H)			
<b>C14</b>	0.81 (t,3H)	1.56 (m,2H)	3.76 (t,2H)	8.53 (s,1H)	8.19 (d,1H)	8.03 (t,1H)	7.74 (t,1H)	8.87 (d,1H)				
<b>C15</b>	0.87 (t,3H)	1.63 (m,2H)	3.81 (t,2H)	8.89 (s,1H)	8.01 (d,1H)	8.04 (t,1H)	8.18 (d,1H)					
<b>C16</b>	0.74 (t,3H)	1.53 (m,2H)	3.83 (t,2H)	9.19 (s,1H)	8.89 (d,1H)	8.31 (d,1H)			8.24 (d,1H)	7.64 (t,1H)	7.69 (t,1H)	8.15 (d,1H)

<sup>a</sup>  $^1\text{H}$ -NMR in DMSO- $d_6$ , 400MHz<sup>b</sup> Me-pyr (CH<sub>3</sub>)<sup>c</sup> Numbering scheme see Scheme 4.1

#### 4.2.1.2 Micro-analysis and ESI- mass spectrometric studies of mononuclear complexes

Some of the mononuclear complexes (**C2 & C4**) were characterised by micro-analysis as shown in Table 4.1. These results confirm the purity of the compounds.

All the copper complexes were also characterised by electron spray ionisation mass spectrometry. The phenomenon of forming a dimeric species was not observed in the case of copper(I) complexes (**C13-C16**) as obtained for mono-nuclear palladium(II) complexes (**Chapter 3**). The fragmentation patterns of these complexes showed similar trends. The first fragmentation is due to the loss of one ligand  $[\text{Cu(I)}\text{L}_2\text{-L}]^+$  forming an unstable copper species  $[\text{Cu(I)}\text{L}]^+$  which readily undergoes demetallation to form the corresponding ligand  $[\text{L}]^+$ . Haddleton *et al* [9] observed the same type of fragmentation pattern for their copper complexes. What was also observed in the mass spectra of these complexes (**C13-C16**) is the appearance of a set of weak signals at  $m/z$  values greater than that of the expected parent ion. These high  $m/z$  peaks correlate well with the calculated molecular mass of oligomeric analogues consisting of three repeat units. The formation of coordination oligomers is not unusual for copper(I) complexes [12-16]. Chandrasokarana *et al* reported the first  $\text{Cu}^{\text{I}}$  coordination polymer of cyclodiphosphazones, which undergo rare reversible transformations into the corresponding mono-nuclear analogues [16]. Recently it has been noted that silver(I) complexes based on bis-tridentate  $N,N'$  donor ligands can also undergo polymeric coordination [15]. It is assumed that these polymeric species are formed during the mass spectral analysis. Single crystal analysis of some of these copper complexes shows no evidence of polymeric species.

#### 4.2.1.3 UV/Vis spectroscopic studies of mononuclear copper(I) complexes

The mononuclear Copper(I) complexes were also characterized by ultra-violet visible spectroscopy. The spectra of these complexes were obtained as DCM solutions at low concentration ( $10^{-5}\text{M}$ ). The electronic absorption spectra of these complexes at room temperature are depicted in Figures 4.2 & 4.3. For all of the complexes (**C13-C16**) three absorption bands are observed. The first absorption band in the region of 235-250 nm are attributed to the intramolecular ligand ( $\pi\text{-}\pi^*$ ) transitions of the aromatic rings (pyridine and quinoline). It is well documented that intense absorptions at  $\lambda_{\text{max}} < 340$  nm can be assigned to ( $\pi\text{-}\pi^*$ ) transitions in such systems [17-23]. The second band at 278-311 nm can be assigned to

$n-\pi^*$  transitions of the azomethine chromophore. van Wyk *et al* and Massa *et al* observed similar transitions for their Schiff base complexes [17-23]. A third absorption band was observed at low energy around 477 nm for pyridine based complexes and at 530 nm for the quinoline based species, **C16** and is attributed to metal-to-ligand charge transfer (MLCT) transitions which are characteristic features of copper(I) complexes when bonded to conjugated organic chromophores such as (C=N) [17].

**Table 4.3:** FT-IR and UV/Vis spectroscopic data for mono-nuclear cationic copper(I) complexes

Complexes	UV/Vis <sup>a</sup> $\lambda_{\max}$ (nm)	FT-IR spectra (cm <sup>-1</sup> ) <sup>b</sup>	
		$\nu$ C=N)	$\nu$ (B-F)
<b>C13</b>	250, 283, 477	1592	1030
<b>C14</b>	247, 278, 477	1593	1032
<b>C15</b>	235, 288, 477	1582	1029
<b>C16</b>	250, 311, 530	1591	1049

<sup>a</sup>10<sup>-5</sup>M, DCM

<sup>b</sup>Neat (ATR)

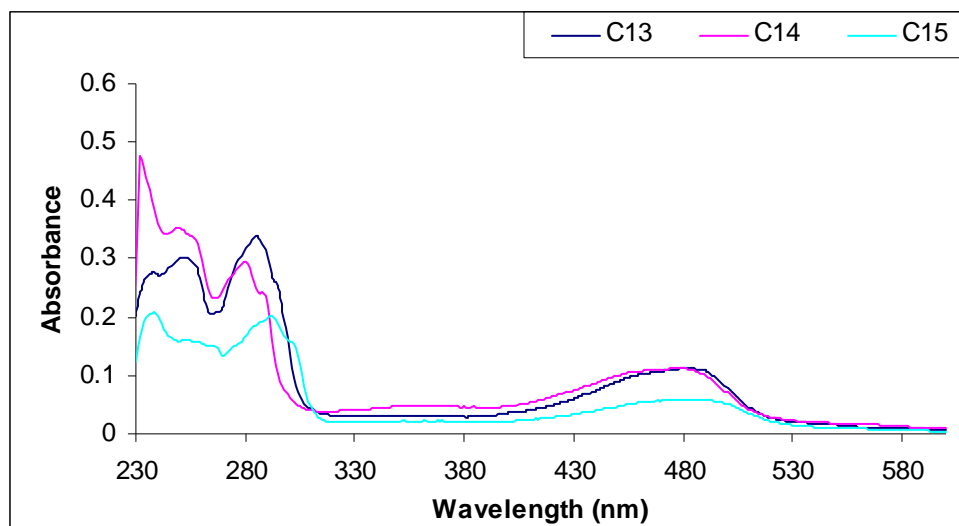


**Figure 4.2:** UV/Vis absorption spectrum of C13-C15 in DCM solution ( $10^{-5}M$ ) at room temperature.

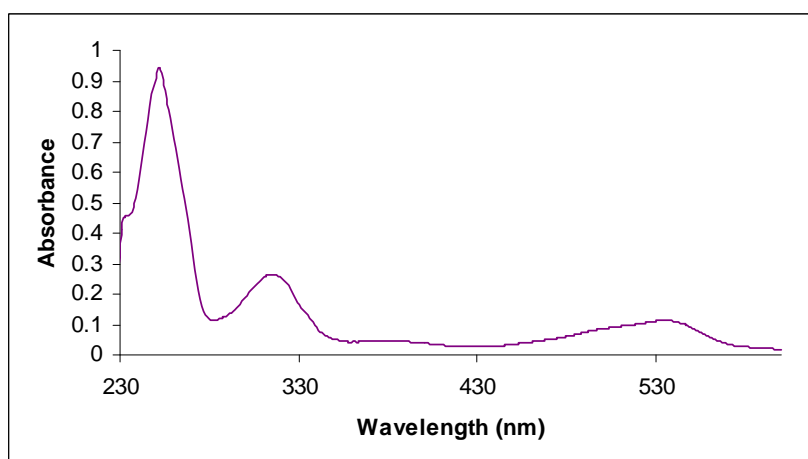


**Figure 4.3:** UV/Vis absorption spectrum of C16 in DCM solution ( $10^{-5}M$ ) at room temperature.

#### 4.2.1.4 Single-Crystal X-ray crystallographic studies of cationic mononuclear Cu(I) complex.

Crystals of **C14** suitable for X-ray diffraction analysis were obtained as already described above. The crystal structural data and crystal refinement parameters of the copper complex are presented in Table 4.4 & Appendix respectively. This complex adopts a distorted tetrahedral geometry. This is a characteristic feature of copper(I) complexes [21]. Haddleton and co-workers reported the same geometry for their [*N*-Alkyl-(2-pyridyl) methanimine] copper(I) complexes [9].



### Structural description of **C14**

The molecular structure of **C14** (Figure 4.4) reveals bis-bidentate chelation of two propyl-pyridin-2-ylmethylene-amine ligands to one copper centre. The geometry around the metal centre is observed to be distorted tetrahedral, which is a typical geometrical arrangement for [N-Alkyl-(2-pyridyl) methanimine] copper(I) systems [9]. The bond angles N(1)-Cu-N(2), N(1)-Cu-N(2)', N(1)-Cu-N(2) and N(2)'-Cu-N(1)' are in the range 81-138° and are significantly different from the ideal 109° angle expected for a tetrahedral conformation. These crystallographic values compared well with those reported by Massa *et al* for their copper(I) complexes with bis-bidentate iminopyridine ligands [10]. Malassa *et al* also reported a distorted tetrahedral zinc 8-amidoquinoline mono-nuclear complex [24].

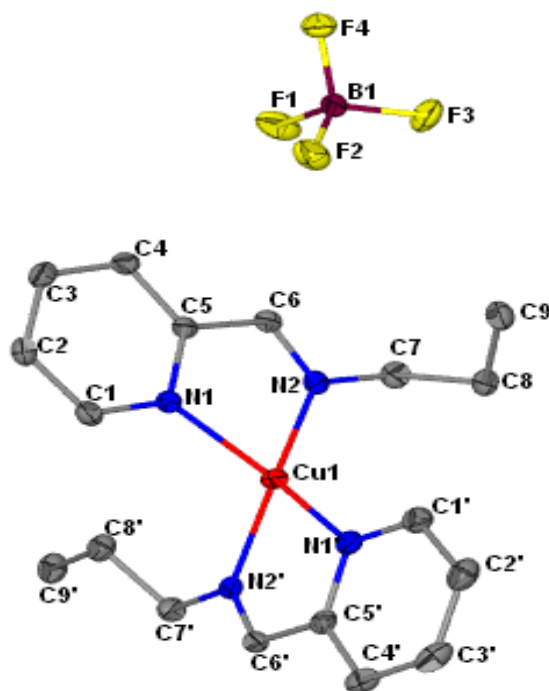


**Figure 4.4:** The molecular structure of **C14** showing crystallographic numbering.

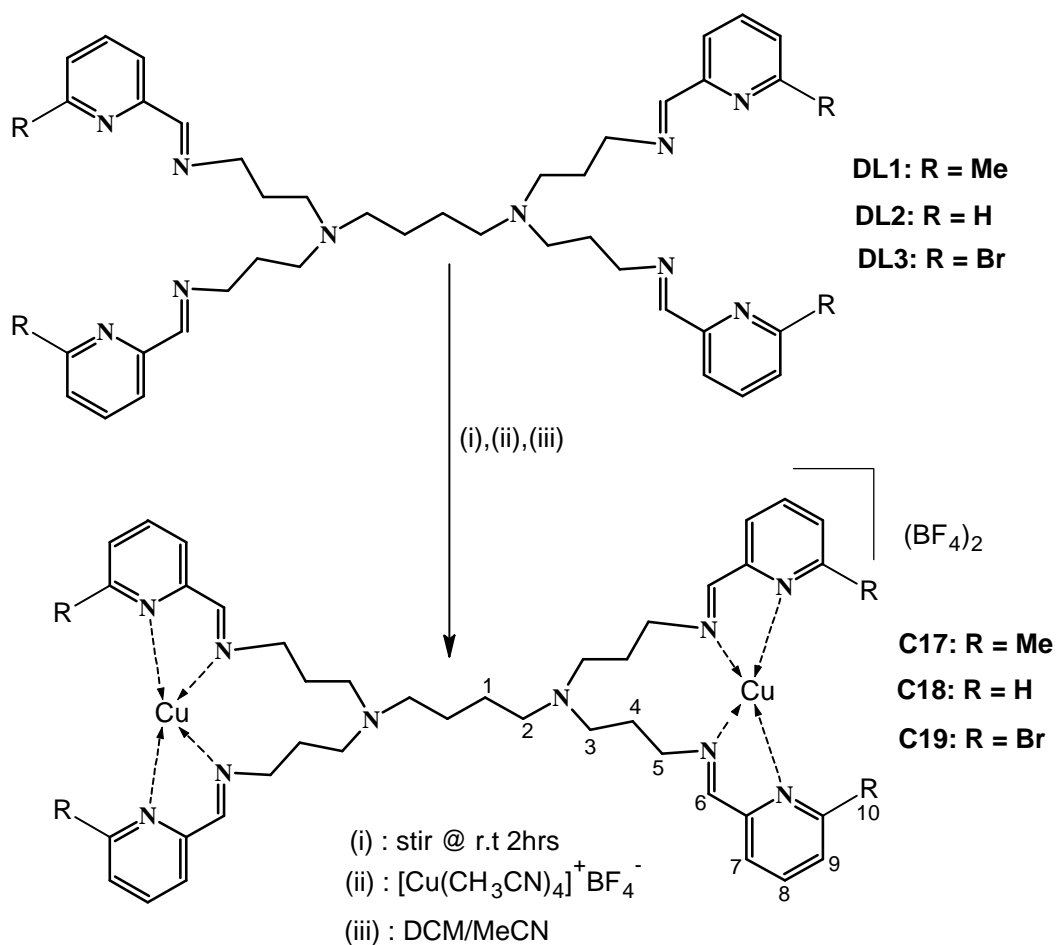
**Table 4.4:** Selected bond lengths (Å) and angles (°) for the core of **C14**

Bond length (Å)		Bond angles (°)	
Cu-N(1)	2.0805 (13)	N(1)-Cu-N(2)	81.55(5)
Cu-N(2)	1.9846 (13)	N(1)-Cu-N(1)'	118.09(5)
Cu-N(1)'	2.0615 (13)	N(1)'-Cu-N(2)	126.35(5)
Cu-N(2)'	2.0015 (13)	N(1)'-Cu-N(2)'	81.37(5)
N(1)-C(5)	1.3537 (2)	N(2)'-Cu-N(2)	138.71(5)
N(2)-C(6)	1.2763 (2)	N(2)'-Cu-N(1)	114.30(5)
N(1)'-C(5)'	1.3523 (2)		
N(2)'-C(6)'	1.2763 (2)		
C(6)-C(5)	1.4705 (2)		
C(6)'-C(5)'	1.4673 (2)		

#### 4.2.2 Synthesis of cationic multinuclear dendrimeric Cu(I) complexes

Again for these complexes the synthetic procedures reported by Haddleton et al [9] and by Fu *et.al* [11] were used. The cationic copper(1) complexes (**C17-24**) were obtained by complexation of generation 1 or 2 pyridylimine and quinolyylimine ligands **DL1-DL8** with tetrakis (acetonitrile) copper(I) tetrafluoroborate as the metal precursor by using different ratios of metal precursor to ligand. In the case of **C17-C20** a 2:1 ratio of copper precursor to ligand was used, and a 4:1 ratio was used for generation-2 copper metallodendrimers (**C21-24**). The synthesis of generation-1 complexes based on pyridine ligands (**C17-C19**) is presented in Scheme 4.2 while Figure 4.5 illustrates the generation-2 metallodendrimers and quinoline based generation 1 metallodendrimers. The dendritic complexes were recrystallised by slow diffusion of diethyl-ether into DCM solutions at -5°C. **C17-19 & C21-C23** were isolated as brown amorphous solids while **C20 & 22** were obtained as purple amorphous solids. These complexes were stable in the solid state but in solution they tend to undergo

some decomposition which is normally observed by a colour change to green. This possibly involves the oxidation of the  $\text{Cu}^{\text{I}}$  to  $\text{Cu}^{\text{II}}$ .  $\text{Cu}^{\text{II}}$  complexes of di-imine ligands tend to be green in colour. These cationic metallodendrimers were soluble in common organic solvents such as DCM,  $\text{CH}_3\text{CN}$  and THF and they were obtained in very good yields. All of the  $\text{Cu}^{\text{I}}$  metallodendrimers were successfully characterized by MS (ESI),  $^1\text{H}$  &  $^{13}\text{C}$ -NMR, FT-IR and, UV/Vis spectroscopies. Some of these complexes were also characterised by micro-analysis and all the analytical data is given in Tables 4.5-4.7.



**Scheme 4.2:** Synthesis of first generation poly (propylene-imine) pyridylimine copper(I) tetrafluoroborate metallodendrimers (C17-C19).

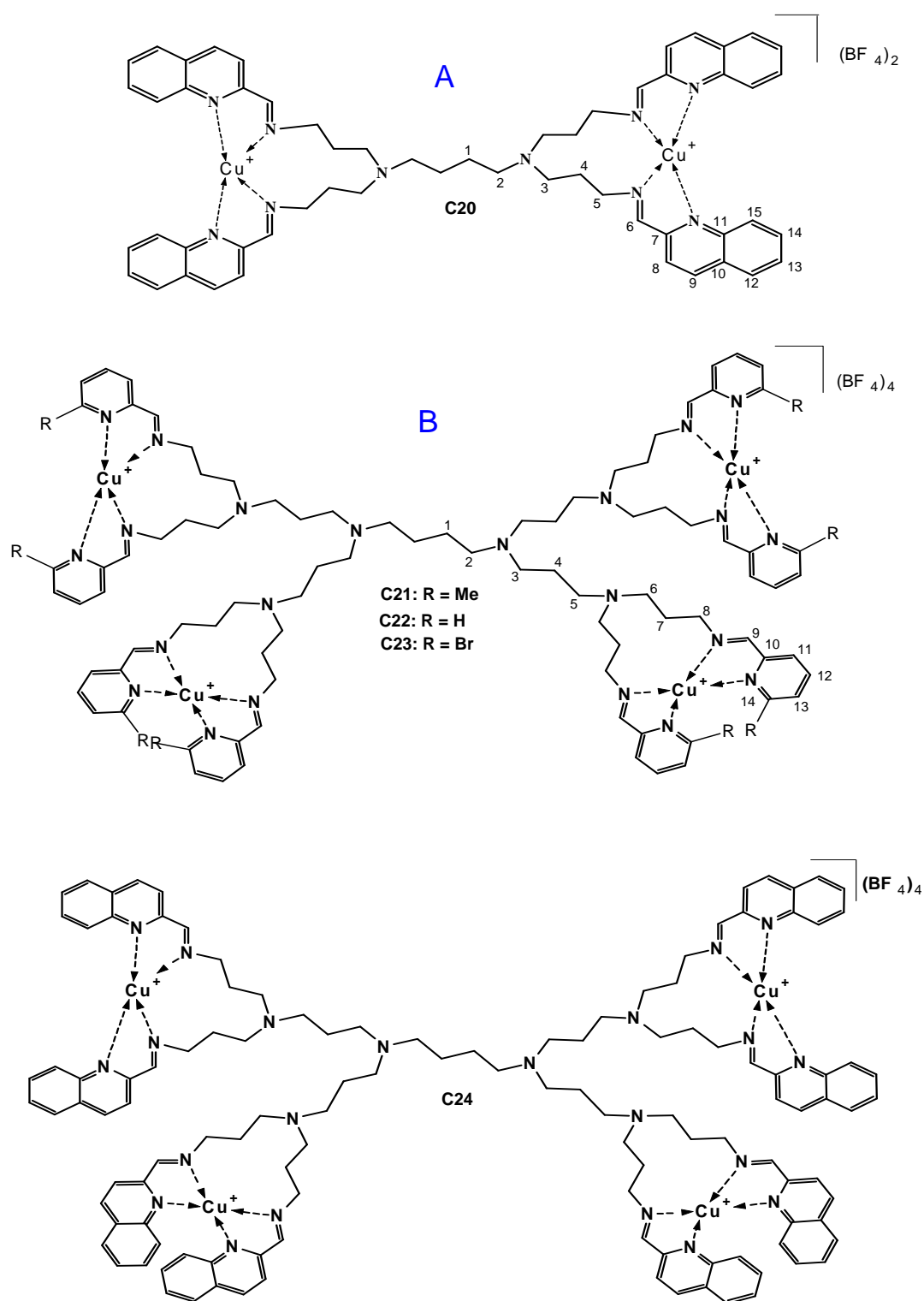


**Figure 4.5:** (A) First generation propylene-imine quinolyimine (B) second generation poly(propylene-imine) pyridylimine and quinolyimine copper(I) tetrafluoroborate metallodendrimers.

**Table 4.5:** characterisation data of cationic copper(I) metallodendrimeric complexes (C17-24)

Multinuclear complexes	Physical Appearance	% Yield	Melting Point (°C)	ESI-MS [M+H] <sup>+</sup> (m/z) Calculated (Found)	Molecular Formula	Micro-analysis Calculated (Found)		
						%C	%H	%N
C17	Deep-red	94	147-149	856.11 (428)	C <sub>44</sub> H <sub>60</sub> B <sub>2</sub> Cu <sub>2</sub> F <sub>8</sub> N <sub>10</sub>	<b>n.d</b>	<b>n.d</b>	<b>n.d</b>
C18	Brown	87	150-155	799.99 (401)	C <sub>40</sub> H <sub>52</sub> B <sub>2</sub> Cu <sub>2</sub> F <sub>8</sub> N <sub>10</sub>	49.35 (46.97)	5.38 (5.31)	14.39 (14.19)
C19	Marrown	90	169-170	1115.58 (557)	C <sub>40</sub> H <sub>48</sub> B <sub>2</sub> Cu <sub>2</sub> F <sub>8</sub> N <sub>10</sub>	<b>n.d</b>	<b>n.d</b>	<b>n.d</b>
C20	Purple	93	169-171	1000.23 (501)	C <sub>56</sub> H <sub>60</sub> B <sub>2</sub> Cu <sub>2</sub> F <sub>8</sub> N <sub>10</sub>	57.30(57.24)	5.15(5.19)	11.93(12.28)
C21	Deep-red	89	166-169	2199.66(734) <sup>a</sup>	C <sub>96</sub> H <sub>136</sub> B <sub>4</sub> Cu <sub>4</sub> F <sub>16</sub> N <sub>22</sub>	<b>n.d</b>	<b>n.d</b>	<b>n.d</b>
C22	Brown	80	155-159	1740.23 (871)	C <sub>88</sub> H <sub>120</sub> B <sub>4</sub> Cu <sub>4</sub> F <sub>16</sub> N <sub>22</sub>	50.63 (49.03)	5.79 (5.98)	14.76 (14.62)
C23	Marrown	87	171-173	2718.61(906) <sup>a</sup>	C <sub>88</sub> H <sub>112</sub> Br <sub>8</sub> B <sub>4</sub> Cu <sub>4</sub> F <sub>16</sub> N <sub>22</sub>	<b>n.d</b>	<b>n.d</b>	<b>n.d</b>
C24	Purple	92	175-179	2140.70 (714) <sup>a</sup>	C <sub>120</sub> H <sub>136</sub> B <sub>4</sub> Cu <sub>4</sub> F <sub>16</sub> N <sub>22</sub>	57.93(58.45)	5.51(6.00)	12.39(11.95)

<sup>a</sup> :triply charged ions

n.d: Not determined

**Table 4.6:**  $^1\text{H}$ -NMR data cationic copper(I) metallodendrimers (**C17-C20**)<sup>a</sup>

Complexes	H1-4	H5	H6	H7	H8	H9	H10	H11
	ppm							
<b>C17</b>	1.54-2.73 br signals, core (12H)	3.89 (t, 8H)	8.88 (s, 4H)	7.86 (d, 4H)	8.09 (t, 4H)	7.67 (d, 4H)	2.21 (s, 4H)	
<b>C18</b>	1.68-2.65 br signals, core (12H)	3.76 (t, 8H)	8.50 (s, 4H)	7.98 (d, 4H)	7.71 (t, 4H)	8.15 (t, 4H)	8.83 (d, 4H)	
<b>C19</b>	2.16-2.72 br signals, core (12H)	3.95 (t, 8H)	8.86 (s, 4H)	7.97 (d, 4H)	8.00 (t, 4H)	8.12 (d, 4H)		
<b>C20</b>	1.56-2.53 br signal, core (12H)	3.81 (t, 8H)	9.19 (s, 4H)	7.66 (d, 4H)	7.70 (d, 4H)	8.21 (t, 4H)	8.31 (t, 4H)	8.87 (d, 4H)

Table 4.6 continued

<b>C21</b>	1.47-2.73 br signal core (24H)	3.80 (t, 16H)	8.89 (s, 8H)	7.87 (d, 8H)	8.12 (t, 8H)	7.68 (d, 8H)	2.22 (s, 8H)	
<b>C22</b>	1.61-2.76 br signal core (24H)	3.72 (t, 16H)	8.53 (s, 8H)	7.99 (d, 8H)	7.82 (t, 8H)	8.3 (t, 8H)	8.88 (d, 8H)	
<b>C23</b>	1.77-2.58 br, signal core (24H)	3.85 (t, 16H)	8.91 (s, 8H)	7.98 (d, 8H)	8.04 (t, 8H)	8.15 (d, 8H)		
<b>C24</b>	1.43-2.55 br signal core (24H)	3.78 (t, 16H)	9.18 (s, 8H)	7.73 (d, 8H)	7.55 (d, 8H)	8.18 (t, 8H)	8.40 (t, 8H)	8.88 (d, 8H)

<sup>a</sup>: 300MHz, DMSO-*d*<sub>6</sub>

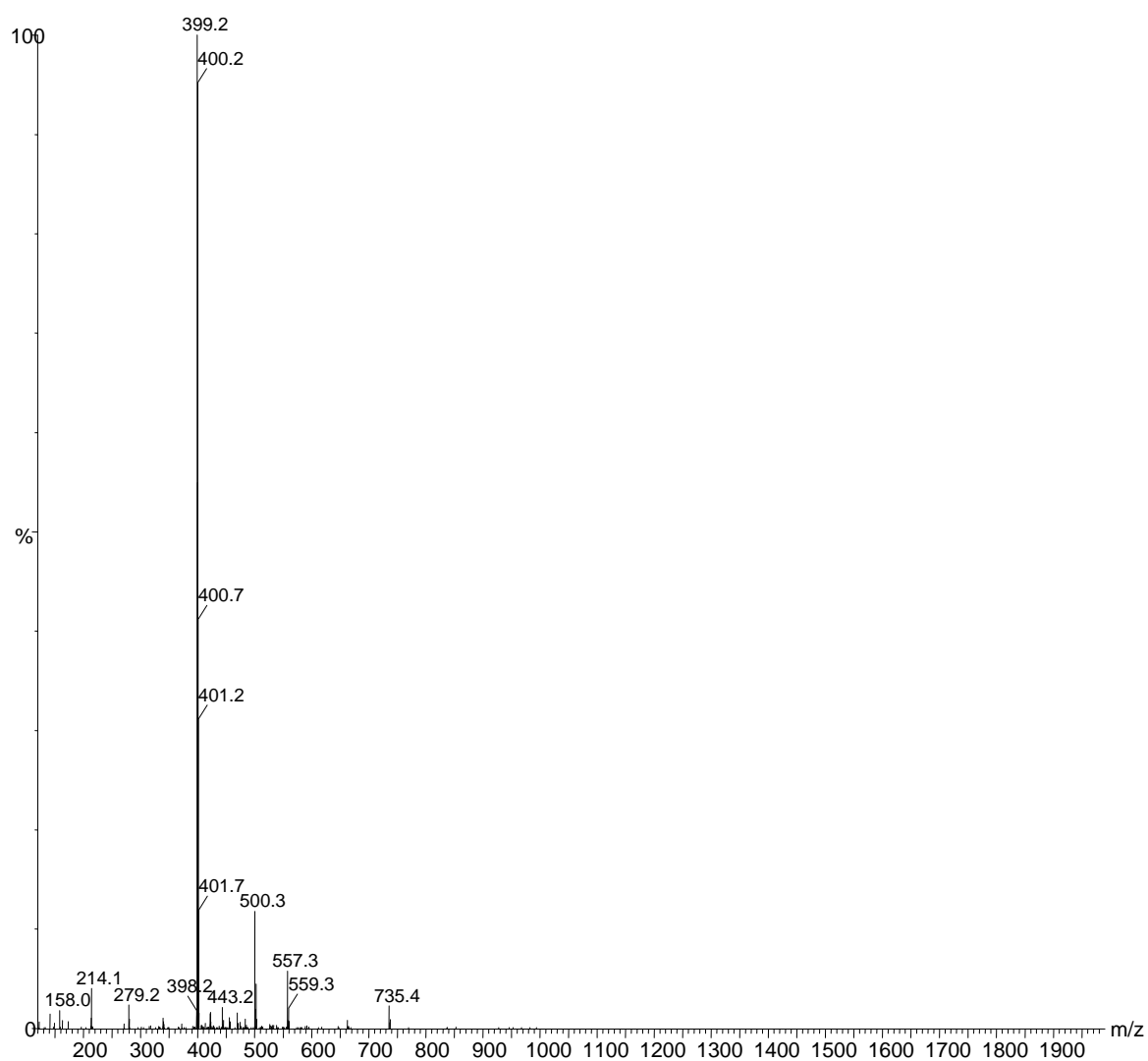


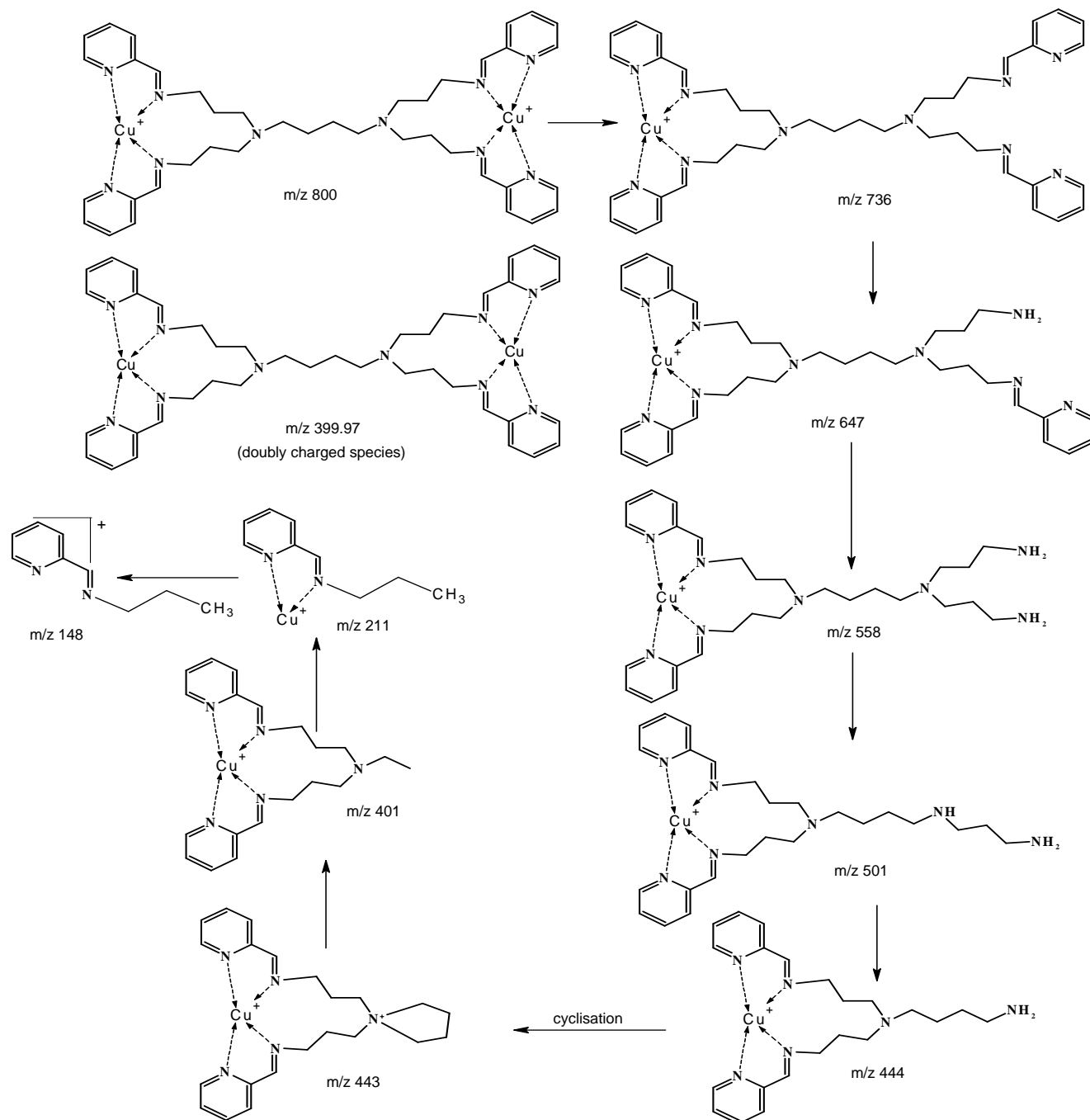
**Figure 4.6:** ESI-MS spectrum of first generation poly(propylene-imine) pyridylimine copper(I) tetrafluoroborate C18.

#### 4.2.2.1 Mass spectrometric studies of polynuclear copper(I) complexes

All metallodendrimeric complexes synthesized were also characterized by ESI-MS. Mass spectra of the complexes show the doubly charged molecular ion peak which correlates well with the calculated monoisotopic molecular mass. All the results are depicted in Table 4.5. For copper metallodendrimers the fragmentation patterns observed show similarities to those of their analogous dendrimeric ligands as discussed in Chapter 2. The most abundant peaks are due to multiply-charged ions. The first fragmentation is due to loss of the metal (demetallation) of one copper, which is followed by loss of peripheral functionalities arms



followed by cyclisation. Generation two metallodendrimers show fragments which correlate well with potassium adducts of **C18** ions as shown in Figure 4.3. All metallodendrimers behaved the same.



**Scheme 4.3:** Fragmentation pathway of first generation poly(propylene-imine) pyridylimine copper(I) tetrafluoroborate complex **C18**.

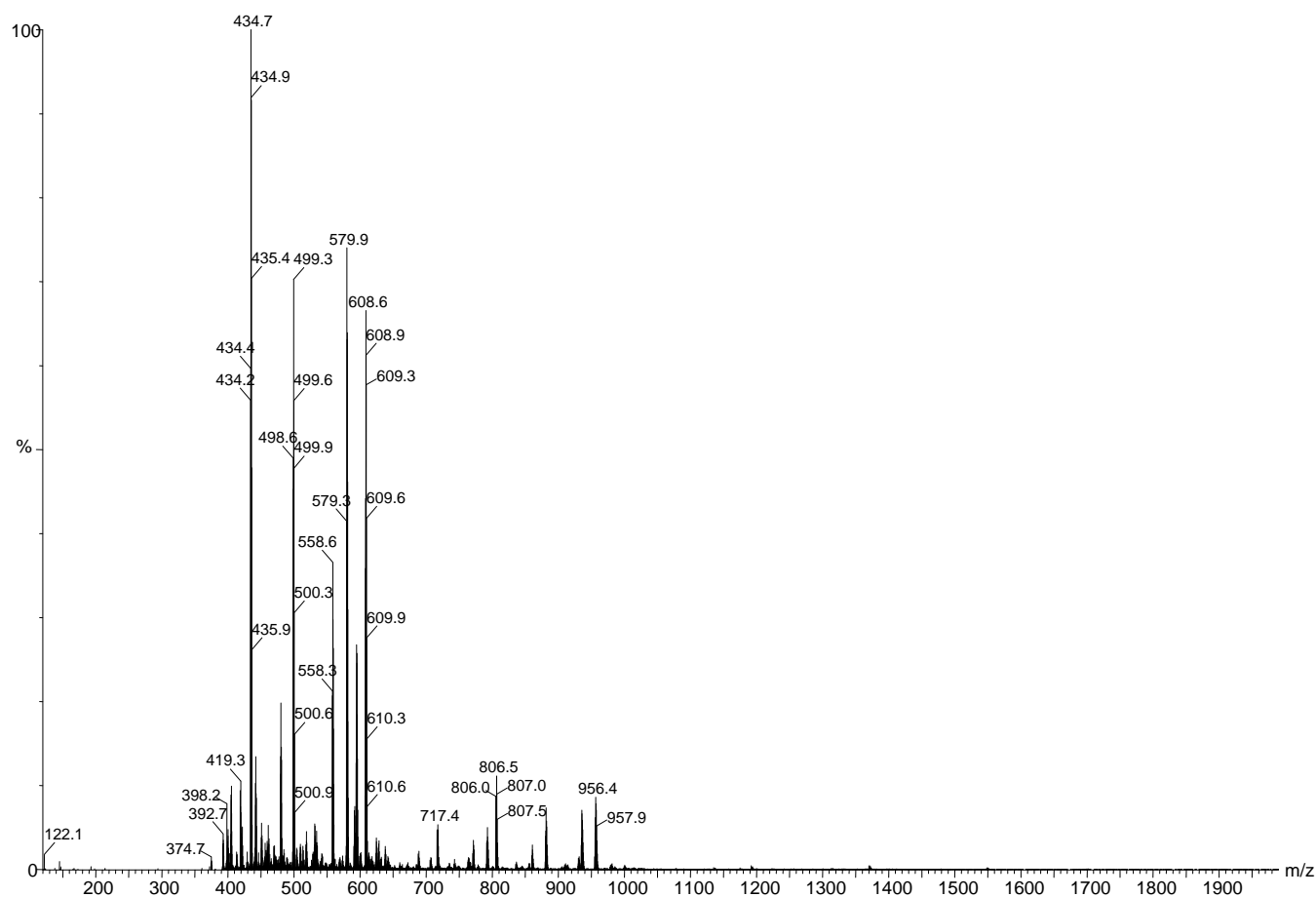
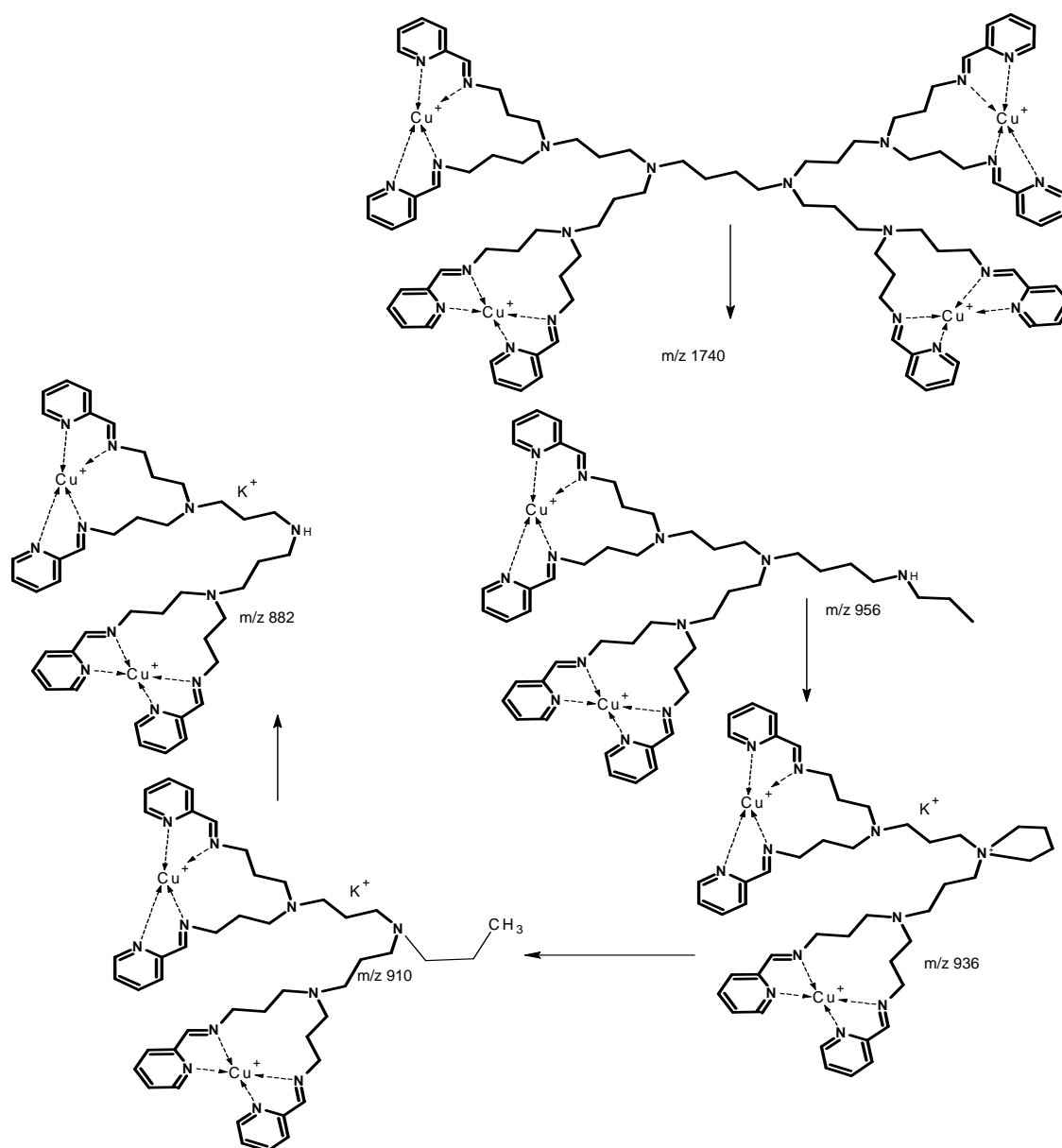


**Figure 4.7:** ESI-mass spectrum of second generation poly(propylene-imine) pyridylimine copper(I) tetrafluoroborate complex **C22**.

#### 4.2.2.2 UV/Vis and Infra-red spectroscopic studies of polynuclear copper(I) complexes

Ultra-violet visible spectra of copper metallodendrimers were recorded in acetonitrile using dilute solutions ( $10^{-5}$ M) at room temperature. The spectra are illustrated in Figures 4.8 & 4.9. For both systems i.e. pyridine and quinoline based, four bands were observed in the spectra of these complexes. The spectra of the quinoline system (**C20 & 24**) were very sharp and intense as compared to their pyridine analogues. The first two absorption bands are observed in the range 223-229 nm and 247-255 nm for the pyridine systems and are assigned to intra ligand  $\pi$ - $\pi^*$  transitions of the pyridine ring. These transitions are observed at 203 nm in the case of quinoline systems. The third band is found in the range 277-288 nm for the pyridine

systems and 289-307 for quinoline system. These bands are attributed to the  $n-\pi^*$  transitions of the azomethine chromophores. The last bands in the UV/Vis spectra of these metallodendrimers which are not observed in the free ligands are assigned to metal to ligand charge transfer (MLCT) transitions. For quinoline systems these bands are observed at very low energy (521 nm) whereas for pyridine metallodendrimers we observe these transitions at slightly higher energies (460-470 nm). The reason for this difference is the fact that the quinoline ring probably has great delocalization of electrons due to the higher conjugated system as compared to the pyridine ring.



**Scheme 4.4:** Fragmentation pattern of second generation poly(propylene-imine) pyridylimine copper(I) tetrafluoroborate complex C22.

**Table 4.7:** Infra-red and UV/Vis spectroscopic data for cationic copper(I) metallodendrimers

Complexes	UV/Vis <sup>a</sup> $\lambda_{\max}$ (nm)	FT-IR spectra (cm <sup>-1</sup> ) <sup>b</sup>	
		$\nu(\text{C=N})$	$\nu(\text{B-F})$
<b>C17</b>	223, 247, 283, 470	1592	1031
<b>C18</b>	224, 248, 277, 470	1593	1032
<b>C19</b>	229, 255, 288, 470	1582	1030
<b>C20</b>	203, 248, 289, 521	1591	1050
<b>C21</b>	223, 247, 284, 470	1592	1032
<b>C22</b>	225, 248, 277, 470	1593	1032
<b>C23</b>	201, 230, 288, 470	1582	1031
<b>C24</b>	203, 248, 307, 521	1591	1051

<sup>a</sup>  $10^{-5}M$ , MeCN solutions<sup>b</sup> Neat ATR

#### 4.2.2.3 Micro-analysis and <sup>1</sup>H-NMR spectroscopic studies of polynuclear copper(I) complexes

Some of the copper(I) metallodendrimers were also analysed by micro-analysis and the results revealed the purity of these compounds (**C18**, **C20**, **C22** & **C24**), see Table 4.5. In this table we also observe the thermal stability of the metallodendrimers. From these results

it can be conclude again that metallodendrimers exhibit high thermal stability as compare to their mononuclear. This phenomenon was also observed in the case of palladium (II) complexes which were discussed in **Chapter 3**. What can be also noted is that Cu (I) metallodendrimers are less stable as compared to the Pd(II) metallodendrimers, see Table 4.5 & 3.7.

Proton-NMR spectroscopy was also used as a characterisation tool for these copper metallodendrimers. The data obtained supports the structures depicted in Scheme 4.2. These results are similar to those of their mononuclear analogues especial the signals of the aromatic protons. The resonance for  $HC=N$  is observed as a sharp singlet downfield as compared to their analogous dendrimeric ligands in the region  $\delta$  8.5-9.19 ppm in the spectra of all complexes. Downfield shift was also observed for signals due to protons of the dendrimeric frame-work (see Table 4.7).

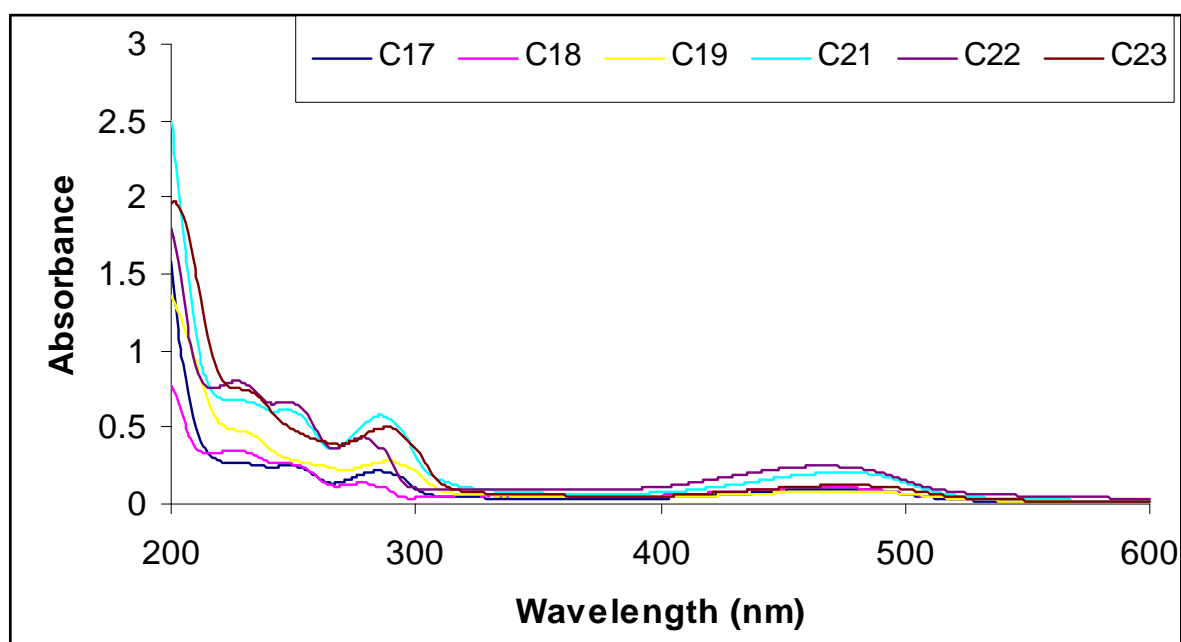


**Figure 4.8:** Absorption spectra of iminopyridyl-copper(I) metallodendrimers in acetonitrile solution ( $10^{-5}M$ ).

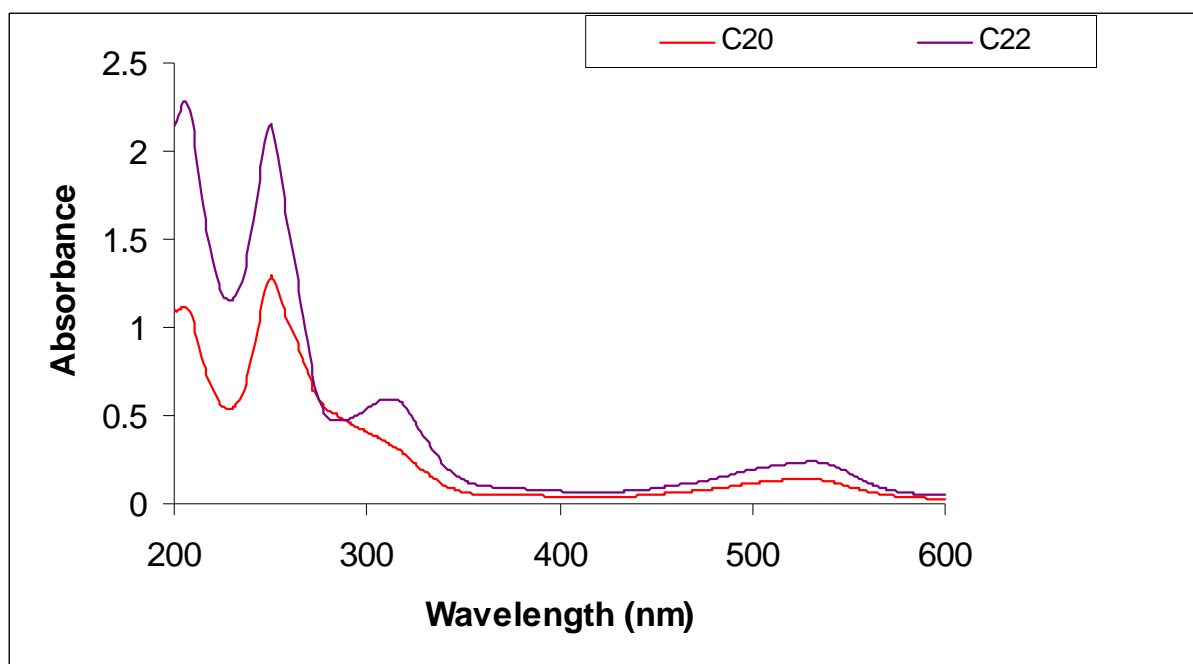


**Figure 4.9:** Absorption spectra of iminoquinolyl-copper(I) metallodendrimers in acetonitrile solution ( $10^{-5}M$ ).

### 4.3 CONCLUDING REMARKS

A range of both mono-nuclear and multinuclear containing copper(I) complexes were successfully obtained by the reaction of various monofunctional and dendrimeric pyridyl and quinolyl-imine based ligands with tetrakis (acetonitrile) copper(I) tetrafluoroborate by using different reaction ratios. All twelve complexes were synthesised by utilising the same procedure that was used by Fu et al. The coordination of these complexes was described as involving two bidentate ligands. All of these complexes were very stable at room temperature but in solution they tend to change colour to green, which is evidence of decomposition. Characterisation of these complexes was performed by using  $^1H$  &  $^{13}C$ -NMR, ESI-MS, FT-IR and UV/Vis spectroscopy. Mono-nuclear complex, **C14** was also characterised by using single X-ray diffraction analysis and the coordination geometry of this complex was discovered to be distorted tetrahedral around copper metal centre. These observations are consistent with molecular structures found in literature. It was observed that UV/Vis spectra of mono-nuclear analogues showed three bands, whereas metallodendrimers showed four bands. The extra band in metallodendrimers is associated with the multifunctionality of the dendrimers. MLCT transitions for **C13-C16** are observed at low

energies as compared with those of **C17-C24**, as well as pyridylimine based complexes versus quinolyimine analogues. These differences can be attributed to electronic factors.

## 4.4 EXPERIMENTAL SECTION

### 4.4.1 *General Remarks and instrumentation*

All manipulations involving air-sensitive and/or moisture-sensitive materials were performed in a nitrogen-filled glove box or under an atmosphere of purified dry nitrogen using standard Schlenk techniques. IR spectra were recorded as solids by using an ATR accessory on a Nicolet Aneta 330- FT-IR spectrometer. NMR spectra were recorded on a Varian Unity Inova instrument ( $^1\text{H}$  at 300 or 400 MHz,  $^{13}\text{C}$  at 75 or 100 MHz). Chemical Shifts are reported in ppm and are referenced to residual proton and carbon signals (7.25 and 77 ppm) for  $\text{CDCl}_3$  respectively and 2.50 and 39.0 ppm for  $\text{DMSO-}d_6$ . Mass spectrometry characterisation was done by using a Waters API Quattro Micro instrument with direct injection of DCM solution, MS settings were as follows: capillary voltage 3.5Kv, cone voltage 15 RF1 40, cone gas 50L/h, desolvation temperature  $400^\circ\text{C}$ , desolvation gas 500L/h and cone gas 50L/h. Elemental analysis was performed by the University of Cape Town Micro-analytical Laboratory.

### 4.4.2 *Materials*

All solvents were purchased from Sigma-Aldrich Ltd or Kimix Chemicals (South Africa), and they were refluxed over appropriate drying agents and distilled prior to use: diethyl ether and toluene over sodium wire and benzophenone, dichloromethane and acetonitrile over phosphorous pentoxide, hexane and pentane over sodium wire. Dimethylsulfoxide (DMSO) was used as received without any further purification. The copper precursor,  $[\text{Cu}(\text{CH}_3\text{CN})_4][\text{BF}_4^-]_4$  was purchased from Sigma-Aldrich and used as received.

## 4.5 SYNTHESIS OF MONO AND POLY-NUCLEAR COPPER(I) COMPLEXES

### 4.5.1 *Mononuclear Bis [N-(n-propyl)-1-(2-pyridyl and quinolyl) - methanimine] Cu(I)Tetrafluoroborate complexes, C13-C16.*

These complexes were prepared using a modified procedure described by Haddleton et al [9] and Fu et al [11]. The synthesis of **C14** is used as an example. Cationic copper tetrakis (acetonitrile) precursor  $[\text{Cu}(\text{CH}_3\text{CN})_4(\text{BF}_4)]$  (0.287 mmol, 0.090 g) was transferred to a 100 ml Schlenk tube which was filled with nitrogen gas. This white solid (precursor) was dissolved in dry DCM (10 ml) by stirring at room temperature for 5 minutes giving a colourless solution. Separately the monofunctional pyridine ligand **ML-2** (0.574 mmol, 0.085g) was dissolved in 5 ml of dry DCM and this yellow solution was added drop-wise by means of syringe to the stirring solution of the copper precursor. An orange-yellow solution was observed during the first 10 drops. As the addition continues, the colour changed to deep red-brown. This reaction was allowed to proceed for 2 hours under nitrogen gas at room temperature. The solvent was reduced to a minimum amount and the product crystallized by slow diffusion of dry  $\text{Et}_2\text{O}$ . The mixture was then stored at  $-5^\circ\text{C}$ . The solvent was decanted and plate-like deep-green crystals were obtained and washed with cold diethyl-ether. Crystals were then dried using vacuum for 2-3 hours and they were suitable for XRD analysis. These complexes were also characterised by  $^1\text{H-NMR}$ , FT-IR and UV/Vis spectroscopy, (+ESI)-MS and Single X-ray analysis.

### 4.5.2 *Multinuclear [G-1&2\_DAB-dendr-(NH<sub>2</sub>)<sub>n</sub>-1-(2-pyridyl and quinolyl)- imine] Cu(I) Tetrafluoroborate complexes, C17-C24.*

Cationic copper complexes based on dendritic scaffolds were prepared using a similar method that was used by Fu *et al* [11] and synthesis of **C18** is used as an example. White cationic tetrakis (acetonitrile) Tetrafluoroborate  $[\text{Cu}(\text{CH}_3\text{CN})_4(\text{BF}_4)]$  (0.0937 g, 0.298 mmol) was transferred to a 100 ml Schlenk tube which was previously filled with nitrogen gas and this white solid (precursor) was dissolved in 10 ml of dry DCM by stirring at room temperature for 5 minutes. A colourless solution was observed. Separately G1 pyridine ligand **DL2** (0.100 g, 0.149 mmol) was dissolved in 5 ml of dry DCM and this yellow solution was added drop-wise by means of syringe in the stirring solution of copper precursor, immediately the colour changed to deep-red-brown. This reaction was allowed to



proceed for 2 hours under nitrogen at room temperature. The solvent was removed by vacuum and a sticky brown residue was obtained, which was then dissolved in dry DCM and it was crystallized by a slow diffusion of dry Et<sub>2</sub>O at -5°C. After removal of solvent by vacuum a dark-brown solid was obtained. All of these complexes (**C17-C22**) were characterised by <sup>1</sup>H & <sup>13</sup>C-NMR, FT-IR and UV/Vis spectroscopy and (ESI)-mass spectrometry, the results are listed in Tables 4.5-4.7.

## 4.6 X-RAY CRYSTALLOGRAPHY

### 4.6.1 Description of crystals for C14 and refinement parameters for data collections, see Appendix.

**C14**: Needle shaped dichroic crystals with approximate dimensions 0.284x0.197x0.100mm. Refinement of 255 parameters based on all 4703 reflections yielded R<sub>1</sub>= 0.0314 and wR<sub>2</sub>= 0.0806 for I > 2σ (I) (4184 reflections).

## 4.7 STRUCTURAL DETERMINATION (C-14)

Single crystals of C1-C4 were mounted on a fine focus sealed tube. The crystal data were collected at 100(2) K on a Bruker APEX-CCD area detector diffractometer with a MoKα radiation (λ = 0.71073 Å) by using a ω-2θ scan mode. Data collection and reduction were performed using *SMART* and *SAINTE* software [ref]. All the structures were solved by direct methods and non-hydrogen atoms were subjected to an isotropic refinement by full-matrix least squares on F<sup>2</sup> using *SHELXTL* package [ref]. Structural refinement and solutions were obtained by *SHELXL* and *SHELXS* respectively.

**4.8 REFERENCE**

- [1] C.T Cunningham, K.L.H Cunningham, J.F Michael, D.R McMillan, *Inorg.Chem.* 38 (1999) 4388.
- [2] D.R McMillan, J.R Kirchhoff, K.V Goodwin, *Coord .Chem .Rev.* 64 (1985) 83.
- [3] N .Armaroli, *Chem .Soc .Rev.* 30 (2001) 113.
- [4] G .A Hogan, A.A .Gallo, K.M .Nicholas, R.S Srivastava, *Tetra. Let .*43 (2002) 9505.
- [5] S .Mahadeva, M .Palaniandova, *Inorg .Chem,* 37 (1998) 693.
- [6] D.R .McMillin, K.M .McNett, *Chem .Rev,* 98 (1998) 1201.
- [7] S.M .Scott, K.C .Gordon, *Inorg .Chem .Rev,* 35 (1996) 2452.
- [8] S.J Lind, T.J Walsh, A.G Blackman, M.I.J Polson, G.I.S Irwin, K.C Gordon, *J.Phys .Chem.* 15 (2009) 3566.
- [9] D.M .Haddleton, D.J .Duncalf, *Eur. J .Inorg .Chem.* (1998) 1799.
- [10] W .Massa, S .Dehghampour, *Inorg .Chem.* 362 (2009) 2872.
- [11] W-F .Fu, X. Gan, *Inorg .Chim. Acta.* 360 (2007) 2758.
- [12] L .Liable-Sands, T .Concolino, A .Rheingold, *Inorg. Chem,* 38 (1999) 6234.
- [13] D .Suresh, M .Balakrishna, J .Magne, *Dalton Trans,* (2008) 3272.
- [14] T .Kuroda-Sowa, M .Munakata, H .Metsuda, S .Akiyama, M .Maekawa, *J. Chem .Soc .Dalton Trans,* (1995) 2201.
- [15] P .Halder, E .Zangrando, T .Pain, *Dalton Trans,* (2009) 5386.
- [16] P .Chandrasokonana, J .Mague, M .Balakrishna, *Inorg .Chem,* 45 (2006) 6678.
- [17] W .Massa, S .Dehghanpour, K .Jahani, *Inorg .Chim,* 362 (2009) 2872.
- [18] A .Diezel, J .Fornies, S .Fuertes, *Organometal.* 28 (2009) 1705.
- [19] L .Zhong, B .Li, Z .Su, *Langmuir ,* 25 (2009) 2068.
- [20] W-J .Wang, C-H .Lim, S-W .Tang, *Mol. Cryst .Liq .Cryst,* 456 (2006) 209.
- [21] Y .Chen, J-S .Chen, X .Gan, W-F .Fu, *Inorg .Chim. Acta,* 362 (2009) 2492.
- [22] P .Yang, X-J .Yang, B .Wu, *Eur .J .Inorg .Chem,* (2009) 2951.
- [23] J.L van Wyk, *Mono-nuclear and multinuclear salicylaldimine metal complexes as catalysts precursors in the oxidation of phenol and cyclohexane*, PhD Thesis, University of the Western Cape (2008).
- [24] A .Malassa, C .Koch, B .Stein-Schaller, H .Gorls, M .Friedrich, M .Westerhausen, *Inorg .Chim. Acta,* 361 (2008) 1405.

**CHAPTER FIVE**  
**SUMMARY AND FUTURE WORK**

---

---

**CONTENT**

5.1 SUMMARY	126
5.2 FUTURE WORK	127

## 5.1 SUMMARY

**Chapter one** of this study provides a brief literature review of the work that has been done for development of oxidative carbonylation reactions especially for alcohols. The challenges and problems that are associated with this catalytic transformation of alcohols are discussed. Attempts to overcome these problems are summarised which includes use of basic additives, chelating ligands, zeolite immobilised catalysts and MCM 41 immobilised catalysts. The chapter concludes with a proposal of how we may attempt to provide possible solutions.

**Chapter two** describe the synthetic approach to a series of new monofunctional ligands [*N*-(*n*-propyl)-1-(2-pyridyl and quinolyl)] methanimine and their peripheral functionalised poly(propylene)-imine dendrimeric ligands based on the 1,4-diaminobutane core. From the results and discussions of this chapter it can clearly be seen that all ligands have been successfully synthesised and characterised.

The third chapter focused on the synthesis and characterisation of Pd(II) complexes. Iminopyridyl and iminoquinolyl-imine ligands discussed in **Chapter two** were complexed with Pd(CH<sub>3</sub>CN)<sub>2</sub>Cl<sub>2</sub> precursor. Similarly **Chapter four** deals with the synthesis and characterisation of Cu(I) tetrafluoroborate complexes. In both chapters mononuclear complexes were also characterised by Single X-ray diffraction analysis. Pd(II) complexes adopted distorted square planar geometry around metal centre whereas Cu(I) complex revealed a distorted tetrahedral rearrangement around metal centre. Characterisation techniques employed includes ESI-MS, <sup>1</sup>H & <sup>13</sup>C{<sup>1</sup>H}-NMR, FT-IR and UV/Vis spectroscopies.

Due to time constraints none of the complexes prepared were actually tested for their catalytic activity in oxidative carbonylation of alcohols. The application of these complexes as catalysts in the above processes is suggested for a future study.

## **5.2 FUTURE WORK**

At this point it is appropriate to shed some light on the future work that can be undertaken using results that have been obtained from this thesis. Firstly it would be interesting to introduce electron donating and electron withdrawing groups on the quinolyl-imine ligands to observe their behaviour when they are subsequently complexed with palladium(II) and copper(I) metal precursors. Another modification would be the use of aromatic amines replacing propyl-amine that will give us many various quinolyl-imine ligands. What can also be done is to use other metals such as platinum, cobalt, zinc etc in order to extend coordination of these ligands. When looking at the dendrimeric based ligands, it will be more interesting to increase the growth of the dendrimers, i.e. look at higher generation dendrimers. Metallodendrimers can also be further characterised by using thermal analysis to test their thermal stability.

Last but not least, these metal complexes can be tested in many catalytic transformations. Pd(II) complexes are active catalysts in oxidative carbonylation of aromatic alcohols whereas Cu(I) complexes are active in oxidative carbonylation of alkyl alcohols.

## APPENDIX

---

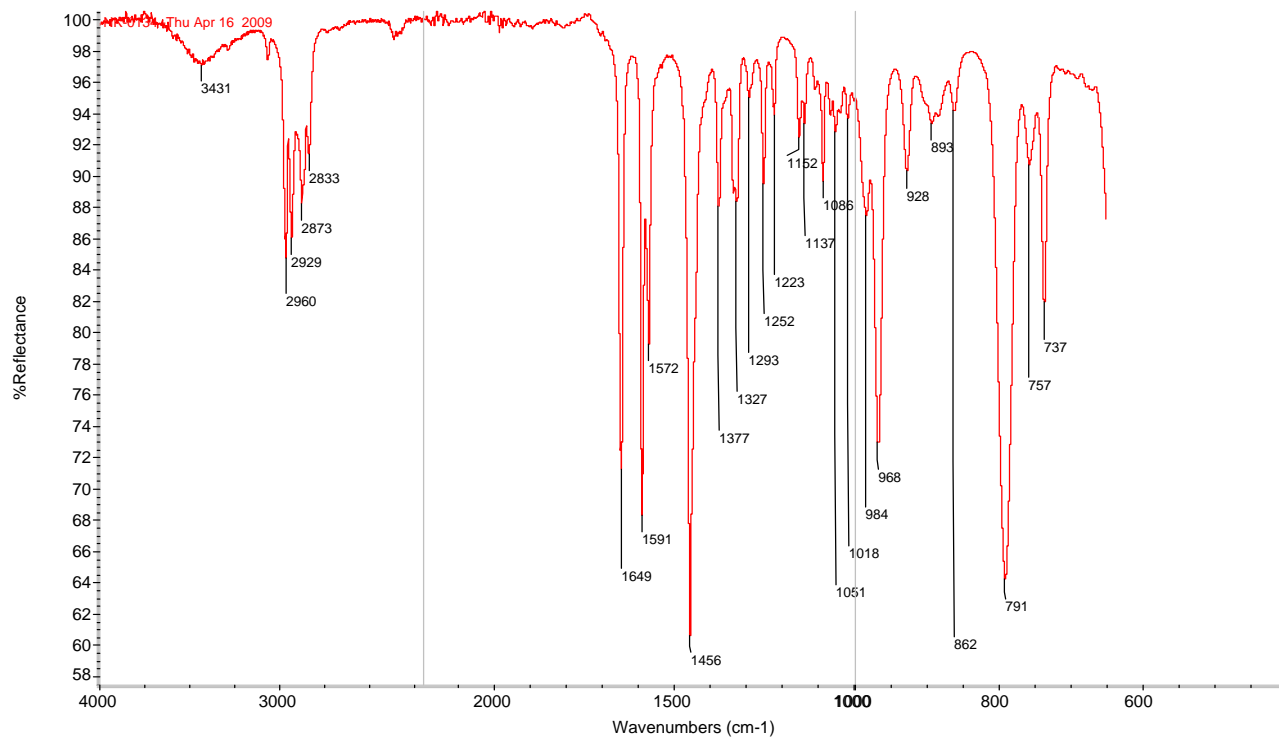
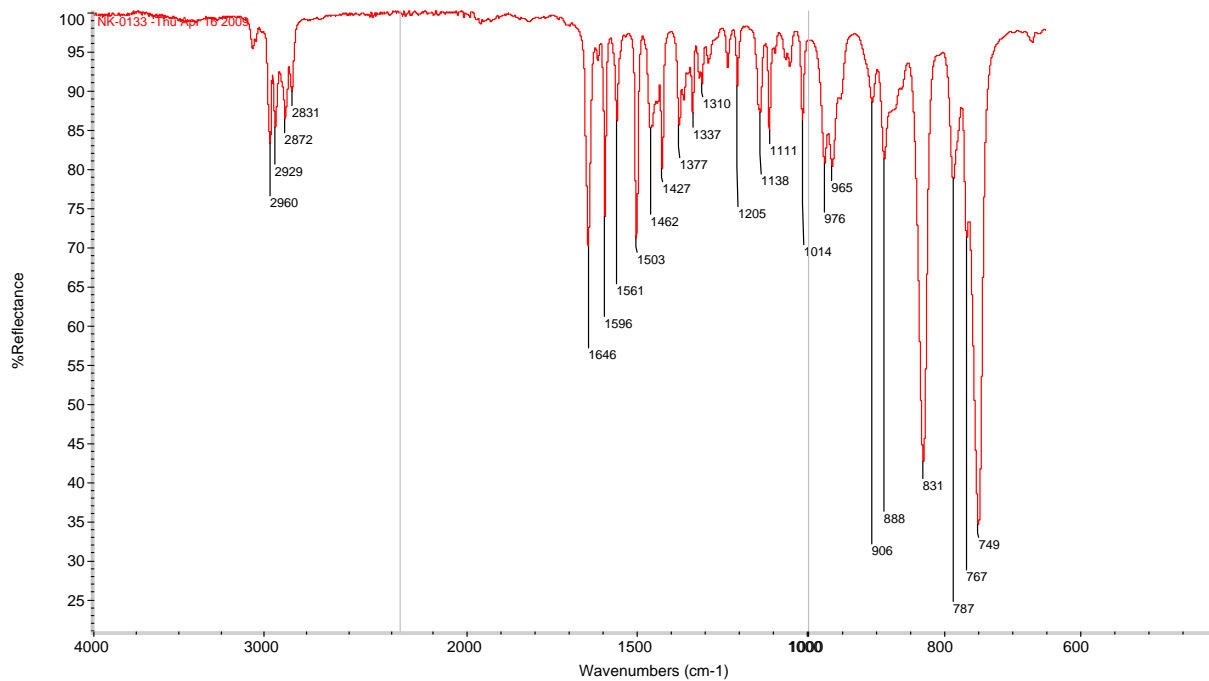
---

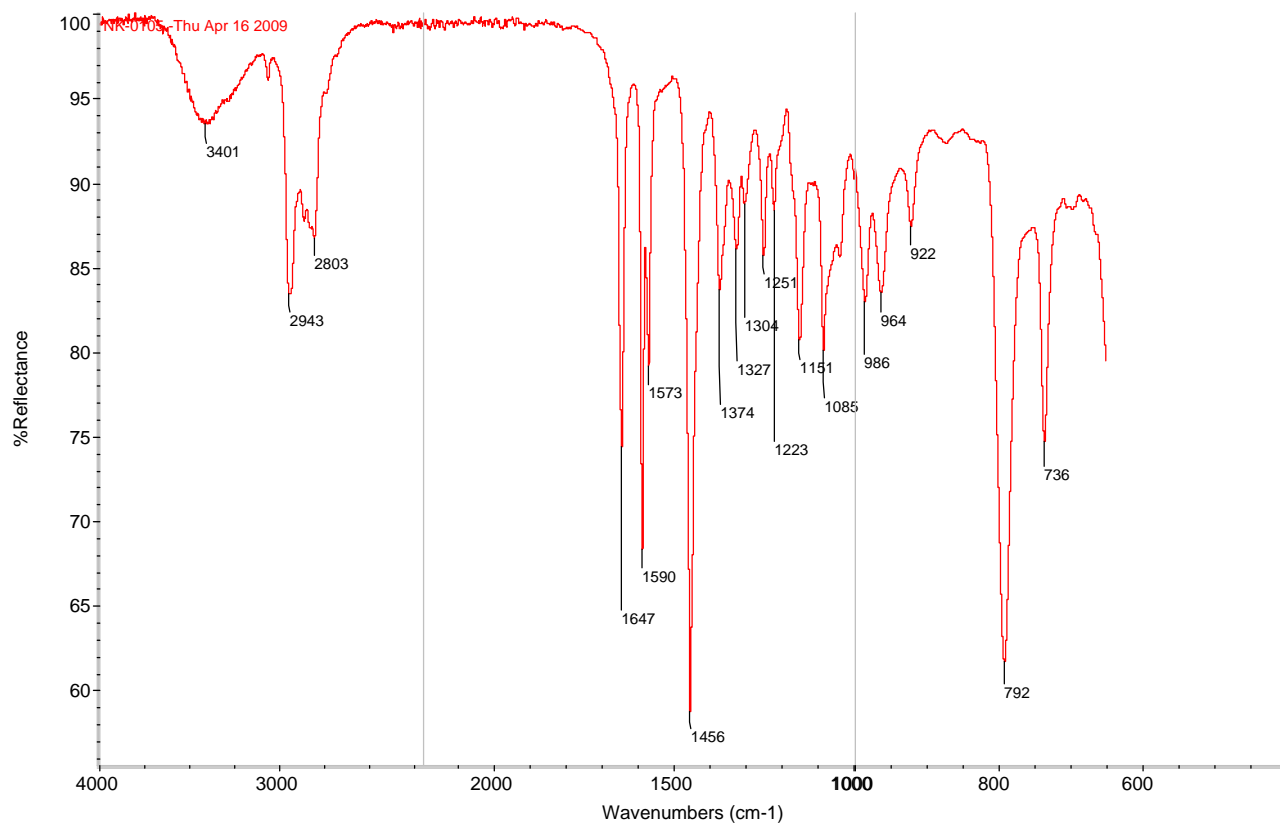
### CONTENT

FT-IR SPECTRA	128
UV/Vis SPECTRA	134
X-RAY DIFFRACTION ANALYSIS	137

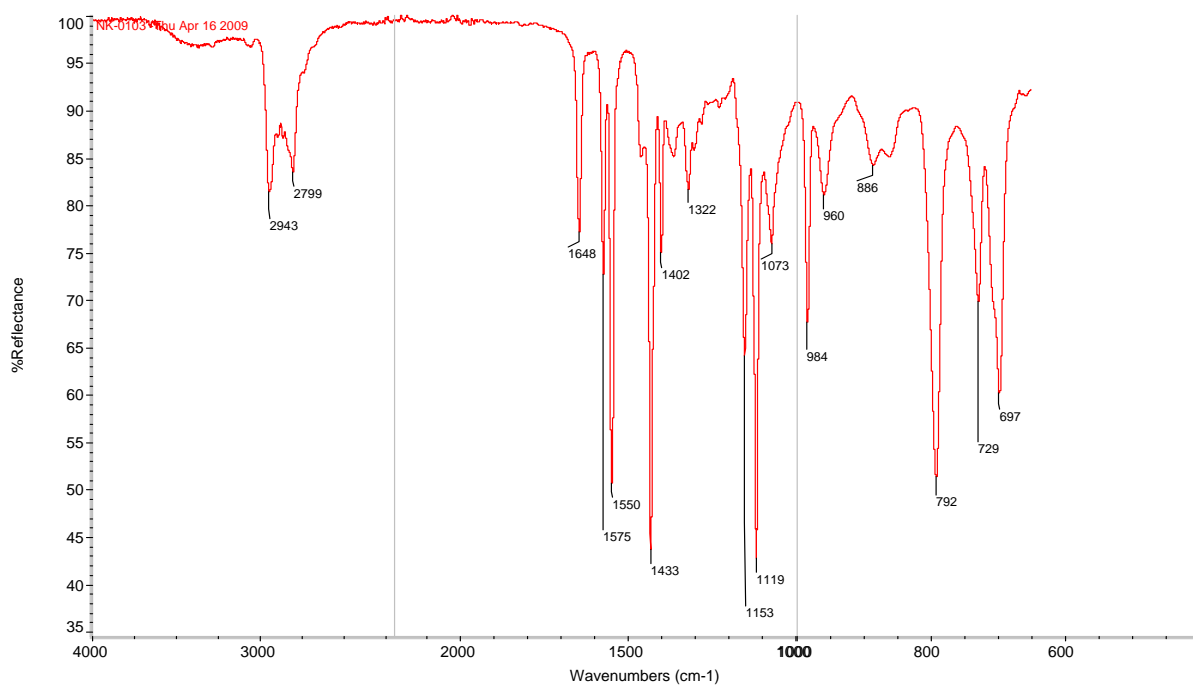
## FT-IR SPECTRA

## Chapter Two:

*Infrared spectrum of N-(n-propyl)-1-(2-pyridyl)-imine ligand ML2**Infrared spectrum of N-(n-propyl)-1-(2-quinolyl)-imine ligand ML4*



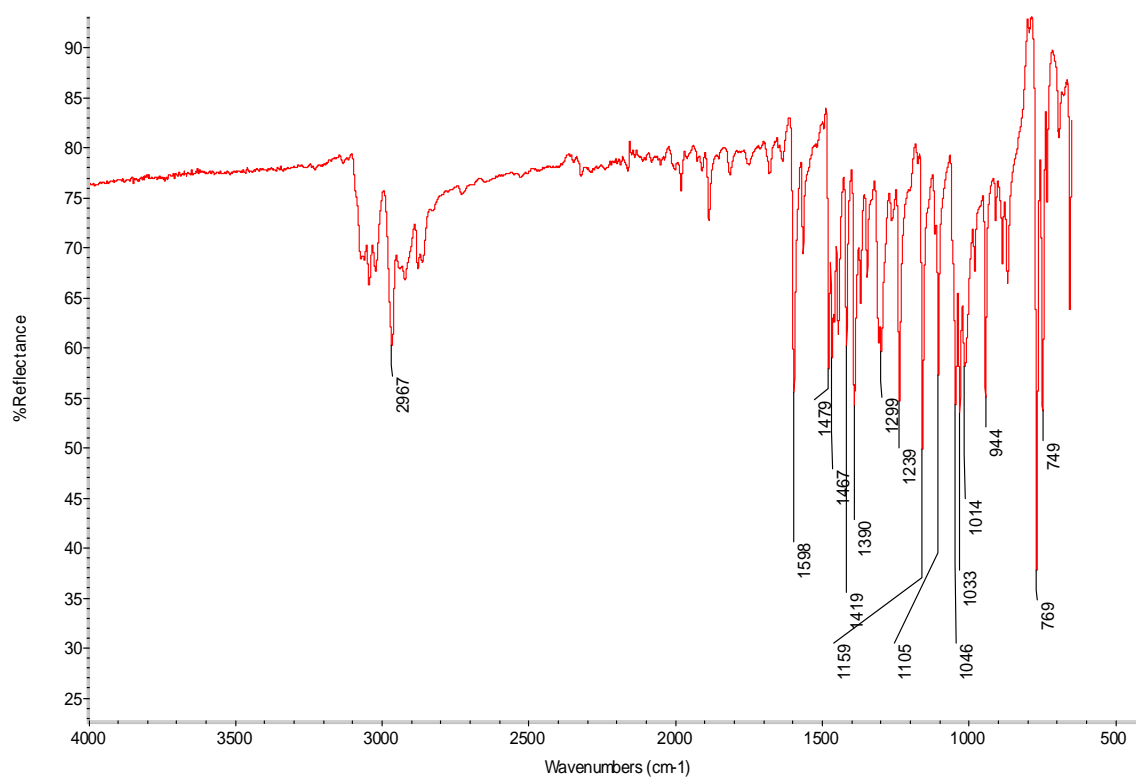
*Infrared spectrum of G1\_poly(propylene)-imine dendrimeric ligand DL1*



*Infrared spectrum of G2\_poly(propylene)-imine dendrimeric ligand DL7*

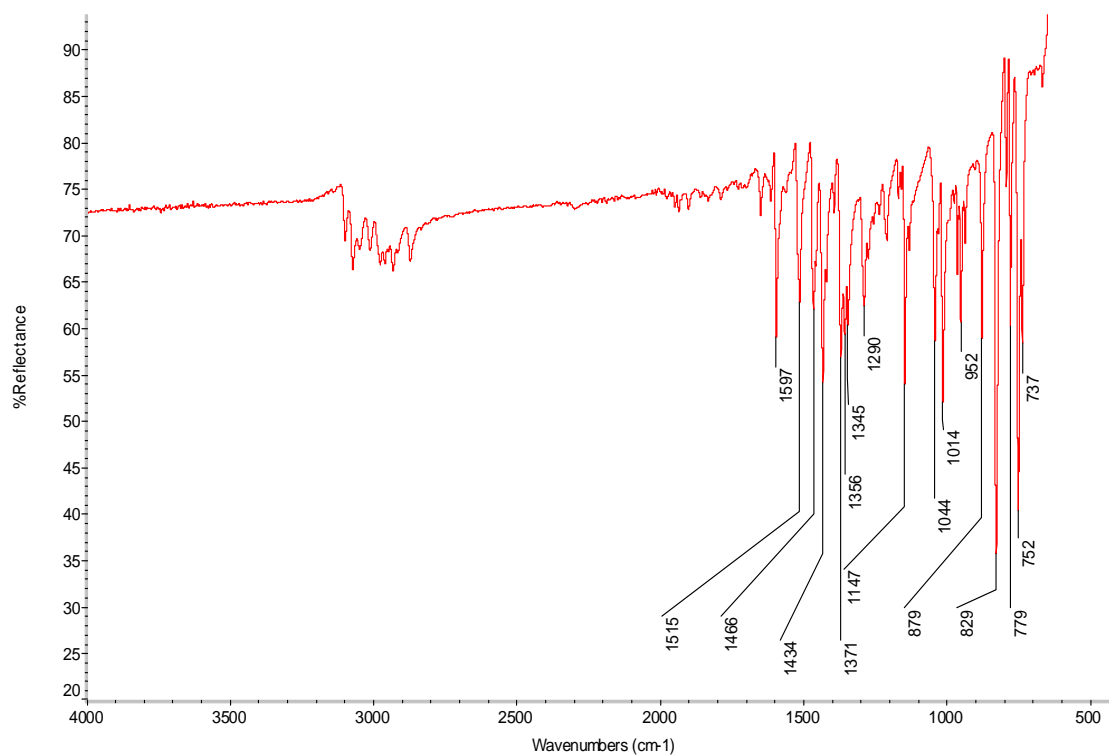


## Chapter Three:



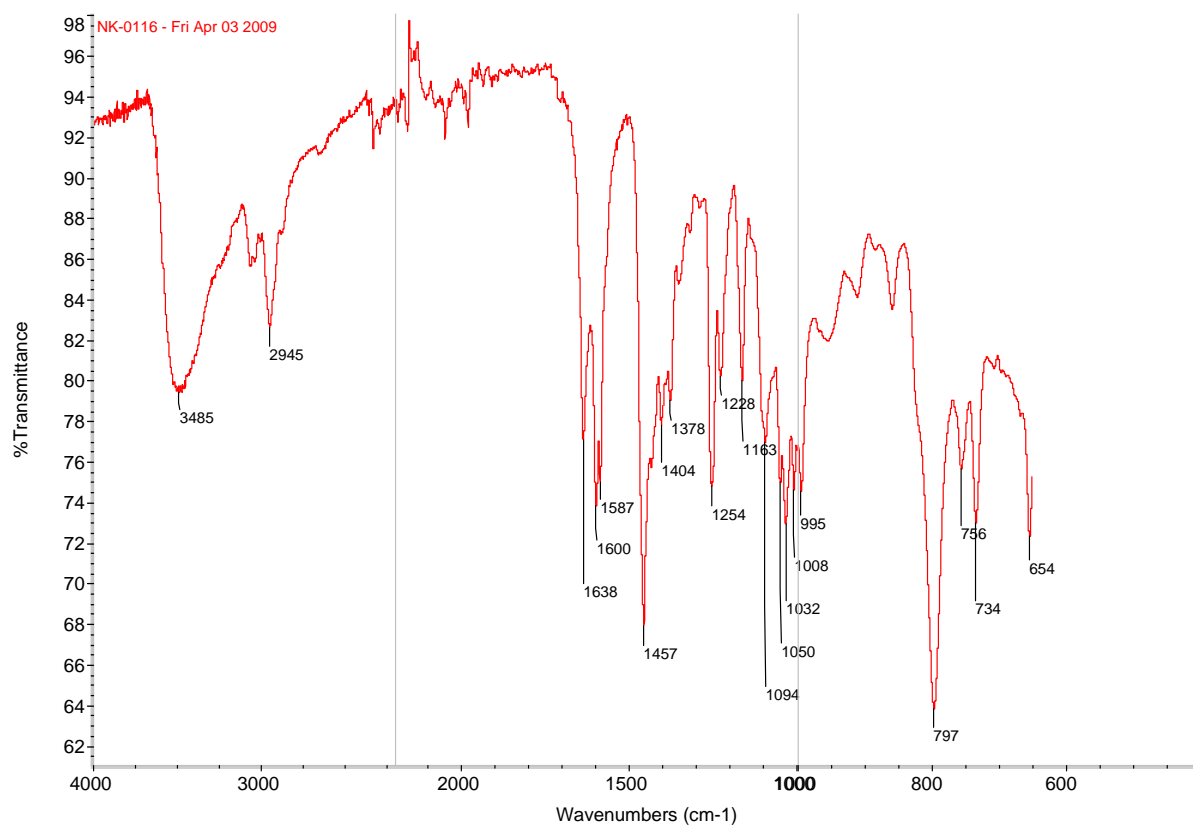
*Infrared spectrum of [N-(n-propyl)-(2-pyridyl)-methanimine] dichloro Pd(II) complex*

**C2**

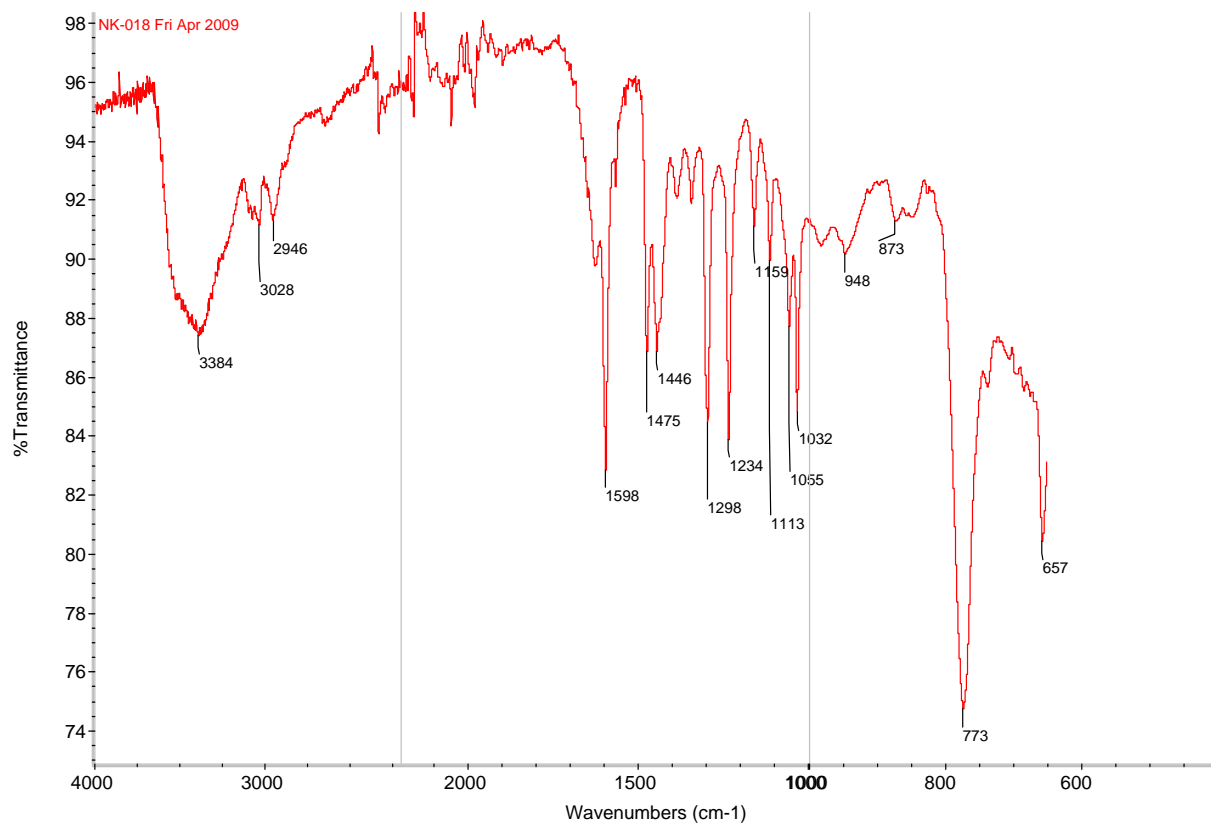


*Infrared spectrum of [N-(n-propyl)-(2-pyridyl)-methanimine] dichloro Pd(II) complex*

**C4**

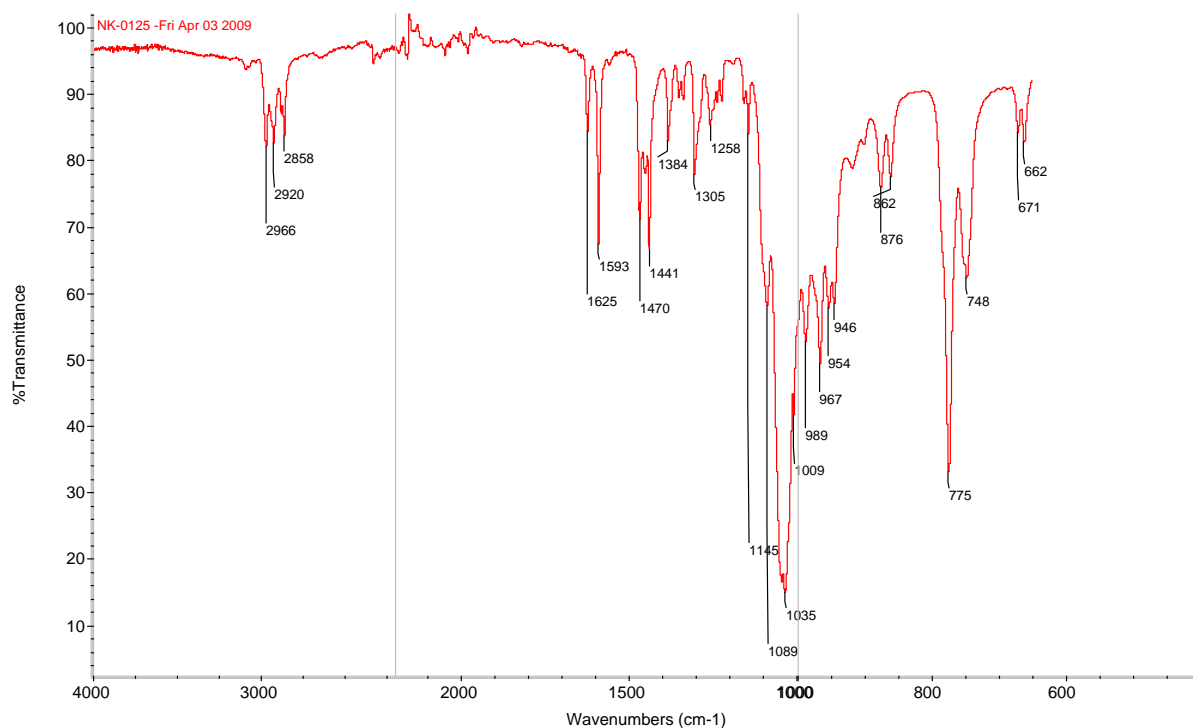


*Infrared spectrum of G1\_Pd(II) dichloro metallodendrimer C5*

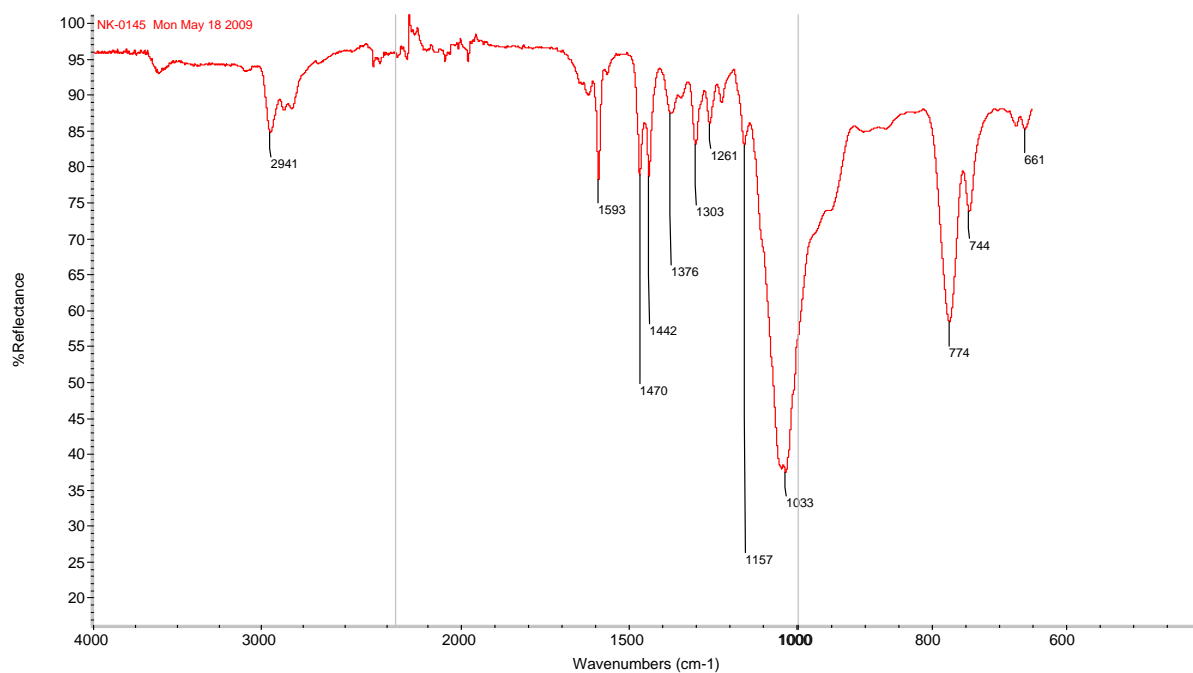


*Infrared spectrum of G1\_Pd(II) dichloro metallodendrimer C6*

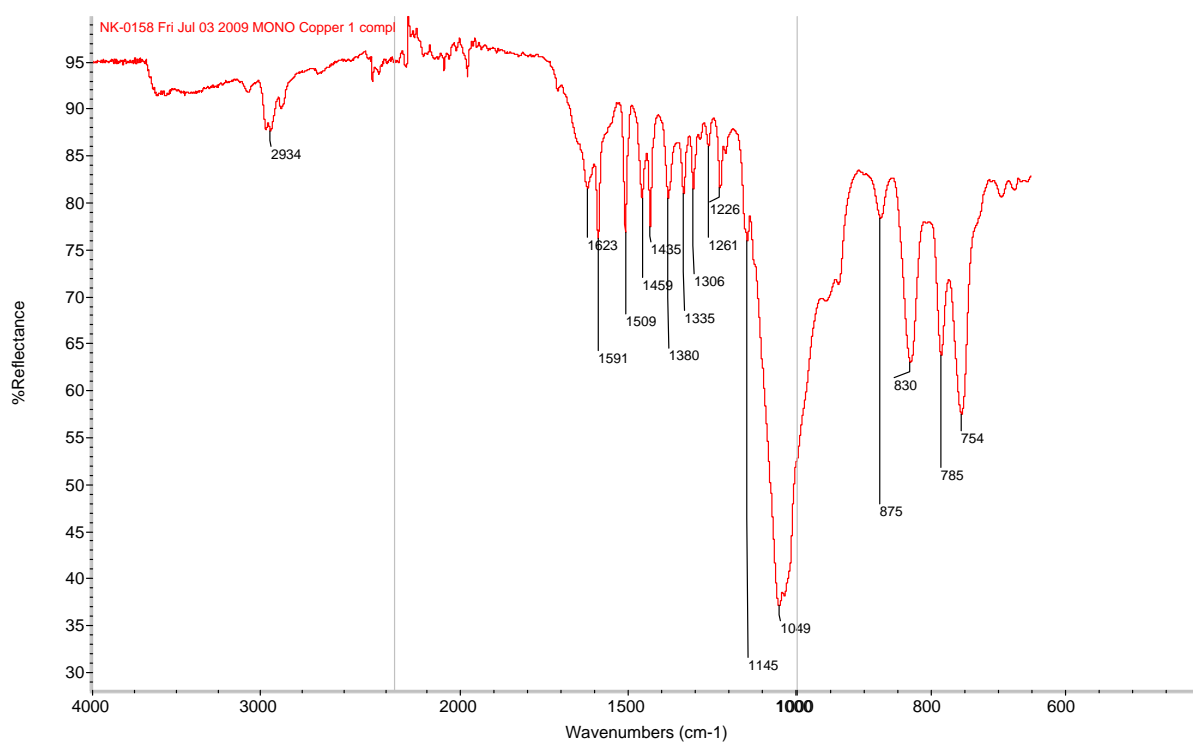
## Chapter Four:



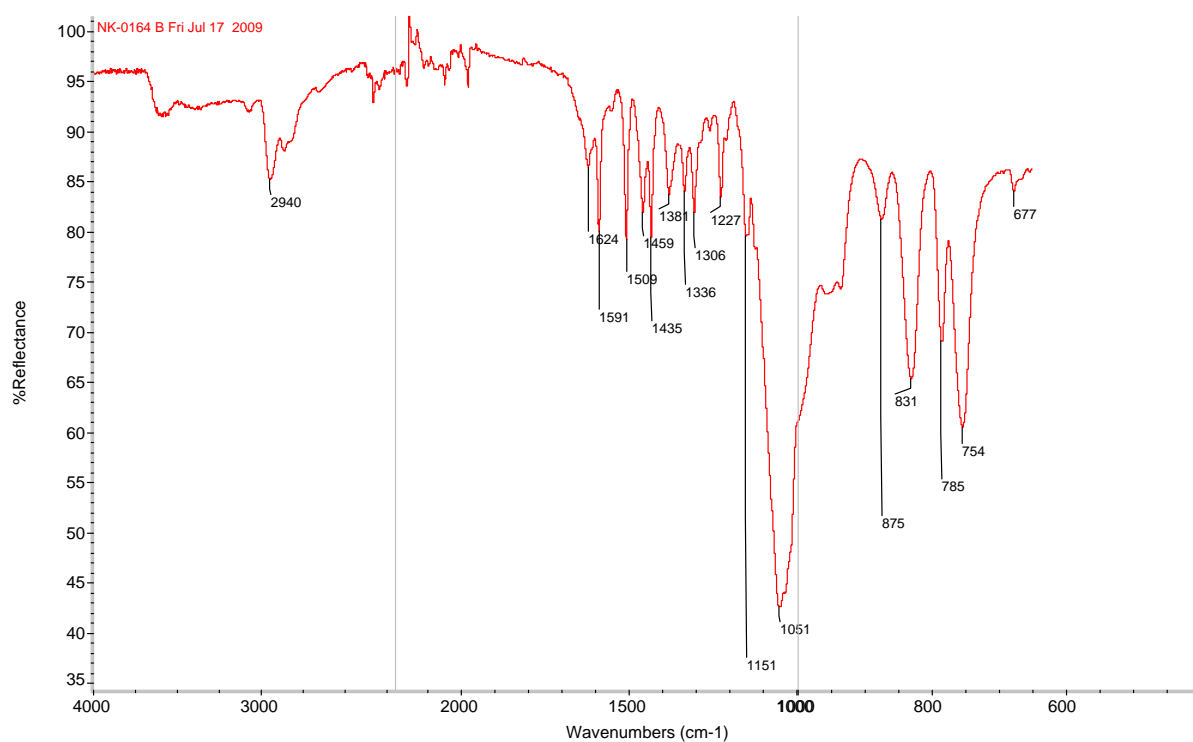
*Infrared spectrum of bis[N-(n-propyl)-1-(2-pyridyl-methanimine)] Cu(I) Tetrafluoroborate complex C14*



*Infrared spectrum of G<sub>1</sub> pyridylimine Cu(I) Tetrafluoroborate metallodendrimer C18*



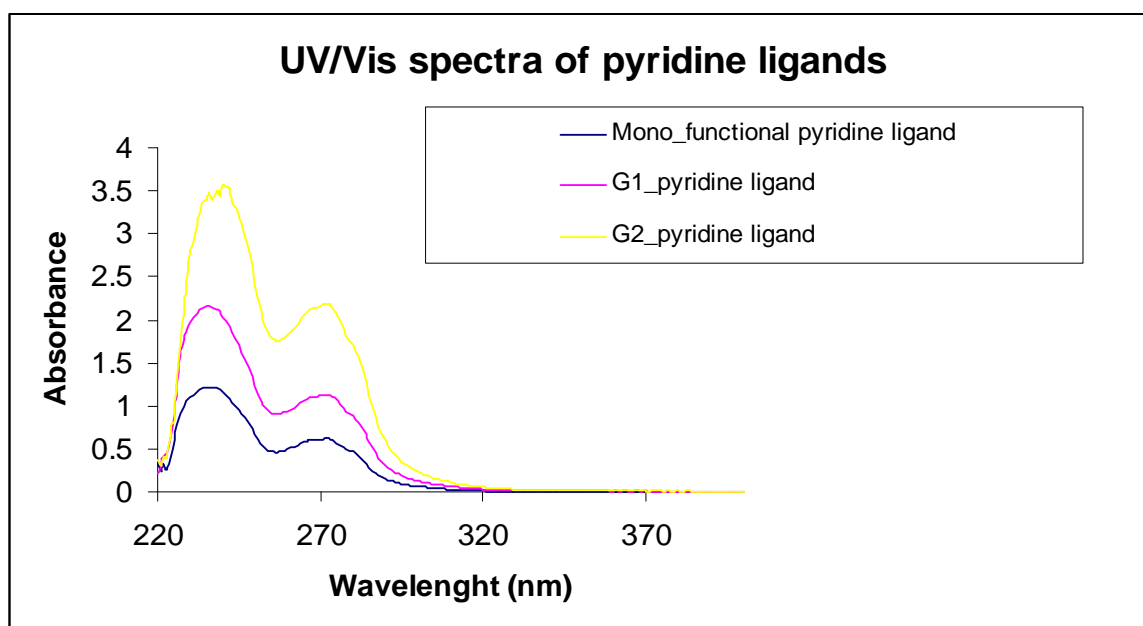
*Infrared spectrum of bis[N-(n-propyl)-1-(2-quinolylyl)-methanimine]  
Cu(I) Tetrafluoroborate complex C16*



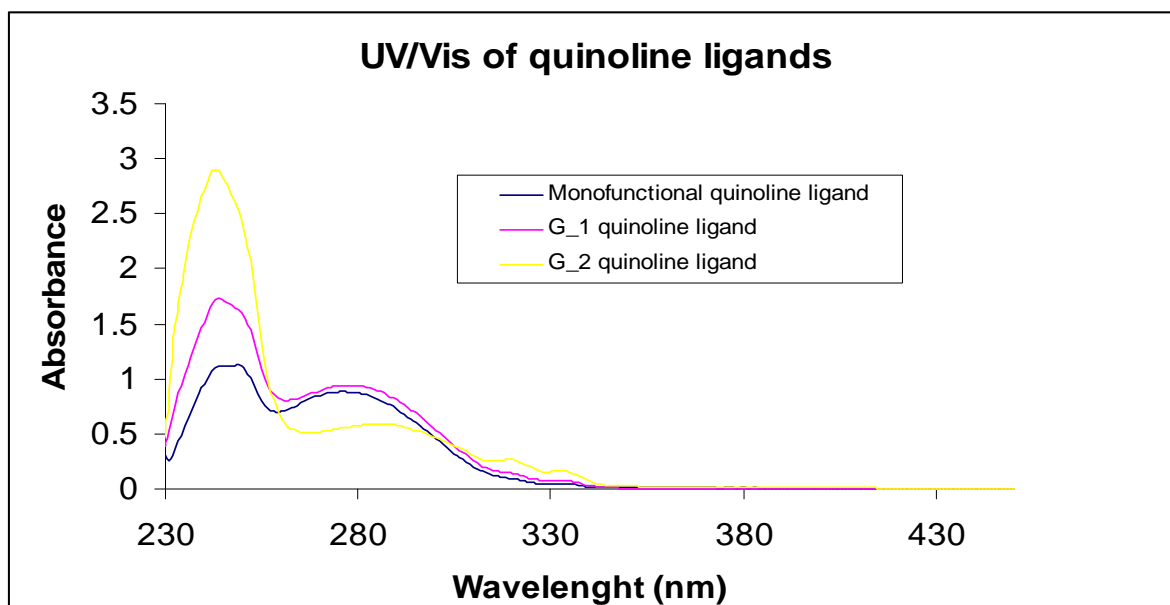
*Infrared spectrum of G\_1 quinolyimine Cu(I) Tetrafluoroborate metallodendrimer  
C20*

## UV/Vis SPECTRA

## Chapter Two:

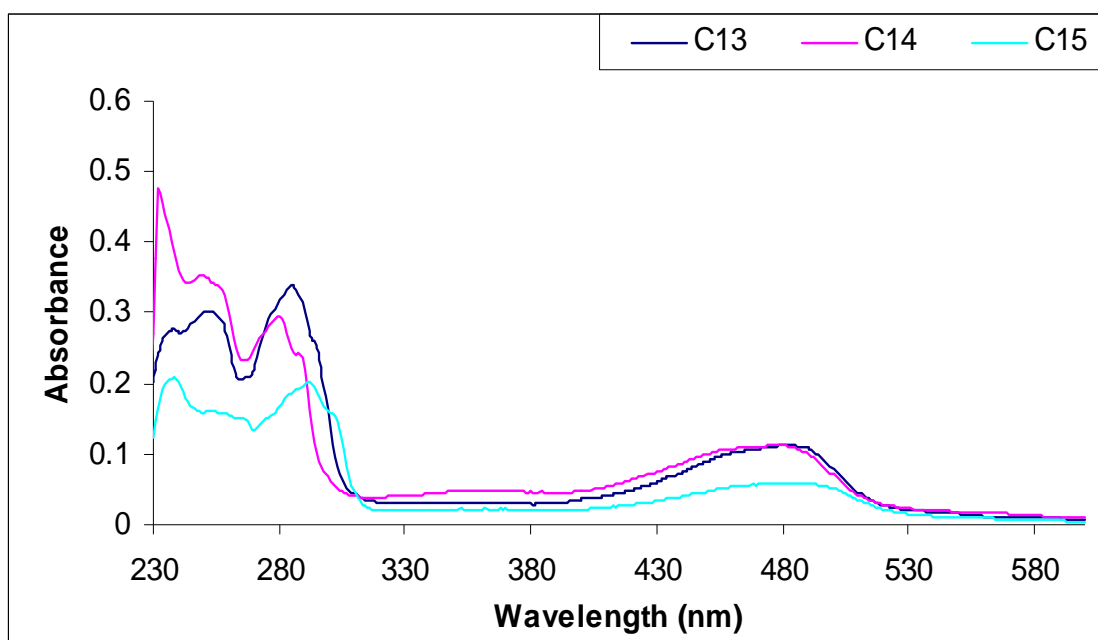


*UV/Vis absorption spectrum of pyridylimine based ligands in acetonitrile solution ( $10^{-5}M$ ) at room temperature.*

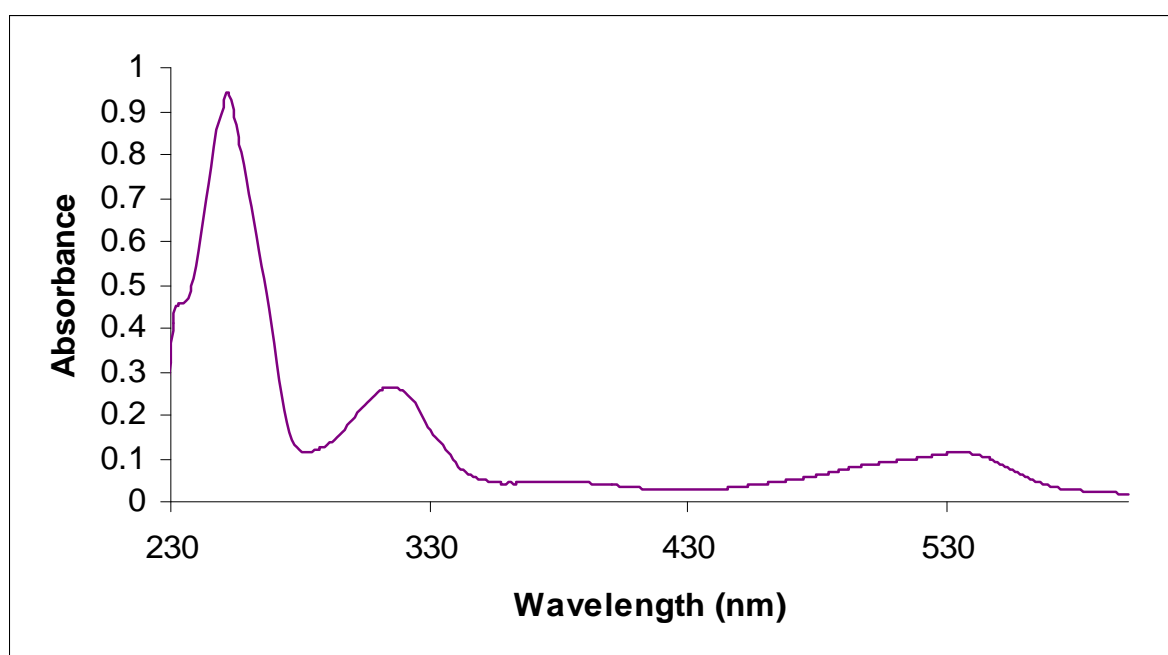


*UV/Vis absorption spectrum of quinolyimine based ligands in acetonitrile solution ( $10^{-5}M$ ) at room temperature.*

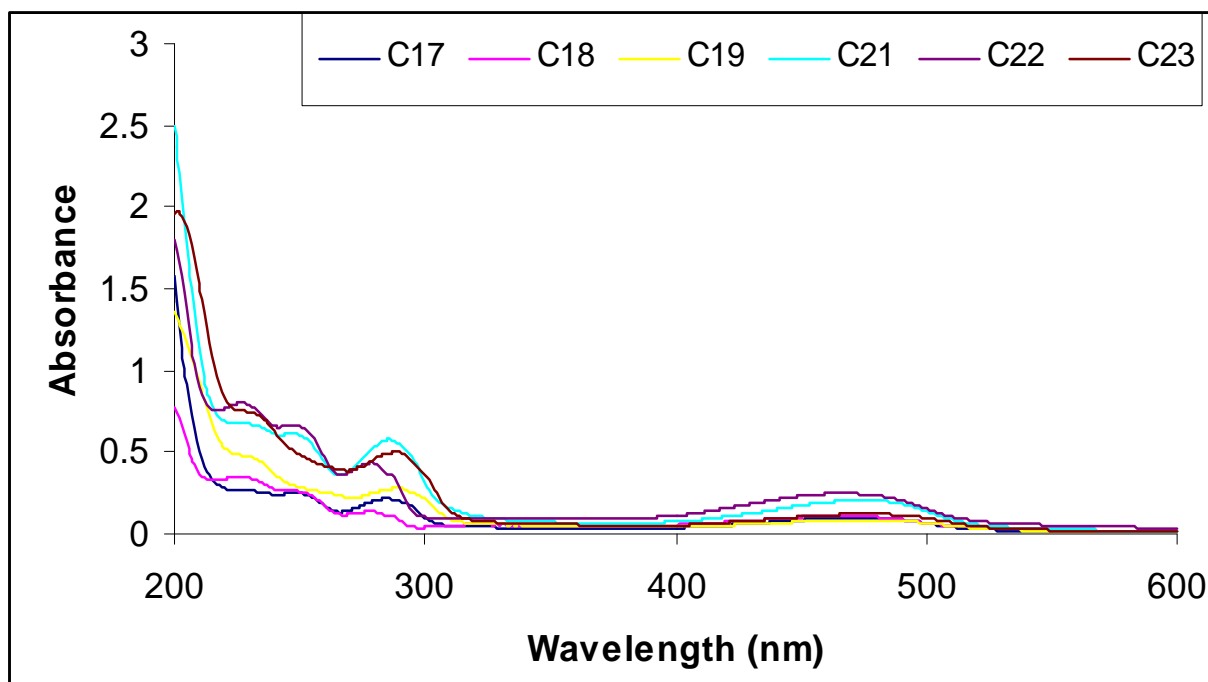
## Chapter Four:



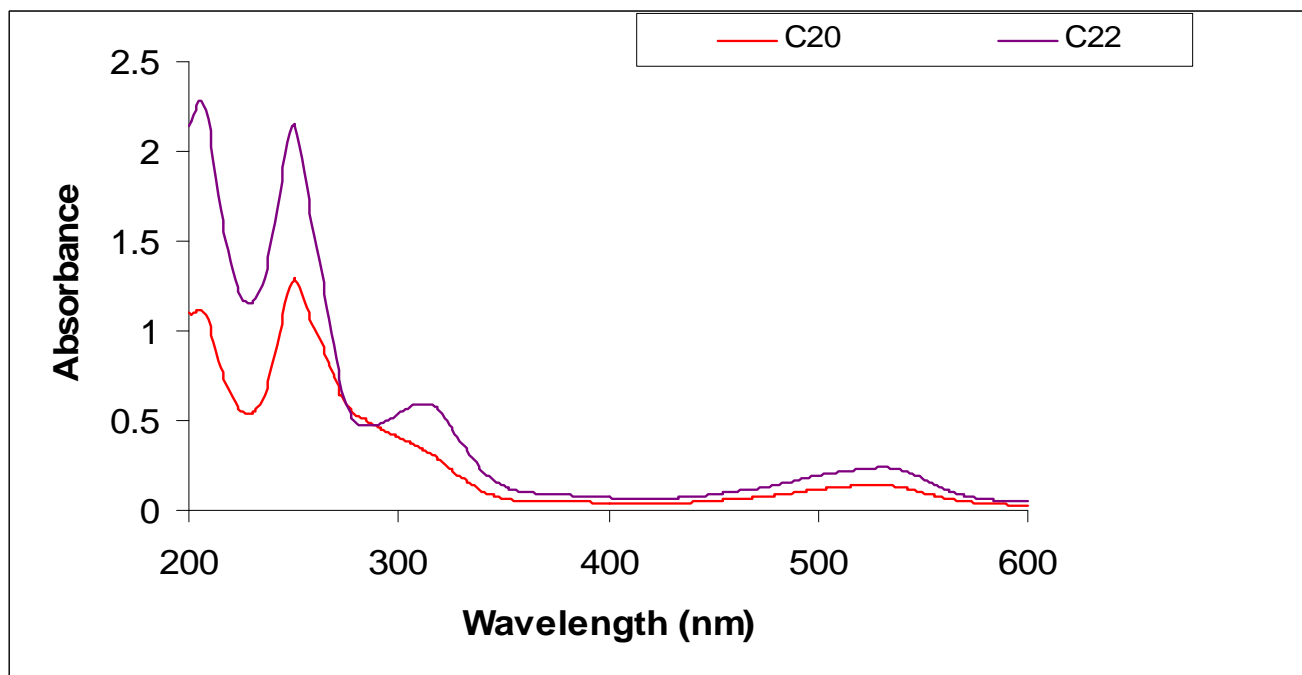
*UV/Vis absorption spectrum of C13-C15 in DCM solution ( $10^{-5} M$ ) at room temperature*



*UV/Vis absorption spectrum of C16 in DCM solution ( $10^{-5} M$ ) at room temperature*



*Absorption spectra of iminopyridyl-copper(I) metallodendrimers in acetonitrile solution ( $10^{-5} M$ ).*



*Absorption spectra of iminoquinolyl-copper(I) metallodendrimers in acetonitrile solution ( $10^{-5} M$ ).*

## X-RAY DIFFRACTION ANALYSIS

## Chapter Three:

Table 1: Summary of X-ray data for complexes 1&amp;2

Data information	C1	C2
Empirical formula	C <sub>10</sub> H <sub>14</sub> Cl <sub>2</sub> N <sub>2</sub> Pd	C <sub>9</sub> H <sub>12</sub> Cl <sub>2</sub> N <sub>2</sub> Pd
<i>Mr</i>	339.53	325.51
Crystal system	orthorhombic	monoclinic
Space group	<i>Pca</i> 2 <sub>1</sub> (No.29)	<i>P</i> 2 <sub>1</sub> / <i>c</i> (No.14)
a (Å)	17.005(2)	8.5500(7)
b (Å)	9.3946(16),	9.4921(8)
c (Å)	7.2658(9)	13.7597(11)
α (°)	90	90
β (°)	90	100.806(5)
γ (°)	90	90
<i>V</i> ((Å <sup>3</sup> ))	1160.8(3)	1096.90(16)
<i>Z</i>	4	4
<i>F</i> <sub>000</sub>	672	640
<i>D</i> <sub>calc</sub> (g.cm <sup>3</sup> )	1.943	1.971
□MoKα(mm <sup>-1</sup> )	2.026	2.139
Temperature (K)	100(2)	100(2)
2□ <sub>max</sub>	59.4°	64.2°
Parameters/Restraints/data	138/7/5996	58/0/14072



$R_1 [I > 2\sigma(I)]$	0.0669	0.0439
wR <sub>2</sub>	0.1571	0.1074
Final <i>Goof</i>	1.019	1.082

**Table 2: Summary of X-ray data for complexes 3 & 4**

Data information	C3	C4
Empirical formula	C <sub>9</sub> H <sub>11</sub> BrCl <sub>2</sub> N <sub>2</sub> Pd	C <sub>13</sub> H <sub>14</sub> Cl <sub>2</sub> N <sub>2</sub> Pd
<i>Mr</i>	248.79	375.56
Crystal system	triclinic	triclinic
Space group	<i>P</i> -1 (No.2)	<i>PI</i> (No.1)
a (Å)	8.3825(8)	8.470(2)
b (Å)	8.5860(8)	8.624(2)
c (Å)	8.6178(8)	9.200(2)
α (°)	84.457(2)	80.696(3)
β (°)	75.637(2)	80.670(2)
γ (°)	74.986(2)	84.051(2)
<i>V</i> ((Å <sup>3</sup> ))	580.00(9)	652.3(3)
<i>Z</i>	4	2
<i>F</i> <sub>000</sub>	448	372
<i>D</i> <sub>calc</sub> (g.cm <sup>3</sup> )	2.849	1.912
□MoKα(mm <sup>-1</sup> )	10.393	1.813
Temperature (K)	100(2)	100(2)
2□ <sub>max</sub>	56.5°	55.8°

Parameters/Restraints/data	137/0/6642	163/0/2725
R <sub>1</sub> [I > 2σ (I)]	0.0231	0.0183
wR <sub>2</sub>	0.0544	0.0450
Final <i>Goof</i>	1.019	1.074

**Table 3: Bond lengths [ $\text{\AA}$ ] and angles [ $^\circ$ ] for C1**

Bond lengths ( $\text{\AA}$ )		Bond angles ( $^\circ$ )	
Pd-N(2)	2.015(7)	N(2)-Pd-N(1)	80.6(3)
Pd-N(1)	2.129(8)	N(2)-Pd-Cl(1)	91.7(2)
Pd-Cl(1)	2.281(2)	N(1)-Pd-Cl(1)	171.5(2)
Pd-Cl(2)	2.304(2)	N(2)-Pd-Cl(2)	175.1(5)
N(2)-C7	1.285(13)	N(1)-Pd-Cl(2)	102.3(2)
N(2)-C8	1.460(12)	Cl(2)-Pd-Cl(1)	85.61(10)
C8-C9	1.525(12)	C7-N(2)-C8	120.8(7)
C8-H8A	0.9900	C7-N(2)-Pd	114.6(6)
C8-H8B	0.9900	C8-N(2)-Pd	124.6(6)
C7-C6	1.460(13)	N(2)-C8-C9	115.2(8)
C7-H7	0.9500	N(2)-C8-H8A	108.5
C2-N(1)	1.353(13)	C9-C8-H8A	108.5
C2-C3	1.418(15)	N(2)-C8-H8B	108.5
C2-C1	1.489(13)	C9-C8-H8B	108.5
N(1)-C6	1.342(12)	H8A-C8-H8B	107.5
C6-C5	1.389(14)	N(2)-C7-C6	118.3(8)
C9-C10	1.536(14)	N(2)-C7-H7	120.9
C9-H9A	0.9900.	C6-C7-H7	120.9
C9-H9B	0.9900.	N(1)-C2-C3	118.8(9)

---

C4-C3	1.329(16)	N(1)-C2-C1	120.9(9)
C4-C5	1.396(14)	C3-C2-C1	120.2(10)
C4-H4	0.9500	C6-N(1)-C2	118.5(9)
C5-H5	0.9500	C6-N(1)-Pd	109.4(7)
C10-H10A	0.9800	C2-N(1)-Pd	132.1(7)
C10-H10B	0.9800	N(1)-C6-C5	124.0(10)
C10-H10C	0.9800	N(1)-C6-C7	117.1(9)
C3-H3	0.9500	C5-C6-C7	118.9(9)
C1-H1A	0.9800	C8-C9-C10	110.1(8)
C1-H1B	0.9800	C8-C9-H9A	109.6
C1-H1C	0.9800	C10-C9-H9A	109.6
		C8-C9-H9B	109.6
		C10-C9-H9B	109.6
		H9A-C9-H9B	108.2
		C3-C4-C5)	119.0(10)
		C3-C4-H4	120.5
		C5-C4-H4	120.5
		C6-C5-C4	117.3(10)
		C6-C5-H5	121.4
		C4-C5-H5	121.4
		C9-C10-H10A	109.5
		C9-C10-H10B	109.5
		H10A-C10-H10B	109.5
		C9-C10-H10C	109.5
		H10A-C10-H10C	109.5
		H10B-C10-H10C	109.5

---

---

C4-C3-C2	122.3(10)
C4-C3-H3	118.8
C2-C3-H3	118.8
C2-C1-H1A	109.5
C2-C1- H1B	109.5
H1A-C1-H1B	109.5
C2-C1-H1C	109.5
H1A-C1-H1C	109.5
H1B-C1-H1C	109.5

---

**Table 4: Bond lengths [ $\text{\AA}$ ] and angles [ $^\circ$ ] for C2**

Bond lengths ( $\text{\AA}$ )		Bond angles ( $^\circ$ )	
Pd-N(1)	2.025(3)	N(1)-Pd-N(2)	80.81(12)
Pd-N(2)	2.022(3)	N(2)-Pd-Cl(1)	93.96(9)
Pd-Cl(1)	2.2784(9)	N(1)-Pd-Cl(1)	174.67(9)
Pd-Cl(2)	2.3052(9)	N(2)-Pd-Cl(2)	175.89(9)
N(2)-C6	1.285(5)	N(1)-Pd-Cl(2)	95.09(9)
N(2)-C7	1.477(5)	Cl(1)-Pd-Cl(2)	90.14(3)
C1-N(1)	1.337(5)	C6-N(2)-C7	121.3(3)
C1-C2	1.395(5)	C6-N(2)-Pd	113.9(2)
C1-H1	0.9500	C7-N(2)-Pd	124.7(2)
N(1)-C5	1.363(5)	N(1)-C1-C2	121.4(3)
C2-C3	1.380(5)	N(1)-C1-H1	119.3
C2-H2	0.9500	C2-C1-H1	119.3
C3-C4	1.391(5)	C1-N(1)-C5	119.2(3)
C3-H3	0.9500	C1-N(1)-Pd	128.3(3)
C4-C5	1.380(5)	C5-N(2)-Pd	112.5(2)
C4-H4	0.9500	C3-C2-C1	119.6(4)
C5-C6	1.454(5)	C3-C2-H2	120.2
C6-H6	0.9500	C1-C2-H2	120.2
C7-C8	1.518(5)	C2-C3-C4	118.7(4)
C7-H7A	0.9900	C2-C3-H3	120.6
C7-H7B	0.9900	C4-C3-H3	120.6
C8-C9	1.533(5)	C5-C4-C3	119.3(4)
C8-H8A	0.9900	C5-C4-H4	120.3
C8-H8B	0.9900	C3-C4-H4	120.3

---

C9-H9A	0.9800	N(1)-C5-C4	121.6(3)
C9-H9B	0.9800	N(1)-C5-C6	114.6(3)
C9-H9C	0.9800	C4-C5-C6	123.7(3)
		N(2)-C6-C5	118.2(3)
		N(2)-C6-H6	120.9
		C5-C6-H6	120.9
		N(2)-C7-C8	116.0(3)
		N(2)-C7-H7A	108.3
		C8-C7-H7A	108.3
		N(2)-C7-H7B	108.3
		C8-C7-H7B	108.3
		H7A-C7-H7B	107.4
		C7-C8-C9	109.8(3)
		C7-C8-H8A	109.7
		C9-C8-H8A	109.7
		C7-C8-H8B	109.7
		C9-C8-H8B	109.7
		H8A-C8-H8B	108.2
		C8-C9-H9A	109.5
		C8-C9-H9B	109.5
		H9A-C9-H9B	109.5
		C8-C9-H9C	109.5
		H9A-C9-H9C	109.5
		H9B-C9-H9C	109.5

---

**Table 5: Bond lengths [ $\text{\AA}$ ] and angles [ $^\circ$ ] for C3**

Bond lengths ( $\text{\AA}$ )		Bond angles ( $^\circ$ )	
Pd-N(2)	2.017(2)	N(2)-Pd-N(1)	80.63(8)
Pd-N(1)	2.142(2)	N(2)-Pd-Cl(1)	91.81(6)
Pd-Cl(1)	2.2776(6)	N(1)-Pd-Cl(1)	172.43(6)
Pd-Cl(2)	2.2948(7)	N(2)-Pd-Cl(2)	176.99(6)
Br-C1	1.878(3)	N(1)-Pd-Cl(2)	101.72(6)
N(1)-C1	1.346(3)	Cl(2)-Pd-Cl(1)	85.84(2)
N(1)-C5	1.372(3)	C1-N(1)-C5	114.7(2)
N(2)-C6	1.270(3)	C1-N(1)-Pd	136.36(17)
N(2)-C7	1.482(3)	C5-N(1)-Pd	108.94(16)
C1-C2	1.394(4)	C6-N(2)-C7	119.7(2)
C2-H2	0.9500	C6-N(2)-Pd	114.94(17)
C2-C3	1.375(4)	C7-N(2)-Pd	125.40(16)
C3-H3	0.9500	N(1)-C1-C2	124.1(2)
C4-C3	1.393(4)	N(1)-C1-Br	121.18(19)
C4-H4	0.9500	C2-C1-Br	114.64(19)
C5-C4	1.376(4)	N(2)-C6-C5	119.4(2)
C6-C5	1.463(3)	N(2)-C6-H6	126.26
C6-H6	0.9500	C5-C6-H6	126.26
C7-C8	1.515(3)	N(1)-C5-C4	124.7(2)
C7-H7A	0.9900	N(1)-C5-C6	116.0(2)
C7-H7B	0.9900	C4-C5-C6	119.3(2)
C8-C9	1.524(3)	N(2)-C7-C8	115.4(2)
C8-H8A	0.9900	N(2)-C7-H7A	108.43
C8-H8B	0.9900	C8-C7-H7A	108.43

---

C9-H9A	0.9800	N(2)-C7-H7B	108.43
C9-H9B	0.9800	C8-C7-H7B	108.43
C9-H9C	0.9800	H7A-C7-H7B	107.47
		C3-C2-C1	119.7(2)
		C3-C2-H2	120.16
		C1-C2-H2	120.16
		C5-C4-C3	118.9(2)
		C5-C4-H4	120.52
		C3-C4-H4	120.52
		C2-C3-C4	110.6(2)
		C2-C3-H3	117.9(2)
		C4-C3-H3	121.05
		C7-C8-C9	110.62(2)
		C7-C8-H8A	109.52
		C9-C8-H8A	109.52
		C7-C8-H8B	109.52
		C9-C8-H8B	109.52
		H8A-C8-H8B	108.08
		C8-C9-H9A	109.47
		C8-C9-H9B	109.47
		H9A-C9-H9B	109.47
		C8-C9-H9C	109.47
		H9A-C9-H9C	109.47
		H9B-C9-H9C	109.47

---



**Table 6: Bond lengths [ $\text{\AA}$ ] and angles [ $^\circ$ ] for C4**

Bond lengths ( $\text{\AA}$ )		Bond angles ( $^\circ$ )	
Pd-N2	2.0184(15)	N2-Pd-N1	80.37(6)
Pd-N1	2.1314(15)	N2-Pd-Cl1	91.71(4)
Pd-Cl1	2.2766(6)	N1-Pd-Cl1	171.98(4)
Pd-Cl2	2.3131(7)	N2-Pd-Cl2	174.85(4)
N1-C9	1.339(2)	N1-Pd-Cl2	103.19(4)
N1-C6	1.389(2)	Cl1-Pd- Cl2	84.793(19)
N2-C10	1.274(2)	C9-N1-C6	116.86(15)
N2-C11	1.481(2)	C9-N1-Pd	109.65(11)
C9-C8	1.404(3)	C6-N1-Pd	133.49(12)
C9-C10	1.461(2)	C11-N2-C11	120.88(15)
C8-C7	1.368(3)	C10-N2-Pd	114.35(12)
C8-H8	0.9500	C11-N2-Pd	124.65(11)
C7-C5	1.404(3)	N1-C9-C8	124.85(17)
C7-H7	0.9500	N1-C9-C10	116.47(16)
C5-C4	1.422(2)	C8-C9-C10	118.67(16)
C5-C6	1.428(2)	C7-C8-C9	118.98(17)
C6-C1	1.412(3)	C7-C8-H8	120.5
C4-C3	1.362(3)	C9-C8-H8	120.5
C4-H4	0.9500	C8-C7-C5	118.90(17)
C3-C2	1.407(3)	C8-C7-H7	120.5
C3-H3	0.9500	C5-C7-H7	120.5
C2-C1	1.373(3)	C7-C5-C4	121.15(17)
C2-H2	0.9500	C7-C5-C6	119.53(16)
C1-H1	0.9500	C4-C5-C6	119.32(16)

---

C10-H10	0.9500	N1-C6-C1	120.67(16)
C11-C12	1.517(2)	N1-C6-C5	120.87(16)
C11-H11A	0.9900	C1-C6-C5	118.47(16)
C11-H11B	0.9900	C3-C4-C5	120.81(18)
C12-C13	1.531(2)	C3-C4-H4	119.6
C12-H12A	0.9900	C5-C4-H4	119.6
C12-H12B	0.9900	C4-C3-C2	119.67(18)
C13-H15A	0.9800	C4-C3-H3	120.2
C13-H13B	0.9800	C2-C3-H3	120.2
C13-H13C	0.9800	C1-C2-C3	121.42(18)
		C1-C2-H2	119.3
		C3-C2-H2	119.3
		C2-C1-C6	120.31(17)
		C2-C1-H1	119.8
		C6-C1-H1	119.8
		N2-C10-C9	119.12(16)
		N2-C10-H10	1 120.4
		C9-C10-H10	1 120.4
		N2-C11-C12	115.76(14)
		N2-C11-H11A	108.3
		C12-C11-H11A	108.3
		N2-C11-H11B	108.3
		C12-C11-H11B	108.3
		H11A-C11-H11B	107.4
		C11-C12-C13	109.50(15)
		C11-C12-H12A	109.8

---

---

C13-C12-H12A	109.8
C11-C12-H12B	109.8
C13-C12-H12B	109.8
H12A-C12-H12B	108.2
C12-C13-H13A	109.5
C12-C13-H13B	109.5
H13A-C13-H13B	109.5
H13B-C13-H13C	109.5

---

## Chapter Four:

Table 7: Summary of X-ray data for complex 14

Data information	C14
Empirical formula	C <sub>18</sub> H <sub>24</sub> BCuF <sub>4</sub> N <sub>4</sub>
<i>Mr</i>	446.76
Crystal system	monoclinic
Space group	<i>P</i> 2 <sub>1</sub> / <i>n</i> (No.14)
<i>a</i> (Å)	10.2859(8)
<i>b</i> (Å)	14.0850(11),
<i>c</i> (Å)	13.8959(11)
$\alpha$ (°)	90
$\beta$ (°)	93.1460(10)
$\gamma$ (°)	09
<i>V</i> ((Å <sup>3</sup> ))	2010.2(3)
<i>Z</i>	4
<i>F</i> <sub>000</sub>	920
<i>D</i> <sub>calc</sub> (g.cm <sup>3</sup> )	1.476
$\mu$ (MoK $\alpha$ mm <sup>-1</sup> )	1.133
Temperature (K)	100(2)
$2\theta_{\text{max}}$	56.4°
Parameters/Restraints/data	255/0/22464
<i>R</i> <sub>1</sub> [ <i>I</i> > 2 $\sigma$ ( <i>I</i> )]	0.0315
<i>wR</i> <sub>2</sub>	0.0774
Final <i>Goof</i>	1.063

**Table 8: Bond lengths [ $\text{\AA}$ ] and angles [ $^\circ$ ] for C14**

Bond lengths ( $\text{\AA}$ )		Bond angles ( $^\circ$ )	
Cu-N2	1.9846(13)	N2-Cu-N2'	138.71(5)
Cu-N2'	2.0018(13)	N2-Cu- N1'	126.35(5)
Cu-N1'	2.0615(13)	N1'-Cu-N2'	81.37(5)
Cu-N1	2.0805(13)	N1-Cu- N2	81.55(5)
F4-B1	1.3879(2)	N2'-Cu-N1	114.30(5)
F2-B1	1.394(2)	N1-Cu-N1'	118.09(5)
F3-B1	1.388(2)	C1-N1-Cu	131.88(11)
F1-B1	1.393(2)	C1-N1-C5	117.61(13)
C1-N1	1.3393(2)	C5-N1-Cu	110.50(10)
C1-C2	1.3889(2)	C6-N2-Cu	114.16(11)
C1-H1	0.9500	C6-N2-C7	118.29(13)
C2-C3	1.3842(2)	C7-N2-Cu	127.46(11)
C2-H2	0.9500	N2-C6-H6	120.51
C3-C4	1.3908(2)	N2-C6-C5	118.98(14)
C3-H3	0.9500	C5-C6-H6	120.51
C4-C5	1.3852(2)	N1-C1-H1	118.56
C4-H4	0.9500	N1-C1-C2	122.87(15)
N2-C6	1.2763(2)	C2-C1-H1	118.56
N2-C7	1.4667(2)	C2-C3-H3	120.67
C6-C5	1.4705(2)	C2-C3-C4	118.66(15)
C6-H6	0.9500	C4-C3-H3	120.67
C8-C7	1.5266(2)	C3-C2-H2	120.42
C7-H7A	0.9900	C3-C2-C1	119.16(15)
C7-H7B	0.9900	C1-C2-H2	120.42

---

C5-N1	1.3537(2)	C5-C4-C3	118.74(14)
C8-C9	1.5187(2)	C5-C4-H4	120.63
C8-H8A	0.9900	C3-C4-H4	120.63
C8-H8B	0.9900	N1-C5-C6	114.63(13)
C9-H9A	0.9800	N1-C5-C4	122.95(14)
C9-H9B	0.9800	C4-C5-C6	122.39(14)
C9-H9C	0.9800	F1-B-F2	109.04(14)
C1'-N1'	1.3405(2)	F4-B-F2	109.83(14)
C1'-C2'	1.3848	F4-B-F1	109.51(14)
C1'-H1'	0.9500	F3-B-F2	109.54(14)
C2'-C3'	1.3815	F3-B-F1	109.86(15)
C2'-H2'	0.9500	F3-B-F4	109.06(14)
C3-N1	1.467(2)	N2-C7-H7B	109.47
C3'-C4'	1.3815(2)	N2-C7-H7A	109.47
C3'-H3'	0.9500	N2-C7-C8	110.87(13)
C5'-N1'	1.3523(2)	H7A-C7-H7B	108.05
C5'-C4'	1.3889(2)	C8-C7-H7A	109.47
C5'-C6'	1.4673(2)	C8-C7-H7B	109.47
C6'-H6'	0.9500	C7-C8-H8A	109.16
C6'-N2'	1.2763(2)	C7-C8-H8B	109.16
N2'-C7'	1.4684(2)	H8A-C8-H8B	107.88
C7'-C8'	1.5152(2)	C7-C8-C9	112.22(14)
C7'-H7A'	0.9900	C9-C8-H8A	109.16
C7'-H7B'	0.9900	C9-C8-H8B	109.16
C8'-C9'	1.5210(2)	C8-C9-H9A	109.47
C8'-H8A'	0.9900	C8-C9-H9B	109.47

---

---

C8'-H8B'	0.9900	C8-C9-H9C	109.47
C9'-H9A'	0.9800	H9A-C9-H9C	109.47
C9-H9B'	0.9800	H9A-C9-H9B	109.47
C9-H9C'	0.9800	H9B-C9-H9C	109.47
		N1'-C1'-H1'	118.31
		N1'-C1'-C2'	123.38(16)
		C2'-C1'-H1'	118.31
		C3'-C2'-H2'	120.64
		C3'-C2'-C1'	118.71(16)
		C1'-C2'-H2'	120.64
		N1'-C5'-C6'	114.79(14)
		N1'-C5'-C4'	122.66(15)
		C4'-C5'-C6'	122.50(15)
		C2'-C3'-H3'	120.49
		C2'-C3'-C4'	119.61(16)
		C4'-C3'-H3'	120.49
		C3'-C4'-H4'	120.62
		C3'-C4'-C5'	118.76(16)
		C5'-C4'-H4'	120.62
		N2'-C6-H6	120.65
		N2'-C6'-C5'	118.71(14)
		C5'-C6'-H6'	120.65
		C6'-N2'-Cu	113.49(11)
		C6'-N2'-C7'	118.49(13)
		C7'-N2'-Cu	127.83(11)
		C1'-N1'-Cu	131.71(11)

---

---

C1'-N1'-C5'	117.44(11)
C5'-N1'-Cu	110.84(10)
N2'-C7'-H7A'	109.17
N2'-C7'-H7B'	109.17
N2'-C7'-C8'	112.18(13)
C8'-C7'H7A'	109.17
C8'-C7'-H7B'	109.17
H7B'-C7'-H7A'	107.88
C7'-C8'-H8A'	109.56
C7'-C8'-H8B'	109.56
C7'-C8—C9'	110.46(14)
C9'-C8'-H8A'	109.56
C9'-C8'-H8B'	109.56
H8B'-C8'-H8A'	108.11
C8'-C9'-H9A'	109.47
C8'-C9'-H9B'	109.47
C8'-C9'-H9C'	109.47
H9A'-C9'-H9B'	109.47
H9A'-C9'-H9C	109.47
H9B'-C9'-H9C'	109.47

---